



Erythrocytes derived microvesicles: their characterisation and potential role as delivery vectors



Presented by
Roberta Cordeiro Freezor

Thesis submission in fulfilment for the degree of
DOCTOR OF PHILOSOPHY (Ph.D)

Director of studies: **Dr. Sheelagh Heugh**
Supporting supervisors: Prof. Jameel Inal and Dr. Gary McLean

Cellular and Molecular Immunology Research Centre (CMIRC)
School of Human Sciences

September 2018

Acknowledgments

I am truly thankful to the director of my study, Dr. Heugh for giving me the opportunity to carry out my research under her supervision, her professional support and guidance throughout my studies at London Metropolitan University. Her ability to overcome issues, intelligent suggestions, and encouragement lure me to further my career in this field.

Besides my director of studies, I would like to thank my supporting supervisors. Dr. McLean for sharing his expertise in virology with me and Prof. Inal. To both, I am grateful for their insightful comments and encouragement and also for the thoughtful questions which incentivised me to widen my research from various perspectives.

My special thanks to Mr. Gonzalez, for sharing his knowledge on proteomics and bioinformatics with me. Thanks to Dr. Haidery who taught me specialised laboratory techniques, and to Miss Velkova for the virus work support. Their passion and dedication to science is an inspiration. They are role models for all PhD students.

I must express my gratitude to Mr. Freezor, my husband, for his continued support, encouragement and love. I was continuously amazed by his skills and willingness to proof read countless pages of “sciences” and for always providing helpful suggestions, by his patience and friendship and I would like to say a big thank you for you being there to experience and listen to all of the ups and downs of my research.

I would also like to thank all the members of staff at London Metropolitan University. To the academic team for answering my questions on the spot, and to the technical team, especially to Mr. Stott, for his willingness to provide bench material for my lab work without notice.

I thank my fellow lab mates for the stimulating discussions, for the sleepless nights when working together before deadlines, and for all the fun we have had in the research lab. They have provided a much needed form of escape from my studies and work commitments. I would also like to thank my mother for her spiritual and personal guidance, and my parents in law for their support and curiosity about my research topic.

I am indebted to them all, without their precious support, it would not be possible to conduct this PhD research and to write this thesis.

Abstract

Extracellular vesicles (EV) are heterogeneous populations of small vesicles released by virtually all cells and are classified depending on their biogenesis and size. Microvesicles (MV) are a subtype of EV and are released under optimal cell conditions and/or upon stimuli. In this study, the influence of erythrocyte derived MV (eMV) on the growth of THP-1 and Jurkat cell lines was observed. HeLa cells and those infected with Human Rhinovirus type 16 derived MV (HRV16iHBMV) were used as parallel samples for all experiments. This is because virus infected cell derived EV have been extensively studied and it is understood that viral-MV uses the virus mechanism of entry to communicate with neighbouring cells. Whereas the eMV mechanism is still not fully understood. Therefore, to understand the mechanism of eMV action on the growth of cell lines, their characterisation was explored.

Flow cytometry analysis using fluorescence sub-micron particle size reference indicates that the samples acquired during this PhD research meet the 'current requirements' in the field, to be classified as MV according to their sizes (100-1000 nm), and that the amount of release of eMV increases depending on the stimulus used (CaCl₂, Normal Human Serum), due to remodelling of the cell membrane. Immunoblotting and flow cytometry surface marker profiling data shows that eMV are composed of key molecules that may allow their survival in the extracellular environment and communication with neighbouring cells. CD235 surface marker confirms their parent cells and the presence of CD47 suggests how eMV may avoid phagocytosis. Surface receptors including CD36, CD58 and CD63 indicate how they may communicate and enter the neighbouring cells through endocytosis. The identification of proteases suggests how eMV may be capable of tissue remodelling and degradation, whereas the presence of miRNAs may indicate how eMV can have an impact on the recipient cell by downregulating gene expression. Fluorescence microscopy shows eMV interacting with the cell membrane and the flow cytometry data suggests that eMV inhibit the growth of THP-1.

The mechanism which clarifies this impact is unknown. Nevertheless, this PhD project has identified key biological molecules which constitute biologically active entities and might therefore, help eMV to transfer information and substances to recipient cells displaying their potential as delivery vectors. Thus, data obtained here can positively contribute towards the EV field.

Publications and accomplishments

Ramirez, M., Amorim, M., Gadelha, C., Milic, I., Welsh, J., Freitas, V., Nawaz, M., Akbar, N., Couch, Y., Makin, L., Cooke, F., Vettore, A., Batista, P., **Freezor, R.**, Pezuk, J., Rosa-Fernandes, L., Carreira, A. C., Devitt, A., Jacobs, L., Silva, I., Coakley, G., Nunes, D., Carter, D., Palmisano, G., Dias-Neto, E., 2018. Technical Challenges of Working with Extracellular Vesicles. *Nanoscale* 10 (3) : 881-906.

Freezor, R., Heugh, S., McLean, G., Inal, J., 2017. Erythrocyte microvesicle engineering: an investigation into methods of induction. Manuscript in preparation.

Freezor, R., Heugh, S., 2017. Membrane markers profiling: Comparative analysis of microvesicles derived from erythrocyte and HeLa cells infected with Human Rhinovirus type 16. Abstract Book: Toronto ISEV2017. *J Extracell Vesicles*, 6:sup1, 1310414.

Freezor, R., Heugh, S., 2017. Identifying immune related miRNAs, studying the differences between erythrocyte and human rhinovirus infected HeLa cells derived microvesicles, a profiling using Firefly particle technology. Abstract Book: Toronto ISEV2017, *J Extracell Vesicles*, 6:sup1, 1310414.

Freezor, R., McLean, G., Heugh, S., 2016. Erythrocyte cells and HRV16-infected HeLa cells derived microvesicles protease profiling. The Fifth International Meeting of ISEV, ISEV2016, Rotterdam, The Netherlands. *J Extracell Vesicles*. 5: 10.3402/jev.v5.31552.

Freezor, R., Heugh, S., 2014. The biological effect and characterization of erythrocyte derived microvesicles. BBTS (British Blood Transfusion Society) 32nd Annual Conference (Harrogate International Centre). <https://www.bbts.org.uk/annualconference/>

Freezor, R., Heugh, S., 2014. Characterization and expression of markers on erythrocyte-derived microvesicles, either naturally released or stimulated with normal human serum. Abstracts from the Third International Meeting of ISEV 2014 Rotterdam, The Netherlands. *J Extracell Vesicles*. 3: 10.3402/jev.v3.24214.

Freezor, R., Heugh, S., 2013. The biological effect of Erythrocytes derived-microvesicles on the growth of Jurkat, THP-1, PC3-M and MCF-7 cell lines. Does this biological function indicate potential therapeutic roles? Second International Meeting of ISEV 2013: Boston, USA. *J Extracell Vesicles*. 2: 10.3402/jev.v2i0.20826.

Freezor, R., Heugh, S., 2013. The clinical importance of microvesicles as diseases biomarkers - developing a reference range for microvesicles in healthy volunteers, to determine the significance of change in disease. ImmunoTools IT-Box-139 Award 2013. <http://www.immunotools.de/html/award/RobertaFreezor.pdf>

List of abbreviations

Adenosine Triphosphate (ATP)
Adenosine Triphosphate enzyme (ATPase)
Antigen presenting cells (APCs)
Bicinchoninic acid (BCA)
Bovine serum albumin (BSA)
Calcium Chloride (CaCl₂)
Calcium ions (Ca²⁺)
Calibration particles (CP)
Carbon dioxide (CO₂)
Cathepsins (CTS)
Cytopathic effect (CPE)
Complete Growth Medium (CGM)
Cluster of Differentiation (CD)
Dendritic cells (DC)
Deoxyribonucleic Acid (DNA)
DL-Dithiothreitol solution (DDT)
Double deionised water (ddH₂O)
Dulbecco's Modification of Eagle's Medium (DMEM)
Ethylene Diamine Tetraacetic Acid (EDTA)
Extracellular Matrix (ECM)
Extracellular vesicles (EV)
Erythrocyte derived Microvesicles (eMV)
Endosomal Sorting Complex Required for Transport (ESCRT)
Flow cytometry (FC)
Fluorescein-Isothiocyanate (FITC)
Gene Ontology (GO)
Glycophorin (GYP)
Glycoprotein (GP)
Glycosylphosphatidylinositol (GPI)
Guanosine Diphosphate (GDP)
Guanosine Triphosphate (GTP)

HeLa derived Microvesicles Control (HeLaMVC)
Hepatitis C Virus (HCV)
Herpes simplex Virus (HSV)
Human Immunodeficiency Virus (HIV)
Human Rhinovirus (HRV)
Human Rhinovirus type 16 (HRV16)
Human Rhinovirus type 16 infected HeLa cells (HRV16iHC)
Human Rhinovirus type 16 infected HeLa derived Microvesicles (HRV16iHMV)
Interleukin (IL)
Intercellular Adhesion Molecule-1 (ICAM-1)
Intraluminal Vesicles (ILVs)
Lymphocyte Function-associated Antigen (LFA)
Kallikreins (KLK)
Major Histocompatibility Complex (MHC)
Matrix Metalloproteinases (MMPs)
Matrix Metalloproteinases Inhibitors (MMPIs)
Membrane Attack Complex (MAC)
Microvesicles (MV)
Multivesicular Bodies (MVBs)
Multiplicity Of Infection (MOI)
Nitric Oxide (NO)
Normal Human Serum (NHS)
Optical Density (OD)
Penicillin-Streptomycin (PenStrep)
Phosphate Buffered Saline (PBS)
Phosphate Buffered Saline Tween-20 (PBST-20)
Phosphatidylserine (PS)
Plaque Forming Unit (PFU)
Polyvinylidene Difluoride (PVDF)
Protein Kinase C (PKC)
Radio-Immunoprecipitation Assay (RIPA)
Red Green Blue (RGB)
Ribonucleic Acid (RNA)
Room Temperature (RT)
Roswell Park Memorial Institute 1640 (RPMI)

Size Exclusion Chromatography (SEC)

Sodium Dodecyl Sulphate (SDS)

Sodium Dodecyl Sulphate Polyacrylamide Gel Electrophoresis (SDS-PAGE)

Soluble N-ethylmaleimide-sensitive factor attachment protein receptors (SNAREs)

Tissue Culture Infective Dose 50% (TCID₅₀)

Tissue Inhibitors of MMPs (TIMPs)

Tumour susceptibility gene (Tsg)

Tunable Resistive Pulse Sensing (TRPS)

Ultraviolet (UV)

Untranslated Region (UTR)

Table of contents

1. Literature review and general introduction	1
1.1 Theoretical background of extracellular vesicles	1
1.1.1 The biogenesis and general characteristics of exosomes.....	2
1.1.2 Microvesicles biogenesis and general characteristics.....	6
1.1.3 Apoptotic bodies	9
1.2 The importance of erythrocyte in circulation	11
1.2.1 Erythrocyte derived MV	12
1.2.2 Cellular mechanisms underlying eMV release	14
1.3 Introduction to Human Rhinovirus	17
1.3.1 Viral-derived MV	19
1.4 Cellular mechanism processes involved in EV uptake	21
1.5 The potential biological interaction between MV and neighbouring cells	23
1.6 EV in circulation	25
1.7 EV as delivery vehicles/vectors	27
1.8 Aim of this PhD research project	31
2. Materials and Methods	33
2.1 Materials	33
2.1.1 Chemicals and kits	33
2.1.2 Technical devices.....	34
2.1.3 Antibodies	34
2.1.4 Buffers and solutions	35
2.1.5 Cell lines	36
2.2 Methods	36
2.2.2 Isolation of erythrocytes	37
2.2.3 HRV16 preparation and infection.....	37
2.2.4 Isolation of MV	40
2.2.5 Flow cytometry analyses	42
2.2.6 qNano standard operating protocol.....	44
2.2.7 Western blotting analyses	45
2.2.8 Proteases profiling	48
2.2.9 miRNA profiling.....	49
2.2.10 MV labelling for fluorescence microscopy	51
2.2.11 The addition of eMV on the growth of different cell lines	52

2.2.12	The addition of HeLaMVC and HRV16iHMV on the growth of HeLa cells	52
2.2.13	Statistical Data Analysis	53
3.	Results	54
3.1	Heterogeneity of MV samples: their concentration and size	54
3.1.1	Introduction	54
3.1.2	Results	56
3.1.3	Discussion	65
3.2	An investigation into key biomolecules required for MV communication and survival	70
3.2.1	Surface markers identification in MV samples	70
3.2.2	Total protein identification in MV samples	86
3.2.3	Proteases identification in MV samples	97
3.2.4	<i>In silico</i> analyses of biomolecules identified in eMV samples	111
3.3	Identifying immune related miRNAs: properties that may allow MV to affect the target cell	117
3.3.1	Introduction	117
3.3.2	Results	120
3.3.3	Discussion	129
3.4	The interaction of MV on the selected cell lines	139
3.4.1	Introduction	139
3.4.2	Results	142
3.4.3	Discussion	151
4.	A model proposition: eMV may act as delivery vectors in circulation	155
5.	Conclusions and further work	160
	References	167
	Appendices	206
	Appendix I	206
	Appendix II	207
	Appendix III	209
	Appendix IV	215
	Appendix V	221
	Appendix VI	224
	Appendix VII	226
	Appendix VIII	229

List of figures

Fig. 1.1.1.1. An example of exosomes biogenesis.....	3
Fig. 1.1.1.2. The SNARE complex.....	6
Fig. 1.1.2.1. An example of MV biogenesis in response to cell stimulation.....	7
Fig. 1.1.3.1. A basic representation of apoptotic bodies biogenesis.....	10
Fig. 1.2.1. Blood cells formation and development.....	11
Fig. 1.4.1. The three main subtypes of endocytosis.....	22
Fig. 1.5.1. A representation of the three general stages of cell communication and signalling in Hairy cell leukaemia.	24
Fig. 1.7.1. The three main classes of cell surface receptors.....	28
Fig. 2.2.3. Determination of infectious titre of HRV16 stock.....	39
Fig. 2.2.4. TCID ₅₀ of HRV16 stock Excel spreadsheet.....	39
Fig. 2.2.7. BSA standard curve for protein concentration.....	46
Fig. 2.2.9.3.1. Summary of the miRNA experimental procedure.....	51
Fig. 3.1.2.1. Dot-plot gating- FC analyses of MV sizing and counting strategy.....	58
Fig. 3.1.2.2. The measurement of MV numbers- assessment by FC analyses.....	60
Fig. 3.1.2.3. MV sizing- assessment by qNano analyses.....	62
Fig. 3.1.2.4. Effect of qEV purification on MV amount of release - assessment by FC analyses.....	64
Fig. 3.2.1.1. Fluorescence intensity measurements – assessment by FC analyses.....	76
Fig. 3.2.1.2. Fluorescence gating - Annexin V (non-specific marker) labelled MV.....	77
Fig. 3.2.1.3. CD percentage fluorescence intensity in all MV samples.....	79
Fig. 3.2.1.4. Fluorescence intensity (in percentage) summary for positive markers	80
Fig. 3.2.1.3.1. Protein interaction network for surface markers present in eMV.....	85
Fig. 3.2.2.1. SDS-PAGE SYPRO® Ruby stain protein gels	90
Fig. 3.2.2.2. Western blotting analyses.....	91
Fig. 3.2.2.3. Western blotting band intensity analyses.....	92
Fig. 3.2.2.3.1. Protein interaction network for total proteins observed in eMV.....	96
Fig. 3.2.3.1. Location of coordinates and the presence of different proteases in each array membrane	103
Fig. 3.2.3.2. The comparison of the relative expression of proteases present in erythrocytes and eMV.....	105
Fig. 3.2.3.3. The comparison of the relative expression of proteases present in HeLa cells and HRV16iH MV.....	106

Fig. 3.2.3.4. The comparison of proteases present in all samples.....	106
Fig. 3.2.3.3.1. Protein interaction network of proteases observed in eMV.....	110
Fig. 3.2.4.1. Cellular component enrichment of biomolecules observed in eMV	113
Fig. 3.2.4.2. Molecular function enrichment of biomolecules observed in eMV	114
Fig. 3.2.4.3. Biological processes enrichment of biomolecules observed in eMV.....	114
Fig. 3.2.4.4. Biological pathway enrichment of biomolecules observed in eMV.....	115
Fig. 3.3.1.1. Firefly particle structure.....	120
Fig. 3.3.2.1. The average signal in RNA spike-in controls and miRNAs selected for data normalisation.....	122
Fig. 3.3.2.2. Comparison of positive RNA spike-in controls to historical values.....	123
Fig. 3.3.2.3. Expression profile comparison of all samples from merged triplicates	125
Fig. 3.3.2.4. Summary of miRNAs present in all samples.....	127
Fig. 3.3.2.5. Summary of miRNAs demonstrating high expression in HeLa cells and their derived MV.....	128
Fig. 3.3.2.6. Summary of miRNAs demonstrating high expression in erythrocytes and their derived eMV.....	128
Fig. 3.3.3.1. Cellular component enrichment for target genes of miRNA observed in eMV.....	134
Fig. 3.3.3.2. Molecular function enrichment for target genes of miRNA observed in eMV	135
Fig. 3.3.3.3. Biological processes enrichment for target genes for miRNA observed in eMV.....	136
Fig. 3.3.3.4. Biological pathway enrichment for target genes of miRNA observed in eMV.....	137
Fig. 3.4.2.1. THP-1 cell and eMV interaction.....	143
Fig. 3.4.2.2. Jurkat cell and eMV interaction.....	144
Fig. 3.4.2.3. Growth rate of cell lines - control against eMV treated cells.....	145
Fig. 3.4.2.4. % Cell viability of control and eMV treated cell lines.....	146
Fig. 3.4.2.5. HeLa cell and their derived MV interaction.....	147
Fig. 3.4.2.6. The impact of HRV16 and MV on the growth of HeLa cells.....	148
Fig. 3.4.2.7. Growth rate of HeLa cells - control against HeLa cells treated with HeLaMVC and HRV16iHMV.....	149
Fig. 3.4.2.8. % Cell viability of HeLaMVC and HRV16iHMV treated HeLa cells.....	150
Fig. 4.2.1. Schematic summary of eMV biogenesis, contents, mechanism of communication and potential impact on a THP-1 cell.....	159

1. Literature review and general introduction

1.1 Theoretical background of extracellular vesicles

Extracellular Vesicles (EV) were first acknowledged when Chargaff & West (1946) identified a “precipitable factor” present in ultracentrifugated platelet-free plasma. They postulated that these fragments were capable of inducing and accelerating the generation of thrombin. Then, Wolf (1967) described these fragments as a residue or by-product of platelet activation that had no real purpose, referring to them as ‘platelet dust’.

Studies in this field, particularly those conducted within the last two decades resulted in different nomenclature being used for these small vesicles, such as, calcifying matrix vesicles (Anderson, 1969), prostasomes (Stegmayr & Ronquist, 1982), plasma-membrane microvesicles (Holme, *et al.*, 1994) ectosomes (Hess, *et al.*, 1999), apoptotic bodies and exosomes (Théry, *et al.*, 2001), tolerosomes (Karlsson, *et al.*, 2001), microparticles (Watanabe, *et al.*, 2003), dexosomes (Patel, *et al.*, 2005) and shedding microvesicles (Cocucci, *et al.*, 2009).

Despite such terms having some use within a specialised field, it became difficult to discriminate between the different types of these vesicles, especially where generic terminology have a different meaning for different things to different investigators. As a result of expanding interest in this field, the International Society for Extracellular Vesicles (ISEV) met in Gothenburg-Sweden, April 2012. ISEV gathered pioneers and active authors in this field to chair a session on the issue of vesicle nomenclature. The authors considered their biogenesis, size, morphology, physical properties, and physiological function. As a result, authors were encouraged to use the generic term “Extracellular vesicles” (EV) for all secreted vesicles, and as a keyword in all publications (Gould & Raposo, 2013).

Research into EV has discovered that these membrane-coated vesicles are released by virtually all cells types and have been found in many biological fluids, including ascites (Andre, *et al.*, 2002), breast milk (Admyre, *et al.*, 2007), amniotic fluid (Keller, *et al.*, 2007), brochoalveolar lavage liquid (Prado, *et al.*, 2008), plasma (Orozco, *et al.*, 2009), urine (Conde-Vancells, *et al.*, 2010), and saliva (Yang, *et al.*, 2014) amongst other

biological samples. It has been suggested that EV can be characterised by antigenic markers exposed on their surface linked to their parent cell origin and are distinguishable by their biogenesis. EV vary in size, biochemical composition, and biological effects (Azevedo, *et al.*, 2007; Distler, *et al.*, 2005).

Currently, there are three main classes of EV: exosomes, microvesicles and apoptotic bodies (Andaloussi, *et al.*, 2013). Each of these types will be discussed in detail in the following chapters of this thesis, elucidating their differences and similarities.

1.1.1 The biogenesis and general characteristics of exosomes

To date, exosomes are the best characterised class of EV and they range between 30-120 nm (Fleissner, *et al.*, 2012; Dozio & Sanchez, 2017). When visualised by electron, transmission electron, and cryo-electron microscopy exosomes appear as a uniform cup-like morphology and round vesicles (Trajkovic, *et al.*, 2008; Conde-Vancells, *et al.*, 2010). Cryo-electron tomography have been used to observe the 3D structure of platelet exosomes in fresh plasma revealing them to be round, electron dense and without a visible lipid bilayer (Yuana, *et al.*, 2013).

Exosomes are considered Intraluminal Vesicles (ILVs) that are known to be released from eukaryotic cells, and are created by inward budding of endosomal Multivesicular Bodies (MVBs). They are the only known secreted EV that originates from internal membrane (Meckes & Raab-Traub, 2011).

Théry, *et al.*, (2001), pioneers in the field, identified proteins including Alix and Tumour susceptibility gene (Tsg) 101 proteins which belong to the Endosomal Sorting Complexes Required for Transport (ESCRT in exosomes derived from dendritic cell (DC). This strongly supports the hypothesis of ESCRT-dependent exosome biogenesis.

Current research indicates that ESCRT consists of four soluble multiprotein complexes: ESCRT-0, ESCRT-I, ESCRT-II, and ESCRT-III which leads to the formation of MVBs. The ESCRT-0 complex initiates the MVB pathway by localising to endosomes through an interaction with an endosome-enriched phospholipid, phosphatidylinositol-3-phosphate (PI3P) (Schmidt & Teis, 2012). This process requires ubiquitination of the cytosolic tail of endocytosed receptors including Tsg101 (Katzmann, *et al.*, 2002), which belongs to the ESCRT-I complex, bind the ubiquitinated (a protein that is inactivated by attaching ubiquitin to it) cargo proteins and activate the ESCRT-II complex (Schmidt & Teis, 2012).

Then, the ESCRT-II complex commences with the oligomerization and ESCRT-III complex follows, MVBs proteins sequestration and recruits a deubiquitinating enzyme, removing the ubiquitin tag from the cargo proteins before sorting them into the ILVs (Mageswaran, *et al.*, 2014). Subsequently, the ESCRT-III complex is dismantled by an Adenosine Triphosphate enzyme (ATPase) (Urbanelli, *et al.*, 2013) which binds to the individual ESCRT-III proteins (associated with a variety of cellular activities), including disassembly by Vacuolar protein sorting-associated protein 4 (Vps4). This may help the membrane deformation permitting ILVs formation (Hanson, *et al.*, 2008). An example of exosomes biogenesis is presented in Fig.1.1.1.1.

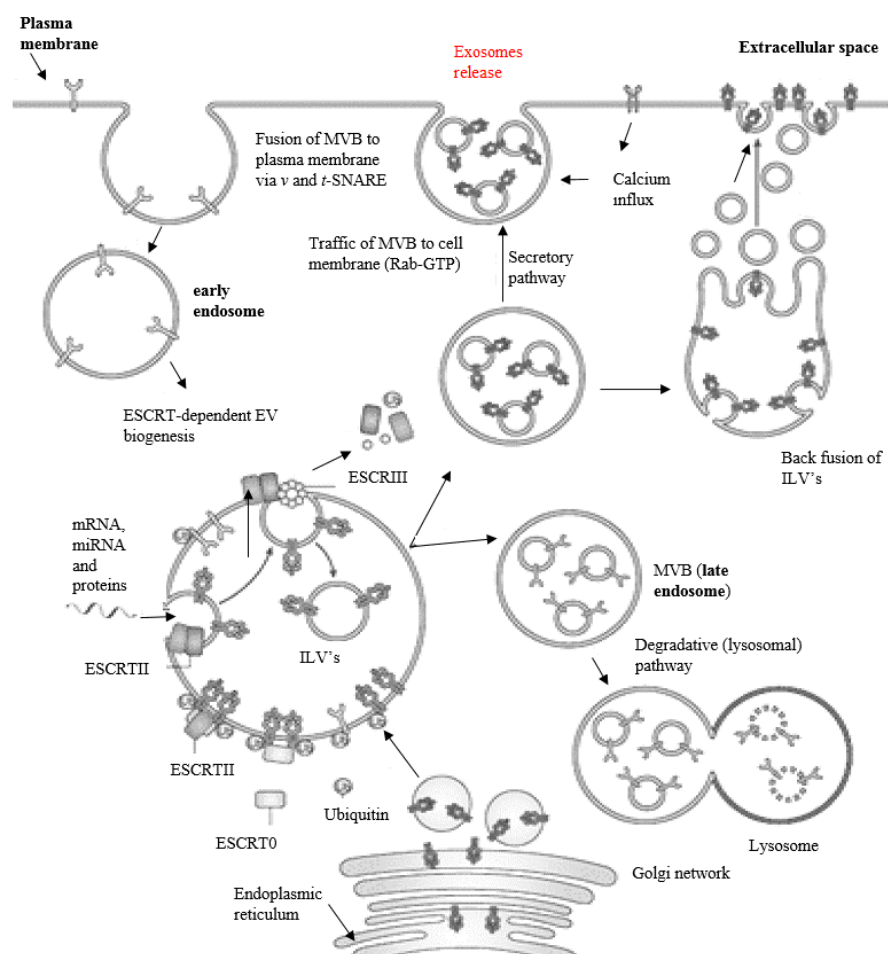


Fig. 1.1.1.1. An example of exosomes biogenesis. Adopted from Robbins & Morelli (2014) and modified by Roberta Freezor using online Pixlr photo editor. After endocytosis of plasma membrane takes place, the transmembrane proteins destined for the lysosome lumen are sorted into the vesicles that bud from the perimeter membrane into endosomes (“early endosomes”). Then when the endosome that has fully developed into a late endosome intermingles with a lysosome, the vesicles in the lumen are sent to the lysosome lumen. MVB membrane invagination and protein sorting are achieved by the concerted function of ESCRT. Then the MVB may follow a degradation pathway fusing with lysosomes or are destined to release the ILVs as exosomes to the extracellular space by exocytosis (Simons M & Raposo, 2009; Théry, *et al.*, 2002).

Some researchers (Trajkovic, *et al.*, 2008; Urbanelli, *et al.*, 2013) suggest that the exosomal sorting of proteolipid protein do not require Tsg101 or Alix, suggesting instead that ceramide (cell membrane proteins made up of a fatty named sphingosine) promotes membrane invagination of ILVs. Bianco, *et al.*, (2009) have suggested that the ceramide role demonstrates an involvement of sphingomyelinases in the biogenesis of exosomes. This was observed in glial cells releasing exosomes and of neutral sphingomyelinase 2 secreting micro-Ribonucleic Acid (RNA), a small non-coding RNA molecule containing vesicles (Kosaka, *et al.*, 2010).

Fang, *et al.*, (2007) postulated that higher order-oligomerization might play a key role in exosome biogenesis as well as sorting proteins into exosomes. This process was demonstrated to be linked to Cluster of Differentiation (CD) 43 (involved in the physicochemical properties of the T-cell surface and in lectin binding) exosomal sorting in Jurkat T-cells. A similar mechanism was proposed a decade before by Johnstone, *et al.*, (1989) using antibody coated (magnetic core bead), obtaining results indicating that exosomes contain the transferrin receptor in reticulocytes as well as other plasma membrane activities, such as the nucleoside transporter and acetylcholinesterase (Vidal, *et al.*, 1997).

Additionally, the Major Histocompatibility Complex (MHC) class II/peptide complexes has also been identified in intestinal epithelial cell derived exosomes (Muntasell, *et al.*, 2007; van Niel, *et al.*, 2003). MHC supports the production of immune responses in preference to the inbuilt tolerance mechanism responses in the context of a systemic challenge. Therefore, controlling the outcomes of the immune response to exosome derived epitopes requires both the mucosal microenvironment and local effector cells in the intestine are proposed to be key players in this.

Exosome composition can depend on what is sorted into them when they are being formed. This may include proteins (ubiquitination) acting as a substrate for the recruitment ESCRT machinery, and the generation of the ESCRT-dependent ILVs. MVBs, for example undergo continuous maturation, and during the process they may lose and/or gain a variety of proteins and lipids (Piper, *et al.*, 2014), small RNA's (Nolte-'t Hoen, *et al.*, 2012), lipids (Subra, *et al.*, 2007), and a variety of proteins (Keerthikumar, *et al.*, 2016). Therefore, without limitations to the endosome membrane and their properties there are no particular restrictions to their cargo, which is dependent on their parent cell.

Exosome movement to the extracellular space requires the fusion of MVBs with the plasma membrane, and this fusion has been proposed as requiring the involvement of a combination of Soluble N-ethylmaleimide-sensitive factor attachment protein receptors (SNAREs) and vesicular SNAREs (*v*-SNAREs) (Urbanelli, *et al.*, 2013). Supporting evidence of this fusion was observed in an erythroleukaemia cell line (K562), where the vesicle (*v*)-SNARE complex, known as TI-VAMP/VAMP7 (vesicular-associated membrane proteins), has been observed as participating in the fusion of exosomes (Fader, *et al.*, 2009; Urbanelli, *et al.*, 2013).

SNAREs and *v*-SNAREs localised on MVBs interact with target SNAREs (*t*-SNAREs) that are bounded on the intracellular side of the plasma membrane to form a membrane-bridging SNARE complex (Chaineau, *et al.*, 2009; Jena, 2009). The arrangement of a SNARE complex between the vesicle and the acceptor membrane tightens the facing membranes together and loses the fusion barrier by undermining the lipid bilayers (Cohen & Melikyan, 2004). The activity of SNAREs can be regulated by many proteins including Rab3, Guanosine Triphosphate-binding proteins that are members of the Ras superfamily, which arrange the initial contact between membranes intended to fuse and assures that only appropriate organelles are tethered (Zerial & McBride, 2001).

Membrane fusion is then coordinated by the arrangement of a quaternary- α -helical *trans*-SNARE complex (bridge two membrane compartments or vesicles), consisting of one *v*-SNARE on the vesicle and two or three *t*-SNAREs on the target membrane. After membrane fusion, the *cis* SNARE complex (after fusion - reside in a single resultant membrane) is disassembled by the ATPase, which catalyses the formation of Adenosine Triphosphate (ATP) from Adenosine Diphosphate (ADP) and free phosphate ion - releasing energy. The N-ethylmaleimide-sensitive fusion (NSF) protein is commissioned to the *cis*-SNARE complex from the cytosol by N-ethylmaleimide-sensitive factor Attachment Protein Alpha (α -SNAP) (Sehgal & Lee, 2011). The SNARE complex is summarised in Fig.1.1.1.2.

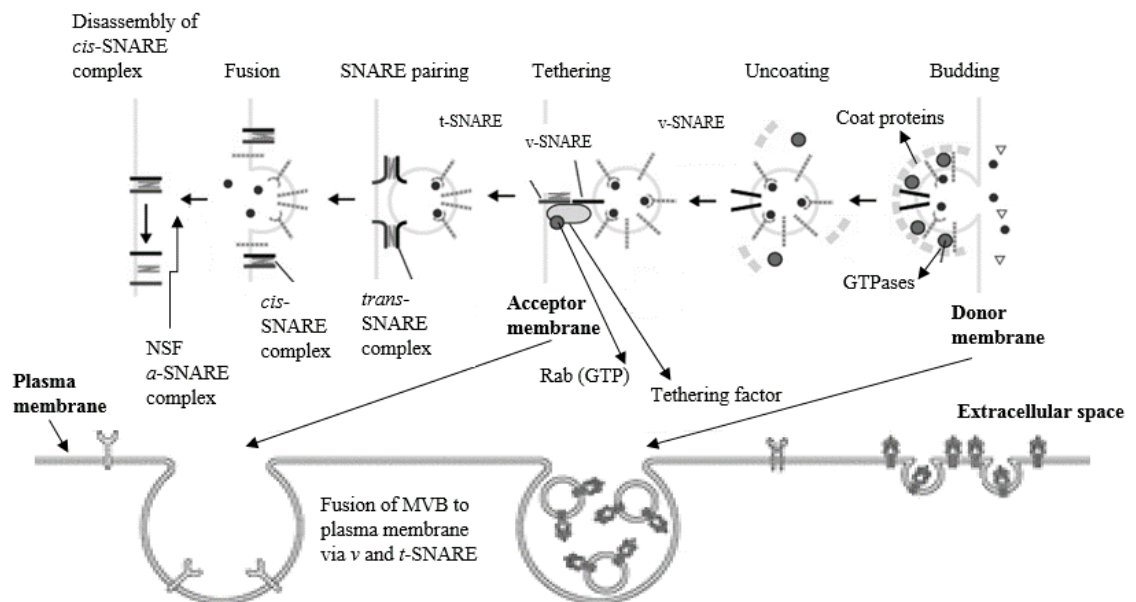


Fig. 1.1.1.2. The SNARE complex. Adopted from Sato, *et al.*, (2005) and modified by Roberta Freezor using online Pixlr photo editor. The portrayal of the various steps involved in the exosome membrane budding and vesicle fusion (general mechanisms) showing the identified molecules. This is where the donor membrane participates in vesicle formation, the process is mediated by GTPases and coat proteins - also involved in sorting of cargo into vesicles. After uncoating, GTPases recruit tethering factors that help *v*-SNAREs on vesicles to join with specific *t*-SNAREs (acceptor membranes-tethering). Subsequently, *v*-SNAREs and *t*-SNAREs are paired, mediating the selective fusion of vesicles with the correct acceptor membrane. The SNARE complexes are detached by NSF and α -SNAP and then recycled (Zhao & Zhang, 2015).

1.1.2 Microvesicles biogenesis and general characteristics

Microvesicles (MV) are another class of EV released from the plasma membrane with cytosolic content instead of internal membranes (exosomes) (Meckes & Raab-Traub, 2011). They are suggested to be larger and more heterogeneous in size in comparison to exosomes, ranging from 100-1000 nm (Sims, *et al.*, 1988; Hind, *et al.*, 2010; György, *et al.*, 2011; Grant, *et al.*, 2011).

The imbalance of the assortment of membrane proteins, the enhancement in cholesterol and diacylglycerol in the membrane asserted to a specific sorting of lipids result in the blebbing of the membrane and the release of MV (Hugel, *et al.*, 2005). The bearing of phosphatidylserine (PS) in the outer leaflet of the membrane is another particular characteristic of MV (Lima, *et al.*, 2009; Sadallah, *et al.*, 2011). This is summarised in Fig 1.1.2.1.

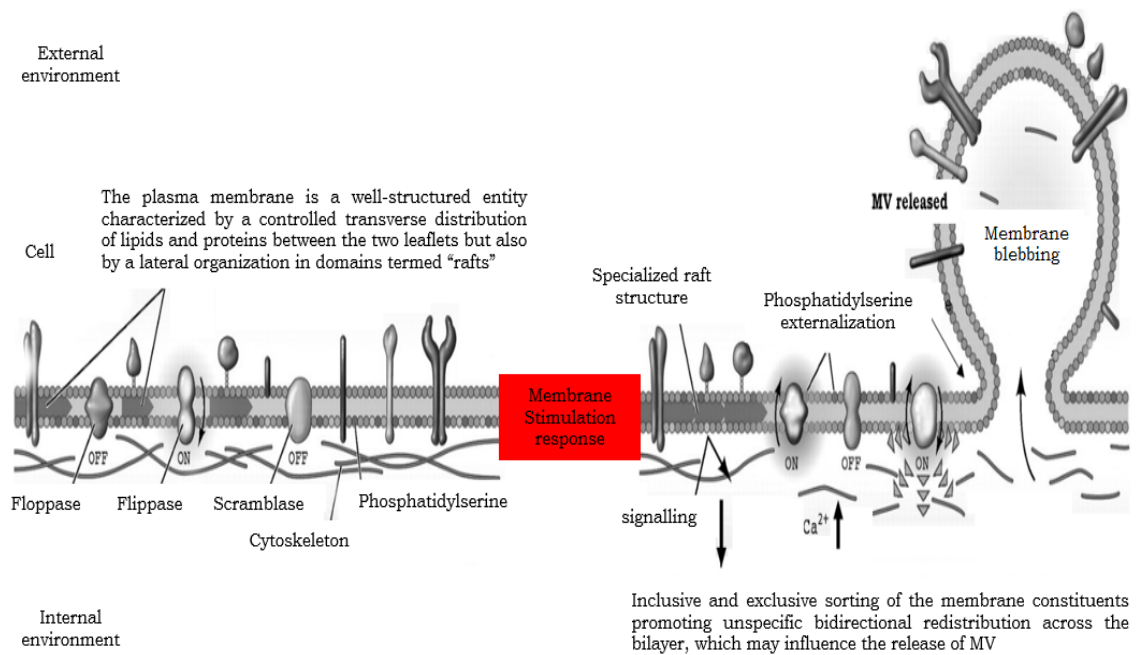


Fig. 1.1.2.1. An example of MV biogenesis in response to cell stimulation. Adopted from Hugel, *et al.*, (2005) and modified by Roberta Freezor using online Pixlr photo editor. The process of MV biogenesis is under the control of three phospholipid pumps: (1) Flippase, an inward-directed pump that is a transmembrane lipid transporter protein responsible for aiding the movement of phospholipid molecules between the two leaflets of the cell membrane (ATPase moves phosphatidylethanolamine and PS from the outer to the cytosolic leaflet); (2) Floppase, an outward-directed pump which uses ATP (ATP-binding cassette known as ABC transporter- moves the phospholipids from the cytosolic to outer leaflet) to transport substrates such as phosphatidylcholine, sphingolipid and cholesterol in opposition concentration gradients in the adverse direction; And (3) a lipid scramblase; which facilitates the movement of lipids along concentration gradients and is responsible for a nonspecific sorting of lipids within the membrane (moves the lipids in either direction, towards equilibrium) (Fadeel & Xue, 2009). These enzymes (flippase, floppase and scramblase) along with translocase (assists in moving other molecules across a membrane usually) and calpain (nonlysosomal, intracellular cysteine calcium-activated neutral proteases) are involved in the microvesiculation process of MV (Piccin, *et al.*, 2007). PS exposure and the presence of transient phospholipid imbalance between the external leaflet at the expense of the inner leaflet gives rise to MV and this is because after cell stimulation, there is a subsequent cytosolic Ca²⁺ increase promoting the loss of the phospholipid asymmetry of the plasma membrane.

It has been suggested that endothelial and circulating blood cells release MV when exposed to distinct induction agents such as complement attack, cell activation, and cell apoptosis (Kriebardis, *et al.*, 2012). Monocyte derived MV can also be induced by bacterial cell wall components, including lipopolysaccharides and platelets MV by activation through thrombin (Xiong, *et al.*, 2012). Also, the inducement of polymorphonuclear cells with N-formyl-methionyl-leucyl-phenylalanine or C5a (protein fragment released from the cleavage of complement component C5) has been observed (Hess, *et al.*, 1999), where with the use of electron microscopy the formation of buds were visualised (diameter of 70-300 nm).

Further evidence of MV release has been demonstrated in microglia cells, where the enzyme acidic sphingomyelinase, is necessary for MV release after Adenosine Triphosphate (ATP) inducement (Bianco, *et al.*, 2009). This acts as a stimulus to secrete MV containing proinflammatory cytokines, which are signalling molecules that are excreted from immune cells including helper T cells and macrophages that promote inflammation (Cruz, *et al.*, 2007). Generally most of the PS and phosphatidylethanolamine are preserved by the active ATP-dependent transport to the cell membrane inner leaflet (translocase) (Connor & Schroit, 1990).

The blockade of the translocase and the activation of Calcium ions (Ca^{2+})-dependent scramblase activities (Zwaal & Schroit, 1997; Sadallah, *et al.*, 2011) cause PS to be externalised to the outer leaflet at the time of cell activation. Also, it is possible that clustering of MV cargo into membrane micro domains drives the MV budding process. This is because the inclusion of membrane targeting motifs to highly oligomeric cytoplasmic proteins has been shown to be sufficient to motivate their secretion from the plasma membrane (Conde-Vancells, *et al.*, 2010).

The examples provided above suggest that different stimuli can differ from one cell to another and that the release of MV from the cell surface is a regulated process (infection, activation, transformation, and stress).

MV have been found to express many of the characteristics of the parent cell, especially membrane components (Camussi, *et al.*, 2010). For example, Sprague, *et al.*, (2008) investigated the ability of platelet MV to communicate activation signals to the B-cell compartment. Their findings demonstrated for the first time that platelet-derived membrane vesicles present CD154, a TNF-related activation protein- expressed on activated human platelets. According to their research, MV alone was sufficient to deliver CD154 to cells which can stimulate antigen-specific IgG production, and modulate germinal centre formation through cooperation with responses elicited by CD4 (+) T cells. Similarly to exosomes, without limitations to the cell membrane and their properties there are no restrictions to their cargo which may be dependent on parent the cell.

Furthermore, MV may also serve as important reservoirs of cytokines, mediators of inflammatory and immune responses (Théry, *et al.*, 2009). In a study by Leroyer, *et al.*, (2008), the direct inducement of endothelial cells with MV associated CD40 ligand suggested that they may aggravate angiogenic responses at the sites of atherosclerosis.

Another example lies on acidic pH which is generally existent in hypo-perfused areas of solid tumours. This might lead to localized splitting of MV and a consequent discharge of their pro-angiogenic and pro-inflammatory load such as vascular endothelial growth factor (Taraboletti, *et al.*, 2006).

1.1.3 Apoptotic bodies

Apoptotic bodies are another subtype of EV, which are larger than exosomes and MV, ranging from 1-5µm in size (Hristov, *et al.*, 2004; György, *et al.*, 2011). Apoptotic bodies have been understudied and this is potentially as a result of them being a by-product of cell death. Nevertheless, they are known to consist of exposed PS and many cellular fragments and organelles, including fragmented Deoxyribonucleic Acid (DNA) (Théry, *et al.*, 2001; Hristov M, *et al.*, 2004).

During apoptosis, EV release occurs in association with blebbing, which is a dynamic redistribution of cellular contents (VanWijk, *et al.*, 2003). The actin cytoskeleton regulates the Rho (Ras Homologous family) Guanosine Triphosphate (GTP)-ases (hydrolase enzymes) (Rho A, B and C), which are intracellular signalling molecules (van Aelst & D'Souza-Schorey, 1997). This is important because Rho proteins exchange Guanosine Diphosphate (GDP) for GTP, transduce signal to the succeeding effector proteins, and decisively retreat to the inactive GDP-bound form by hydrolysing the bound GTP. Two isoforms of serine/threonine kinase, Rho-associated protein kinases (ROCK) I and ROCK II have been identified as effectors of Rho (Liao, *et al.*, 2007).

ROCK proteins attach to and are initiated by GTP-bound Rho and the deletion of the carboxyl-terminal region of ROCK trigger the amino-terminal kinase domain and the initiation of ROCK proteins which assigns to the stabilization of filaments actin, phosphorylation of myosin light chains, myosin ATPase activity and the coupling of actin-myosin filaments to the plasma membrane. These events lead to elevated actin-myosin force generation and cell contractility leading to the release of apoptotic bodies (Fackler & Grosse, 2008; Mitra, *et al.*, 2011). This process is summarised in Fig. 1.1.3.1.

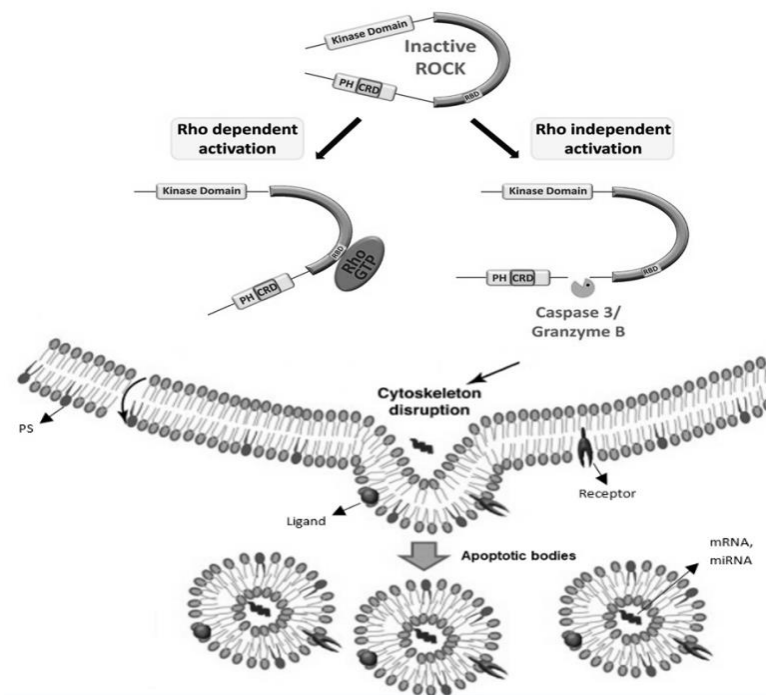


Fig. 1.1.3.1. A basic representation of apoptotic bodies biogenesis. Adopted from Martinez, *et al.*, (2011) and Julian & Olson (2014) and then merged and modified by Roberta Freezor using online Pixlr photo editor. In a variety of cell types, trigger of Rho-associated kinase ROCK I by caspase 3-interposed cleavage intensifies phosphorylation of myosin light chain, which order further actin myosin contraction, membrane blebbing and the formation of apoptotic bodies. The occurrence of apoptotic blebbing has been reported to be dependent on the function of ROCK but not on that of Rho, specifically ROCK I being cleaved during apoptosis by initiated caspases, promoting a truncated kinase with elevated intrinsic activity. This cleaved form of the kinase is satisfactory to promote cell contraction and membrane blebbing without caspase initiation, which is dependable to a direct effect of ROCK-induced cell contractility on the formation of the apoptotic morphology (Coleman, *et al.*, 2001).

Apoptotic bodies have been observed to relocate their load, including oncogenes and DNA, between cells, and have been shown to be important in antigen presentation and immunosuppression (Meckes & Raab-Traub, 2011). A specific example suggested that apoptotic bodies from mature endothelial cells are taken up by endothelial progenitor cells, increasing their number and differentiation state, suggesting that such a mechanism may simplify the adjustment of injured endothelium and may serve as a new signalling pathway between progenitor and injured somatic cells (Hristov M, *et al.*, 2004). Thus, further proving apoptotic bodies to be of biological function and interest, but again a heterogeneous class of EV.

Erythrocytes are probably the only cell type that does not form exosomes. In mature erythrocytes only membrane vesicles may be formed due to their lack of organelles and nucleus. Little is known about the role of these membrane vesicles, therefore, it is important to distinguish, characterise and understand erythrocytes derived EV.

1.2 The importance of erythrocyte in circulation

Originating from stem cells in the bone marrow, human erythroid cells are differentiated through a process named erythropoiesis (controlled by erythropoietin) to become mature erythrocytes (see Fig. 1.2.1). Commonly termed red blood cells for their bright red colour, and accounting for approximately 40-45 percent of human venous blood, they are the most abundant cell type in the blood with a lifespan in the circulatory system of about 100-125 days (Lodish, *et al.*, 2000).

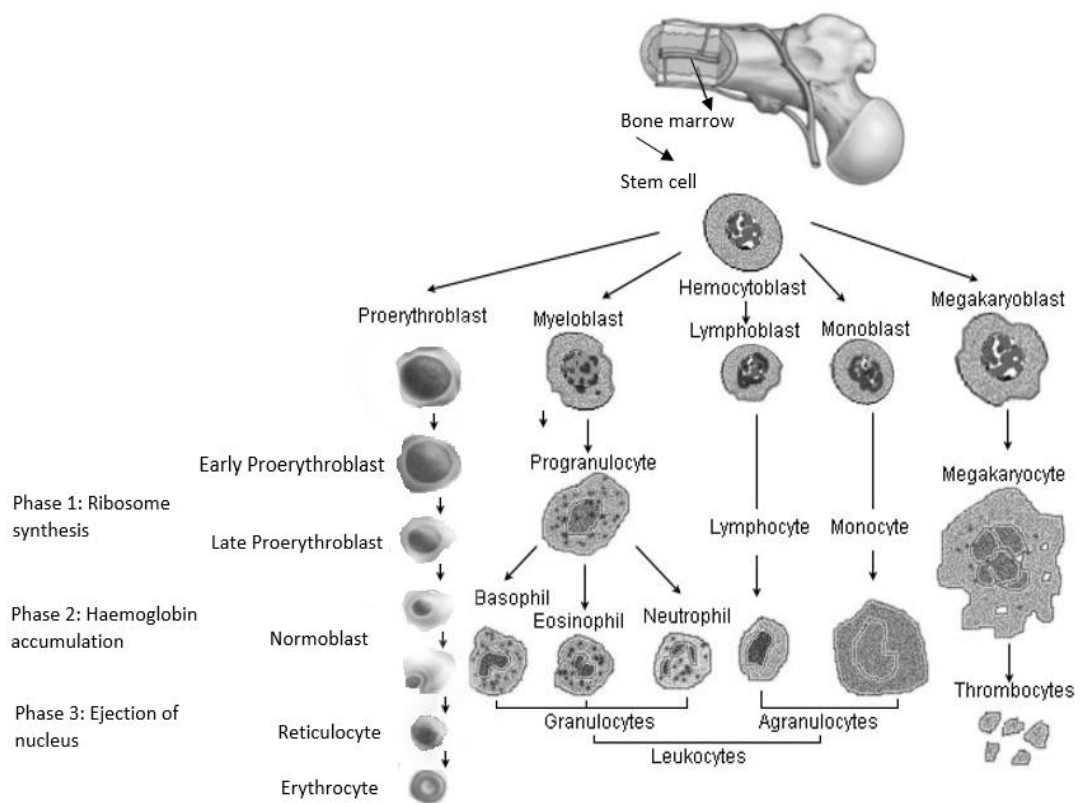


Fig. 1.2.1. Blood cells formation and development. Adopted from SEER training modules (2008), modified and expanded by Roberta Freezor using online Pixlr photo editor. Where, the rate of blood cell production is controlled by the body's needs. The development of erythrocyte (Erythropoiesis) is the process which produces erythrocytes according to the stimulation by less O₂ in circulation, which is recognised by the kidneys that then release the hormone erythropoietin that stimulates proliferation and differentiation of cell precursors. Additionally, the bone marrow yield and discharge more white blood cells (leukocytes) in reaction to infections agents, and it also discharges more platelets (thrombocytes) in response to bleeding.

When arterial blood arrives in peripheral capillaries erythrocytes integrate the narrow capillaries one by one (Hamasaki & Okubo, 1996). This is because mature erythrocytes are approximately 7000 nm and relatively basic and conversely unique due to the lack of organelles and a nucleus. These characteristics allow erythrocytes to easily change their shape, leading to an advantage in flexibility and movement throughout the blood stream.

The dominant cytoplasmic constituent is haemoglobin, which is required for binding and releasing Oxygen (O_2) as well as Carbon Dioxide (CO_2). The CO_2 is immediately hydrated to Carbonic Acid (H_2CO_3) by Carbonic Anhydrase, and the H_2CO_3 rapidly estranges into Hydrogen Ion (H^+) and Bicarbonate (HCO_3^-). Then the leading erythrocyte integral membrane protein Band 3, exchanges the cellular HCO_3^- with Chloride in plasma. Following the anion exchange, H_2CO_3 is converted to a strong acid, Hydrochloric Acid (HCL), and then the intracellular pH becomes acidic which generates for the dissociation of O_2 from oxyhemoglobin (HbO_2). The dissociated O_2 is given to tissues that metabolically generate CO_2 . Then the protons that were formed are accepted by the groups of oxyhemoglobin (HbH^+), and the pH level within erythrocytes is re-established to prevent continuous dissociation of oxygen from HbO_2 generating more CO_2 . CO_2 are provided with more O_2 from HbO_2 in tissues (Hamasaki & Okubo, 1996; Hamasaki & Yamamoto, 2000; Diez-Silva, *et al.*, 2010). Therefore, erythrocytes are essential for optimal homeostasis (Diez-Silva, *et al.*, 2010).

Due to their vital function within the human body, erythrocytes have been studied extensively. Their plasma membrane (De Rosa, *et al.*, 2007), the functions of haemoglobin (Giardina, *et al.*, 1995), their proteome (Kakhniashvili, *et al.*, 2004), and their lipidome (Timperio, *et al.*, 2013) are well documented.

Also, a large part of human iron is embedded in erythrocytes (haemoglobin) and the regulation of iron distribution acts as an innate immune mechanism against invading pathogens (Cassat & Skaar, 2013). The lysis of erythrocytes by bacteria, causes their haemoglobin to release their contained free radicals, which have been suggested to break down the pathogen's cell wall and membrane, leading to pathogen death (Jiang, *et al.*, 2007; Minasyan, 2014). A role in modulating T cell proliferation and survival by enhancing cytokine secretion and induction of the Interleukin 2 Receptors (IL2R) through downregulation of oxidative stress and modulation of $CD4^+/8^+$ (immune system helper and killer cells, that flight against infections) ratios has also been suggested (Fonseca, *et al.*, 2003; Minasyan, 2014).

1.2.1 Erythrocyte derived MV

Erythrocyte derived EV are an extracellular and heterogeneous population of small vesicles released from the plasma membrane of erythrocytes. They have been reported as being smaller (from 100-400 nm) than other MV subtypes (Hind, *et al.*, 2010). Therefore,

considered MV (eMV) due to their general size (100-100 nm) (Borges, *et al.*, 2013). These are the EV type that forms the focus of this PhD research.

Erythrocytes undergo a series of biochemical and physical changes known as storage lesions during the aging process, including lipid and protein oxidation conjointly a reduction in deformability and osmotic stability (Solberg, 1988). The latter results in noticeable haemolysis, with the discharge of free haemoglobin and iron, leading to erythrocytes losing approximately 20 percent of their haemoglobin and membrane surface area over time due to the discharge of MV (Alaarg, *et al.*, 2013).

eMV release has been observed to increase significantly during storage, therefore patients receive large numbers of MV during blood transfusions, which is dependent on the age of the unit (Zecher, *et al.*, 2014). This can lead to the hypothesis of transfused eMV being linked to post blood transfusions adverse events/complications. These may include Posttransfusion purpura, Transfusion-associated graft versus host disease, iron overload, and immune-modulation, including bacterial and viral infection complications. (Sahu, *et al.*, 2014; Bosman, *et al.*, 2008; Dellinger & Anaya, 2004).

MV release has also been observed as significantly lower in pre-menopausal women than in age-matched men in a study comparing age and sex specific differences in blood-borne MV from apparently healthy humans (Gustafson, *et al.*, 2015).

Elevated levels of eMV release have also been associated with numerous diseases, including Paroxysmal Nocturnal Haemoglobinuria (Sloand, *et al.*, 2004), β Thalassaemia intermedia (Habib, *et al.*, 2008), Malaria (Mantel, *et al.*, 2013), Hereditary Haemolytic Anaemia (Alaarg, *et al.*, 2013), and Sickle-cell disease (Kasar, *et al.*, 2014). Their clinical relevance has also been observed (Tissot, *et al.*, 2010) in transfusion complications (Jy, *et al.*, 2011), thrombin generation (Rubin, *et al.*, 2013), cardiovascular complications (Tantawy, *et al.*, 2013) and systemic inflammation by thrombin-dependent activation of complement (Zecher, *et al.*, 2014).

According to Bicalho, *et al.*, (2013), eMV release does not disturb glycerophosphocholine and sphingomyelin erythrocyte membrane organisation. This was observed when erythrocytes and eMV were set side by side to understand the membrane compositional features of out of date blood bank-stored erythrocytes. Their results revealed that phospholipidomics could potentially provide a superior understanding of the eMV release process, suggesting that eMV release may not be such a negative phenomenon to the

erythrocytes. Additionally, it could be suggested that eMV can potentially help to clear certain molecules from the blood flow. This is because of the function of their parent cell, erythrocytes remove particular harmful agents including denatured haemoglobin, C5b-9 complement attack complex, band 3 neo-antigens, and/or immunoglobulin G that accumulates during their lifespan (Willekens, *et al.*, 2008). MV in general contain similar characteristics of those present in their parent cell (see page 8).

Only recently a study of eMV characterisation (Nguyen, *et al.*, 2016) and a summary review of eMV biological roles was reported, suggesting that eMV has a role in oxidative stress, in inflammation, Nitric Oxide (NO) homeostasis, thrombosis and foam cell formation (Harisa, *et al.*, 2017). However, the role of eMV in biological functions is not yet fully understood.

1.2.2 Cellular mechanisms underlying eMV release

The mechanism leading to the release of EV is initiated by an increase in cytosolic Ca^{2+} , which causes enzymatic activation (see Fig. 1.1.2.1). The introduction of Ca^{2+} containing buffer to normal erythrocytes promotes a global and transient rise in free Ca^{2+} concentration of $2\mu\text{M}$ (Bogdanova, *et al.*, 2013). Nevertheless, the concentration decreases in the course of the time until it reaches its resting value, because of the intracellular system maintaining the Ca^{2+} homeostasis (Constantin, *et al.*, 1998).

Erythrocytes are known to shed MV *in vitro* under several other conditions too. For instance, when erythrocytes are depleted of their ATP content by incubation at $37\text{ }^{\circ}\text{C}$ they have been observed to decrease their total ATP, glucose and water content (Nagy, *et al.*, 1998). The depletion of ATP leads to the assumption that they begin to produce MV due to the remodelling of the membrane, and this is because the membrane fluctuations have been ascribed to ATP-dependent phosphorylation of structural proteins associated with the membrane (Levin & Korenstein, 1991). The consequence of strongly buffered energy-driven maintenance of cell integrity has been postulated to be through the dissociation of actin from spectrin at nodes in the cell cytoskeleton, which could contribute to the energy expenditure (Kuchel & Benga, 2005). Also, there is a significant lag period between the depletion of ATP (caused by blocking glycolysis) and gross changes in cell shape which could cause microvesiculation in general and probably even more from ATP-depleted erythrocytes (Lutz & Bogdanova, 2013). This is because ATP is necessary for maintaining cell shape and flexibility, repairing membrane lipids, and energizing

metabolic pumps (Gov & Safran, 2005). The diffusible diacylglycerol partitions into the outer monolayer also contributes to membrane budding (Müller, *et al.*, 1981).

The release of small haemoglobin-containing vesicles from human erythrocytes treated with Ca^{2+} and ionophore A23187 (mobile ion-carrier that forms stable complexes with divalent cations), appears to accelerate membrane fusion events and provides a convenient model system that might be relevant to more general aspects of biological membrane fusion (Bever, *et al.*, 1992). It has been a while since the treatment of erythrocytes with Ca^{2+} -ionophore was suggested to induce a large variety of concomitant biochemical changes, including calcium influx (Allan, *et al.*, 1976). The breakdown of polyphosphoinositide's (phosphatidylinositol 4-phosphate + phosphatidylinositol 4,5-bis-phosphate) with a consequent rise in 1,2-diacylglycerol and phosphatidate concentrations can cause several alterations in membrane polypeptide pattern. The aggregation of protein components catalysed by transamidase, the conversion of polypeptide 2.1 molecular weight about 200kDa into lower-molecular-weight components, especially polypeptide 2.3 (~175kDa) and the probable proteolysis of polypeptide 4.1 (~78kDa) increase the intracellular free Ca^{2+} levels (Allan & Thomas, 1981).

Bever, *et al.*, (1992), suggested that calcium influx initiates a variety of cellular responses. For example, in blood platelets and erythrocytes, these responses include marked shape changes with evagination of the cell surface and the shedding of MV. The formation of MV indicated to involve fusion between opposing segments of the plasma membrane and may be accompanied by a local collapse of the normal asymmetric distribution of plasma membrane phospholipids'. Particularly if the aminophospholipid translocase, which restores phospholipid asymmetry by specifically translocating phosphatidylserine and other aminophospho-lipids to the membrane inner leaflet is inhibited.

Furthermore, Antibody-Antigen binding could induce the disruption of membrane organisation in erythrocytes (Zimring, *et al.*, 2005; Powers, *et al.*, 2007), and therefore may cause microvesiculation (Canellini, *et al.*, 2012). The complement activity (attack) is due to the antibody-mediated or otherwise initiated activation of the complement cascade, and the presence of complement factors such as C5b-9 MAC can stimulate the release of MV (Hamilton, *et al.*, 1990).

The complement system is a 'key player' in inflammatory responses (antibodies attachment to a specific antigen). It provides recognition, warning signals and the initial fast response upon exposure to foreign organisms. Comprised of three activation pathways (Classical, Alternative and Lectin), it culminates in the formation of the convertases, which in turn generate the major effectors of the complement system including Opsonins (C3b, iC3b, and C3d), anaphylatoxins (C3a and C5a), and Membrane Attack Complex (MAC- C5b through C9) (Dunkelberger & Song, 2010) (see Appendix I).

Landsteiner's "law" explains that the reactions between the erythrocytes and serum are related to the presence of markers (antigens) on the erythrocytes and antibodies in the serum, postulating that two different antigens (A and B) are found on the surface of erythrocytes. The "naturally occurring" antibodies against these antigens are found in the plasma of individuals. Erythrocytes of a particular person hold antigens on their surfaces that correlate to their blood group, and antibodies in the serum that recognise and integrate with the antigen sites. Naturally occurring antibodies are therefore a result of immunisation; the manufacture of antibodies in response to an antigen. (Landsteiner & Donath, 1904; Schwarz & Dorner, 2003; Berkman & Lawler, 2018).

Spalter, *et al*, (1999) suggested that Normal Human Serum (NHS) contains naturally occurring antibodies and therefore complement when IgM and IgG antibodies reactive with autologous blood group antigens were present in the immunoglobulin (Ig) fraction of NHS. That is because natural IgG anti-A antibodies purified from IgG of individuals of blood group A exhibited an affinity for A trisaccharide antigen. Therefore, it is reasonable to speculate that NHS may be used as an inducer for microvesiculation in erythrocytes (Canellini, *et al.*, 2012).

In contrast to erythrocytes, general viral derived EV have been extensively studied. It is well understood that viral-EV use the virus mechanism of entry to communicate with and enter neighbouring cells (receptor-mediated endocytosis), and it is well known that viral infection also induces the release of EV (Meckes Jr, 2015; van Dongen, *et al.*, 2016). Whereas with eMV such a mechanism is still not understood. Nevertheless, there have not been any reported articles that analyse MV release from Human Rhinoviruses type 16 (HRV16) infection, thus HRV16 is the HRV type used for this research as a parallel sample for all experiments.

1.3 Introduction to Human Rhinovirus

Human Rhinoviruses (HRV) are prevalent respiratory pathogens related with mild and self-limited upper respiratory tract infections. They are understood to be associated with the exacerbation of respiratory diseases such as asthma and chronic obstructive pulmonary disease (Khetsuriani, *et al.*, 2008), and are answerable for serious disease manifestations such as bronchiolitis in young children and the immunosuppressed (Miller, *et al.*, 2007).

HRVs are responsible for more than 50 % of upper respiratory tract infections and it is considered to be the common cold that commonly fades away within seven days. The symptoms usually include nasal stuffiness, sneezing, coughing, and a sore throat but about 12–32 % of HRV infections in children of less than 4 years of age are asymptomatic (Jacobs, *et al.*, 2013). A variety of polymorphisms in cytokine genes have been shown to impact the severity of HRV infection, implying a genetic predisposition (Tregoning & Schwarze, 2010).

Up to date, only palliative (drugs without side effects will be accepted by otherwise healthy patients) treatment is offered, and vaccination as well as approved antivirals are still not available (Blaas & Fuchs, 2016), despite HRVs being seemingly the world's most causative factor of respiratory diseases.

HRVs are unusually disinclined transmitters, infecting about 50% those of susceptible in family environments (including day care and the home). Peltola, *et al.*, (2008), suggested that HRV are spread mainly by aerosol, rather than by fomites or personal contact because it requires close contacts between virus donors and recipients. Rhinoviral infection of a minuscule fraction of airway epithelial cells motivates the creation of an array of cytokines and chemokines, which leads to the enrolment of immune cells to the airways and increases airway inflammation (Stokes, *et al.*, 2011).

Numerous serotypes exist and molecular methods have described more than 150 complete or partial genome sequences of all known HRV, that have been published (Fuchs & Blaas, 2012; McIntyre, *et al.*, 2013).

Phylogenetic analyses have grouped HRV into three species:

1. HRV-A;
2. HRV-B; and

3. HRV-C.

HRV can be divided into major (HRV-A) or minor (HRV-B) group strains. The division is determined by their recognition via Intercellular Adhesion Molecule-1 (ICAM-1) or the Low-Density Lipoprotein (LDL) receptor (Fuchs & Blaas, 2012). The newest and most distinct group of HRV (HRV-C), has been suggested to use human cadherin-related family member 3, a transmembrane protein that enables HRV-C binding and replication in normally unsusceptible host cells (Bochkov, *et al.*, 2015).

HRV are non-enveloped, single-stranded RNA (ssRNA) with a (+) RNA genome, of approximately 7100 base viruses that belong to the *Picornaviridae* family, genus *Enterovirus*. They are composed of 60 copies, each of four polyomavirus (natural hosts are primarily mammals and birds) capsid proteins. Viral Protein (VP) 1, VP2, VP3, and the small myristoylated (lipidation modification) VP4 are arranged on an icosahedral (30 nm in diameter) triangulation number 1, and lattice point 3 (Harutyunyan, *et al.*, 2013). The VP1, VP2, and VP3 proteins elucidate the virus antigenic distinctiveness, whereas VP4 anchors the RNA core to the capsid. Each of the four capsid proteins has 60 copies, which contributes to the virion an icosahedral structure, with a canyon in VP1 that acts as the site of attachment to cell surface receptors for the major group through ICAM-1 only (Jacobs, *et al.*, 2013).

Virus uptake occurs via clathrin-dependent, independent endocytosis or micropinocytosis, which is dependent upon the receptor type. This is where the virions experience conformational changes and promote hydrophobic subviral particles, an action that is originated by ICAM-1 (major group) and/or the low-pH environment in endosomes (Blaas & Fuchs, 2016). The RNA genome passes through the endosome membrane into the cytosol via a pore organised by viral proteins or succeeding membrane rupture. While in the cytosol, the host cell ribosome translates the positive-sense, single-stranded RNA into a polyprotein that is refined into its assorted components. The decrease in pH promotes viral uncoating (first stages of the viral replication cycle- transcription) (Fuchs & Blaas, 2010).

Negative-strand (parental) RNA is replicated along as being translated into structural (capsid) and non-structural proteins. The virion is then assembled and confined before cellular export via cell lysis takes place (Jacobs, *et al.*, 2013). The viral double-stranded RNA (dsRNA) formed at the time of HRV replication is identified by the host pattern

recognition receptor, called the Toll-like receptor 3, along with melanoma differentiation-associated gene 5 and retinoic acid-inducible gene I (Kato, *et al.*, 2008; Wang, *et al.*, 2009).

1.3.1 Viral-derived MV

Belonging to group A, HRV16 uses the receptor Intercellular Adhesion Molecule (ICAM) 1 to enter cells and are referred to as the major group (Palmenberg, *et al.*, 2009; Oliveira, *et al.*, 1993). The release of exosomes and MV has been observed in many viral infections including Epstein-Barr virus, Herpes simplex virus (HSV), Human Immunodeficiency Virus (HIV) Retroviruses, Hepatitis B virus and poxviruses and Hepatitis C virus (HCV) (Meckes & Raab-Traub, 2011), but not in HRV16 infection to date.

There are a vast amount of studies demonstrating EV discharge from viral infected cells harbour and distribute regulatory factors to recipient cells (Robbins & Morelli, 2014). These include viral RNA and proteins, viral and cellular miRNA, as well as host functional genetic elements to nearby cells. This leads to production of infections particles and modulating cellular responses including the spread or limitation of infection conditional on the type of pathogen and target cells. EV have been exploited as candidates for the development of antiviral or vaccine treatments (Chahar, *et al.*, 2015), showing the potential of MV derived from viral infection.

The study of MV secretion during viral infection is complex because of their similarity in size and the density of EV and infectious viral particles, making it a challenge to tell them apart. For example, HIV particles have biophysical properties indistinguishable to exosomes secreted from the same cells. Including size similarity because they are approximately 100 nm, have a buoyant density of 1.13 to 1.21 g/L, and functional effects on immune cell activation (Wang, *et al.*, 1999; Cantin, *et al.*, 2008). HRV16 on the other hand is approximately 30 nm and much smaller than MV and has no lipid envelope (Tuthill, *et al.*, 2010) like HIV, they may therefore be considered to be separated entities.

MV have been found to be beneficial either to the host cell or to the infectious agent via the packaging and transfer of functional proteins, messenger RNA/miRNA, and other cytosolic components, (Manjunath, *et al.*, 2009). Virally infected cells have been proven to be advantageous to exemplify the role of microvesiculation in intercellular communication (Wurdinger, *et al.*, 2012).

All types of viruses retain individual properties that allow protection from immune attack. Wurdinger, *et al.*, (2012), outlined the influential immune modulatory steps involved in virus-induced MV arrangement and release during different viral infections. According to their review report in accordance with other studies (De Gassart, *et al.*, 2009; Klibi, *et al.*, 2009), the conservancy of the virus relies on MV release of infected cells.

MV released by infected cells consist of particular components of the cell and the virus, including some that may promote the capability of virions to remain in an unfavourable antiviral immune environment. Intercellular processes are well orchestrated and it depends on the virus type and their viral cycle to produce specific cellular and immune outcomes. These highlight some aspects of EV that are hijacked by viruses (enveloped) to assist in their spread or avoidance of the immune system (Wurdinger, *et al.*, 2012).

HSV for example, targets the MHCII molecule processing pathway by viral envelope glycoprotein (GP) B. The antigen-presenting cells consistently organise the MHCII surface receptor human leukocyte antigen to MHCII compartments for presenting peptide antigens to the immune system, to elicit or suppress T-helper cell reaction that encourages B-cell generation of antigen-specific antibodies (Temme, *et al.*, 2010). MV containing viral tegument proteins and GP's, can prime nearby cells for beneficial infection and lessen immune recognition. This demonstrate their potential of evading the host immune system (Wurdinger, *et al.*, 2012).

In relation to HRV16 (*enterovirus*- non envelope), there may be numerous hypothesis (not the aim of this PhD study) including that it may use the viral RNA synthesis, protein translation, protein processing and the general intracellular localisation of viral proteins. This may be embedded in MV to disrupt host-cell functions including nucleo-cytoplasmic trafficking because this was demonstrated in HRV infected HeLa cells (Amineva, *et al.*, 2011).

Furthermore, Walker, *et al.*, (2016) suggested that the HRV16 genome encodes two proteases specifically, 2A and 3C as well as a precursor protease, 3CD. These proteases are necessary for adequate virus replication, for the precise localisation of proteins during infection and for the temporal regulation of 2A and 3CD/3C protease activities during HRV16 infection. Therefore, these proteases may be hypothesised to be embedded in MV because MV generally express some of the characteristics of their parent cell, suggesting

that MV derived from HRV16 infected cells could potentially be hijacked by the virus to spread infection.

Indeed, EV derived from viral infection do not replicate as an independent entity. They can however facilitate the movement of infectious material through tissues and may be the cause of pathologies resulting from the infection (Lagana, *et al.*, 2013; Schwab, *et al.*, 2015).

Pegtel, *et al.*, (2010) suggested that viral particles can enter monocyte-derived dendritic cells using EV to safely spread their miRNAs. This is because MV are undetected by the immune system, resulting in the undetected miRNAs of non-host origin facilitating the rapid spread of the virus, using the exosomes/MV to transport viral miRNAs. Additionally, MV and exosomes have been observed to be increased in HIV-1–infected Monocyte-derived macrophages, showing that EV derived from viral infection not only serves as a model for cell to cell communication but also serves as an inducer for microvesiculation (Kadiu, *et al.*, 2012).

1.4 Cellular mechanism processes involved in EV uptake

A variety of mechanisms for EV uptake have been proposed during the past few decades including receptor-mediated endocytosis, phagocytosis, macropinocytosis, and plasma or endosomal membrane fusion. These mechanisms have been summarised by Mulcahy, *et al.*, (2014) in their review article. Endocytosis is the action of capturing a substance or particle from outside the cell by swallowing it up. This occurs when the membrane folds over the substance and it becomes utterly confined by the membrane and the membrane-bound sac (vesicles) compresses and the substance is then moved into the cytosol. The three main subtypes of endocytosis are summarised in Fig. 1.4.1.

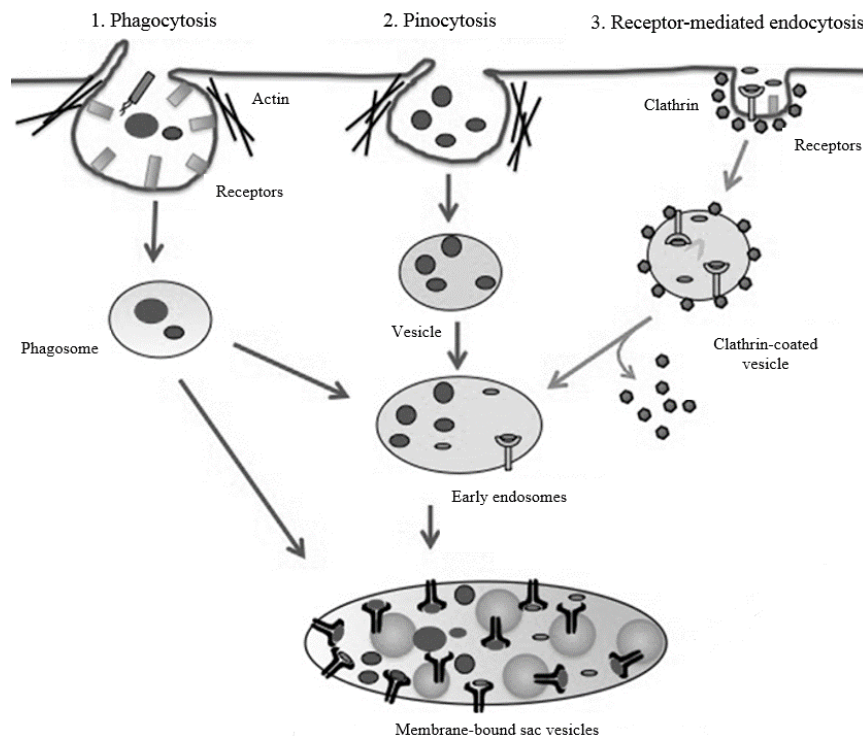


Fig. 1.4.1. The three main subtypes of endocytosis. Adopted from Zhenzhen & Roche (2015) and adapted by Roberta Freezor using online Pixlr photo editor. An example showing the three main types of endocytosis in dendritic cells. Where 1. Phagocytosis represents cellular eating - plasma membrane engulfs the solid material and unambiguous association with the internalised material is not necessary, it comprises the internalisation of specific crude matter, such as bacteria and fragments of apoptotic cells. This is a receptor-mediated event that engages the progressive arrangement of invaginations nearby the molecules intended for internalisation, independently of the cooperation of enveloping membrane extensions (Doherty & McMahon, 2009). 2. Pinocytosis (engulfs vesicles) represents cellular drinking - membrane bend inward to design a channel granting dissolved substances entry to the cell. The disarranged extensions of the plasma membrane extend beyond cell surface and envelop an area of extracellular fluid, which is then internalised completely, due to the blending of the membrane projections amongst themselves or back with the plasma membrane (Swanson, 2008). And 3. Receptor-mediated endocytosis, where a particular receptor on the cell surface binds securely to the extracellular macromolecule (the ligand) - the plasma membrane domain accommodating the receptor-ligand complex then under goes endocytosis, becoming a transport vesicle. This process comprise the arrangement of particular membrane patches called pits, which are determined by the presence of the cytosolic protein clathrin (Alberts, *et al.*, 2002).

There has been evidence suggesting that EV are consumed into endosomal compartments through endocytosis (Morelli, *et al.*, 2004). Uptake of EV have been considered to be fast, being pinpointed inside cells from as soon as 15 minutes after initial admittance (Feng, *et al.*, 2010). Several studies have demonstrated that when cells are incubated at 4°C, their potential to internalise EV is quantitatively reduced. Thus suggesting that the uptake is an energy-requiring process, that might be affected by the decreased fluidity of the lipid layer at lower temperatures, as the fatty acid tails of the phospholipids become more rigid at cold temperatures and that the process requires a functioning cytoskeleton, both of which are indicative of endocytic pathways (Escrevente, *et al.*, 2011; Tian, *et al.*, 2013).

It has been suggested that the fusion of the EV with the cell plasma membrane (lipid bilayers are carried into close concurrence and the outer-leaflets come into absolute association), leads to the creation of a hemi-fusion stalk with fused outer-leaflets. The stalk expansion creates the hemi-fusion diaphragm bilayer from which a fusion pore opens and as a result, the two hydrophobic cores mix, creating one steady structure with the collaboration of a variety of protein families including SNAREs, Rab proteins, and Sec1/Munc-18 related proteins (Valapala & Vishwanatha, 2011).

Parolini, *et al.*, (2009), demonstrated EV fusion by showing diffusion of lipids in the membrane of recipient cells, explaining how EV could release their internal content into the cytosol of recipient cells through lipid interaction (Kosaka, *et al.*, 2010). It also revealed significant EV involvement in physiological processes such as immunomodulation, inflammation, coagulation, and intercellular communication (Distler, *et al.*, 2005; Tissot, *et al.*, 2010; Théry, 2011; Fleissner, *et al.*, 2012).

Each case presented above, indicates that bioactive ligands disclosed on the MV surface are believed to be answerable for a variety of regulatory processes that may change recipient cells random circulation of MV in tissue and body fluids, or even by directional uptake of MV based mechanisms. Nevertheless, further studies are necessary in order to fully understand these mechanisms, especially when considering EV heterogeneity.

1.5 The potential biological interaction between MV and neighbouring cells

MV have demonstrated characteristics of delivering molecular signals using lipids, proteins, nucleic acids, and/or functional transmembrane proteins that are the same as in the parent cell. This is through interaction with surrounding cells, mimicking the characteristics of a long-distance cell-cell communicator (Ardoin & Pisetsky, 2008; Bruno, *et al.*, 2009).

Generally, during cell communication, the signalling cell discharges a distinct signalling molecule that is then recognized by the target cell, which may lead to cleavage by receptor molecules, internalisation and cellular responses. An example of the three general stages of cell signalling is summarised in Fig. 1.5.1.

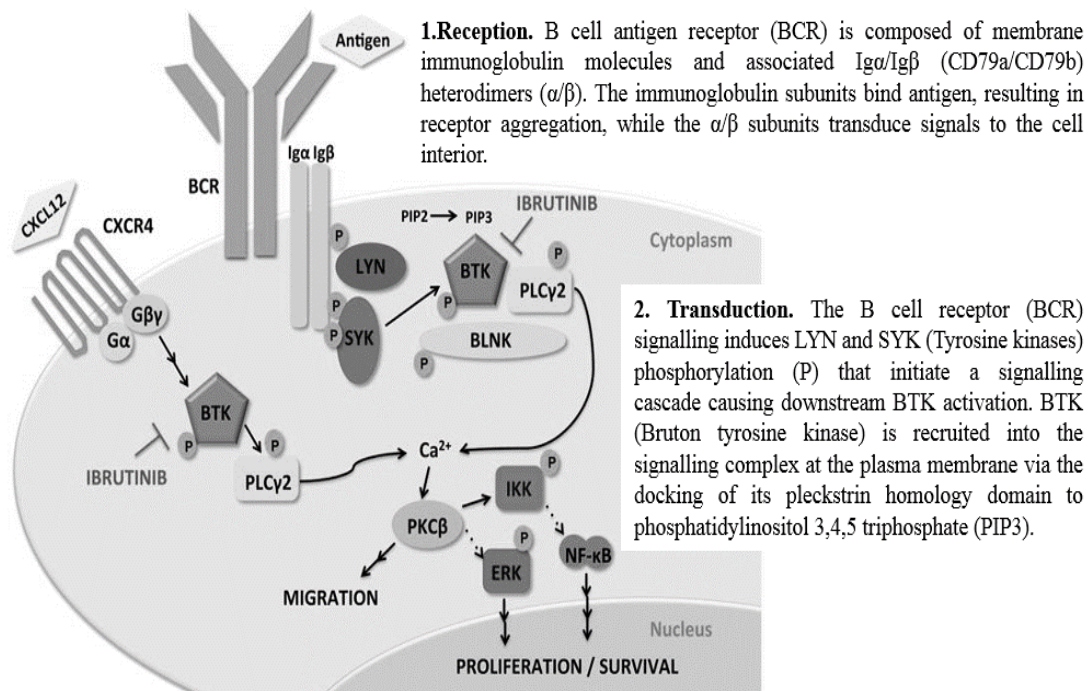


Fig.1.5.1. A representation of the three general stages of cell communication and signalling in Hairy cell leukaemia. Adopted from Sivina, *et al.*, (2014) and adapted by Roberta Freezor using online Pixlr photo editor. Where (1) represents the target cell detecting a signalling molecule present in the exogenous environment (a signal molecule-ligand) which binds to a receptor protein (receptor), compelling it to change shape. (2) where the conversion of the signal to a configuration that can generate a particular cellular response (the cascades of molecular interactions broadcast signals from receptors target the molecules in the cell) and (3) where the particular cellular effect generated by the signalling molecule reacts and the cell signalling advances to the regulation of transcription or cytoplasmic activities including protein synthesis by switching particular genes on or off within the nucleus.

A challenge for the EV field is understanding how EV may reinforce physiological and pathophysiological processes while being able to exhibit EV transferring material among cells. EV and cell interactions have been suggested as occurring locally, regionally or systemically via lymph and blood vessels (Cocucci, *et al.*, 2009; Castellana, *et al.*, 2010; Swartz & Lund, 2012; Lee, *et al.*, 2011). They are often external by nature, as a result of straightforward surface-to-surface interaction and stimulation between the target cell and the EV surface. This lead to the assumption that EV may act via surface interactions with receptor molecules on target cells, or act as delivery vectors by directly transferring their contents, including RNA (Diehl, *et al.*, 2012), bioactive lipids, and proteins into the recipient cell (Watanabe, *et al.*, 2003; Cardo, *et al.*, 2008).

The cargo of MV have been demonstrated to be active in recipient cells, and are not just a means for the removal of cellular waste (Thebaud & Stewart, 2012), and can either be internalised or be cleaved at the cell surface where they remain (Robbins & Morelli, 2014). The protein architecture of EV may regulate their performance in different manners. Surface-exposed receptors and ligands are answerable for dissemination, for the cleavage of EV to target cells or to the extracellular matrix. This is where EV may invoke intracellular signalling pathways through a simple intercommutation with the surface receptors or ligands of target cells or by going through internalisation (Yáñez-Mó, *et al.*, 2015).

EV interaction with target cells may be dependent on the recipient cells and its ability may be dependent on the phagocytic capabilities of the recipient cell in general (Feng, *et al.*, 2010). Whereas with viral-EV in particular, ESCRT components have been observed as being recruited to the site of budding, leading to the development of the “Trojan exosome hypothesis”. This hypothesizes that retroviruses have adapted to use host exosome machinery for the arrangement and transfer of virions by a non-viral route, but retrovirus-directed transmission. This is with the particular lipid composition of retroviral particles, the host cell proteins existent in retroviral particles, the complex cell biology of retroviral discharge, and the skill of retroviruses to infect cells free of envelope protein–receptor interactions (Gould, *et al.*, 2003).

1.6 EV in circulation

Previous studies have shown that purified exogenous EV, artificially introduced into circulation, is rapid. For example, biotinylated rabbit EV demonstrated rapid clearance in rabbit circulation, in approximately 10 minutes (Rand, *et al.*, 2006). Other examples were observed in EV from splenocyte supernatants (Saunderson, *et al.*, 2014) eMV (Willekens, *et al.*, 2005) and EV from B16 melanoma cells (Takahashi, *et al.*, 2013) all of which showed a clearance of more than 90% after 30 minutes (Yáñez-Mó, *et al.*, 2015). But human platelet concentrate-derived EV persisted in the circulation for 5 ½ hours (Rank, *et al.*, 2011).

EV derived from human monocyte-derived dendritic cells and cells of B lymphocyte cells may be able to protect themselves from complement-mediated lysis because they express GPI-anchored CD55 and CD59. EV removal from circulation may be due to storage and apprehension in target organs (Clayton, *et al.*, 2003). Indeed, a

biodistribution study with eMV showed an uptake by the liver (44.9%), bones (22.5%), skin (9.7%), muscles (5.8%), spleen (3.4%), kidneys (2.7%) and lungs (1.8%) (Willekens, *et al.*, 2005).

An extensive example of in EV in circulation was demonstrated by Lai, *et al.*, (2014), in which Human embryonic kidney (HEK) 293T cells transduced with lentivirus vectors were investigated. Engineered EV displayed a supremely delicate and adaptable membrane system reporter named EV-GlucB (*Gaussia* luciferase- Gluc fused to a biotin acceptor domain, a metabolically biotinylated in mammalian cells in the existence of biotin ligase). Fluorescence-mediated tomography was used to identify and record the circulation of intravenously administered EV *in vivo* labelled with streptavidin-Alexa680 conjugate, and EV-GlucB with Phosphate Buffered Saline (PBS; control) were injected into athymic nude mice. After 30 minutes of coelenterazine injection of EV-GlucB-injected, mice showed a significant amount of Gluc signal in the spleen and liver. No signal was observed in the control mice. EV signal depreciated by more than half from 30 to 60 minutes in the liver and the kidneys, while, the spleen and the lungs levels stayed relatively steady. Then at 360 minutes, the spleen and the heart showed the most EV signal (spleen 22.4 %; heart 9 % of initial levels), while the lungs showed 4 %, the liver 1.3 % and the kidneys showed 0.6 %. The brain indicated the least EV distribution, showing signal only at 120 minutes and the muscle retained a significant fraction of activity (9 %) out to 120 minutes.

Even though a particular mechanism for EV distribution is not yet fully elucidated, the examples presented above, suggest that the bio distribution of EV may be dependent on the parent cell source, as well as the ability of different target cell types to internalise the circulating EV. To further support this statement, EV from distinct parent cells may show divergent innate homing capabilities *in vivo*. An observation of the bio distribution of EV derived from 3 different mouse cell sources, including a muscle cell line (C2C12), a melanoma cell line (B16F10), and primary immature bone marrow-derived DC was conducted to compare intrinsic tropisms (Wiklander, *et al.*, 2015). Where, C2C12-derived EV displayed 71% liver accumulation compared to B16F10-EVs (56%) and DC-derived EVs (46%). The lung accumulation was 5% for C2C12-EVs, 13% B16F10-EV and 10% in DC-EV. In the gastrointestinal tract B16F10-EV accumulated 15%, C2C12-EVs (8%) and DC-EVs (10%). Furthermore, DC-EV demonstrated elevated accumulation in the spleen (28%) in comparison to EV derived from C2C12-EVs and B16F10-EV, which displayed similar splenic distribution (both 12%).

Despite substantial progress in this field, the complexity and challenges associated with EV research remain considerable. EV released from different cell types and even from a single cell type are heterogeneous in size and composition.

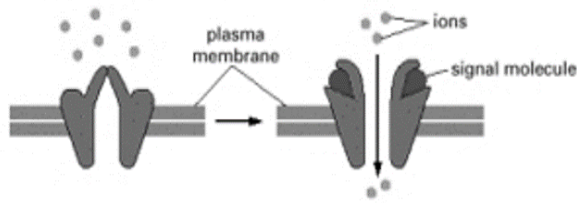
1.7 EV as delivery vehicles/vectors

EV are potentially unique in terms of functioning as natural delivery vectors because they can be seen as free, membrane coated, relatively stable entities due to the lipid content of their membranes, specially exosomes (Record, *et al.*, 2014) that may be involved in cell communication within the extracellular space through ligand-receptor interactions. EV surface molecules are of particular interest as biomarkers because surface molecules in general (cells) perform essential biological functions, including the mediation of cell communication and reply to external signals (see chapter 1.5).

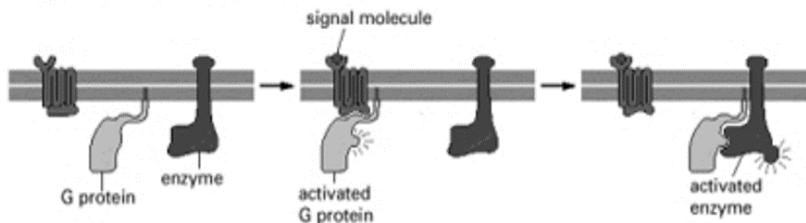
The cell “surfaceome” specifies phenotypic and practical diversity between cell types, and between normal and abnormal cells, such as cancer cells (Mirkowska, *et al.*, 2013). There are three main classes of cell-surface receptors, that can transduce extracellular signals in different ways and this is summarised in Fig. 1.7.1.

Target cells may use a range of intracellular mechanisms to react to an increasing concentration of an extracellular signal or to change a short-lasting signal into a long-lasting reaction. They may often reversibly accommodate their sensitivity to a signal to allow the cells to react to changes in the concentration of a specific signal molecule, across a variety of concentrations (Alberts, *et al.*, 2014).

1. Ion-channel linked receptors



2. G-protein-linked receptors



3. Enzyme-linked receptors

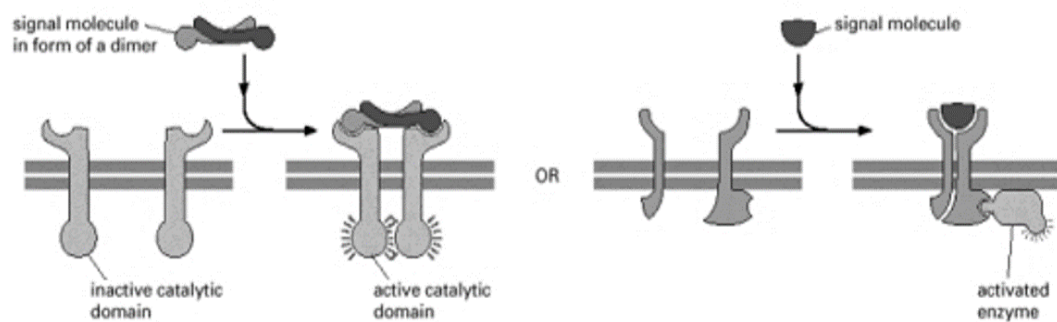


Fig. 1.7.1. The three main classes of cell surface receptors. Adopted from Alberts, *et al.*, (2002) and slightly modified by Roberta Freezor using online Pixlr photo editor. Where (1), the Ion-channel-linked receptors are transmitter-gated ion channels that give or block access briefly in return to the binding of a neurotransmitter; (2) G-protein-linked receptors discursively trigger or block plasma-membrane-bound enzymes or ion channels via trimeric GTP-binding proteins (G proteins); and (3) Enzyme-linked receptors can operate precisely as enzymes or are associated with enzymes. They are generally protein kinases that phosphorylate particular proteins in the target cell, and the functional signalling complexes are often assembled using modular binding domains (one or more domain binding to the same ligand) in the signalling proteins (Pawson, *et al.*, 2002). These domains allow different protein assemblies to function in signalling networks (Alberts, *et al.*, 2014).

Despite their seemingly homogeneous characteristics, EV surface composition carries various membrane lipids, such as the anionic phospholipid phosphatidylserine and altered membrane lipids besides transmembrane proteins (Wang, *et al.*, 2014). MV surface also exhibits antigens that are particular for the membranous elements of the cell of origin (Liu, *et al.*, 2016) making them heterogeneous.

It has also been suggested that surface receptors can potentially alter the cell function that interact with the MV. For example, MV transfer using Glycosyl phosphatidylinositol (GPI)-anchored proteins (peripheral membrane proteins tethered to the cell through a lipid anchor- alpha subunits of heterotrimeric GTP binding proteins-G proteins) CD55 and CD59 to erythrocytes can correct paroxysmal nocturnal

haemoglobinuria by inhibiting complement-mediated erythrocytes (Sloand, *et al.*, 2004). Additionally, CD24 (GPI-linked protein) cell surface receptor has been shown to promote apoptosis in developing B cells and induces B cells to release MV (presenting CD24) (Ayre, *et al.*, 2015).

EV have been demonstrated as having important physiognomy for intracellular delivery (specificity and selectivity), and compelling characteristics for the systemic delivery of experimental agents. For example, Sun, *et al.*, (2010) tested EV for the delivery of anti-inflammatory agents including curcumin (a substance in turmeric) via the Lipopolysaccharide -induced septic shock model (mouse) into activated myeloid cells *in vivo*. This is where the target specificity was selected by exosomes, and the advancement of curcumin activity was accomplished by conducting curcumin to inflammatory cells affiliated with therapeutic, but not toxic effects.

In addition to MV potential role in interacting with cell surface receptors and markers as well as, in directly stimulating target cells, their potential role in transferring bioactive molecules present inside MV (cargo) has been investigated intensively for the past decade. This is due to their possibly most important potential function, that is their biological effect on neighbouring cells (Collino, *et al.*, 2010; Ratajczak & Ratajczak, 2016).

It has become progressively clearer that a large class of small noncoding RNAs (ncRNAs) function as important regulators of a wide range of cellular processes, modulating gene expression (van Rooij, 2011). These classes include small interference RNAs (siRNAs), micro RNAs (miRNAs), repeat-associated siRNAs (rasiRNAs) and piwi (P-element induced wimpy testis) interacting RNAs (piRNAs). Small RNAs act as repressors of gene expression in plants, animals and many fungi (Finnegan & Matzke, 2003). Different sequence and/or structural elements in the precursor transcripts of small RNAs engage RNA-processing enzymes and proteins which are accountable for small RNA maturation, and for the subsequent congregation of these RNAs into effector complexes that reveal their function (Ruby, *et al.*, 2007; Farazi, *et al.*, 2008).

Valadi, *et al.*, (2007) demonstrated that EV contain and transfer genetic information, in the form of messenger RNAs (mRNAs) and non-coding RNAs (miRNAs), between mast cells regulating protein expression of recipient cells. EV transference of intact, functional mRNAs to recipient cells was also accomplished by studying the treatment of murine bone marrow mononuclear cells with embryonic stem cell-derived EV enriched in Oct4 mRNA. This led to the enhancement of Oct4 protein expression in the bone marrow cells,

while pre-treating the EV with RNase abrogated this effect (Ratajczak, *et al.*, 2006). Endothelial progenitor cell-derived EV have also been demonstrated as transferring functional mRNAs to microvascular endothelial cells, thus triggering neoangiogenesis (Deregibus, *et al.*, 2007).

The remarkable stability of extracellular miRNAs is hypothesised by the formation of miRNA-vesicle package, MV directly packing miRNAs by forming a protrusion and then detaching from the cell surface (Muralidharan-Chari, *et al.*, 2009). They can easily translocate across the cell membrane, which easily facilitates miRNA entry into recipient cells and mediates cell-to-cell communication (Hunter, *et al.*, 2008).

The understanding that EV might function as a vehicle/vector to transfer genetic information and are able to regulate gene expression in target cell opened up a completely new field of research regarding intercellular communication mechanisms. Currently, there is increasing evidence that the effect of EV on target cells is mainly dependent on their intravesicular miRNAs expression (Diehl, *et al.*, 2012). The study conducted by Valadi, *et al.*, (2007) demonstrates that by incubating human mast cells with mouse mast cell-derived EV, murine miRNAs can indeed be relocated to the recipient cells by EV where they were translated into murine proteins, but EV did not demonstrate functional machinery for the protein synthesis.

It is important to be selective with EV parent cells (their properties) in order to produce uninduced and/or induced/engineered EV. This is because uninduced EV might transfer naturally occurring biological effects to the neighbouring cells, while induced/engineered EV samples may have greater potential as delivery vehicles because of their scalability and the possibility of overexpressing specific molecules (Lässer, *et al.*, 2018). For example, the photoreceptor cryptochrome (CRY) 2 has been observed to be expressed on the inside of EV, and this can help load proteins carrying the CRY-interacting basic-helix-loop helix (CIB) 1 into the EV (Liu, *et al.*, 2008). Yim & Choi (2016), made good use of this information and implemented this into their EV protein-loading system, named exosomes for protein loading via optically reversible protein-protein interactions (EXPLORs), where CIBN (a truncated version of CIB1), was fused with CD9 (usually enriched in EV), and CRY2 was fused with a cargo protein which was visualised being recruited to the plasma membrane. Eventually secreted as EV cargo, it successfully delivered several functional proteins such as Cre recombinase, a Type I topoisomerase from bacteriophage that catalyses the site-specific recombination of DNA between loxP sites,

into the target cells. It is also important because loading and injection of purified EV has been suggested by other research groups (Alvarez-Erviti, *et al.*, 2011; Kooijmans, *et al.*, 2013).

Therefore, there is supporting evidence that EV transfer biological functional molecules such as proteins and miRNAs to target cells, which shows their increasing potential as novel regulators in intercellular gene regulation (Pfeifer, *et al.*, 2015).

1.8 Aim of this PhD research project

Increased levels of eMV have been observed during blood storage and have been associated with numerous diseases (see chapter 1.7.1). Therefore, it is important to acknowledge their biological role and cargo because they are free entities present in the bloodstream and may be able to deliver vital information to neighboring cells. The objective of this PhD research was to characterise eMV and analyse their cargo with a specific interest in cell communication helper molecules.

The decision to study MV derived from a different source (Hela cells infected with HRV16) in parallel, is based on the rationale of being able to carry out a comparative study with a control sample to produce substantial parameters. Also, because the mechanisms by which viral infections induce the release of EV and because viral derived EV enter and communicate with neighbouring cells have been well studied and shown to be of use on this role for this study.

This study proposes to answer:

1. What are the size and concentration of eMV? Does it differ when erythrocytes are induced with CaCl₂ and CaCl₂+NHS?
2. Do eMV interact with neighbouring cells? What entry mechanism do they use?
3. If they do interact with neighbouring cells, what is the overall message that eMV pass on once inside the cells?

Chapter 3.1 investigates whether erythrocyte induced by exposure to different inducers (CaCl₂ and with CaCl₂ + NHS) yield a different amount and/or produced a greater number of detectable eMV in comparison to the uninduced sample. It compares instrument detection of eMV sizes using FC (sub-micron Particle size ranging between 0.5-2000 nm) and qNano (polystyrene calibration particles ranging between 115-1150 nm). This

chapter also investigates eMV extraction methods by comparing classic ultracentrifugation and Size Exclusion Chromatography approaches.

Chapter **3.2** investigates and compares surface markers, total proteins and proteases using different immunoblotting techniques, to identify the potential presence of intracellular/extracellular molecules in uninduced and induced samples. This is because these proteins may enable eMV to communicate with neighbouring cells and may allow their survival in the extracellular environment.

In results chapter **3.3**, an investigation and comparison is conducted on the potential presence of an immunology panel composed of 68 miRNA in all samples (including parent cells), to understand whether eMV could affect recipient cells by down-regulation of gene expression.

In results chapter **3.4**, a variety of cell lines were used to observe whether eMV directly interacts with the cell membrane using fluorescence microscopy. If so, to observe the impact of eMV on the growth rate of the observed cell lines using FC Guava ViaCount software.

2. Materials and Methods

2.1 Materials

2.1.1 Chemicals and kits

BD Vacutainer™ Safety-Lok™ Blood Collection Sets (Fisher Scientific REF 367286)
BD Vacutainer Plastic K2EDTA Tube 10 mL with Lavender Hemogard Closure-10 mL (Fisher Scientific REF 367525)
Bicinchoninic Acid Protein Assay Kit (Thermo scientific B2161296)
Bovine Serum Albumin (Sigma-Aldrich)
Calcium Chloride (Sigma-Aldrich)
Clarity™ western ECL substrate (BIO-RAD 170-5061)
Crystal Violet Solution (Sigma-Life sciences V5265-250 mL)
DL-Dithiothreitol Solution (Sigma-Aldrich 646563)
Exosome-depleted FBS media supplement (SBI EXO-FBS-50A-1)
Ficoll-Paque™ Plus (GE healthcare 17-1440-02)
Foetal Bovine Serum (Sigma-Aldrich)
Flow cytometry Sub-micron Particle Size Reference Kit (Molecular probes-Life technologies F13839)
GlutaMAX™-I Dulbecco's Modification of Eagle's Medium (Gibco 31966-021)
Herpes buffer solution (Sigma-Life sciences-83264-100 mL)
Laemmli 2X sample buffer (Bio-Rad 161-0727)
MegaCell™ RPMI 1640 medium (Sigma-Aldrich m3817-500 mL)
Mini-PROTEAN TGX™ Stain-Free™ precast gels 4-20% (BIO-RAD 456-8093)
mirVana™ miRNA isolation kit, with phenol (ThermoFisher scientific AM1560)
Multiplex miRNA Assay Immunology Panel - Circulating (ab204064)
Non-fat dried milk power (Marvel-original less than 1% fat)
Penicillin-Streptomycin (Sigma-Aldrich)
Pierce® reversible protein stain kit - for PVDF (Thermo scientific 24585)
Precision Plus Protein™ dual colour standards (BIO-RAD 161-0374)
Phosphate Buffered Saline (PBS) (Sigma-Aldrich p4417-100TAB)

Protease Inhibitor Cocktail (Sigma-Aldrich P8340-5 mL/013M4034V)
Proteome Profiler Human Protease Array Kit (R & D systems ARY021)
Radio-Immunoprecipitation Assay (RIPA) (Sigma-Aldrich R 0278)
Sodium Bicarbonate (Sigma-Aldrich)
Sypro®ruby Protein Gel Stain (Invitrogen tm s12000)
Trans-Blot® Turbo™ Mini PVDF transfer packs (BIO-RAD 170-4156)
Trans-Blot® Turbo™ Mini Nitrocellulose Transfer Packs (BIO-RAD 170-4158)
Tris-Glycine-SDS buffer 10x (BIO-RAD 161-0732)
Triton® X-100 (Sigma-Aldrich T8532-500L)
ViaCount Reagent (Guava technologies)

2.1.2 Technical devices

Cell culture flask 100x20 mm with vent (Sigma-Aldrich)
Dishes Nunclon™ Surface (Thermo scientific)
FLUOstar omega plate reader (BMG labtech, UK)
GelDoc-it imaging system (UVP systems, UK)
Guava EasyCyte flow cytometry (MerckMillipore)
LumaScope™ 500 Series (Etaluma)
Mini-PROTEAN Tetra cell vertical electrophoresis system (BIO-RAD)
NanoDrop® ND-1000 UV-Vis Spectrophotometer (ThermoFisher)
Trans-Blot® Turbo™ Transfer System (BIO-RAD)
qEV Size Exclusion Column (IZON science)
qNano particle analyser (IZON science)
UVP ChemiDoc-it system (UVP systems, UK)

2.1.3 Antibodies

2.1.3.1 ImmunoTools IT-Box-139.3 Roberta Freezor 2013 award (anti-human) Flow cytometry application includes:

FITC: CD14 (18D11 antibody), CD36 (antibody TR9), CD46 (antibody MEM-258), CD54 (antibody 1H4), CD58 (antibody MEM-63), CD63 (antibody MEM-259), CD235ab (antibody HIR2), HLA-ABC (antibody W6/32), Control-IgG1 (clone PPV-06), and Annexin V (detection of Phosphatidylserine).

2.1.3.2 Western blotting application includes:

Anti-CD47 AB mouse (ab3283)

Active human CD47 protein fragment standard (ab174029)

Monoclonal Anti- β -Actin, Clone AC-74 (Sigma-Aldrich A2228)

Monoclonal Anti-Human Band 3, clone BIII-136 (Sigma-Aldrich B 9277)

Monoclonal Anti-Protein Kinase C AB mouse (Sigma-Aldrich P 5704)

Monoclonal Anti-Glycophorin (α) AB mouse (Sigma-Aldrich G 7900)

Monoclonal Anti-spectrin (β), AB mouse (Sigma-Aldrich S 3396)

HRP conjugated Goat anti-mouse Ig-polyclonal (BD Pharmingen™ 554002)

2.1.4 Buffers and solutions

2.1.4.1 Complete Growth Medium (CGM)

500 mL RPMI 1640 or DMEM

50 mL Foetal bovine serum or exosome free serum 10% (v/v)

5 mL Pen/strep 1% (v/v)

2.1.4.2 Human Rhinovirus (HRV) medium

500 mL DMEM

5 mL Pen/strep 10% (v/v)

10 mL Herpes 2% (v/v)

5 mL Sodium Bicarbonate 1% (v/v)

10 mL exosome free serum 2% (v/v)

2.1.4.3 Cell freezing medium

100 μ L DMSO 10% (v/v)

100 μ L Foetal bovine serum or exosome free serum 10% (v/v)

800 μ L cell containing Complete Growth Medium 80% (v/v)

2.1.4.4 Western blotting washing buffer (PBST-20)

1 mL tween-20 in 999 mL PBS (v/v)

2.1.4.5 Western blotting blocking buffer

3 g BSA non-fat powdered milk in 100 mL PBS (w/v)

2.1.5 Cell lines

HeLa Ohio cells, passage +6 (European collection of cell culture 2013)

Jurkat cells, passage +8 (European collection of cell culture 2013)

THP-1, passage +13 (European collection of cell culture 2013)

PC-3, passage +6 (European collection of cell culture 2013)

MCF-7, passage +9 (European collection of cell culture 2013)

2.2 Methods

2.2.1 Maintenance of cell lines

The passage history for maintaining all cell lines was recorded throughout this PhD research and the following procedures were used consistently for the entire project.

2.2.1.1 Non-adherent cell lines

Non-adherent cell lines were maintained in the Roswell Park Memorial Institute 1640 (RPMI) Complete Growth Medium (CGM), at 37°C in a 5% CO₂ incubator. The cells were normally sub-cultured every three days. They were centrifuged at 160 g for 5 minutes to remove depleted medium and the pellet was suspended with 5 mL of sterile Phosphate Buffered Saline (PBS), pH 7.4 and centrifuged at 160 g for a further 5 minutes 3 times consecutively. The retained cells pellet was diluted in an appropriate volume of CGM according to cell number and prepared as required for further analysis.

2.2.1.2 Adherent cell lines

Depending on the cell line, adherent cell lines were maintained in either RPMI CGM, or Dulbecco's Modification of Eagle's Medium (DMEM) CGM. The cells were normally sub-cultured every three days by removing the depleted medium from the flask and rinsing once with 200 nm filtered PBS, pH 7.4. Subsequently, 5 mL trypsin was introduced to the flask, and the cells were incubated for approximately 5 minutes at 37°C in 5% CO₂. The flask was tapped several times to detach any remaining cells and 1 mL of CGM was added to inactivate the trypsin. The cells were then centrifuged at 200 g for 5 minutes, and the retained cell pellet was suspended with 5 mL of sterile PBS, pH 7.4, and centrifuged at 200 g for a further 5 minutes 3 times consecutively. The retained pellet

was diluted in an appropriate volume of CGM, according to cell number and prepared as necessary for further analyses.

2.2.2 Isolation of erythrocytes

Human venous blood was collected (0.75 in size needle used) into Ethylene Diamine Tetra-acetic Acid (EDTA)-containing tubes (10 mL) from a healthy donor. The same donor provided blood throughout this research and was screened regularly as a National Health Service Blood and Transplant, Tissue Service donor. This donor was approved by the London Metropolitan University Ethics Committee.

Blood cells were purified and isolated utilising the Ficoll-Paque PLUS method, according to the manufacturer protocol. The blood was diluted with 200 nm filtered PBS, pH 7.4 (ratio 1:1) and carefully layered on top of the required volume of Ficoll-Paque PLUS, maintaining approximately the same height of the Ficoll-Paque PLUS 2.4 cm and of diluted blood sample 3 cm accordingly. Volumes of blood were adjusted and processed with the same efficiency of separation by increasing the diameter of the centrifuge tube, while maintaining approximately the same height of the Ficoll-Paque PLUS, and centrifuged at 4,000 *g* for 30 minutes at 18-20°C.

Once the blood was separated into layers (erythrocytes at the bottom, followed by the Ficoll-Paque PLUS, the white cells, platelets and finally the diluted plasma at the top) they were transferred into separate tubes and suspended with 200 nm filtered PBS, pH 7.4. The erythrocytes were centrifuged at 200 *g* for 10 minutes with 200 nm filtered PBS, pH 7.4 and the pellet was ready for further procedures.

2.2.3 HRV16 preparation and infection

Plaque-based assays are the standard method used to determine infective virus concentration in terms of viral infectious substances. The viral titre is a quantitative measurement of the biological activity of a virus and it can be determined by enumerating plaque forming units per volume (PFU/ mL), or alternatively multiple replicates of the virus dilution are made and the 50% Tissue Culture Infective Dose (TCID₅₀) titre is calculated from the 50% endpoint of the inoculated culture medium.

2.2.3.1 HRV16 replication

A stock of HRV16 was stored at -80°C in 5 mL aliquots (kindly supplied by Dr. McLean). The aliquot was thawed for 5 minutes in a water bath at 37°C and 7.5 mL of HRV medium was added. This was then added to a T175 fully confluent flask of HeLa cells and incubated for 1 hour at Room Temperature (RT) using a platform shaker. Subsequently, 12.5 mL HRV medium was added to the flask and incubated at 37°C , 5% CO_2 for 24 hours. Cells were then lysed by two freeze thaw cycles (-80°C) and the medium was clarified by centrifugation at 4,000 g for 1 hour at 4°C . The resultant supernatant was centrifuged at 25,000 g for 90 minutes (optimised step for this project), at 4°C . The supernatant stock was used immediately or stored at -80°C until further analysis.

2.2.3.2 HRV16 quantification

HRV16 stock was serially diluted ten-fold (10^{-1} to 10^{-9}), 6 replicates per dilution. Then 1.8 mL of HRV medium was added to 9 different dilution vials and 200 μL of the stock of virus was added to the 10^{-1} vial. Next, 200 μL of the 10^{-1} vial was serially diluted to 10^{-9} . In a 96 well plate, 50 μL of HRV medium was added into each control well (cells only) and 50 μL virus (relevant dilution) was added to each virus well. 150 μL of HeLa Ohio cells were added (cell number $\sim 5 \times 10^5$ / mL and viability $> 95\%$ was recorded prior experiment), and incubated for 5 days at 37°C , 5% CO_2 . The cytopathic effect (CPE) was observed by microscopy (5 days) to identify the differences between virus dilutions and control wells.

At day 5 (end of CPE observation) the HRV medium was gently removed from the 96 well plate and 50 μL /well of crystal violet solution containing 0.1% in ddH₂O (v/v) was added into each well and incubated for 10 minutes to stain adherent cells by binding to proteins and DNA. Then the cells were washed gently with ddH₂O for 4-5 minutes and the 96 well plate was allowed to dry at RT for 1 hour. Subsequently, stained cells were dissolved in 30 μL Sodium Dodecyl Sulphate (SDS) in a platform shaker for 1 hour at RT and the absorbance Optimal Density (OD) at 560 nm was recorded (Fig. 2.2.3) using the FLUOstar omega plate reader.

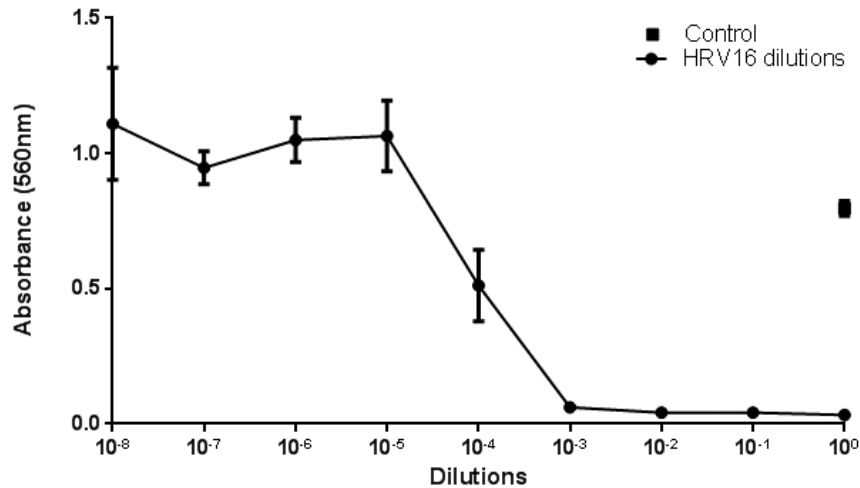


Fig. 2.2.3. Determination of infectious titre of HRV16 stock. A representation of the CPE in a quantifiable manner, to determine the infectious titre of the virus in the tissue culture. It is related to how the 50% Tissue Culture Infective Dose (TCID₅₀) which is calculated by the sum of positive (plaques formation) and negative tests (absence of plaques) over the period of 5 days while cells in culture remain viable. Where 10⁻¹ to 10⁻⁹ dilution was prepared at 6 replicates for each sample including infected and control (not infected cells) samples. Wells with destroyed cell monolayers were observed manually for 5 days (data not shown here) under an inverted microscope. Then, automatically using a viable colorimetric/cytotoxicity assay known as crystal violet assay. This assay quantifies the cytotoxic effect as a function of the number/viability of remaining cells after the infection. The assay was performed at day 5 (graphed- as the dilution rate of HRV16 decreases cell viability increases). Graph Pad version 7.3 was used, where Group family XY was used connecting lines with error bars (the values represent mean ± SEM - 95% confidence interval of independent replicates).

The optimal TCID₅₀ of viral infection dose (concentration required to induce cell death and/or pathological changes in 50% of cultures inoculated), was determined by using the following formula utilising an excel spreadsheet based on the Reed & Muench (1938) method (Fig. 2.2.4) as follows:

- Log of lowest dilution (**L**) -Difference of stepwise dilution (**d**) x (Sum of positive tests (**S**) - volume of the virus used)

L	d	S	µl			
-1	1	5.33	50			
				L=Log of lowest dilution		
				d=Difference of stepwise dilution		
				S=Sum of positive tests		
				(1) TCID 50=10E-5.83		
				TCID50/ml		
				1.35E+07		

Fig. 2.2.4. TCID₅₀ of HRV16 stock Excel spreadsheet. The TCID₅₀ method is a statistical derivative of the PFU/ mL assay. Instead of counting individual plaques, multiple replicates of the virus dilution were prepared (Fig.2.2.3). The TCID₅₀ titre is calculated from the 50% endpoint of the tissue culture (wells). The spreadsheet represents the TCID₅₀/ mL obtained during an experiment.

The following formulae were then used to determine the titre in PFU/ mL and Multiplicity Of Infection (MOI) of the viral stock:

- $\text{PFU/ mL} = \text{TCID}_{50}/ \text{mL} * 0.69$ (Poisson distribution $1\text{TCID}_{50}=0.69 \text{ PFU}$)
Example: $1.35 \times 10^7 * 0.69 = 9 \times 10^6 \text{ PFU/ mL}$
- Total PFU needed = cell number * desired MOI
Example: $8 \times 10^5 * 0.2 = 1.6 \times 10^5 \text{ PFU}$
- Total amount of virus needed : $\text{PFU/ mL} \div \text{PFU}$
Example: $9 \times 10^6 \text{ PFU/ mL} \div 1.6 \times 10^5 \text{ PFU} = 56.25 \text{ mL}$
In $\mu\text{L} = 1000 \div 56.25 \text{ mL} = 17.78 \mu\text{L}$ in suspension

2.2.3.3 HeLa cells HRV16 infection

HeLa cells were maintained on 100x20mm culture dishes prior to and whilst performing the infection experiments. For the experimental work, 95% or greater confluent flasks containing HeLa cells were used and the CGM was gently removed. Subsequently, the dishes were rinsed twice with 200 nm filtered PBS, pH7.4 and then the flasks were treated with 5 mL of HRV16 containing medium (MOI 0.2) apart from the control. The control wells were treated with the same volume added for the HRV16 wells, but only HRV medium was added instead. All flasks were incubated at 37°C, 5% CO₂ for 12 hours (~5 x10⁵/ mL). The supernatant of cultures were collected 24 hours after infection to extract derived MV. Cell number and cell viability was also recorded after the supernatant was removed.

2.2.4 Isolation of MV

In order to understand the properties present in MV, all MV samples used during this PhD project were produced and extracted using the same method for all experiments.

2.2.4.1 Isolation of eMV

The retained pellet (erythrocytes concentrate), which yields approximately 4.5 mL, was used for the extraction of eMV. The eMV were prepared in three different ways:

- (i) Control - erythrocyte pellet with 10 mL 200 nm filtered PBS pH 7.4;
- (ii) As in (i) with the addition of 20 μL of 2 mM of CaCl₂; and

- (iii) As in (i) with the addition of 1 mL 20 nm filtered normal human serum (NHS) in 10 mL 200 nm filtered PBS pH 7.4 and 20 μ L of 2 mM of CaCl_2 .

All samples were incubated for 45 minutes in a 37°C water bath, and placed on ice for approximately 5 minutes to stop the reaction, then centrifuged at 600 g for 5 minutes to pellet the cells and the supernatant was collected and centrifuged at 4,000 g for 60 minutes.

The supernatant was collected once again and sonicated for 5 minutes to disperse aggregation and centrifuged at 25,000 g for 90 minutes at 4°C. The resultant pellet was suspended in 200 nm filtered PBS, pH 7.4 (or RPMI 1640 used if eMV were to be introduced to cell lines). They were used immediately, or frozen at -80°C to store until further analysis.

2.2.4.2 Isolation of HeLaMVC and HRV16iHMOV

Conditioned medium was collected from cell cultures (infected and healthy cells) at specific times (depending on experiment demands) and centrifuged once at 200 g for 5 minutes. Then the supernatant was collected and sonicated for 5 minutes, and centrifuged at 4,000 g for 60 minutes and subsequently centrifuged at 25,000 g for 90 minutes at 4°C. The resultant pellet was suspended in 200 nm filtered PBS, pH 7.4 (or DMEM used if MV were to be introduced to cell lines) and used immediately or frozen at -80°C to store until further analysis.

2.2.4.3 An alternative method for EV extraction

The preparation for the use of the Size Exclusion Chromatography (SEC) column was carried out according to the manufacturer's instructions (IZON sciences). Briefly, the column was placed in a holder and levelled vertically, leaving the bottom Luer-slip cap in place, then the top-cap was removed. Subsequently, the column was equilibrated by removing the lower Luer-slip cap and removing the bed volume (10 mL) by rinsing the column with 10 mL 200 nm -filtered PBS buffer.

With the bottom Luer-slip cap on, the PBS buffer above the top filter was removed, then the sample (prepared as in 2.2.4.1 and 2.2.4.2, after the 4000 g centrifugation step) was introduced. The bottom Luer-slip cap was removed and 0.5 mL fractions were collected immediately (the first six fractions were discarded because it is the void volume and does not contain MV). Then, 200 nm -filtered 10 mL PBS buffer was introduced to the column. Immediately after the void volume was discarded, a fraction of 1 mL of the sample was

collected. After the collection of the MV fractions, the column was rinsed with 10 mL of PBS buffer, the bed volume (10 mL) was reintroduced to the column and then stored at 4°C until further use (reused for same sample type 3 times).

The samples were then centrifuged at 25,000 g for 90 minutes at 4°C to concentrate MV. The resultant pellet was suspended in 200 nm filtered PBS, pH 7.4 and used immediately or frozen at -80°C to store until further analysis.

2.2.5 Flow cytometry analyses

The Guava flow cytometry (FC) EasyCyte HT system allows complex biological studies such as cell counting and viability testing, cytokine detection, cell activation marker analysis and discriminates events between different cells/particles based on their size, granularity and fluorescence staining. The Guava FC can be used to perform ten different assays, but, for this PhD study only two assays were utilised. These were the ViaCount assay (for counting cells and determining viability) and ExpressPlus assay (MV concentration, size and surface marker analyses).

2.2.5.1 Cell number and viability

The quantitative measure of cell number and percentage (%) viability was an important consideration for performing cell culture and/or cellular assays. This evaluation was fundamental for this research.

For cell analysis, the ViaCount assay (FC) was used. After wash and suspension, the cells were seeded into 96 wells plate and stained with Guava ViaCount reagent (ratio 1:1). The cells were then analysed via Guava ViaCount software. Cell number/ mL and % viability was recorded using EasyFit.

The remaining stock of the cells was transferred into a culture flask to allow growth, or was seeded into well plates at $\sim 13 \times 10^5$ / mL (only cells of 95% viability or greater were used for the experiments).

2.2.5.2 MV enumeration and sizing

The size range of bioparticles in the experimental sample was estimated by comparing the side scatter signals (SSC) with forward scatter signals (FSC) provided by the reference microspheres sizes (500 to 2000 nm), using the FC Sub-micron Particles size reference kit.

The ExpressPlus assay software was used to perform all measurements using the Guava FC EasyCyte HT system. The settings were adjusted by establishing the threshold value to less than or equal to 5000 events per sample (for very low flow) for accurate particle counting (particles/ mL). The voltages (using the SSC and FSC parameters) were adjusted by evenly distributing the particles between 10^0 and 10^8 , allowing discrimination of sizes.

The accepted background “noise” consisted of events per second when 200 nm filtered PBS, pH7.4 was used as a blank solution. Debris or other unwanted events were excluded (accepted that MV are larger than 100 nm) during analysis using the FCS Express FC De Novo Software (optimized for use with Guava instruments), which allowed gating of specific areas, discrimination of sizes and sample population. To obviate MV aggregates, samples were sonicated briefly before analysis and the total amount of MV samples were seeded into 96 wells plate to allow the MV to be counted singly.

2.2.5.3 Fluorescence detection

The size range and % fluorescence detection of MV was estimated by comparing the SSC with those of the reference microspheres sizes (500 to 2000 nm) as established in chapter 2.2.5.2 but utilising the green scatter (GRN-Log) parameter instead of FSC-Log, using the ExpressPlus software.

To determine the expression of surface markers (fluorescence), MV samples were labelled with a specific panel of cluster differentiation (CD) Fluorescein-Isothiocyanate (FITC)-Conjugated antibodies in PBS containing 1 % BSA and 0.09 % sodium azide -pH 7.4. The antibodies were free of unconjugated FITC and adjusted for direct use, therefore, no reconstitution was necessary for the direct method of labelling.

A percentage of total volume (up to $\times 10^6$ / mL), of each MV sample was diluted with 100 μ L binding buffer and incubated for 30 minutes at RT. The relevant CD was added (5 μ L-recommended by manufacture) and incubated for 1 hour at RT. Subsequently, the MV samples were concentrated via ultracentrifugation at 25,000 g for 90 minutes at 4°C. The resultant pellet was then diluted with 200 nm filtered PBS, pH7.4 and washed through centrifugation at 25,000 g for 90 minutes at 4°C, and seeded into 96 wells plate. Samples were then analysed by FC Guava Express Plus software.

2.2.6 qNano standard operating protocol

Nanopore (NP) size 300 (target size between 115-1150 nm- MV samples sizes expected to be 100- 1000 nm), was used along with the Polystyrene calibration particles (CP) CPC200 particles matching the expected size range of unknown particles, to accurately estimate the size of unknown particles/samples.

The CP was vortexed rapidly to ensure homogeneity and sonicated briefly to remove aggregates. Then they were diluted in 200 nm -filtered PBS (as sample buffer), to the target desired concentration (1×10^9 / mL).

80 μ L of 200 nm -filtered PBS was applied and removed from the lower fluid cell, to reduce the risk of air bubble formation under the nanopore when applying the electrolyte to the lower fluid cell.

The nanopore was then placed onto the 4 arms of the instrument and the digital callipers were used to measure the distance between two opposite arms and enter the distance in mm into the stretch input field. Subsequently, the calibrate stretch option was set to 47 mm and 80 μ L of 200 nm -filtered PBS was introduced and removed from the lower fluid cell to allow more flexibility to the pore.

Then, the upper fluid cell and shielding cage was placed on the nanopore, and 40 μ L of diluted CPC200 was introduced in the upper fluid cell. The variable pressure module was used to apply ≥ 0.8 kPa positive pressure, and the stretch was reduced to 44 mm, whilst analysing the blockade events caused by the CPC200 and observed in the signal trace panel. The particle rate measurements were recorded until 500 particles were reached, which provided a stable baseline current for appropriate measurement of the samples.

The CPC200 was then removed from the upper fluid cell, which was washed three times with 1000 μ L 200 nm-filtered PBS to remove residual particles. Then the samples were introduced into the upper fluid cell with baseline current within 3% observed during measurement, showing particle rate plot display constant sample detection.

2.2.7 Western blotting analyses

Western blotting is a widely used analytical technique used in molecular biology, immunogenic and other molecular biology disciplines to detect specific proteins in a sample of tissue homogenate or extract.

2.2.7.1 Preparation of sample lysates

After the removal of the final (wash) PBS buffer from the cells and MV, an appropriate volume of RIPA Buffer was added (1 mL for 0.5 to 5×10^7 cells) with protease inhibitor cocktail (1X). For MV samples the volume of RIPA was optimised to $200 \mu\text{L}$ to maximize concentration/dilution. Then the cells were incubated on ice for 5 minutes, and MV incubated for 1 hour on ice. Samples were rapidly vortexed and placed on ice for 5 minutes, and the lysates were centrifuged at $8000 g$ for 10 minutes at 4°C to pellet the debris. Then, the supernatant containing the soluble proteins from all samples were ready for analysis.

2.2.7.2 Total protein concentration and SDS-PAGE sample preparation

Following the manufacturer's instructions, $200 \mu\text{L}$ of working reagent (WR) is required per sample ($25 \mu\text{L}$). The WR is made up using reagent A (sodium carbonate, sodium bicarbonate, bicinchoninic acid and sodium tartrate in 0.1 M sodium hydroxide) and reagent B (4% cupric sulphate) at ratio 50:1 (v/v). In parallel, a dilution series of Bovine Serum Albumin (BSA) stock solution was prepared and used as a standard in the later evaluation of unknown concentrations. Applied concentrations of the standard ranged between 0 - $2000 \mu\text{g}/\text{mL}$ BSA. The preparation of the working reagent was determined by the following formula:

- $(\text{No. of standards} + \text{No. of unknowns}) \times (\text{No. of replicates}) \times (\text{Vol. of working reagent per sample}) \text{ total} = \text{Total volume required.}$

Subsequently, the 96 well plate containing the standards and samples was incubated at 37°C for 30 minutes. The plate was allowed to cool down at RT and the OD at 562 nm readings were recorded, using the FLUOstar Omega microplate reader. Protein concentrations of the unknown samples were determined by interpolation on the standard curve (Fig. 2.2.7).

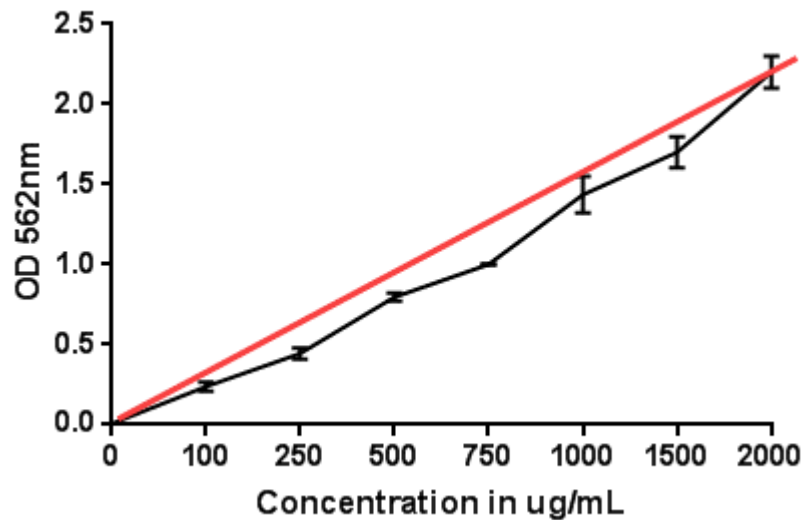


Fig. 2.2.7. BSA standard curve for protein concentration. Where 0- 2000 $\mu\text{g}/\text{mL}$ BSA dilution in triplicates are shown (blank corrected data). The response values (absorbance) were plotted against known concentrations and a best-fit line drawn through the points. The unknown protein concentration of samples was determined by reference to the standard curve. Graph Pad version 7.3 was used, where Group family XY was used connecting lines with error bars (Mean and Error).

Subsequently, 50 $\mu\text{g}/\text{mL}$ (total protein concentration) of the samples were diluted with (2X) Laemmli sample buffer and reducing agent Dithiothreitol (DTT-1M to 950 μL of ddH₂O for 50 mM DDT solution). Finally, the samples were boiled for 5 minutes at 95°C to ensure denaturation/reduction. The samples were then allowed to cool before loading onto an SDS-PAGE gel.

2.2.7.3 SDS-PAGE standard procedure

Polyacrylamide Gel Electrophoresis (SDS-PAGE) 4-20% Mini-PROTEAN Tris-Glycine eXtended (TGX)TM Stain-FreeTM precast gel (which retains Laemmli-like separation characteristics while using a standard Tris-glycine running buffer system) was placed into the electrode assembly device, inside a clamping frame in the tank of the Mini-PROTEAN Tetra cell vertical electrophoresis system. Then the Tris-glycine-SDS buffer (1x) was added to the inner and outer chambers of the tank, and the plastic comb of the gel was carefully removed. The Precision plus proteinTM dual colour standards ranging between 250-10 kDa were applied by loading 10 μL into the gel. Subsequently, appropriate concentrations/volumes of samples were distributed along the wells. Electrophoresis separations were performed at 150V (constant voltage), until the SDS sample buffer reached the end of the gel.

2.2.7.4 SYPRO® Ruby protein gel stain

After electrophoresis, the gel was washed with ddH₂O and placed in a clean container with 100 mL of fix solution containing 50 mL of 99.8% pure methanol, 7 mL acetic acid and 43 mL ddH₂O (v/v), and agitated on a platform shaker for 30 minutes and fix solution was discarded. Then 60 mL of SYPRO® Ruby protein gel stain was added to the container and placed in the microwave (80-85°C) for 30 seconds, agitated for 3 seconds to distribute heat evenly, and microwaved for a further 30 seconds (80-85°C) and then agitated for 5 minutes. The gel was reheated for 30 seconds and agitated for 23 minutes (30 minutes total staining time). Subsequently, the gel was transferred to a clean container with 100 mL of wash solution containing 10 mL of 99.8% pure methanol, 7 mL acetic acid and 83 mL ddH₂O (v/v) for 30 minutes and briefly washed with ddH₂O before protein bands visualization with GelDoc-it imaging system.

2.2.7.5 Membrane transfer

The Trans-blot Turbo blotting system was used throughout this research (semi-dry transfer). The gels (protein bands) were transferred to Trans-Blot® Turbo™ Mini Nitrocellulose (for western blotting procedure) and/or Polyvinylidene Difluoride (PVDF) (for visualisation of bands - to test successful band transfer) membrane Transfer Packs. The membrane packs allowed the gels to be sandwiched between sponge and paper and all are clamped tightly together, to ensure no air bubbles were formed. The sandwich was placed in the centre of the cassette bottom and the lid was placed on the top of the membrane, and the cassette was locked by turning the knob clockwise. When the cassette was inserted into the instrument, the BIO-RAD existent protocol for 3 minutes mini gel transfer was selected. The membrane was then ready for further analysis.

2.2.7.6 MemCode reversible protein stain kit- PVDF membranes

To verify successful protein transfers to the membrane (PVDF only), the membrane was manually rinsed with ddH₂O three times and quickly decanted. MemCode™ sensitizer was poured into the container, and agitated at RT for 2 minutes on a rotary platform shaker, at moderate speed, and the solution was decanted. Then MemCode™ reversible stain was poured into the container and the membrane was agitated for 1 minute at RT, then the solution was decanted. Subsequently, the membrane was rinsed with the MemCode™ destain solution three times, quickly decanted and stained protein bands were visualised by eye.

The membrane was then submitted to the eraser/methanol solution, agitated for 20 minutes at RT on a platform shaker and rinsed with ddH₂O. Western blotting was performed with PVDF membrane for trial purposes only (data not presented here).

2.2.7.7 Western Blotting standard procedure

The resultant nitrocellulose membrane was incubated for 1 hour at RT with western blotting blocking buffer. Following blocking, the membrane was washed 3 times for 10 minutes in a platform shaker with PBST-20 and incubated with the relevant primary antibody in the desired dilution (diluted with Western blotting blocking buffer and according to the manufacturer's instructions) for 2 hours at RT, or overnight at 4°C and washed with PBST-20 (3 times for 10 minutes in a platform shaker). Subsequently, the membrane was incubated with the relevant secondary antibody for 2 hours at RT, and washed 3 times for 10 minutes in a platform shaker with PBST-20.

Visualization of positive protein bands detection was performed using the enhanced chemiluminescence reagent system (ECL), where reagent A and B (ratio 1:1) was added to the membrane and incubated for 5 minutes at RT under dark conditions. The images were visualised using the UVP ChemiDoc-it system.

2.2.8 Proteases profiling

2 mL of array buffer 6 (buffered protein based with preservatives serving as a blocking buffer) was added into each well of the 4-well multi-dish. Then each sample membrane (each containing 34 different capture antibodies printed in duplicates) was placed in the wells (4-well multi-dish: 4 samples: 4 membranes), and incubated for 1 hour on a rocking platform shaker.

Sample preparation and total protein concentration procedures were carried out as in chapters 2.2.7.1 and 2.2.7.2.

Cells and MV lysates were diluted and adjusted to a final volume of 1.5 mL (50 µg/ mL of protein) with array buffer 4 (buffered protein based with preservatives serving as diluent buffer) and 15 µL of reconstituted protease detection antibody cocktail (diluted in 100 µL of DDH₂O) and incubated at RT for 1 hour. Then the array buffer 6 was aspirated from the wells of the 4-well multi-dish containing the sample-membranes, and the prepared antibody mixtures, with the corresponding sample was introduced to the membranes and incubated overnight at 2-8°C on a rocking platform shaker. Each

membrane was removed and placed into individual plastic containers with 20 mL of 1X Wash Buffer and washed 3 times for 10 minutes.

Then, 2 mL of 1X streptavidin-HRP was introduced into each well of the 4-well multi-dish (the 4 samples-4 membranes) and incubated for 30 minutes at RT, on a rocking platform shaker. Each membrane was then washed 3 times with 20 mL of 1X Wash Buffer for 10 minutes. 1 mL of the prepared chemi Reagent Mix (1:1 ratio) was evenly introduced onto each membrane and incubated for 1 minute. The image/stained spots were detected using the UVP ChemiDoc-it system (UVP systems, UK).

2.2.9 miRNA profiling

miRNA profiling involves comparisons between two or more groups of different biological samples, to therefore calculate the differences of miRNA expression between groups and/or samples.

2.2.9.1 miRNA extraction

PBS was removed from all samples (N=3: erythrocytes, eMV control, eMV CaCl₂, eMV CaCl₂ + NHS, HeLa cells, HRV16iHc, HeLaMVC, and HRV16iHMOV), and 300–600 µL Lysis/Binding Solution for 10⁰-10⁷/ mL cells was added. Approximately 300 µL for small numbers of samples (hundreds), and closer to 600 µL when isolating RNA from larger numbers of cells (thousands/millions).

Then, 1/10 volume of miRNA homogenate additive was added to all samples, which was mixed well by vortexing and inverting the tube several times and incubated for 10 minutes on ice. A volume of Acid-Phenol Chloroform that was equal to the original lysate volume (before addition of the miRNA homogenate additive) was added. Samples were vortexed for 30–60 seconds and centrifuged for 5 minutes at 10000 g at RT to separate the aqueous and organic phases. The aqueous phase was recovered without disturbing the lower phase and transferred to a fresh tube.

Subsequently, 1/3 volume of 100% ethanol was added to recover the aqueous phase, and the samples were mixed thoroughly by vortexing. Samples were then, introduced into the filter cartridge (one per sample) which was supported by the collection tubes, and centrifuged for 15 seconds at 10000 g and the filtrate collected.

2/3 volume of 100% ethanol was added to the filtrates and mixed thoroughly. The mixture was introduced to a second filter cartridge, centrifuged for 15 seconds at 10000 g and the filtrate discarded. Then the filter was washed with 700µl miRNA wash solution by centrifuging all samples for 15 seconds at 10000 g. Then, the filter was washed twice with 500 µl wash solution (centrifuged for 15 seconds at 10000 g).

100 µl of pre-heated (95°C) elution solution was introduced to the centre of the filter and centrifuged 30 seconds at 10000 g. At the end of this procedure, the eluate was collected and samples were ready for analysis or stored at –80°C until further analysis.

2.2.9.2 miRNA quantification

The RNA concentration range was measured within manufacturer specifications for the NanoDrop® ND-1000 UV-Vis Spectrophotometer, and the ultraviolet (UV) absorbance measurements were acquired under the RNA-40 settings at RT.

The concentration of the samples was assessed by pipetting 2µl of each sample directly onto one measurement pedestal, a measurement of the elution buffer was recorded and acted as a blank (background-subtracted). The ratio of A260 to A280 was used because it provides an indication of RNA purity. After this procedure samples were diluted with elution buffer to attain the required concentration (aiming at 10 µg/ mL).

2.2.9.3 Firefly™ circulating miRNA profiling assay (immunology panel)

Each sample prepared in 2.2.9.1 and quantified in 2.2.9.2 went through the procedure presented in Fig. 2.2.9. All samples (N=3: erythrocytes, eMV control, eMV CaCl₂, eMV CaCl₂ + NHS, HeLa cells, HRV16iHc, HeLaMVC, and HRV16iHMOV) were sent to Abcam and scanned on an EMD Millipore Guava 8HT flow cytometry (technical replicates of each sample were independently analysed by Abcam), and the resultant data was analysed with the Firefly™ Analysis Workbench software.

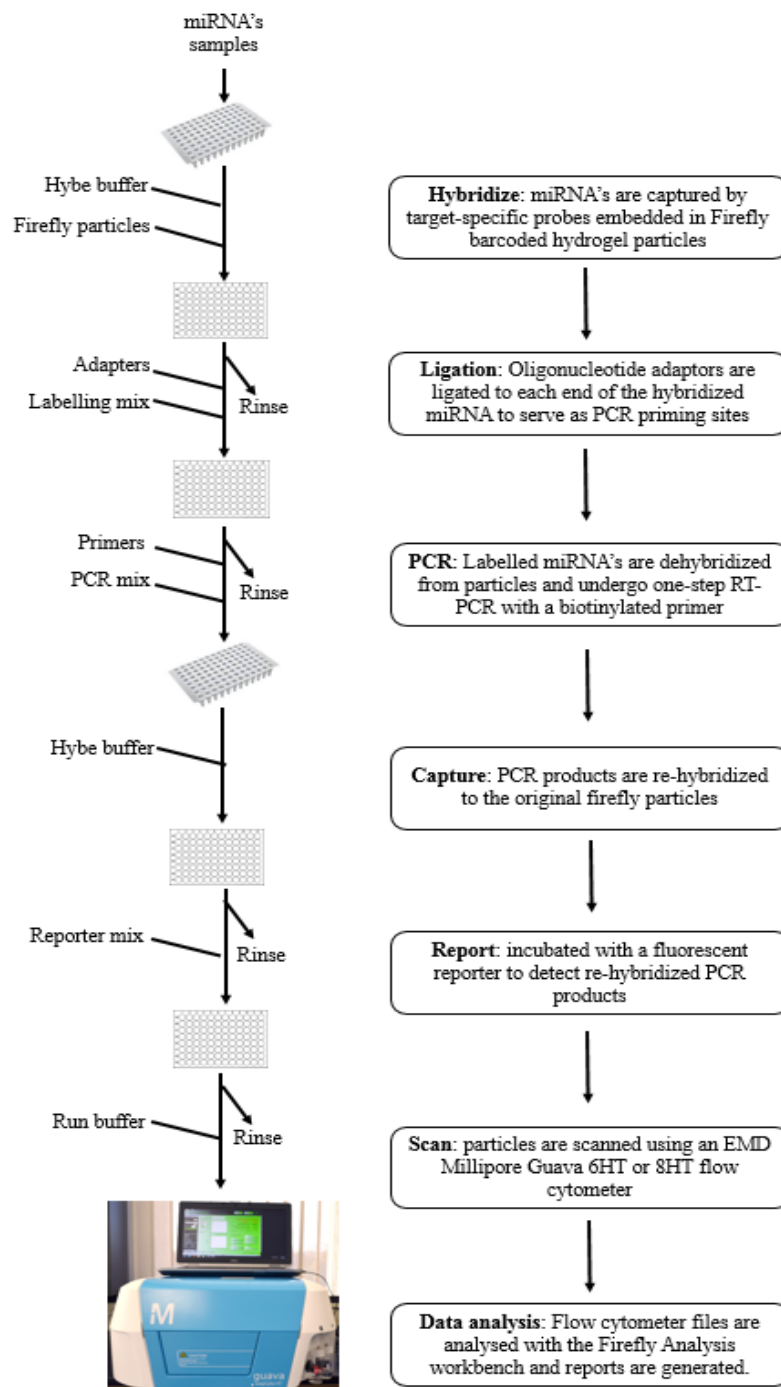


Fig. 2.2.9.3.1. Summary of the miRNA experimental procedure. The workflow diagram was built on information provided by Abcam (2015), and it represents the step by step experimental procedure used for the miRNA profiling. It permits profiling of up to 68 miRNAs across multiple samples, with readout on a standard flow cytometry. A detailed procedure is provided in Appendix I.

2.2.10 MV labelling for fluorescence microscopy

For MV-cell interactions, Annexin-V-FITC-Conjugated was used to label the MV samples, the purified antibody used here was conjugated with FITC- free of unconjugated FITC, under optimum conditions and adjusted for direct use, no reconstitution was necessary. A percentage of total volume of the MV samples were diluted (ratio 1:1 with cells) with binding buffer and incubated for 30 minutes. 5 μ L of Annexin-V-FITC-

Conjugated was added to each MV sample and incubated for 1 hour at RT. Subsequently, the MV samples were concentrated/washed through centrifugation at 25,000 g for 90 minutes at 4°C. The labelled MV were added to the 95% or greater viable cells, and MV to cell interaction was observed using time-lapses settings, utilising an automated system alternating between bright field and fluorescence using LumaScope™ 500 Series Fluorescence Microscope LED imaging analysis. Photographs of interactions and/or outcomes were recorded every two minutes for 15 minutes.

2.2.11 The addition of eMV on the growth of different cell lines

For the observation of the impact of eMV on the growth of cell lines, THP-1, Jurkat, PC-3 and MCF-7 cells were used. The cells in the exponential phase were washed and quantified accordingly using the flow cytometry ViaCount assay as in 2.2.5.1. Cells (treated with exosome free serum CGM) were seeded into sterile 24 well plates at $\sim 13 \times 10^5$ / mL cell (only cultures with 95% viability or greater were used) in triplicate. Then RPMI 1640 diluted eMV control (quantified using FC Express Plus software as in 2.2.5.2) were added to each well (except controls- RPMI 1640 only) containing the different the cell lines, THP-1, Jurkat, PC-3 and MCF-7, at 1:1 ratio.

Plates were incubated at 37°C in a 5% CO₂ incubator and left untreated for the duration of the experiment (96 hours). Cell growth rate was analysed (concentration and viability determined) every 24hours against eMV treated cells.

2.2.12 The addition of HeLaMVC and HRV16iHVMV on the growth of HeLa cells

To investigate the effect of HeLaMVC and HRV16iHVMV on the growth rate of HeLa cells, HeLa cells in the exponential phase were washed as in chapter 2.2.1.2 and quantified accordingly as in chapter 2.2.5.1. Cells were seeded into 24 well plates at $\sim 16 \times 10^5$ / mL cell (only cultures with 95% viability or greater were used) in triplicate.

Quantified by FC and DMEM diluted HeLaMVC and HRV16iHVMV (ratio 1:1) were added to each well (except controls) containing the HeLa cells treated with DMEM CGM (exosome free serum). The plates were then incubated at 37°C in a 5% CO₂ incubator and left untreated for 24 hours. HeLa cells control samples were observed against MV-treated cells (1:1 ratio) and concentration/ mL and viability was determined every 4 hours after an initial incubation period of 12 hours to determine the effect of MV on the growth of the cell line before cells were apoptotic (MOI 0.2).

2.2.13 Statistical Data Analysis

Statistical analysis for all data presented in this PhD thesis, unless noted otherwise in figure description, were performed by using multiple T test for comparison between groups (one unpaired t test per row- per period of time). The points and connecting line are shown as Mean and Error (XY graph family). The statistical significance between groups was determined correcting for multiple comparisons using the Holm-Sidak method, where $\alpha=0.05$ with fewer assumptions. This analysed each row individually, not assuming consistent Standard deviation. $P > 0.05$ considered not significant (NS), and $P < 0.05$ ($P < 0.05$ *, $P < 0.005$ **, $P < 0.0005$ *** and $P < 0.00005$ *****) were considered statistically significant utilising GraphPad Prism version 7.2 for Windows (GraphPad Software, USA).

3. Results

3.1 Heterogeneity of MV samples: their concentration and size

3.1.1 Introduction

Due to the large number of publications in this field, EV may be referred to as entities that contain material which may mirror the content of the parent cell. Nevertheless, it is important to acknowledge that EV are heterogeneous in size, biogenesis, composition and can derive from diverse sets of biological/immunological processes which may be dependent on their parent cells, and their biology requires further elucidation.

The physiological, pathophysiological processes and biological functions of EV are becoming increasingly characterised. Most, if not all cells secrete at least one type of EV, which comprise heterogeneous populations of vesicles of different compositions, physiochemical properties and sizes (Sadallah, *et al.*, 2011; van der Pol, *et al.*, 2012; Tissot, *et al.*, 2013; Yáñez-Mó, *et al.*, 2015). As previously mentioned (chapter 1.2.1- pages 12-13), MV are considered to be a subtype of EV and are the focus of this PhD research.

The concept of induced microvesiculation is not new and has been observed by a variety of study groups (chapter 1.2.2). For example, microvesiculation can be induced by a plethora of cellular events including cell death, hypoxia, stress, expression of oncogenes, differentiation and infection by viruses (Inal & Jorfi, 2013).

An early report by Liepins (1983), focused on cytoskeletal disruption as a mechanism for MV formation and reported that treatment of mouse mastocytoma P815 cells with colchicine (β - tubulin interactor), vinblastine (cell cycle regulation), and cold temperatures disrupts the microtubule cytoskeleton. These treatments appear to cause a localized rupture of the plasma membrane from the underlying cytoskeleton, as well as subsequent blebbing due to hydrostatic pressure differences (Jiang & Sun, 2013).

Furthermore, it has been suggested that even a single cell may release more than one type of EV and that induced microvesiculation may lead to heterogeneous populations of EV (concentration and size). For instance, in platelets, where isolation protocol, the quantity

and protein content were compared in microvesiculation induced by thrombin, collagen, lipopolysaccharide and, Ca^{2+} ionophore generated different results (Aatonen, *et al.*, 2014).

In addition to sample stimulation, MV general sample preparation and extraction is yet to be standardised, despite there being many studies attempting to establish clinical standards (Bobrie, *et al.*, 2012; Witwer, *et al.*, 2013). There are numerous uncertainties over protocol standardisation and how to define the pre-analytical and analytical variables, which may influence the interpretation of the results (Mora, *et al.*, 2016).

Donor heterogeneity factors, such as diet and age should be considered in order to facilitate understanding of the analytical parameters/variables and to ensure that MV can be reliably quantified in patients and other clinical settings. Other factors including sample collection, sample handling, storage period, and isolation/extraction conditions can affect the results. Therefore, standardised protocols are essential because variation in the steps of the protocol used can lead to significant fluctuations in MV numbers and their purity, resulting in unreliable experimental results (Witwer, *et al.*, 2013).

Indeed, EV extraction and identification/characterisation technologies have been widely investigated, and this area of research has accumulated increasing interest and knowledge. Nevertheless, it is generally accepted this is an area of research that is unprepared for clinical applications/practice. It may be suggested that this area of research is still early stage, particularly the ability to state that EV-data can unquestionably be used for clinical purposes. Considering their heterogeneity, more data is needed to positively reveal EV concentration, size and their biological role.

In this results chapter, the investigations focus on the characterisation and comparison of eMV released from uninduced erythrocytes (control) with those induced with CaCl_2 and CaCl_2 +NHS (Hela cells derived MV were used for source differentiation purpose) considering:

1. eMV size and concentration isolated from ultracentrifugation procedure using the FC Express Plus assay;
2. eMV size distribution using the Tunable Resistive Pulse Sensing (TRPS) principle (qNano instrument); and
3. eMV concentration isolated from ultracentrifugation compared to the Size Exclusion Chromatography (SEC) column approaches analysed using the FC Express Plus assay.

The primary functions of Flow Cytometry (FC) are to measure the scattering of light caused by a particle, hence the FC Sub-micron Particle Size Reference Kit. Forward scatter (FSC) is light from the illuminating laser beam that has been bent (refracted or otherwise deflected) at a small angle as it passes through a particle. The intensity of the FSC signal is proportional to the particle's size (Tzur, *et al.*, 2011). Therefore, it is possible to analyse the size of bioparticles using a standard FC by comparing their FSC signals with that of a population of microsphere standards that have known diameters.

The Guava EasyCyte™ HT system FC Express Plus Software (used for this PhD research), allows analysis of large numbers of MV using very small volumes (5-200 µL). It is also used for performing one-, two-, and three-colour assays, and is designed for measuring intracellular or cell surface marker expression. It can also be adopted for a range of assays including accurate quantification and sizing of samples (MerckmilliporeGroup, 2015).

Secondly, with the aim of understanding eMV size distribution, the qNano instrument was used. This is because it compares the resistive pulses caused by the unknown particles with the resistive pulses caused by calibration particles with a known diameter. This can be done because the concentration and rate of blockades are linearly proportional (Willmott, *et al.*, 2010). Using a single calibration sample, together with particles of known concentration and particle size allows for the measurement of size distribution of an unknown sample (Maas, *et al.*, 2014).

Additionally, due to research technologies rapidly expanding in the field of the EV, a Size Exclusion Chromatography (SEC) was used as an alternative method to extract MV samples to test whether it provided a better MV isolation procedure compared to the classic ultracentrifugation method.

3.1.2 Results

Chapter 1.2.2 hypothesised how different cell inducers may stimulate the release of MV. Therefore, in an effort to increase the production yield of eMV, erythrocytes were induced with CaCl₂ and CaCl₂ + NHS and compared to uninduced erythrocytes (control eMV), (Hela cells were infected with HRV16 to act as a parallel sample) as described in chapter 2.2.4.

The FC size analysis of MV is shown in Fig. 3.1.2.1, where the events were plotted using the side scatter (SSC-allows for particles/cellular differentiation within a heterogeneous population) against forward scatter (FSC - allows for discrimination of particle sizes) parameters. Both were set at the common logarithmic (Log) scale because data is condensed to a substantial degree at the high end in comparison to the low end (natural logarithm- In), which provides a more suitable view for data with very different medians (Bushnell, 2017).

Fig. 3.1.2.1a represents the known populations of the size beads ranging between 500-2000 nm and 200 nm-filtered PBS (blank buffer/noise) that were used to create the MV optimized gate. This was performed according to the predicted MV size ranging between 100-1000 nm. The size beads were overlaid over each other and the MV gate was activated in order to investigate particles/MV sizes.

The triggering threshold (minimum value) was set on forward scatter below the power of particles scattered light but above the systems background noise (PBS gate). The background noise subpopulations of particle events disappear after the gating system is activated (bottom left dots next to the Y axis). This is when the noise is subtracted from the event count (5000 maximum for all analysis), and the true centre of the gated population acts as a reference for all samples.

eMV control (Fig. 3.1.2.1b), eMV CaCl₂ (Fig. 3.1.2.1c), and eMV CaCl₂ +NHS (Fig. 3.1.2.1d) samples (N=3) show similar characteristics in terms of sizing and FC position, with the majority of samples (dots) laying within the MV gate created. These samples appear to be smaller than 500 nm when observed against the size beads (reference), with a significant population positioned below the area established at 500 nm. The eMV control and eMV CaCl₂ samples appear to be smaller than the eMV CaCl₂ +NHS sample, as the dots shifted further right and upwards when observed against the created MV gate.

HeLaMVC (Fig. 3.1.2.1e) and HRV16HiMV (Fig. 3.1.2.1f) were demonstrated as being larger than eMV samples in general. More particles/dots appeared outside the gate created and they presented similar characteristics to the eMV CaCl₂ +NHS sample (dots shifting further right and upwards).

Also, a small number of particles/dots were observed as present below the MV gate created, suggesting that smaller particles were present in the samples and showed more heterogeneity in terms of their sizes.

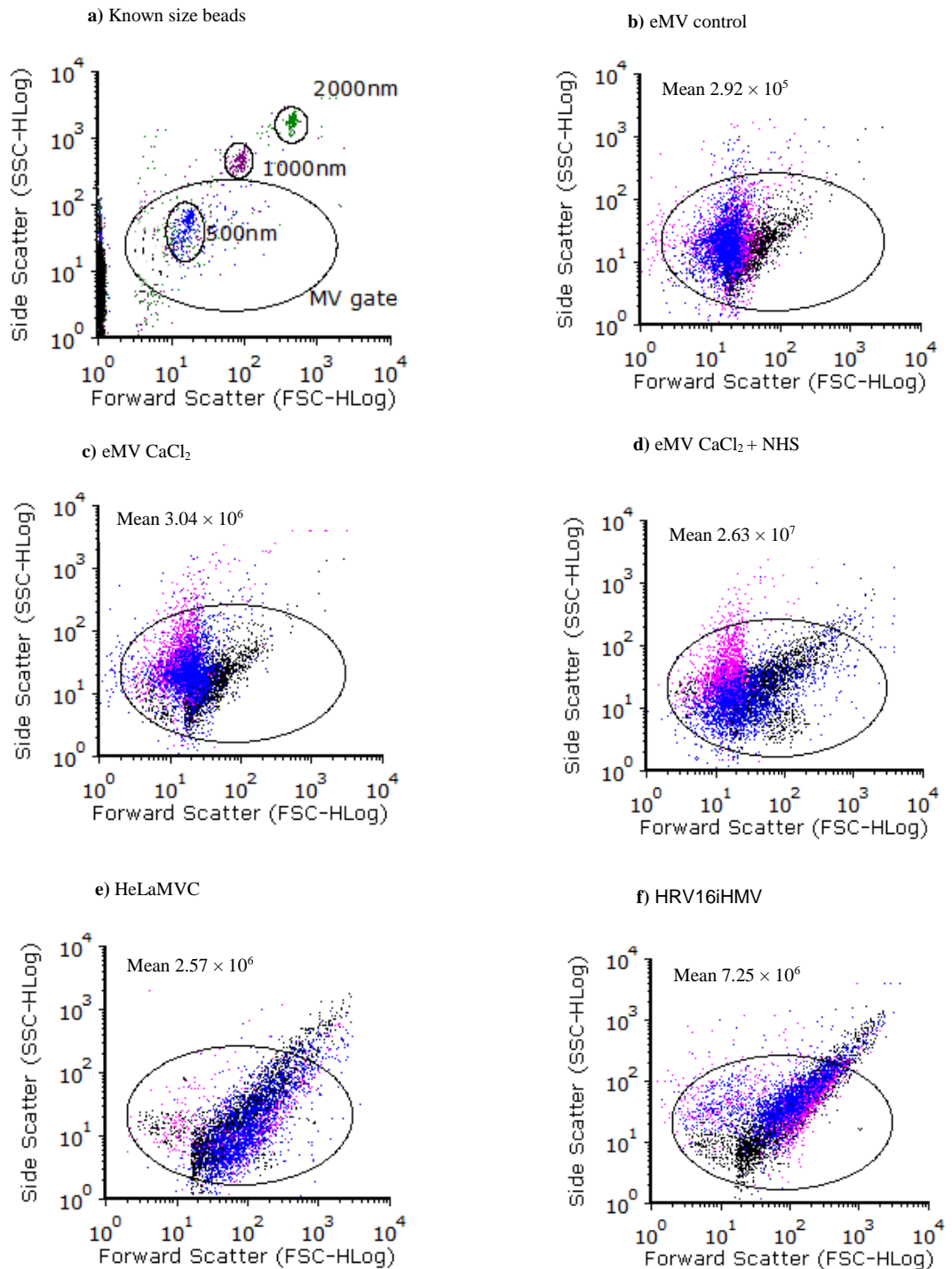


Fig. 3.1.2.1. Dot-plot gating- FC analyses of MV sizing and counting strategy. Where a) represents the dot plots acquired from the size beads overlaid over each other and displayed as the SSC HLog vs. FSC-HLog separated by sizes (gated) and showing events which were used to create the MV gate and to establish appropriate instrument settings. Each dot represents a single particle, and the characteristic position of the different populations is determined by differences in particle sizing and granularity. The MV gate was defined as >100 nm and <1000 nm by verifying resolution capabilities of the FC against beads, which was also used to define the size distribution of all samples. The gate showing 500 nm particles was purposely used for the MV sizing and counting and PBS was used as buffer control which was excluded from background when analysing MV numbers (Fig. 3.1.2.2). Fig. 3.1.2.1 b), c), d), e) and f) represent MV samples (N=3) as labelled above each diagram. FCS Express 6 FC and Image Cytometry Software was used for the analysis.

To compare the concentration of eMV population released in the presence of CaCl₂ and CaCl₂ + NHS, with the amount released from eMV control each condition was assessed in Fig. 3.1.2.1. This was achieved using parameters established in Fig. 3.1.2.1a, where the concentration of samples were analysed excluding particles/MV (dots) that did not fit within the parameters used for the MV gate.

As shown in Fig, 3.1.2.2a, erythrocytes released higher levels of eMV in the presence of CaCl₂ (N=3, mean 3.4×10^6 / mL) when compared with uninduced erythrocytes/eMV control (N=3, mean 4.5×10^4 / mL). The production of eMV was further increased when erythrocytes were induced with CaCl₂ and NHS (N=3, mean 2.9×10^7 / mL), in comparison to eMV control. Furthermore, eMV CaCl₂+NHS yield a greater amount when compared to eMV CaCl₂ suggesting that there is an additive effect as a result of NHS in eMV production.

The data obtained (Fig 3.1.2.2) supports the assertion that it is possible to produce reproducible MV populations when using FC settings (gate created), because eMV CaCl₂ and eMV CaCl₂+NHS did not show significant inaccuracy for the amount released within the same group (N=3, Mean and Error). However, eMV control samples did show a small variation between samples (Mean and Error). eMV CaCl₂ and eMV CaCl₂+NHS samples showed an increased trend in their amount of release (statistical significance) when compared to uninduced samples (eMV control).

To relate the amount of eMV produced with the number of erythrocytes, it can be suggested that all eMV samples show less than a 1:1 ratio production in comparison with the original erythrocyte numbers ($\sim 5.9 \times 10^9$ /mL) used for the experiment.

In addition, to further compare the amount of MV released from erythrocytes, MV from HeLa cells (HeLaMVC) and HeLa cells infected with HRV16 (HRV16iH MV) were used. HeLaMVC (N=3, mean 2.4×10^6 / mL) and HRV16iH MV (N=3, mean 7.5×10^6 / mL) also produced a greater amount of MV when HeLa cells were infected with HRV16. However, it did not show inaccuracy between MV types for the amount released within the same group (N=3, Mean and Error). In relation to the number of cells used (2.5×10^7 HeLa cells/mL) it also suggests that HeLa cells produce less than 1 MV per parent cell.

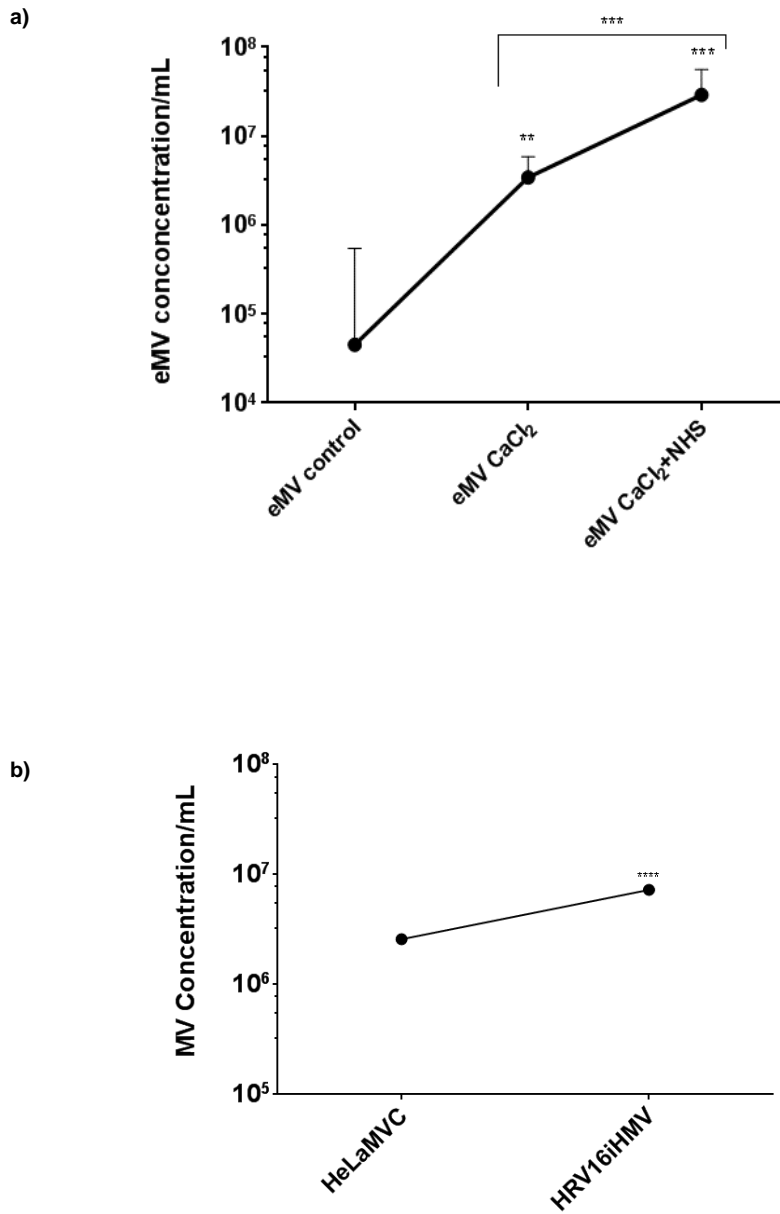


Fig. 3.1.2.2. The measurement of MV numbers- assessment by FC analyses. Comparison of the total concentration of the MV samples. Where Fig a) represents triplicates of each sample (Mean and Error) estimated per $\sim 5.9 \times 10^9$ mL erythrocytes where statistical analysis was performed between groups (eMV control vs eMV CaCl₂ P<0.001, eMV control vs eMV CaCl₂+NHS P<0.0001, and eMVCaCl₂ vs eMV CaCl₂+NHS P< 0.0001) and Fig b) represents triplicates for HeLaMVC and HRV16iHMV estimated per $\sim 2.5 \times 10^7$ mL (N=3, Mean and Error) showing statistical significance between HeLaMVC vs HRV16iHMV (P<0.00004). The strategy used here allows the total concentration of the samples to be estimated by activating the gate created using the size beads, where only particles/MV lying within the MV gate created in Fig. 3.1.2.1a were considered for the concentration analysis.

To further analyse/characterise and confirm the size range of MV samples against FC analyses the qNano (TRPS technology) was used. The measurement of MV sizing was obtained using the reference beads within expected samples sizes being 100- 900 nm and the polystyrene CP200 that complements the nanopore (NP300 115 - 1150 nm).

Fig. 3.1.2.3 demonstrates that eMV size is dependent on the stimulation used. The size dispersal can be practical in terms of noticing the intervals between spikes that may be notably plentiful (visible as peaks). An increase in concentration distribution of eMV samples was observed to be greater (size spectrum ranging 100nm to 800nm) for induced samples. In Fig. 3.1.2.3a (N=3, eMV control) peaks are more concentrated between 170 nm to 220 nm (size ranging between 100 nm to 370 nm). Whereas in Fig. 3.1.2.3b (eMV CaCl₂), a greater concentration distribution (peaks) is shown between 150 nm to 250 nm (size ranging between 100 nm to 600 nm). In Fig. 3.1.2.3c (eMV CaCl₂ +NHS) an increased concentration distribution is shown between 120 nm to 350 nm (size ranging between 100 nm to 750 nm).

HeLaMVC samples (N=3) show greater concentration distribution between 120 nm to 250 nm (size ranging between 100 nm to 600 nm) and HRV16iHVMV (N=3) appears larger, with the concentration distributed between 120 nm to 370 nm (size ranging between 100 nm to 600 nm).

Notably, overall qNano data indicated that the concentration of small MV (< 400 nm) is greater than the larger MV (>500 nm- which can be due to MV aggregation, variation of the pore dimension, and electronic noise) at all of the testing points. The peaks demonstrate that concentration distribution varies between each MV sample. It also shows that the majority of MV analysed here stand between 100 nm and 800 nm, which confirms the MV gate used the FC analyses (Fig. 3.1.2.1) gated system (<1000 nm), but it contradicts that HeLaMVC and HRV16iHVMV are larger (in comparison to eMV samples analysed with FC).

Despite the fact that the qNano analysis provided a more accurate manner to understand the size range of MV samples, the FC analysis is the method of choice for further experiments during this PhD research. This is because it proved to be an accurate and valuable tool for the concentration measurement of MV, which were the measurements required for further experiments (following results chapters).

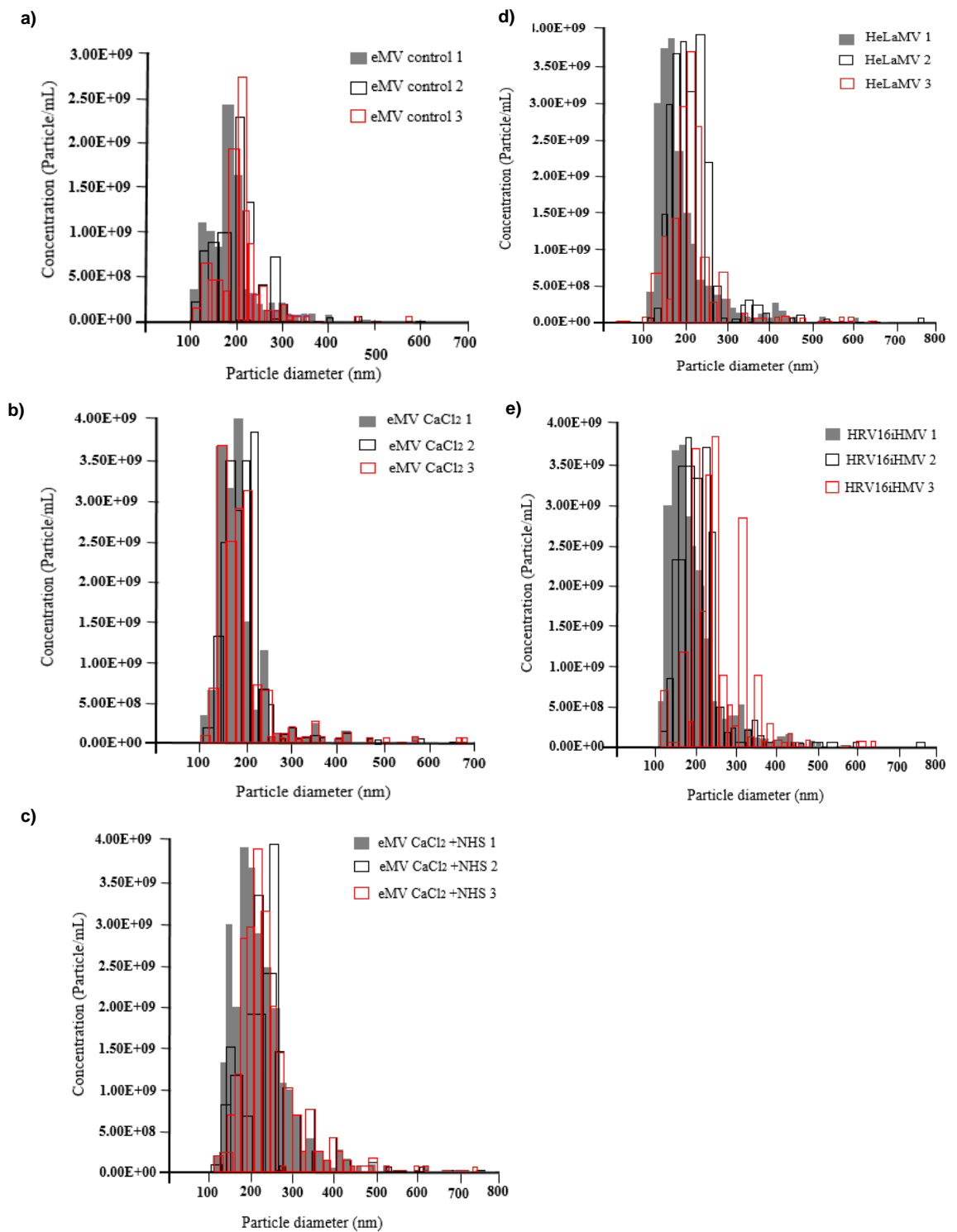


Fig. 3.1.2.3. MV sizing- assessment by qNano analyses. Size comparison of the MV group population (obtained by differential sample preparation). Where the size distribution of MV was plotted against CPC200. Fig a) to e) represents an overlay of each MV sample (N=3) as labelled on the right hand corner of each diagram. The size distribution profile for a single sample shows a fairly monodisperse profile allowing the estimation of sizes, which suggests that all MV analysed here are >100 nm and <800 nm. The IZON Control Suite software was used for the analysis of all platforms for both data acquisition and particle analysis.

To compare MV isolation methods, two approaches were employed and tested. Samples were divided as follow:

1. In approach one, samples were prepared using the classic ultracentrifugation method as in 2.2.4.1 and 2.2.4.2; and
2. In approach two, samples were submitted to the Izon qEV SEC as prepared in 2.2.4.3.

Both approaches were centrifuged at 4,000 g for 60 minutes and MV concentrated at 25,000 g. In approach two, samples were passed through the column, MV samples were loaded on the SEC and fractions were collected and gathered for concentration. All samples were analysed by FC using the protocol described in chapter 2.2.5.2 and settings in Fig. 3.1.2.1a.

The SEC method using qEV columns provided a poor MV recovery rate in terms of concentration when compared to the classic ultracentrifugation method. As Fig.3.1.2.4 shows eMV Control recovery decreased from 2.7×10^5 / mL (ultracentrifugation) to 1.3×10^5 / mL (column), eMV CaCl₂ from 2.1×10^6 / mL to 1.8×10^5 / mL and eMV CaCl₂ + NHS from 5.8×10^7 / mL to 1.9×10^7 / mL. Similarly, HeLaMVC recovery decreased from 3.1×10^5 / mL (ultracentrifugation) to 1.2×10^5 / mL (column) and HRV16iHMOV from 2.2×10^6 / mL to 2.1×10^5 / mL. The decrease may be due to the loss of particles associated with density gradient purification but, no significant differences (N=3, Mean and Error) in MV amount of release within the same method were observed.

The results presented here show that EV isolation methodologies differently affect the MV preparation/extraction and alter the quantification of total MV release. In this line, although new technology tools could represent a quick and easy method suitable for implementation, the results here (Fig.3.1.2.4) suggest otherwise. The influence of the isolation methods may lead to a different yield of MV in general and therefore, the ultracentrifugation method was used for further experiments (following results chapters).

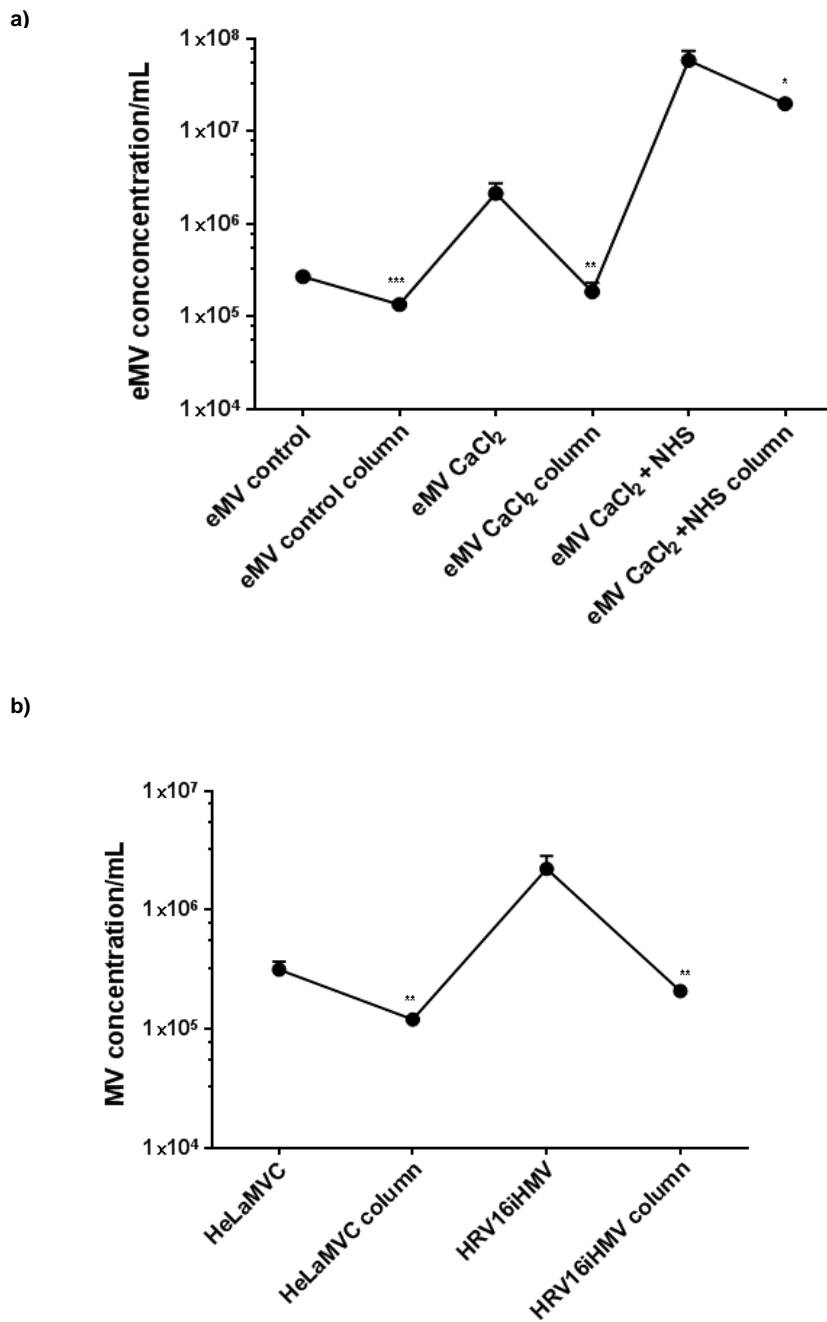


Fig. 3.1.2.4. Effect of qEV purification on MV amount of release - assessment by FC analyses. Comparison between ultracentrifugation and qEV SEC extraction methods of each MV type (N=3). Profile shows that the qEV SEC purification causes a statistically significant decrease in concentration of the samples submitted to the qEV SEC. The Mean and Error was calculated according to the variability of samples within the same group/MV type, which suggests accuracy, but statistical significance was observed whilst comparing groups of MV samples (ultracentrifugation method against column), showing P value of 0.0007 for eMV control, 0.005 for eMV CaCl₂, 0.01 for eMV CaCl₂ + NHS, 0.0032 for HeLaMVC, and 0.005 for HRV16iHMV samples.

3.1.3 Discussion

In this research, induced microvesiculation mechanisms, CaCl₂, CaCl₂ + NHS and HRV16, were used and the data obtained (Fig. 3.1.2.2) suggests that membrane perturbation can lead to a loss of phospholipid asymmetry and MV release which is in accordance with previous studies (chapter 1.2.2). The MV samples obtained in this study imply that CaCl₂, CaCl₂ + NHS, and HRV16 can induce cells to release an increased number (amount) of MV.

FC data also suggests that induced eMV samples do not significantly differ in sizes, with eMV control, eMV CaCl₂, and eMV CaCl₂ and NHS fitting in with the created MV gate (>100 nm and <1000 nm). However, HeLaMVC and HRV16iHMCV demonstrated more heterogeneity in size (larger), with a small percentage of total amount of samples observed as being present outside the gate created (<1000 nm).

However, induced samples do show statistical significance for the amount released, in comparison with the control samples. The size and concentration of a particular type of EV may be relevant to the sample quality. For example, Ferreira, *et al.*, (2013) indicated that the size of EV (the larger) secreted by human embryos could be associated with decreasing embryo quality. Their data suggested that average EV size could potentially be used to predict embryo aspects and improve the assessment of slow developing embryos. Likewise, the concentration and diameter of EV secreted by embryos derived from *in vitro* fertilisation differed from those secreted by parthenogenetic activation embryos, demonstrating that the characteristics of the population of EV vary depending on embryo competence (Mellisho, *et al.*, 2017).

FC is the widely used method of choice for MV phenotyping (Pospichalova, *et al.*, 2015; Pockley, *et al.*, 2015). The primary concern over FC analyses is the ability to reliably distinguish between EV that carry specific protein markers, and to accurately measure EV proportion and the use of proper controls that robustly validate the test and establish background levels, which are still unavailable (Hulspas, *et al.*, 2009). Nevertheless, in order to relate the measured light scattering to a particle size the FC can be calibrated by using beads that refer to the Mie theory (Hergert & Wriedt, 2012), assuming spherical particles of known refractive index. As beads meet these criteria, Mie theory can be used to determine particle-size distribution, resulting in dedicated FC being the most accurate in sizing particles with the hypothesis that MV are spheres with a refractive index (van

der Pol, *et al.*, 2014), which was previously estimated (Konokhova, *et al.*, 2012) and compatible to the refractive index of cells (van Manen, *et al.*, 2008). Here, the beads proved to be useful not only for the measurement of MV sizes, but also for the concentration as MV samples fitted with the created gate. An advantage of general FC is the knowledge of the analysed sample volume, such that the particle concentration can also be determined without calibration with beads (van der Pol, *et al.*, 2014).

In relation to MV concentration distribution, according to their sizes, the qNano proved to be a helpful apparatus by accurately distributing the concentration of MV according to their size spectrum. The qNano analyses demonstrated that MV are <800 nm.

Size profiling of different types of EV has also been suggested to be successfully measurable by Tunable Resistive Pulse Sensing (TRPS) (Harry, *et al.*, 2013). Using the IZON qNano, the movement of particles through the nanopore (NP100 target size range 40 - 320 nm, NP200 target size range 80 - 640 nm, and NP300 target size range 115 - 1150 nm) is determined by electro-kinetic (electrophoretic and electro-osmotic) and fluidic forces (Vogel, *et al.*, 2012). However, even when applying significant pressure (which is necessary sometimes), the electro-kinetic forces can, depending on particle surface charge, remain non-negligible (Kozak, *et al.*, 2012).

The accurate sizing of EV by TRPS requires that the electrical conductivity of a particle is negligible, in comparison with the conductivity of the electrolyte. Both polystyrene beads and MV meet this requirement (van der Pol, *et al.*, 2014). Nevertheless, the measurement restrictions made the TRPS measurements impractical for use in this study and when working with EV, operating the instrument was challenging and this may be due to particle aggregation. These challenges consisted mainly of a high rate of nanopore blocking (sudden drop in baseline current). The inability to recover baseline currents within 3% of calibration measurement, or to identify significant differences in particle rates between identical samples is another down side to this technology. Resulting in a measurement time of several hours, and losing the total concentration of samples.

Additionally, electron microscopy (EM) and Cryo-electron microscopy (cryo-EM) has considerably helped EV studies. Nevertheless, the nanometre-scale proposing strength of transmission electron microscopes also has pitfalls including elongated sample preparation time, deficiency of multi-parametric phenotyping, and low throughput capacity (Trajkovic, *et al.*, 2008; Conde-Vancells, *et al.*, 2010; Yuana, *et al.*, 2013).

Nanoparticle Tracking Analysis is another popular method for EV characterisation (Gardiner, *et al.*, 2016). This is a technique that uses laser light scattering and the Brownian motion of particles (Frissen, 2001) to calculate concentration and size distribution. It recognises the particles' speed in a medium of noted temperature and viscosity which may allow the calculation of its hydrodynamic diameter as well as providing specific results for labelled EV in fluorescent mode (Dragovic, *et al.*, 2011). However, it should be noted that it depends upon a variety of optimization steps by an experienced operator in order to identify convenient settings for the video capture and analysis. The high error bars in the results are regularly generated by the diversity of particle counts between each measurement (vary between samples), and this variation in the number of particles encountered is directly linked to the imprecision of the particle concentration provided by this technique (Filipe, *et al.*, 2010).

To avoid contamination of other peripheral cells Ficoll-Paque™ PLUS was used to isolate the erythrocytes pellet. This is a sterile, ready to use density gradient medium for purifying blood cells in high yield from small or large volumes of blood, and it uses a fast centrifugation procedure based on the method developed by Bøyum (1968) so that purity can be obtained (Amersham Biosciences, 2002). This is because when erythrocytes are aggregated, lymphocytes may be trapped in clumps and precipitate erythrocytes which is avoided by diluting the blood with PBS because it reduces the size of the red cell clumps. Also, erythrocyte aggregation may occur because of higher temperatures (37°C), and at lower temperatures (>20°C) the rate of aggregation is decreased (Neumann, *et al.*, 1987).

Ultracentrifugation is a common and well reported method, but similar to other methods variation in protocols (rotors speed and time) may also modify the final concentration of EV samples (Cvjetkovic, *et al.*, 2014; Lobb, *et al.*, 2015). Linares, *et al.*, (2015) reported that ultracentrifugation induces the formation of EV aggregates composed of a mixture of EV of various phenotypes and morphologies. This may cause incorrect interpretation with respect to the existence of EV bearing surface antigens from divergent cells. Throughout this PhD research, samples were sonicated briefly before FC analyses, to allow the MV to be counted as single events and avoid aggregation. Also, there are other extraction methods that may be helpful in this case, density gradient centrifugation for example, may also be used as an alternative because it enables the greater purification of EV and the potential separation of distinct subpopulations by size (Heijnen, *et al.*, 1999; Théry, *et al.*, 2001).

The SEC did not show advantages in this research. As shown in Fig. 3.1.2.4, this process loses a large number of MV compared to FC analysis and just adds an extra step to the classic ultracentrifugation method. Supporting the assertion that the classic ultracentrifugation method is still a valuable procedure to reveal the actual amount of MV that have been released under different conditions. Nevertheless, according to IZON the SEC purification of vesicles is able to remove >99% of contaminating free proteins and provides 95% removal of contaminating high-density lipoproteins from EV samples. Therefore, it might be beneficial for biological samples including urine, plasma, serum and/or ascites fluid for further characterisation/proteomic analysis.

The technical approach of the combination of SEC, also known as qEV Size Exclusion Column separation and TRPS analysis of EV are supposed to provide valuable results for EV analysis. Maas, *et al.*, (2014) demonstrated that it is possible to accurately measure the size of MV in general. However, distinguishing between MV aggregates can also be problematic, but for this research, samples were sonicated briefly before analysis, to allow the MV to be counted as single events.

Isolation of MV is a time-consuming process that increases the difficulty of large-scale sample preparation and detection. As a result it may be more practical and convenient if MV could be obtained in a shorter time, hence the alternative method. The results obtained by this PhD research using the ultracentrifugation method may meet the up to date requirement for sample collection, thus assisting in the batch processing of samples and promoting the development of MV detection. An excessive centrifugation speed might lead to fragment contamination of the MV pellet, and appropriate speed is critical for intact MV isolation. The data obtained during this research indicates that the classical ultracentrifugation (alone) at 25,000 *g* for 90 minutes is sufficient to achieve the requirements of MV sample isolation acquired for this research, and therefore this is the method of choice for subsequent analysis. Nevertheless, there are other extraction tools available today, that may be useful and can be used individually or combined for the isolation of EV including density-gradient separation, polymer-based precipitation, immune selection, microfluidic, and Tim4-based isolation methods. It is important to note that each of these methods, whilst they have been acceptable, also have their limitations (Greening, *et al.*, 2015; Furi, *et al.*, 2017).

EV/MV surfaceome and profiling (explored in the following chapters 3.2 and 3.3) in general is important in general in order to adopt the concepts mentioned above. This is

because of their heterogeneity and they may express different characteristics between induced and not induced samples. Utilising purer isolates consisting of a single subpopulation of EV, and using the knowledge regarding influence and advantage of unlike subpopulations of EV, it can become possible to judge whether subpopulations display therapeutic potential and indeed activity as mentioned by Tkach, *et al.*, (2017) in their opinion article.

A combination of the different approaches described here may be able to provide useful information on the amount of MV released from inducements. These methods should be further assessed and validated by comparing measurement results, so that precise, reliable, and fast extraction methods and measurements analysis can eventually be translatable from the bench to the clinic, in which are being addressed by researchers (yearly ISEV meetings/workshops). Indeed, this field of research is rapidly developing and extraction methodologies/tools are advancing, but reliable studies on EV profile and content in general are needed for a better understanding of their role and for a possible use in clinical settings, for example, the use of MV in tissue regeneration (Panagiotou, *et al.*, 2016). These may include combining complementary characterisation approaches, which are investigated during this research (following results chapters 3.2 and 3.3).

3.2 An investigation into key biomolecules required for MV communication and survival

The communication network between the cell microhabitat and the cell centre is vital to understand their potential behaviour, and the Extracellular Matrix (ECM) components perform a significant role in signalling network transduction. This is because of their capacity to travel to the nucleus upon attachment to the cell's interior mediated by adhesion molecules (Lelièvre & Bissell, 1998). Important information may be transduced from the membrane to the nucleus of cells, and the potential function of MV in communication and intercellular signalling is dependent on their cargo (as it is for cells), including different biomolecules particularly when taking into account their biogenesis (Valadi, *et al.*, 2007; Subra, *et al.*, 2010).

As a result of standing-in as inducers and coordinators of biochemical cascades, these biomolecules including proteins, can promote the chemical and mechanical mechanisms of intracellular signalling (Lelièvre & Bissell, 1998). Therefore, this chapter intends to identify the biomolecules present in MV samples acquired during this PhD research that may be involved in the communication network, and how MV can potentially survive in the microhabitat.

3.2.1 Surface markers identification in MV samples

3.2.1.1 Introduction

MV composition (especially their membrane) contains general characteristics inherited from their parent cell making them naturally non-immunogenic, which may allow them to communicate and to resist fast clearance from circulation and thereby increase delivery efficiency to target tissues (Johnsen, *et al.*, 2014; Wiklander, *et al.*, 2015). Identifying/profiling EV “surfaceome” might not only lead to the identification and development of new diagnostic markers and therapeutic targets, but it could also provide insight into the biology of unknown substances, including environmental interactions and the identification of important cellular subtypes and signalling pathways (Gedye, *et al.*, 2014). This includes possible ways to communicate with neighbouring cells (see chapter 1.5).

Cluster of Differentiation (CD) antigens can act as ligands and receptors, and can control cell adhesion, cell signalling and even adaptive immunity. The concept of the receptor-

ligand interaction is an important component to the activity of biological systems (Engin, *et al.*, 2017), and it may allow MV/cells to transmit a message to one another. A MV/cell might present a receptor in its membrane and when it binds to a complementary ligand on a nearby MV/cell, may allow the receptor to operate its function.

An example of this receptor-ligand interaction is CD58 (widely expressed in erythrocytes and tested for in this chapter), a Lymphocyte Function-associated Antigen 3 (LFA-3) interaction with CD2 (for example). CD2 is a transmembrane glycoprotein commonly expressed on virtually all T cells and functions in both T cell adhesion and activation processes (Tibaldi, *et al.*, 2002). CD2 is known to bind to the CD58 through counter-receptor interaction, which empowers the opening stages of T cell connection with the antigen presenting cells (APCs) (Meuer, *et al.*, 1984). The adherence of domains between CD58 and CD2 allows the antigen recognition activity by supporting cell-cell contact (Tibaldi, *et al.*, 2002).

Bierer, *et al.*, (1998) demonstrated that LFA-3+ L cells (can be found in the ileum, large intestine-colon, duodenum and jejunum), together with anti-CD3 (a T cell co-receptor allows the activation of the cytotoxic T cell, CD8+ naive T cells, as well as T helper cells, CD4+ naive T cells monoclonal antibody) or with doses of Phytohaemagglutinin (PHA) (a mitogenic agent used as a red-cell agglutinating agent that promotes proliferation of human peripheral blood T cells) promotes proliferation of human peripheral blood T cells. Moreover, proliferation was inhibited by monoclonal antibodies directed against either CD2 or LFA-3 and resulted in the increased expression of key molecules including the interleukin-2 receptor (IL-2R). Their data supports the fact that LFA-3 plays a role in CD2-dependent T cell activation.

Given the importance of surface markers to a wide range of biological processes and their broad utility as research and clinical tools for identifying specific characteristics of biological samples, this PhD research studied a panel of surface markers to test the hypothesis that markers signify MV differentiation, identification and potential role including:

1. Annexin V binds specifically to phosphatidylserine (PS), a phospholipid component of the cell membrane, acting as important activators in cell cycle signalling, specifically in relation to apoptosis (Lizarbe, *et al.*, 2013). FITC-conjugated Annexin V can be used as a fluorescent probe to label the phosphatidylserine of the plasma membrane from the inside surface to the

outside surface. The exposure of PS on the cell membrane of cells draws a signal for recognition and engulfment by phagocytic cells (Vance & Tasseva, 2013). Annexin V is extensively used in this research area and it is categorised as a marker for MV in general due to the exposure of PS (Chandler, 2016; Kong, *et al.*, 2015).

2. CD235ab (antibody HIR2) recognises N-terminal of glycophorin (GYP) A and faded signal of GYP (B) and are the major transmembrane sialoglycoproteins. These are a combination of sialic acid and glycoprotein/GYP, itself sugar and protein expressed on erythrocytes and their precursors. They supply the cells with a substantive amount of mucin-like surface, minimising aggregation between erythrocytes in the circulation. GYPA is the carrier of blood group M and N specificities, while GYPB accounts for S, s and U specificities (Poole, 2000).
3. CD54 is a transmembrane glycoprotein (GP) expressed on many cells including T lymphocytes, B lymphocytes, monocytes, macrophages, granulocytes, activated endothelial cells, epithelial cells, and dendritic cells. The expression of CD54 is upregulated by activation. It binds to Intercellular Adhesion Molecule 1 (ICAM-1) and mediates cell adhesion by binding to integrins CD11/CD18. The interaction of CD54 with Lymphocyte function-associated antigen-1 enhances antigen-specific T-cell activation (Roebuck & Finnegan, 1999). CD54 has been reported being a cell surface entry receptor for HRV (Shukla, *et al.*, 2017).
4. CD46 (antibody MEM-258) is a type I membrane protein that identify an epitope on SCR4 (the membrane-proximal SCR) domain. CD46 is expressed on platelets, granulocytes, monocytes, T and B lymphocytes, fibroblast, epithelial and endothelial cells. It is negative on erythrocytes under normal circumstances. CD46 in its monomeric form is an important governor of the complement activation cascades (classical and alternative), by preventing amplification of the activities on CD46 presenting cells by factor I to the proteolysis of deposited C3b and C4b. Thus, protecting the host cell from damage by complement activity (Liszewski & Atkinson, 2015). CD46 also serves as a receptor for several human pathogens (both bacteria and viruses). When CD46 is expressed on T lymphocyte its ligation alters the polarization toward antigen-

presenting cells or target cells, inhibiting lymphocyte function (Barilla-LaBarca, *et al.*, 2002; Persson, *et al.*, 2010).

5. CD14 (18D11 antibody) is a lipopolysaccharide (LPS) receptor. It is a 55 kDa Glycosylphosphatidylinositol (GPI)-anchored GP, constitutively expressed on the surface of mature monocytes, macrophages, and neutrophils. CD14 serves as a multifunctional LPS receptor. It is also released to the serum as a secreted and in an enzymatically cleaved GPI-anchored form. CD14 binds to the lipopolysaccharide molecule in a reaction catalysed by lipopolysaccharide-binding protein (an acute phase serum protein). CD14 affects allergic, inflammatory and infectious processes and it is a specific marker for monocytes/macrophages (Pugin, *et al.*, 1998; Ziegler-Heitbrock & Ulevitch, 1993).
6. CD36, antibody TR9 reacts with glycoprotein integrin beta 3 subunit –GPIIIb, a fatty acid translocase (FAT) - beta subunit of the platelet membrane adhesive protein receptor complex. It is a ditopic glycosylated protein that belongs to the class B family of scavenger receptors, and is widely expressed. It operates in affinity with tissue uptake of long chain fatty acids, and helps lower excessive fat supply to lipid assembly and metabolic impairment. CD36 can bind to multiple ligands with its alliance with other transmembrane proteins, supplying to the diversity of its signal transduction. The ligands can diversely control CD36 signalling and downstream protein-protein interactions within metabolic protein clusters (Pepino, *et al.*, 2014; He, *et al.*, 2011).
7. CD58, is widely expressed by both haematopoietic and non-hematopoietic cells, often on antigen presenting cells. CD58, antibody MEM-63 reacts with the Lymphocyte Function-associated Antigen (LFA)-3, an immunoglobulin family adhesion molecule. As previously mentioned in this chapter, it serves as a ligand of CD2, an interaction that is essential for T cell-mediated immunity. In its transmembrane form, CD58 activate kinase activity and its GPI-anchored form interactions are associated with protein kinases (Li, *et al.*, 2009; Itzhaky, *et al.*, 1998).
8. CD63, is a 40-60 kDa tetraspanin GP expressed by platelets, monocytes/macrophages, granulocytes, endothelial and T cells. CD63 antibody

MEM-259 reacts with lysosome-associated membrane protein LAMP-3. Cellular surface exposition of CD63 is usually activation-dependent. CD63, the LAMP-3 is a GP of tetraspanin family, and is present in lysosomes, late endosomes, and secretory vesicles from a variety of cell types. CD63 also serves as a T-cell co-stimulatory molecule (Pols & Klumperman, 2009).

9. Human Leukocyte Antigen (HLA)-ABC monoclonal antibody recognises an epitope common among 43 kDa chains of the HLA-ABC antigens. HLA-ABC are detectable on virtually every human nucleated cell. HLA-ABC reacts the human Major Histocompatibility Complex (MHC) class I. HLA-A, B, and C, and the frequency of this antibody makes it a very good candidate for a positive control for HLA tissue typing and cross matching. MHC class I antigens associated with β 2-microglobulin are expressed by all human nucleated cells and are central in cell-mediated immune response and tumour surveillance (Giacomini, *et al.*, 1997).

As previously described (see chapter 3.1.1) FC is a higher-throughput technique, allowing rapid analysis of significant numbers of MV in liquid suspension. Nevertheless, a persistent concern in FC analyses is the inability to reliably distinguish between the positive and negative population of samples and to accurately measure the positivity of labelling without appropriate control. This is useful to describe quantitatively, and qualitatively the degree of separation between the populations that may be present in the same sample. A prerequisite for exploiting these tools is the proper use of control samples to confirm that the test sample was prepared correctly and to establish the level of machinery background (noise) (Hulspas, *et al.*, 2009).

This chapter aims to identify EV surface markers, and direct labelling was used because it can provide reliable information about their expression, as well providing an insight into their distribution in heterogeneous samples. FC utilise chemically or fluorescently tagged antibodies to detect surface markers. The assay is specific, sensitive and reproducible, and can provide information at the level of individual MV (Gedye, *et al.*, 2014).

3.2.1.2 Results

In this result chapter, the investigation focused on the percentage (%) fluorescence signal of surface markers of labelled eMV control, eMV CaCl₂, and eMV CaCl₂ +NHS

(HeLaMVC and HRV16iHMV as parallels) samples. This was performed by using fluorescence FC Sub-micron Particle Size Reference, to act as a reference for the MV samples fluorescence intensity/expression utilising the FC Express Plus assay.

The FC Sub-micron Particle Size Reference Kit provides a set of green fluorescent microsphere suspensions to serve as reliable size references for FC users. All the microspheres are green (excitation and emission maxima at 505 nm and 515 nm), and the beads show excitation and emission profile similar FITC (excitation and emission maxima at 490 nm and 525 nm) stained samples. This is ideal for the Guava EasyCyte HT system because the green fluorescent dye molecules are localised within the bead polymeric matrix, which makes the beads brighter and photo stable and therefore, selected for use in this work.

The Dot plots in Fig. 3.2.1.1a represent the levels of fluorescence versus reduced wide-angle SSC-log. The analysis was conducted by raising the fluorescence threshold, and noise events could also be eliminated, and then 500 nm and 2000 nm-sized fluorescent beads were subjected to FC measurements set at SSC-Log. These allow for particles/cellular differentiation within a heterogeneous population against Green fluorescence-Log (GRN-Log), differing from those applied in chapter 3.2.1, Fig 3.1.2.1a, where SSC-Log against FSC-Log was used. The beads were overlaid over each other and the MV gate was created, discriminating vesicles that did not fit within the parameters created according to the fluorescence size beads and fluorescence scale.

The green fluorescence-based thresholding was used to analyse the fluorescence intensity of the beads and the events are shown in Fig. 3.2.1.1b against PBS buffer (left hand side of the histogram). This demonstrated a low fluorescence signal against high fluorescence provided by the size beads (right) threshold, where the amount of fluorescent signal obtained is equivalent to the number of fluorochrome molecules on the particles. The histogram peaks allow the intensity of the fluorescence to discriminate positively or negatively labelled samples and to assess the percentage fluorescence in the sample. As the sample penetrates the laser beam spot, it precipitates scattered light and fluorescence signals that display in a stream of electrons (current) from the anode of the photomultiplier tube (PMT). The extent of the current is equivalent to the number of photons that touch the photo cathode, which is also equivalent to the intensity of the scatter or fluorescence signal created by the sample. While the sample joins the laser beam spot, the production of the PMT increases, achieving peak volume and where the particle is

fully illuminated, reaching the greatest total of optical signal. This production of a pulse is considered the “event”, where height signifies the maximum amount of current output by the PMT, area signifies the integral of the pulse, and width signifies the time interval in the course of pulse occurrence (BIO-RAD laboratories, 2014).

The fluorescence expression of the size beads acted as a reference for fluorescence intensity for the MV samples. This is shown in red representing the positive (+VE for >50% stained) labelled samples. Grey represents the negative (-VE for <50% stained) labelled samples. Additionally, the background fluorescence and background noise were excluded in Fig. 3.2.1.1a positioned in the left hand side of the dot plot diagram along with the fluorescence signal of the size beads (500 nm-2000 nm), shown in Fig. 3.2.1.1b.

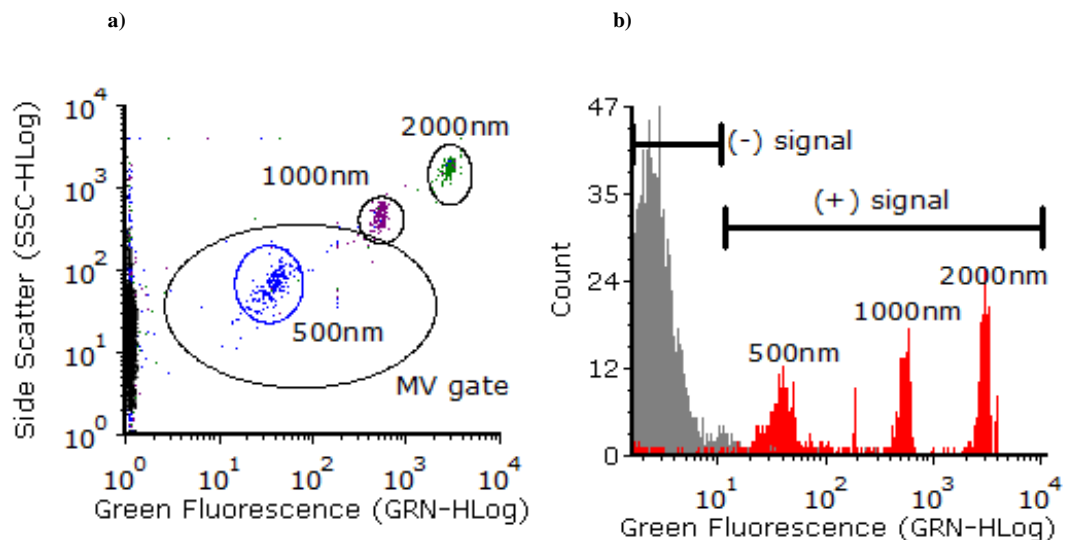


Fig. 3.2.1.1. Fluorescence intensity measurements – assessment by FC analyses. Where a) represents the dot plots acquired with the fluorescence size beads, which were used to create the MV gate and to establish appropriate instrument settings against buffer/noise (left hand corner of the diagram). The MV gate was defined as >100 nm and <1000 nm, by verifying the resolution capabilities of the FC against beads, which was also used to define the size distribution of all samples according to the fluorescence intensity. The dot plot cluster of the 500 nm was purposely used to create the MV gate. In b) the % intensity of each sample (size beads) is shown. On the left hand side (grey), samples/events represent negative staining and low fluorescence intensity, whereas the events (fluorescence size beads) shown on the right (red), represent positive fluorescence intensity. The parameters (histogram) were plotted as channel vs. number of events and FCS Express 6 FC and Image Cytometry Software was used for the analyses.

Generally, any cell membrane disruption/remodelling can cause non-specific binding of Annexin-V to PS from the inner face of the plasma membrane to the cell surface. FC analysis revealed that samples obtained here reacted with Annexin V, suggesting PS exposure on their surface, where all MV samples were positively (fluorescence signal) labelled with PS/Annexin V, representing a non-specific marker. This can be observed in Fig. 3.2.1.2 using the parameters established in Fig. 3.2.1.1. Annexin V stained MV samples (red histograms) were plotted against unstained MV samples (black histograms),

and the majority of the peaks show the highest intensity to be between 10^1 and 10^2 against unstained samples ($<10^1$). eMV control displayed a different profile (less concentrated) due to the length of time in the laser beam spot. It is important to note that because Log scales cannot exhibit samples with zero or negative values, these particles are compressed on the Y axis in the Log displays (black histograms) present.

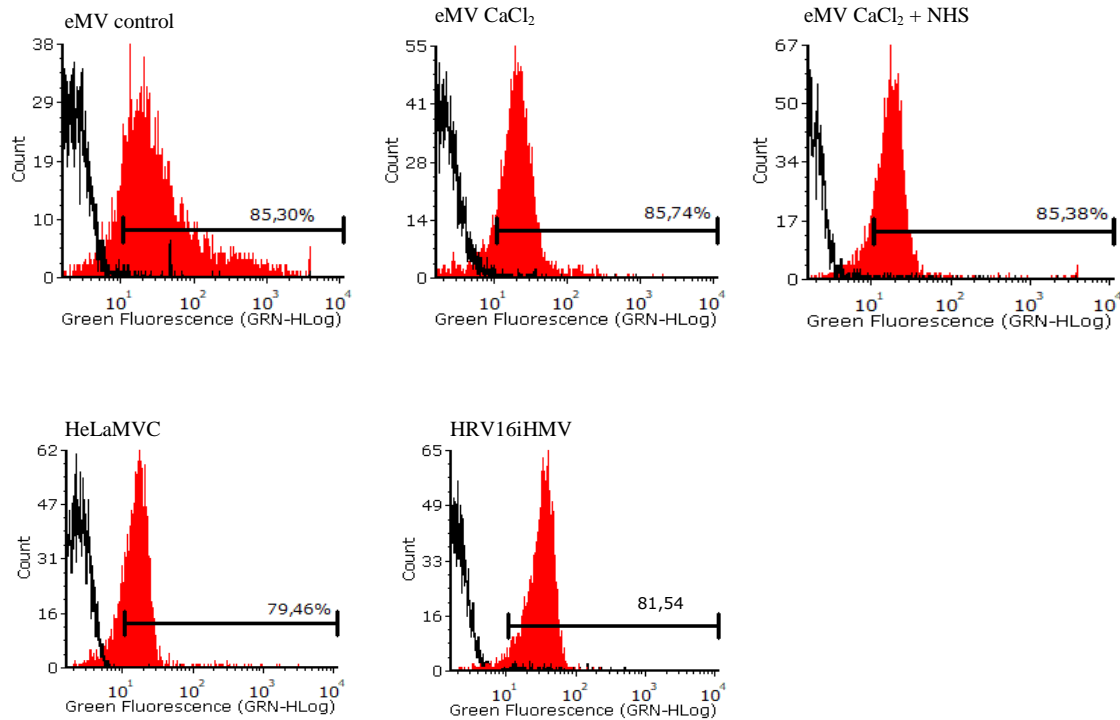


Fig. 3.2.1.2. Fluorescence gating - Annexin V (non-specific marker) labelled MV. Represents % fluorescence gated according to the parameters established in Fig. 3.2.1.1. The MV gate was defined as <1000 nm by verifying resolution capabilities of the FC against beads, which was also used to define the size distribution of all samples displayed as the SSC HLog vs. FSC-HLog. The positive fluorescence intensity of all MV samples (as titled) was established according to the settings in Fig. 3.2.1.1b. Unlabelled MV samples (different for each MV type) were overlaid over Annexin V labelled samples to provide differentiation between % fluorescence signals. FCS Express 6 FC and Image Cytometry Software was used for this analyses.

To observe the general changes (switches) between samples showing positive fluorescence intensity and those showing unlabelled features, the parameters established in Fig. 3.2.1.1 were used. Each and all MV samples were tested for non-specific IgG1-negative isotype control and the same IgG1-negative isotype stained sample was used for its type of MV. For example, one IgG1-negative isotype eMV control was used for all CD tested here for eMV control samples. The black histograms (IgG1-negative isotype stained samples) may appear differently in different plots, and this is due to the number of events occurring within labelled samples (more events), when overlaid over positively stained samples.

The IgG1-negative isotype control labelled samples displayed similar characteristics to the unstained MV samples (Fig. 3.2.1.2). This is showing particles being compressed on the Y axis in the Log displays (black histograms) particularly for eMV control and HeLaMVC. Whereas the other MV samples displayed a slight switch to the left side of the histogram, displaying a small amount of positive staining (<50% is considered to be the negative threshold).

The expression of several CD's used here, have been reported showing specific expression on the MV cell of origin (source - generally accepted surface profile). This was investigated and the results are set out in MV samples prepared here (Fig. 3.2.1.4). The results revealed that the MV originated from and were positively stained for the surface markers present in their source of origin (erythrocytes and HeLa cells) in accordance with their basic characteristics. For instance, the erythrocyte marker CD235ab, showed positive fluorescent signal on all eMV samples with >92% expression, and it was negative for HeLaMVC and HRV16iHMV (Fig. 3.2.1.4a) showing >93% positive stain for the negative marker (fluorescence intensity). Another example that justifies sample purity (source/parent cell) is set out in Fig. 3.2.1.4b, where all MV samples were tested for CD54, and showed >72% fluorescence intensity (positive marker) for HeLaMVC and >96% for HRV16iHMV (typically expressed on endothelial cells and a positive marker for ICAM1-receptor for HRV16), but >83% for the negative marker for all eMV samples.

CD46 (Fig. 3.2.1.4c), the preventer of complement cascade amplification displayed >69% for the negative marker in eMV samples, and >84% positive staining in HeLaMVC and HRV16iHMV samples.

MV samples did not bind to CD14 (Fig. 3.2.1.4d), confirming that samples obtained here were derived from the expected sources (erythrocytes and HeLa cells), whereas CD58 (Fig. 3.2.1.4e) and CD36 (Fig. 3.2.1.4f) were positive in all samples. In contrast, CD63 (Fig. 3.2.1.4g), was not observed in the eMV control, but was slightly expressed in the other samples (>60%). HLA-ABC (Fig. 3.2.1.4h) was negative in all eMV samples, but present in HeLaMVC and HRV16iHMV samples (>90% positive).

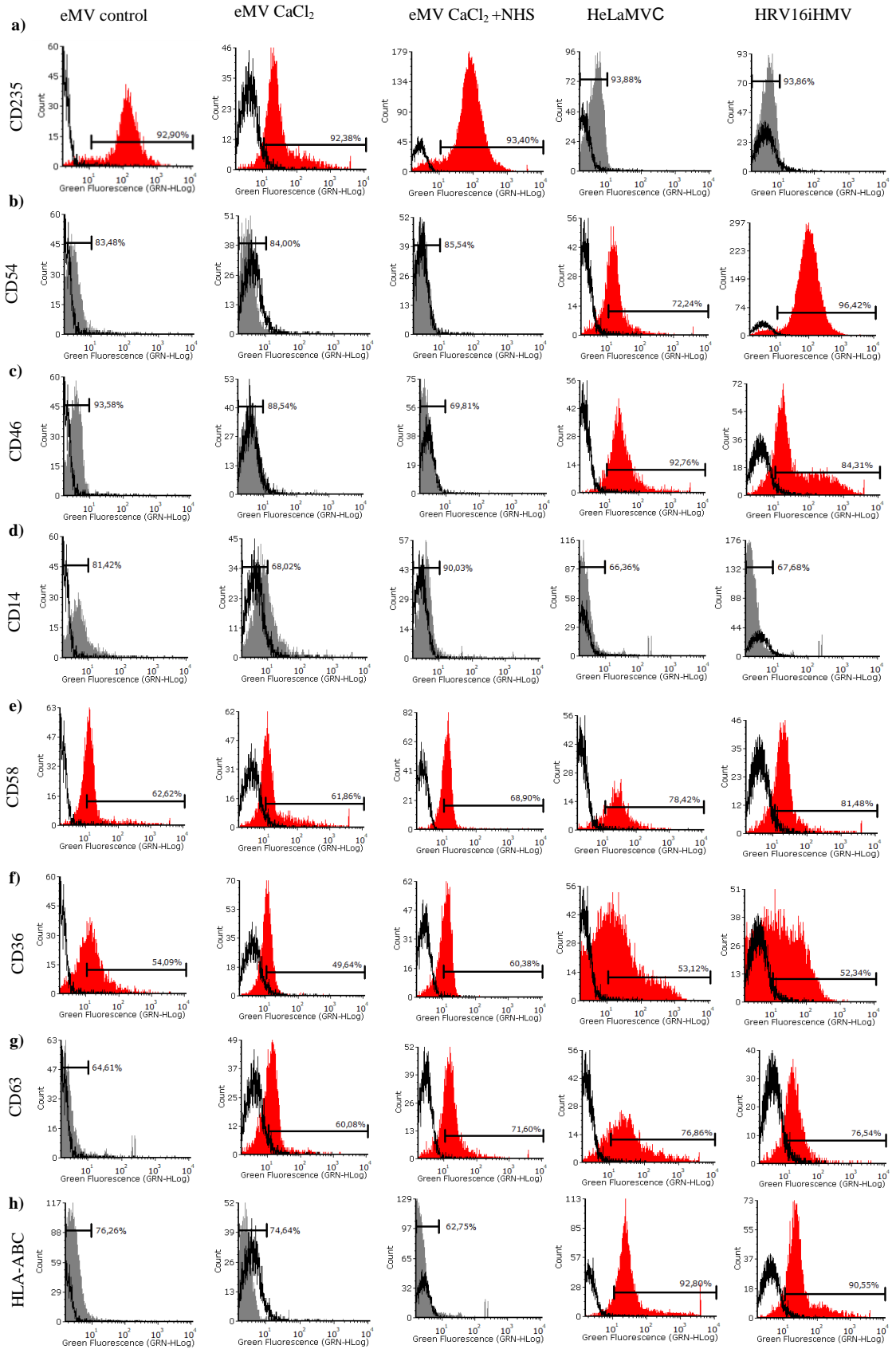


Fig. 3.2.1.3. CD percentage fluorescence intensity in all MV samples. Fluorochrome-conjugated Mouse IgG1 (negative isotype control- black overlaid line) was plotted against events (counts) of positive (red) and negative (grey) markers established in Fig. 3.2.1.1. This was used to discriminate/divide between positive and negative events according to the parameters established using the fluorescence size beads. Each MV sample was tested for Mouse IgG1 (negative isotype staining control) and used against all CD's markers for each sample (overlaid over positively or negatively stained samples). These events are drawn to include the % of staining as seen in the events created with the MV gate (fluorescence size beads). FCS Express 6 FC and Image Cytometry Software was used for this analyses.

The selected panel of surface expression is shown in summary in Fig. 3.2.1.4, where MV samples were labelled with different CD's, including (-VE) and (+VE) labels, and analysed via Guava Express Plus software (Fig. 3.2.1.3). Not all MV samples were positive or negative for the same label, which simultaneously highlights their differences and their similarities, which may be dependent on the stimuli used (or control) and/or differentially regulated biological processes between them. The triplicates of each MV sample did not demonstrate a significance (Mean and Error) between expression within themselves (same type of MV), apart from eMV CaCl₂ +NHS labelled with CD46 and CD63, which showed expression between the (-VE) and (+VE) markers (established in Fig.3.2.1.1b).

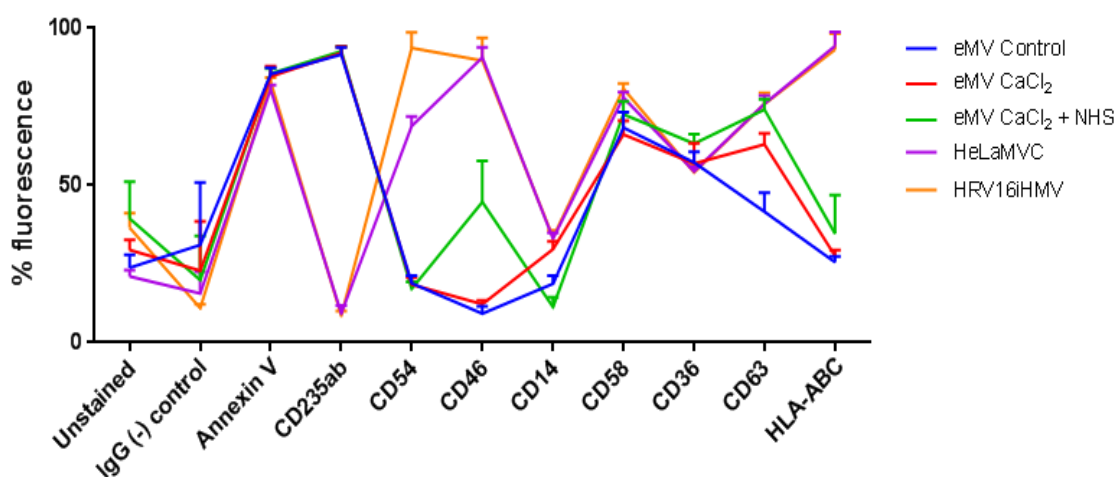


Fig. 3.2.1.4. Fluorescence intensity (in percentage) summary for positive markers. Represents the Mean Fluorescence Intensity (MFI) in % of all three repeats of each MV sample against each label and according to parameters established in Fig. 3.2.1.1b. This compared to the appropriate controls (unlabelled and IgG negative control MV samples- N=3) which provides differentiation between % fluorescence signals. The increase in percentage indicates the increase in marker/antibody binding. FCS Express 6 FC and Image Cytometry Software was used for the percentage analyses and GraphPad Prism was used to plot the XY graph (Mean and Error).

3.2.1.3 Discussion

Accurate and specific phenotyping analysis of EV is important due the implementation of biomarker profiling and its use in the clinical setting, but the issues are well understood and this is mainly due to their heterogeneity. The Journal of Extracellular Vesicles (official journal of ISEV) and ISEV members have released a variety of position statements and articles outlining experimental requirements, and suggestions for EV characterisation including Lötval, *et al.*, (2014) and Van der Pol, *et al.*, (2016). Despite, providing valuable information, this field still requires further development.

It is a widely accepted that Annexin V, a specific ligand to phosphatidylserine (PS) exposure on the cell surface is a common feature of MV release (György, *et al.*, 2011) because this phenomenon has been observed in MV derived from different cell types. For instance, platelets and erythrocytes (Jayachandran, *et al.*, 2012). PS exposure on the surface is considered a specific characteristic in apoptosis and it is due to the affluence of phospholipid in membranes, its negative charge and its talent to exchange interactions with other lipids priming the disruption of lipid rafts (Balasubramanian & Schroit, 2003; Demchenko, 2013).

Nevertheless, PS exposure is not only conditional for apoptosis and may indicate different pathological conditions. For instance, it has been reported that the occurrence of PS expression on the surface of endothelial cells of tumour vasculature and stressed tumour cells, and has demonstrated its potential as a biomarker for non-invasive imaging and drug targeting (Stafford & Thorpe, 2011). The exposure has also been observed on platelet activation, being a part of the blood clotting process (Heemskerk, *et al.*, 2002).

The surface marker profile of MV samples observed here correlates with those from their parent cells when specific markers were used. CD235 is a specific marker for erythrocytes (Grisendi, *et al.*, 2015), and CD54 is a specific marker for ICAM-1 (HRV16 receptor) (Shukla, *et al.*, 2017). Therefore, there was an expectation of a positive result for their derived MV also providing evidence of a strategy for determining sample quality of their original source (parent cells).

CD46 expression was observed on HeLaMVC and HRV16iHVMV during this study. It is well understood that this encoded protein can act as a receptor for a variety of viruses including the Edmonston strain of measles virus, human herpesvirus-6, and type IV pili of pathogenic *Neisseria* (Plant & Jonsson, 2006). It is also known to be conserved in Adenovirus (Gaggar, *et al.*, 2005). The binding to HRV16iHVMV samples may be because HRV expresses a cytosolic 3C protease that has been hypothesised to mediate antagonism, which was predicted to cleave complement C3 (Tam, *et al.*, 2014). It is also known that CD46 is expressed by all nucleated human cells (Joubert, 2014), which may provide an explanation of why it was weakly (negative) bounded to eMV CaCl₂+NHS, and negative for eMV control and eMV CaCl₂ (erythrocytes do not have nucleus). Moreover, the role of this membrane cofactor protein in regulation of C4b and C3b deposited on cells, is interesting because this expressed complement regulatory protein safeguard host cells from complement activity. This type-I membrane GP serves as a cofactor for the serine

protease factor I, to mediate inactivation of C3b and C4b deposited on host cells (Liszewski & Atkinson, 2015).

It is notable that erythrocytes have previously been considered negative for CD36, whereas in this research there was a slight expression in eMV samples. The results obtained here are consistent with an early study by Van Schravendijk, *et al.*, (1992), detecting CD36 on the majority of normal adult erythrocytes. Particularly, when comparing with staining for GYPA, LFA-3, and CR1, the level of expression of CD36 was low, but nonetheless present. However, FC technology has advanced since then. Nevertheless, normal erythrocytes can adhere to plastic coated with anti-CD36 monoclonal antibodies, suggesting that the level of expression of CD36 on normal erythrocytes is sufficient to be important in cell adherence. This may suggest that eMV could inherit this molecule during microvesiculation.

Additionally, CD36 is a membrane GP present on platelets, mononuclear phagocytes, adipocytes, hepatocytes, myocytes, and some epithelia. Moreover, CD36 in a variety of cells is localised in specialised cholesterol-rich membrane microdomains and may interact with other membrane receptors, including tetraspanins and integrins. Recognition of CD36 signalling pathways in specific cells evoked in response to specific ligands may result in novel targets for drug development (Silverstein & Febbraio, 2009).

The process of erythrocytes accumulation under low flow conditions by the capture and adhesion of normal erythrocytes to surface-adherent neutrophils and platelets observed, is distinct from the process of passive entrapment within fibrin fibres (Goel & Diamond, 2002). Goel & Diamond hypothesised that under venous flow conditions erythrocytes via receptor-mediated adhesion could attach to activated neutrophils, activated platelets, and surface-deposited fibrin. Their research implicate inflammatory responses causing neutrophil or platelet arrest and activation on activated endothelium, with subsequent receptor-mediated capture of erythrocytes under low flow conditions in the development of deep vein thrombosis. Erythrocytes attach to a thrombospondin-coated purified fibrin surface, but do not adhere to purified fibrin. Goel & Diamond visualised short-lived adhesion events (< 5 seconds) between erythrocytes and platelets, neutrophils, or fibrin as well as firm adherence of erythrocytes. All interactions were assisted by erythrocyte membrane deformation and membrane tethering upon binding.

Likewise, CD58 is not a traditional erythrocyte marker. The influence of the age of the erythrocytes within its lifecycle at the time of blood donation on the erythrocytes storage lesion is still not well understood (Bicalho, *et al.*, 2013). Nevertheless, the expression of cell adhesion molecules including CD58, GYPA and PS on young and old erythrocytes density separated prior to storage was determined by FC (Sparrow, *et al.*, 2006). According to their results, older erythrocytes showed significantly reduced expression of GYPA throughout storage. Storage in the presence of leukocytes caused a significant decline in the expression of CD58 and GYPA, whereas erythrocytes that were pre-storage leukocyte depleted, maintained a relatively consistent level of expression throughout storage. Increased levels of Annexin V were detected in the supernatant of erythrocytes stored in the presence of leukocytes, with significantly greater supernatant levels found in older erythrocytes when compared to young erythrocytes. These findings provided an insight into the erythrocytes storage lesion and indicated that erythrocyte age at the time of donation may impact upon the quality of stored erythrocyte concentrates. This was acknowledged during this PhD research (storage time), and erythrocytes were immediately used after separation from other blood cells. However, these processes were not tested during this research project.

Among tetraspanins CD63 has a broad tissue distribution, while others are restricted to specific cells. For example, CD37 and CD53 in haematopoietic cell and microscopy studies have shown that tetraspanins are abundant on various types of endocytic membranes and have been widely used as exosomal markers (Andreu & Yáñez-Mó, 2014). However, since tetraspanins are ubiquitous in the plasma membrane, they may be present in the wider subpopulations of EV, and in some cases, do not permit successful discrimination of exosomes from other EV because all EV subtypes originate through budding from the plasma membrane and could not be distinguished from exosomes only by CD63.

eMV did not show a positive signal for HLA-ABC. This is because their parent cells (erythrocytes) do not generally have HLA molecules (De Villartay, *et al.*, 1985), in contrast to HeLa and HRV16 MV samples. Likewise, CD14 was negative for all MV samples in this research. It is a known specific marker for peripheral monocytes, and it was used here as a negative antibody control in order to enhance the hypothesis that the samples collected here only derived from the original source of choice. Nevertheless, this assumption could not be proven because erythrocytes probably picked up other cell

markers in circulation (CD36, CD58 and CD63), which were then assumed to be passed on to eMV or eMV adhering to these molecules whilst in the microenvironment.

Byron, *et al.*, (2010), explained the manner that adhesion receptors may be used to regulate chemical signalling by controlling the spatial-temporal congregation of enzymes and adaptors. This is demonstrated evidence that cell and ECM interactions also perform as sites of mechanotransduction, transferring short-range elastic force beyond the plasma membrane and understanding long-range alterations in tissue. Important information was acquired into the duty of integrins as mechanosensitive receptors that present catch-bond characteristics.

The interaction network for the surface markers observed here (eMV samples) is extensive and their ligand-receptor arrangement potential is shown in Fig. 3.2.1.3.1. This is where the receptors-ligand may reveal a surprising quantitative and qualitative variation in receptor binding strengths providing a substantial source of novel recognition pathways and biological support, revealing the likely communication paths further motivating the need to understand the challenges and opportunities in pursuing selected target molecules. Each and every one of these proteins proposes different ways to communicate/signal with nearby cells. However, the communication network will also depend on the surface markers (receptor/ligands) present in the neighbouring cells for the MV-cell communication to occur successfully, according to the principles of cellular communication introduced in chapter 1.5.

Legend:

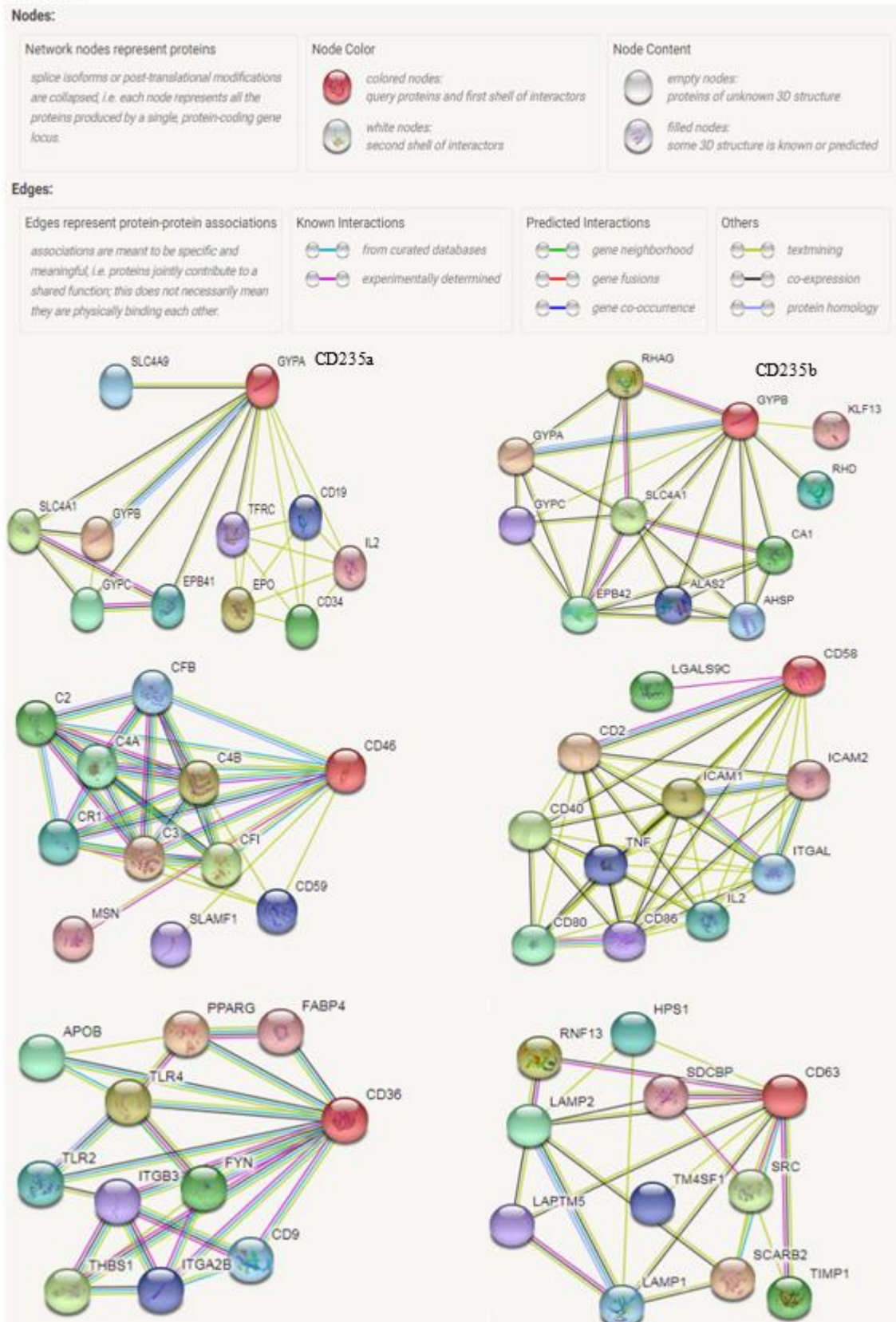


Fig. 3.2.1.3.1. Protein interaction network for surface markers present in eMV. String database- CONSORTIUM 2017 (Szklarczyk, *et al.*, 2015). The analysis provides a system-wide understanding of all functional interactions between the surface markers present in eMV. The data is collected from a variety of sources and aims to integrate the information in a single diagram, by consolidating known and predicted protein-protein association data. The associations in this database include direct (physical) interactions, as well as indirect (functional) interactions, as long as both are specific and biologically meaningful to the protein (name) provided.

3.2.2 Total protein identification in MV samples

3.2.2.1 Introduction

A large proportion of cell surface receptors respond to the specialised actions of transmitters including hydrophobic signal molecules such as steroid and thyroid hormones that can diffuse across the plasma membrane of the target cell, and activate intracellular receptor proteins that directly regulate the transcription of specific genes (Cooper, 2000), and/or by triggering heterotrimeric guanine nucleotide binding proteins (G proteins). The binding of a G protein is consummate by the dissociation of their subunits which in turn modulate target effectors (Robillard, *et al.*, 2000). They commonly operate as molecular triggers in the intracellular environment because they transmit signals from various biological processes from the external to the internal environment. A large number of G-protein-coupled receptors have been demonstrated to induce multiple signalling pathways when expressed in a variety of cells (Hutchings, *et al.*, 2010), because they act as signal transducers (see chapter 1.5), converting the extracellular binding event into intracellular signals that alter the behaviour of the target cell (Alberts, *et al.*, 2014).

When MV are released into the extracellular space they can bind to neighbouring cells by acting locally or by travelling passively through the bloodstream for a more paracrine destination, or they can even be directed by marginal zone phagocytes in the spleen and liver (Robbins & Morelli, 2014). Therefore, once released by a variety of cell types, MV may have several fates themselves as well as being able to transfer molecules/messages to neighbouring cells and changing their fate, all of which dictate their potential function and survival depending on their cargo.

This chapter aims to identify a number of proteins to test the hypothesis that their characteristics, signify MV differentiation and identification as well as, their potential survival in the extracellular space including:

1. CD47 (integrin-associated protein) is a ubiquitously expressed cell surface transmembrane glycoprotein (GP). CD47 interacts with several integrins that attach the cytoskeleton to the extracellular matrix, and biochemically, by sensing whether adhesion has occurred and regulating their functions. Through soluble ligands or counter-receptors, CD47 modulates various signalling pathways including the activation of heterotrimeric G-proteins. CD172a (signal regulatory

protein α , SIRP α), an immune inhibitory receptor on macrophages ligates with CD47 resulting in CD47-positive cells that can avoid phagocytosis (Oldenberg, 2013).

CD47 has displayed the capability to have an impact on a variety of additional biological processes through interaction with different receptors, or because of the signalling within its intracellular cytoplasmic domain. For example, cooperation of CD47 with thrombospondin-1 (TSP-1) or vascular endothelial growth factor receptor 2 (VEGFR2) retarding angiogenesis and restraining tumour development (Kaur, *et al.*, 2014; Bazzazi, *et al.*, 2017).

2. Protein Kinase C (PKC) are a large family of protein kinases. There are fifteen isozymes, which are divided into three subfamilies (Webb, *et al.*, 2000):
 - a. Conventional (or classical) isoforms α , β_I , β_{II} , and γ , require Ca^{2+} , diglyceride, and a phospholipid such as phosphatidylserine for activation;
 - b. Novel, include the δ , ϵ , η , and θ isoforms, and require diglyceride. They do not require Ca^{2+} for activation; and
 - c. Atypical, include the $M\zeta$ and ι / λ isoforms. They do not require either Ca^{2+} or diacylglycerol for activation.

PKC's regulate the activity of proteins by phosphorylating the hydroxyl groups of their threonine and serine residues. Recurring themes are that PKC is involved in receptor desensitisation, modulation of membrane structure events, regulation of transcription, mediation of immune responses, regulation of cell growth, cell learning and memory, cell shape and regulation of cell-cell contact (Newton, 1995).

3. Spectrins were originally discovered in erythrocytes by Marchesi, *et al.*, (1968). Now spectrins are recognised as a large class of proteins found in all vertebrate, and invertebrate cells that are differentially expressed during development (Chorzalska, *et al.*, 2010). The antibody used here localizes the 220 kDa (β) and 240 kDa (α) bands of human erythrocyte spectrin staining. A large number of spectrin-like molecules have been found in non-erythroid cells. β Spectrin for instance, includes mammalian erythrocytic β -spectrin, non-erythroid β -spectrin/fodrin (β -G, the general form of β -spectrin is expressed in multiple

tissues), a novel β -G spectrin (ELF1-4- protein coding gene) that lacks the C-terminal pleckstrin homology domain, the brain-specific SPTBN2 (gene), and β -V spectrin (SPTBN5 gene). They help to support of membrane integrity, stabilisation of cell-cell interactions, axonal growth, normal functioning of the Golgi complex and organisation of synaptic vesicles (Gallagher & Forget, 1996)

4. Glycophorin A (GYPA) is one of the major intrinsic membrane protein of the erythrocyte. The external membrane N-terminal glycosylated segment bears the classification of human blood, the MNSs blood group system, which required two genes, GYPA and GYPB on chromosome 4 for expression. They are major sialoglycoproteins, a combination of sialic acid and GP's. GYPA is important for the function of SLC4A1, a gene that provides instructions for making a protein known as anion exchanger 1. GYPA is needed for high activity of SLC4A1 and it might have an involvement in the translocation of SLC4A1 to the plasma membrane. It also appears to have a role in facilitating the movement of band 3 to the cell surface during biosynthesis (Tanner, 1993).
5. Band 3 is a transmembrane protein responsible for the anion channel across the erythrocyte plasma membrane, and a cytoplasmic domain (large amino terminal segment exposed) displaying modular functions. This interaction is electrostatic and it is influenced by oxygenation (Galtieri, *et al.*, 2002). Band 3 protein is the major integral membrane protein of erythrocytes and consists of 911 amino acids. The NH₂-terminal 360 amino acid residues form a water soluble, with long domain that act as an attachment site for the binding of the membrane skeleton and other cytoplasmic proteins. The abundance of Band 3 has made it a useful model for the study of structure/function relationship in the transport protein. Band 3 protein assumes two conformational states during the exchange process, the inward facing form which can bind an anion from the intracellular surface and the outward facing form which can bind an anion from the extracellular surface (Passow, 1986; Hamasaki, 1999).

3.2.2.2 Results

In this result chapter, the investigation focused on the expression of different proteins that were present in the lysate of MV samples compared with their parent cells. This was assessed by Western blotting analyses to further investigate the hypothesis that MV

express the same characteristics as their original sources (parent cells). And are therefore, able to identify molecules that may enable MV to communicate with nearby cells and their potential ability to survive in the extracellular environment.

Erythrocytes, eMV, eMV control, eMV CaCl₂, eMV CaCl₂ + NHS, HeLa cells, HeLaMVC, and HRV16iHMV samples were subjected to SDS-PAGE SYPRO® Ruby protein gel staining (Fig. 3.2.2.1) following procedures set out in chapters 2.2.7.1-2.2.7.4. This was performed to identify potential proteins by their size position ranging between 250-10 kDa, where the migration distance depends on the protein charge, its size, and the pore size of the gel which could be further investigated using Western blotting analyses.

In Fig. 3.2.2.1a erythrocytes visually presented stronger intensity bands compared to eMV samples, despite the amount of total protein being the same for all samples (50 µg/mL). The same bands appear to be present in all samples but were expressed at different levels (lower intensity) for eMV samples, in particular for eMV control.

In Fig. 3.2.2.1b HeLa cells and their derived MV presented more bands at different intensities. Particularly, HeLaMVC which demonstrated to be less concentrated despite the same amount of total protein concentration being loaded (50 µg/mL).

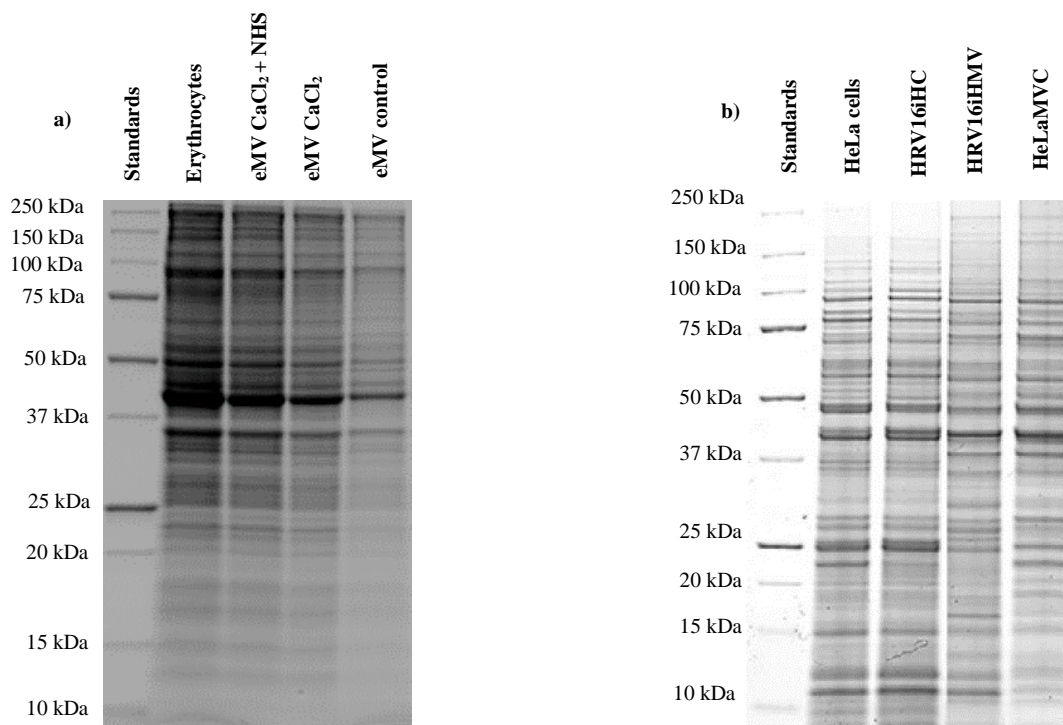


Fig. 3.2.2.1. SDS-PAGE SYPRO® Ruby stain protein gels. Representation of different proteins bands being separated by size. The molecular masses are indicated in kDa. All samples consisted of 50 µg/mL (volume varied for each sample, therefore diluted with PBS buffer to make up for 25 µl per well) determined by BSA assay interpolation of standard curve (Fig. 2.2.7) Precision plus protein™ dual colour standards ranging between 250-10 kDa and 10 µL were loaded into gel and it acted as a size guide for stained bands.

To identify the bands present in Fig. 3.2.2.1, the Western Blotting immunoassay test was performed (Fig. 3.2.2.2). The presence of β Spectrin, PKC, CD47, and β actin was confirmed in all samples. Whereas Band 3 and GYPA was only present in erythrocytes and their derived MV, suggesting that each MV population did not differ in total protein presence when compared to their cell source.

The exploration and confirmation that the chosen proteins were in fact present in the samples, was performed using β actin which acted as a "housekeeping protein", to correct for protein loading and transfer efficiency (present in all samples). This technique is commonly used and provides a useful reference in protein expression studies (Ferguson, *et al.*, 2005).

Also, in order to validate the assay and the true binding of the antibodies a gold protein standard was used (CD47 standard -Protein fragment), labelled as "CD47 standard". This is where only the protein fragment was loaded into the gel well (no MV sample), along

with samples tested against CD47 itself. This protein fragment acted as a separate entity-sample (standard) for the measurement of its binding ability in a functional antibody assay.

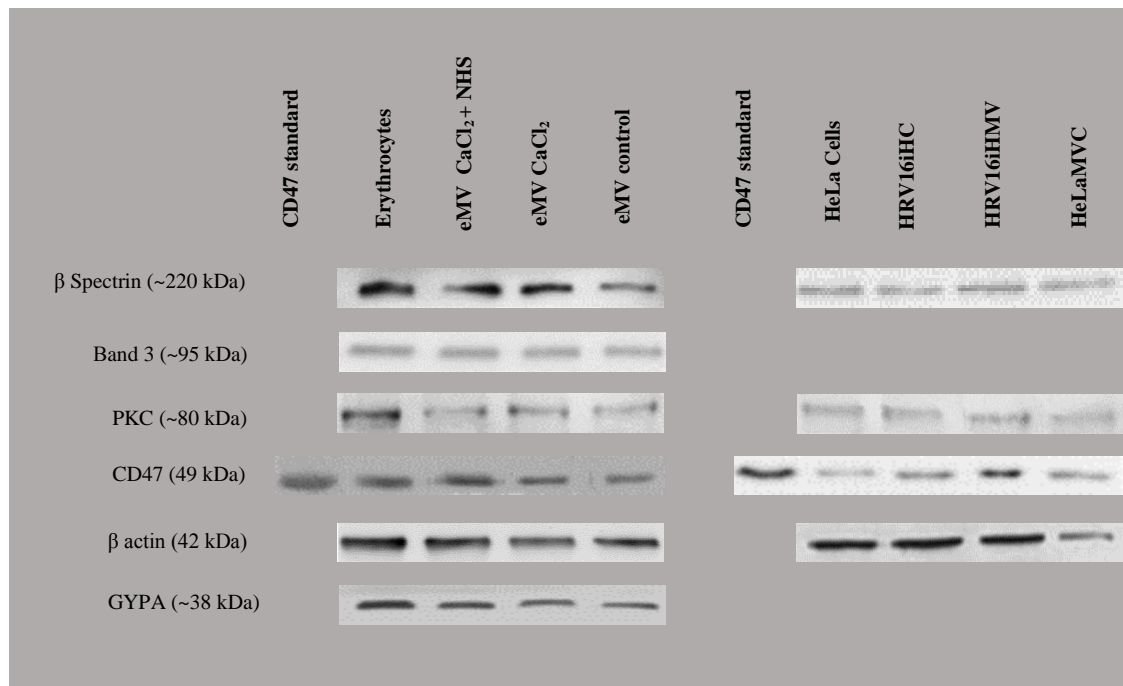


Fig. 3.2.2.2. Western blotting analyses. A representation of six different experiments performed for erythrocytes and eMV samples (as labelled) and four experiments performed for HeLa cells and their derived MV (as labelled). Note, each of the samples consisted of the same amount of total protein (50 $\mu\text{g}/\text{mL}$), determined by BSA assay interpolation of standard curve when loaded into the gel. Therefore representing different levels of antibody expression is a result of the content of each sample (total protein), indicating the approximate size (kDa) for each of the monoclonal antibodies tested here.

The band intensity reflects specific antibody binding and to demonstrate that band intensity correlates with a specific antibody. Here reference samples (parent cells) and PBS negative binding control (blank spot) were used as a reference for intensity brightness subtraction, a parameter used for every test measurement in Fig. 3.2.2.3a. This was performed to compare band intensity across all samples. As shown in Fig. 3.2.2.3b (erythrocytes and their derived eMV) and Fig. 3.2.2.3c, all proteins were expressed at different levels which differ according to each sample.

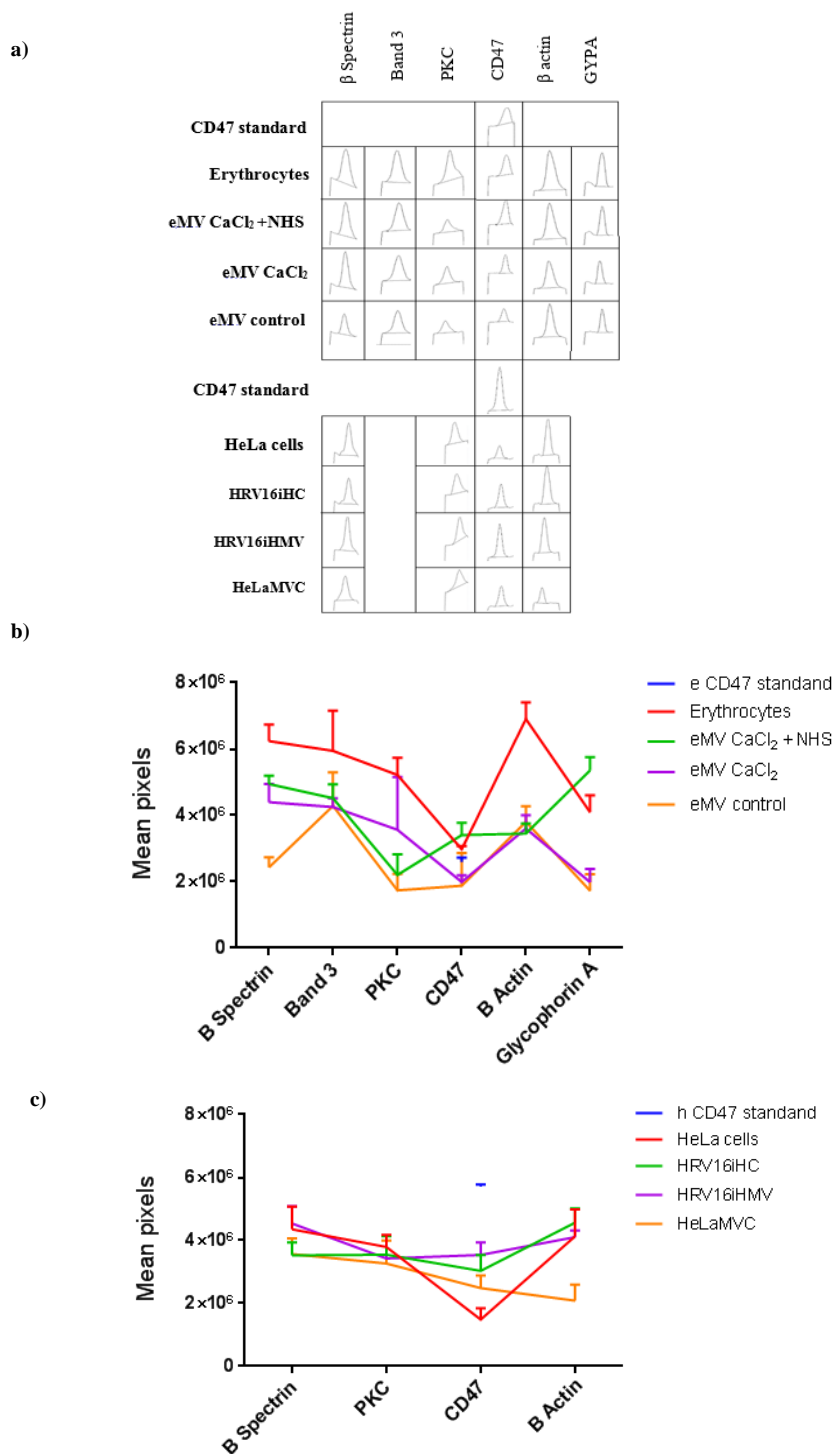


Fig. 3.2.2.3. Western blotting band intensity analyses. The measurement of each band for each sample and each antibody binding is shown in a) representing the histograms, indicating the intensity of each of the bands (the larger the histogram peak, the brighter the band, the more protein binding). This was subtracted against PBS binding control samples clear spot (band). The summary of all samples and all antibodies tested here (in triplicates) is shown in b) erythrocytes and their derived eMV and c) HeLa and their derived MV, which represents the intensity of each band per sample as a numerical value (in pixels). The brighter the band, the higher the number. The analyses was performed using the Image J software and GraphPad Prism was used to generate the XY graphs (Mean and Error).

3.2.2.3 Discussion

It is important to acknowledge that the data obtained with a Western Blot is typically semi-quantitative, only proving a relative comparison of protein levels, and not an

absolute measure of quantity. The factors influencing this are due to variations in sample loading and transfer rates between the samples in separate lanes, which are different on separate blots. For a more precise comparison to be made, processing needs to be standardized and the signal generated by detection needs to be linear across the concentration range of samples. A nonlinear signal was produced, and therefore, should not be used to model the total concentration in each sample (Mahmood & Yang, 2012).

There are additional complementary techniques that supplements and may support Western Blotting analyses which could be employed in future work.

The Enzyme-Linked Immunosorbent Assay (ELISA) for example, can be used to assess the affluence of a target protein providing strong sensitivity, protein concentration (standards) and reduce experiment timing (less than 4 hours). However, it can be expensive due to the cost of readily available kits and the expensive machinery required to conduct the analysis (Haab, *et al.*, 2013).

Another technique commonly employed is the Liquid Chromatography Mass Spectrometry (LC/MS) for the analysis and detailed assessment of proteins. It can provide distinguishable benefits over ELISA as well as Western Blotting techniques, because the distinctions between different proteins as well as their isoforms is achievable with a greater degree of sensitivity and over a broad dynamic scope. But again, it requires highly specialised, expensive equipment and also technical expertise (Bass, *et al.*, 2017).

Notably, CD47, PKC and β -spectrin showed expression in all samples. This was expected because these proteins are not tissue/sample specific. But yet, it proves that the MV samples obtained here express similar characteristics to those of their original source (parent cells).

CD47 serves as the ligand of SIRP α , which is expressed on phagocytic cells and, when activated, initiates a signal transduction cascade resulting in the inhibition of phagocytosis (Barclay & Brown, 2006). A number of studies suggest that blocking CD47 efficiently enhances macrophage phagocytosis in both physiological and pathological conditions including human myeloma cells (Kim, *et al.*, 2012) and MKN45 and MKN74 gastric cancer cells (Yoshida, *et al.*, 2015). Thus, suggesting that CD47 positive MV have a greater chance of survival in the extracellular environment because they will not be depleted by phagocytic cells due to the “do not eat me signal” that they produce.

Nevertheless, Burger, *et al.*, (2012) noticed that aged erythrocytes attach to SIRP using CD47 because it undergoes a conformational alteration during aging stimulated by oxidative stress which allows erythrocytes to be recognised after the binding of thrombospondin-1, 28, and 29, and therefore to be phagocytosed. This finding supports the statement provided in chapter 3.1.3 (page 65) by Ferreira, *et al.*, (2013) that sample quality may affect the enumeration of eMV samples, because in this case, if eMV present characteristics similar to their parent cells it will also present the “eat me” signal. It also suggests that eMV derived from younger erythrocytes may have a higher chance of survival in the microenvironment, because this is before they undergo the conformational alteration.

A study by Alkan, *et al.*, (2005) has suggested that PKC activation plays an important role in the survival of chronic lymphocytic leukaemia. They investigated the expression pattern of PKC isoforms, which this PhD research did not address. Nevertheless, their findings suggest that PKC activation overall, is important for chronic lymphocytic leukaemia cell survival and that inhibitors of PKC may have a role in the treatment of patients with chronic lymphocytic leukaemia. Moreover, it appears that the function of PKC is dependent on the different isoforms present, for instance PKC δ acts as a pro-survival factor in human breast tumour cells *in vitro* (McCracken, *et al.*, 2003). The activation of PKC ϵ may improve retention, survival, and differentiation of transplanted primary mesenchymal stem cells in myocardia (He, *et al.*, 2016).

Therefore, PKC may also play a role in MV survival in the extracellular environment and may be involved in the MV role of cell growth regulation on neighbouring cells, as influential cell cycle-specific impacts of PKC signalling that can either favourably or adversely affect the proliferation of cells (Black & Black, 2012; Redig & Plataniias, 2008). Integrin proteins may link specific integrins to PKC (Zhang, *et al.*, 2001), the family of phospholipid-dependent serine and threonine kinases that is understood to partake in a vast range of biological activities (see Appendix II, table 5 and 6). The activation of cytosolic PKC by phorbol ester or diacylglycerol occurs in parallel with PKC translocation to cellular membranes. Membrane association has also been suggested to specific PKC interactions with phosphatidylserine (Jaken & Parker, 2000; Igumenova, 2015) which is present in MV samples (Fig. 3.2.1.2).

Spectrins are a critical component of the cell membrane skeleton, maintaining cell shape by conferring strength and elasticity as they associate with the plasma membrane through

protein–protein and protein–lipid interactions. Ankyrin is a key component in this network, because it binds both to spectrin and transmembrane proteins, thus linking spectrin to the plasma membrane (Clarkson, *et al.*, 2014). In non-erythroid cells, spectrins form an extended protein network just below the plasma membrane bilayer by linking various actin fibres and many integral membrane proteins. They are also present in the cytosol, and can bind other proteins via numerous interaction motifs, such as the SRC Homology 3 Domain (proto-oncogene) (Chorzalska, *et al.*, 2010). Therefore, the presence of spectrin in the eMV samples can only highlight their strength and ability to maintain MV shape intact.

More specifically, Band 3 and GYPA are the two most abundant integral proteins of the erythrocyte membrane and were detected in eMV samples acquired here, probably due to their biogenesis (erythrocytes). The main functions of Band 3 are for membrane anion transport and the maintenance of erythrocyte membrane stability, through interaction with the cytoskeleton. Whereas, GYPA plays an important role in the prevention of erythrocyte aggregation in the circulation and contribution to the glycocalyx (Poole, 2000).

GYPA has been well characterised in erythrocytes. This is a protein with abundant glycosylation, and studies have suggested that resistance of target cells to natural killing may be correlated with the level of GYPA expression (Ouagari, *et al.*, 1995). In their native state GYPA do not seem to control membrane material properties and/or cell shape. Instead the binding of ligands may lead to a rise in membrane rigidity and a reduction in the lateral mobility of these molecules, which may have resulted from increased association of the cytoplasmic domain of GYPA with the skeletal network. This may be adjusted by the modifications on the exoplasmic domain (where the binding of ligand occurs), and can be considered a form of signal transduction in which ligand induce changes in cellular behaviour. This was described in granulocytes and platelets (Chasis & Mohandas, 1992).

The presence of the proteins observed in this chapter, also suggests that the eMV cargo is likely to depend on the parent cell (same characteristics - similar to chapter 3.2.1) and that MV function and survival chances may be dependent on the molecules that they may express, combined with the proteins observed in this chapter (see Fig. 3.2.2.3.1 for protein interaction network). The availability of different target cell types to internalise the circulating MV is broad and provides a variety of possible mechanisms in which MV may

be able to process. The targeting by specific adhesion molecules may play a role in determining EV bio distribution (Yáñez-Mó, *et al.*, 2015).

Legend:

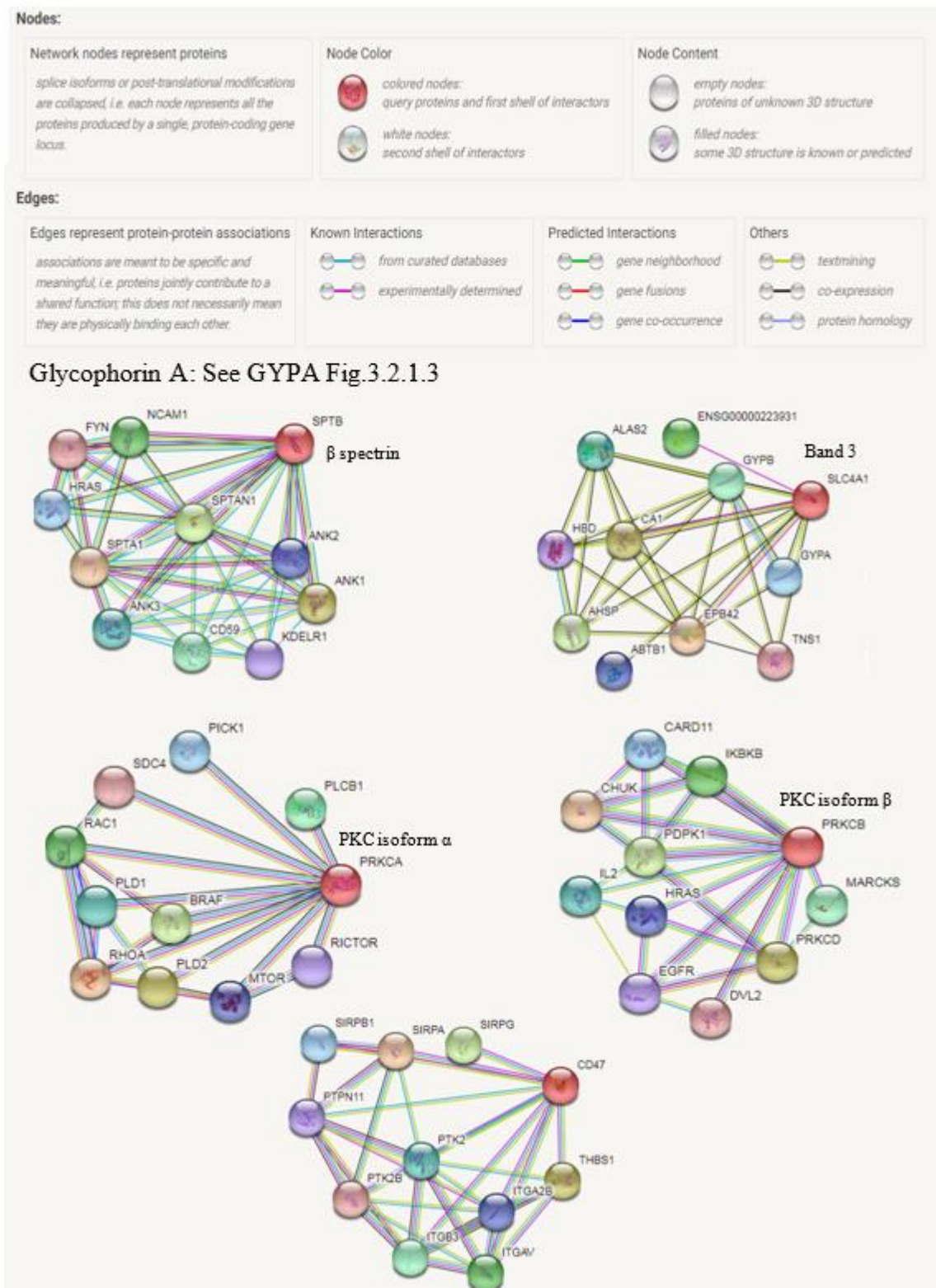


Fig. 3.2.2.3.1. Protein interaction network for total proteins observed in eMV. String database- CONSORTIUM 2017 (Szkarczyk, *et al.*, 2015). Also see Fig. 3.2.1.3.1. The contact of these molecules with each other may induce a variety of interactions and associations among other proteins. Predicting the protein functionality is one of the main objectives of the network, which can be based on their contrasting structural and functional characteristics, in which each may have different biological effect outcomes.

3.2.3 Proteases identification in MV samples

3.2.3.1 Introduction

Proteases, are recognised as peptide hydrolases that have been observed in a variety of biological processes, in distinction to protein degradation in lysosomes to cell division. They are enzymes that perform proteolysis, which is the beginning of protein catabolism by hydrolysis of the peptide bonds that link amino acids together in a polypeptide chain (Castro, *et al.*, 2011). Proteases represent 1- 4% of the genes per genome that have been sequenced and have been observed to be present in various species from viruses to mammalia. The human genome exhibits more than 670 proteases, of which approximately 31% are serine proteases, 25% cysteine proteases, 33% metalloproteases, and 4% are aspartic proteases (Bromme, *et al.*, 2011).

Proteases can be considered molecular scissors that engage a significant role in the intracellular environment during regulatory processes consuming little energy. Therefore it is important to understand its specificity, considering that it determines the selection of its interactions in the protein-protein interface of cleavage-substrates (Fuchs, *et al.*, 2013). The requirements to substrate specificity of regulatory proteases, participating in limited proteolysis of inactive precursors of enzymes and (or) hormones is even greater, particularly in physiological conditions, where the proteolytic reaction is irreversible, representing the main difference of proteolysis from a set of *ad hoc* regulatory mechanisms (Rodriguez, *et al.*, 2010; Berg, *et al.*, 2002).

In organisms of a higher organisation level, the domain composition of proteins is more complex and combinations of domains are more diverse (Chothia, *et al.*, 2003). During the acquisition of new domains, several unique proteases with various catalytic or inhibiting domains encoded by the same gene were formed, and it is believed that the key mechanisms for the appearance of new proteins are gene duplications (Zhang, 2003).

The high biological significance of proteolysis explains the origin of multiple, highly diverse types and familial proteases (Rao, *et al.*, 1998). The diversity of proteolytic enzymes is resultant to a certain degree because of distinctions in the conditions of their functioning in various cellular structures including organisms from different ecological niches, the pH, the temperature, the redox potential of the medium, and hydrophilic and hydrophobic surroundings (Nemova & Lysenko, 2013). Thus, they play a key role in various physiological processes, including division, differentiation, migration, aging,

cellular apoptosis, thermal shock, morphogenesis, reorganisation of tissues, angiogenesis, immunity, haemostasis, wound healing, ovulation and fertilisation (Nemova & Lysenko, 2013; Shah, *et al.*, 2012). Therefore a panel of different protease families was studied during this research including:

1. ADAMs is a disintegrin and metalloproteinase family of multidomain transmembrane proteins belonging to the zinc protease superfamily (characterised by their manifestation of metalloprotease and integrin receptor-binding activities). The ADAMs family has forty gene members currently identified of which 21 are functional in humans. Human ADAM's include precursor forms of growth factors, cytokines, growth factor receptors, cytokine receptors, and several different types of adhesion molecules (Duffy, *et al.*, 2011). The cytoplasmic domain, observed in many family members specify binding sites for various signal-transducing proteins (Seals & Courtneidge, 2003). Murphy's work (2008), suggested ADAMs to be involved in the control of membrane fusion, cell migration, cytokine and growth factor shedding, fertilisation, muscle development, cell fate determination, involvement cell-cell and cell-matrix interactions.
2. ADAMTS is also a disintegrin and metalloprotease family of proteases with thrombospondin motifs; a novel family of extracellular proteases. ADAMTS are distinguished from the ADAMs family members based on the multiple copies of thrombospondin 1-like repeats. The ADAMTS family members are speculated by their structural domains to be Extracellular Matrix (ECM) proteins, with an extensive range of activities and functions including, growth factors and adhesion receptors (Kelwick, *et al.*, 2015; Seals & Courtneidge, 2003)
3. Cathepsins (CTS) are cysteine proteases that constitute one of the five catalytic types of proteases. The common feature is their catalytic mechanism, the increase in the rate of a chemical reaction by the active site of a protein. All cysteine proteases utilise a Cys residue as a nucleophile and a His residue as a general base for proton shuttling (Berg, *et al.*, 2011). Based on sequence homology and three-dimensional structure similarity, they have been divided into clans, each consisting of one or more families. The most intensively studied cysteine proteases are papain and its relatives, including the lysosomal cysteine CTS in clan CA which comprises family C1 (Berdowska, 2004). The activity of

lysosomal cysteine CTS can be regulated in several ways, the most important being zymogen activation and inhibition by endogenous protein inhibitors (Turk, *et al.*, 2001). The N-terminal pro-regions of the lysosomal cysteine CTS, which are removed during maturation, act as potent reversible inhibitors of the mature enzymes, preventing inappropriate activation of the protease zymogens. CTS have long been believed to be responsible for intracellular protein degradation (Mohamed & Sloane, 2006). Overall, CTS's catalyse the hydrolysis of a variety of protein substrates with different specificities and are involved in a wide range of biological processes including, tumour metastasis, muscular dystrophy, emphysema and arthritis (Agarwal, 1990; Jedeszko & Sloane, 2004).

4. Kallikreins (KLKs) are serine proteases present in diverse tissues and biological fluids. The KLKs enzymes have been split into two major groups, the Plasma KLKs and the Tissue KLKs. These differ notably in their molecular weight, substrate specificity, immunological characteristics, gene structure, and type of kinin (structurally related polypeptides) released (Yousef & Diamandis, 2001).

The Plasma KLKs are encoded by a single gene located on human chromosome 4q35 (Yu, *et al.*, 1998) and their function is to participate in the process of blood clotting and fibrinolysis and, in the regulation of vascular tone and inflammatory reactions (Bhoola, *et al.*, 1992; Yousef & Diamandis, 2001). Whereas, tissue KLK have diverse expression patterns and physiological roles, including cell growth regulation, invasion, angiogenesis, and metastasis in cancer. Tissue KLKs are part of a large multigene family, with similarities in the tertiary structure as well as at the gene and protein level. This has been demonstrated in numerous studies (Riegman, *et al.*, 1991; Murtha, *et al.*, 1993; Nelson, *et al.*, 1999; Yousef, *et al.*, 1999; Yousef, *et al.*, 2000; Koumandou & Scorilas, 2013).

Matrix Metalloproteinases (MMPs) are the family of calcium-dependent zinc-containing endopeptidases associated with tissue remodelling and degradation, and the removal of the ECM from the tissue; including collagens, elastins, gelatin, matrix GP's, and proteoglycan (Yadav, *et al.*, 2011). Nevertheless, it has been suggested that the breakdown of ECM molecules or cell surface molecules changes cell-matrix and cell-cell interactions, and the release of growth factors that are bound to the ECM that model them for cell receptors. MMPs

are generally expressed in normal physiological conditions providing homeostatic maintenance (Loffek, *et al.*, 2011).

MMPs are derived from a number of connective tissue and pro-inflammatory cells such as fibroblasts, osteoblasts, endothelial cells, macrophages, neutrophils and lymphocytes. MMPs are expressed as zymogens, the active form result from processing by other proteolytic enzymes including, serine proteases, furin, plasmin, and others that leads the active forms. Under normal physiological conditions, the proteolytic activity of the MMPs is controlled at any of the following identified stages:

1. Activation of the zymogens;
2. Transcription; and
3. Inhibition of the active forms by various TIMPs (Verma & Hansch, 2007).

MMPs are regulated by hormones, growth factors, and cytokines, and are involved in ovarian functions (Verma & Hansch, 2007). These highly active proteases require tight physiological control via endogenous MMP inhibitors (MMPIs) and Tissue Inhibitors of MMPs (TIMPs) that if overexpressed can result in a variety of pathological disorders (Liu, *et al.*, 2006). In addition, a number of non-ECM molecules are also potential substrates of MMPs (Nagase, *et al.*, 2006).

In relation to MV, EV proteomic analysis has suggested that metalloproteinases including the cell surface-anchored sheddases and metalloproteinases, and cell surface-bound and soluble MMPs are involved in EV activity from a variety of sources. Metalloproteinases, have been shown to impact not only ECM remodelling, but also cellular interactions. In particular, some of the metalloproteinases in EV have been shown to be proteolytically active, proposing that they may change the contents of EV by proteolytic processing and assist in EV-mediated cell–cell communication (Shimoda & Khokha, 2013). In addition, the release of metalloproteases from tumour cell derived MV has been observed to promote tumour invasion and metastases (Dolo, *et al.*, 1999).

The expression profile of proteases is fundamental for understanding their roles in normal cellular function, their dysregulation in diseases such as cancer, and their therapeutic applications (Craik, *et al.*, 2011). Therefore, this chapter aims to identify

proteases/families present in MV samples using The Human Protease Array Kit (R & D systems) which is a rapid, sensitive, and economical tool to simultaneously detect protease and the relative expression differences between samples.

3.2.3.2 Results

In this results chapter, the investigation focused on the expression of different proteases that were present on the lysate of MV samples and their parent cells. These were assessed by selected capture antibodies (in duplicates) on nitrocellulose membranes, where the signal is produced in proportion to the amount of protein bound. Chemiluminescence was detected in the same manner as Western blotting analyses (results chapter 3.2.2.2).

Erythrocytes were isolated from fresh venous blood utilising the Ficoll-PaqueTM Plus method. eMV control was extracted by incubating the erythrocyte pellet as in chapter 2.2.4. HRV16iH MV were extracted from conditioned medium (exosome free serum), after 24 hours infection/incubation period. These MV samples were isolated following various steps of centrifugation: 200 g for 5 minutes; 4,000 g for 60 minutes; and 25,000 g for 90 minutes. Subsequently, these MV samples and their parent cell were lysed with RIPA buffer and protease inhibitors (see chapter 2.2.7.1).

Total protein concentration was determined with BCA assay and 50 µg/ mL of each sample was used for this experiment. All experimental design was followed according to the manufacturer instructions (Proteome Profiler Human Protease Array Kit, R & D systems (see chapter 2.2.8).

Parent cells (erythrocytes and HeLa cells) were used to overcome substantial limitation, such as a relative protein recovery from a limited volume of eMV control and HRV16iH MV samples. The same amount of total protein (50 ug/ mL) was used for each sample, which was created to normalise the relative quantitative changing of the proteases array, and negate the lack of a housekeeping protein.

Fig. 3.2.3.1 displays the membrane images acquired during the analysis, where the spots positioned at A1 and A2, A19 and A20, and E1 and E2 represent the positive controls. The absence of spots in positions E9 and E10 signifies the negative control, indicating the specificity of the antibody cocktail. The complete list of analyte names and position/mapping is available in Fig. 3.2.3.1a. This is where the position of each coordinate is shown in column 1 and the analyte ID is shown in column 2. All positions

can be identified/mapped in each membrane by placing the transparency overlay template (Fig. 3.2.3.1b). The signals for each array membrane (the samples) are displayed in Fig. 3.2.3.1 c, d, e, and f which were quickly identified by placing the transparency overlay template onto the array image and aligning it with the pairs of reference spots in the three corners of each membrane.

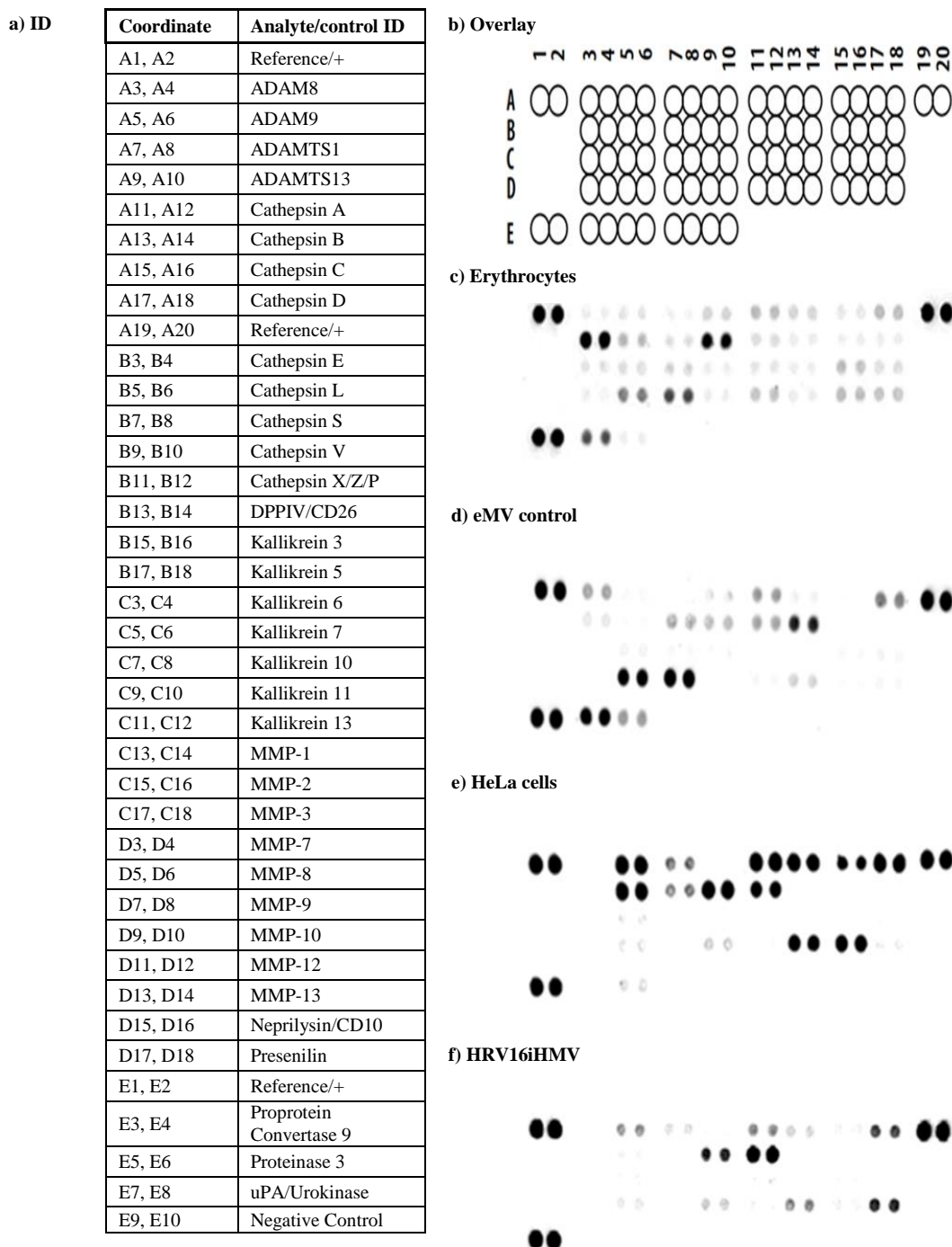


Fig. 3.2.3.1. Location of coordinates and the presence of different proteases in each array membrane. The positive signals seen in each membrane were identified using Fig. a) which provides the coordinate and ID of each spot, b) represents the overlay template and c), d), e) and f) representing the samples used as labelled.

For the following sets of comparison graphs (Fig. 3.2.3.2- Fig. 3.2.3.4), Image J software was used to calculate the mean pixel densities of each analyte. This was performed by creating a template to analyse pixel density in each spot of each membrane, then the average signal (pixel density) was calculated using the pair of duplicate spots representing each analyte. This was determined by subtracting an averaged background signal from each spot, against the negative control spots as a background value. The signals on different membranes were used to determine the relative change in analyte level between samples (established as 535x210 pixels; 8-bit; 110k for all membranes), using the Red Green Blue (RGB) images and the results were calculated using brightness values. RGB pixels are converted to brightness values using the formula $V=(R+G+B)/3$, or $V=0.299R+0.587G+0.114B$ if "Weighted RGB Conversions" were checked. For these analyses the following parameters were recorded: length, angle (straight lines only), mean, standard deviation, mode, min, max, and bounding rectangle.

Fig. 3.2.3.2 show changes between positive and negative detection of the proteases in MV samples with respect to their parent cells (erythrocytes). Considerably, 34 relatively positive signals were observed in the erythrocytes membrane (that is 34 out of 35 tested proteases, some at very low level, but expression is observed), showing that the proteases analysed here may attach to erythrocytes in circulation (RIPA buffer lysed samples/total proteins analysis was obtained here). In comparison, 21 proteases (positive signal) were detected out of 34 for the eMV sample, showing that eMV inherit some but not all of the proteases present in their parent cells.

Both, erythrocytes and eMV samples appear to be enriched with CTS D and V, KLK 7 and 10, MMPs 3, 8 and 9, and PC9 (more than 2×10^2 / mean pixels), whereas eMV demonstrated a higher concentration/expression of CTS D, E and V, DPPIV, KLK 10 and PC9 than erythrocytes (more than 3×10^2 / mean pixels) and with a significant expression of MMP9 of more than 5.5×10^2 / mean pixels.

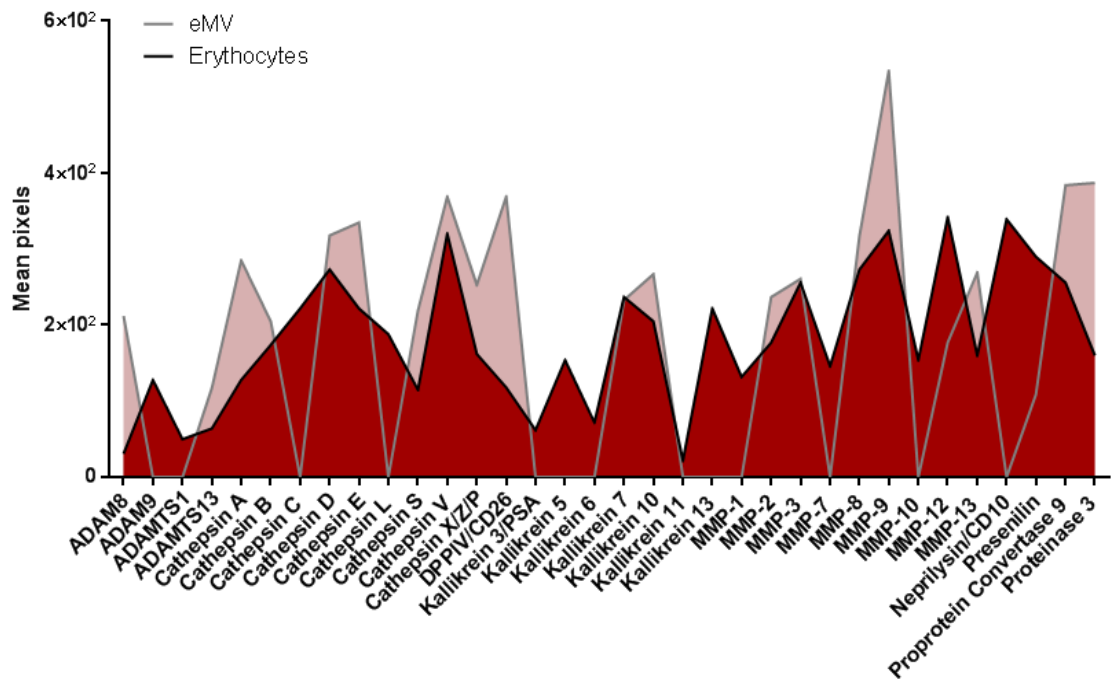


Fig. 3.2.3.2. The comparison of the relative expression of proteases present in erythrocytes and eMV. The graph shows the identified positive expressions/signals highlighting the differences between the samples, where MV shows less proteases binding, but demonstrates higher concentration/intensity for the proteases present.

In contrast, much lower positive/binding signal was observed in HeLa cells, with 17 proteases against 11 detected proteases in HRV16iHMV (Fig. 3.2.3.3), when compared to Fig. 3.2.3.2. Nevertheless, similarly the majority of proteases present in MV cell shows expression in parent cells, apart from MMP10 which was not present in HeLa cells. PC9, Presenilin, MM9, KLK7 and CTS L, C and S was not present in HRV16iHMV. CTSC appears to be present only in the HeLa, which shows a significant change for both sets of parent cells (erythrocytes and HeLa), demonstrating a trend of assay validation.

Neprilysin showed strong expression in HeLa and HRV16iHMV (more than 4.0×10^2 mean pixels). It was also present in erythrocyte, but absent in eMV. Additionally, ADAM9, ADAMTS1, and MMP10 were expressed strongly on HRV16iHMV. CTS D and V, KLK 7 and 10, MMPs 3, 8 and 9 did not show presence in HeLa and HRV16iHMV samples (not present in the graph), in contrast to erythrocytes and eMV.

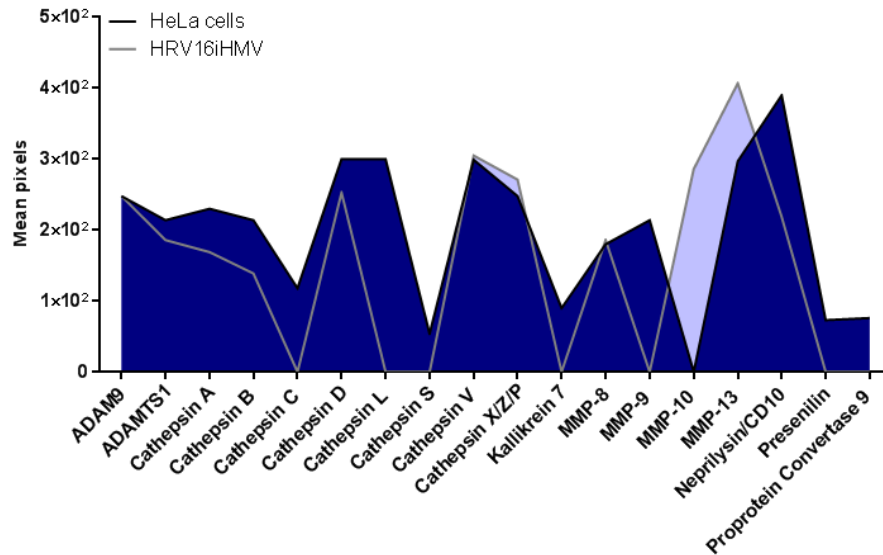


Fig. 3.2.3.3. The comparison of the relative expression of proteases present in HeLa cells and HRV16iHMV. The graph shows the identified positive expressions/signals highlighting the differences between the samples, where MV shows less proteases binding signal, but demonstrates higher concentration/intensity for the proteases present.

All the samples expressed a significant level of some CTS's and ADAM's family (Fig. 3.2.3.4), where a set of proteases appear to progressively increase in terms of positive signal/binding. Especially for the CTS family with a progressive trend of A, B, D, V and Z showing more than 3.0×10^2 mean pixels. MMP8 and MMP13 is also present in abundance in all samples when all samples are compared.

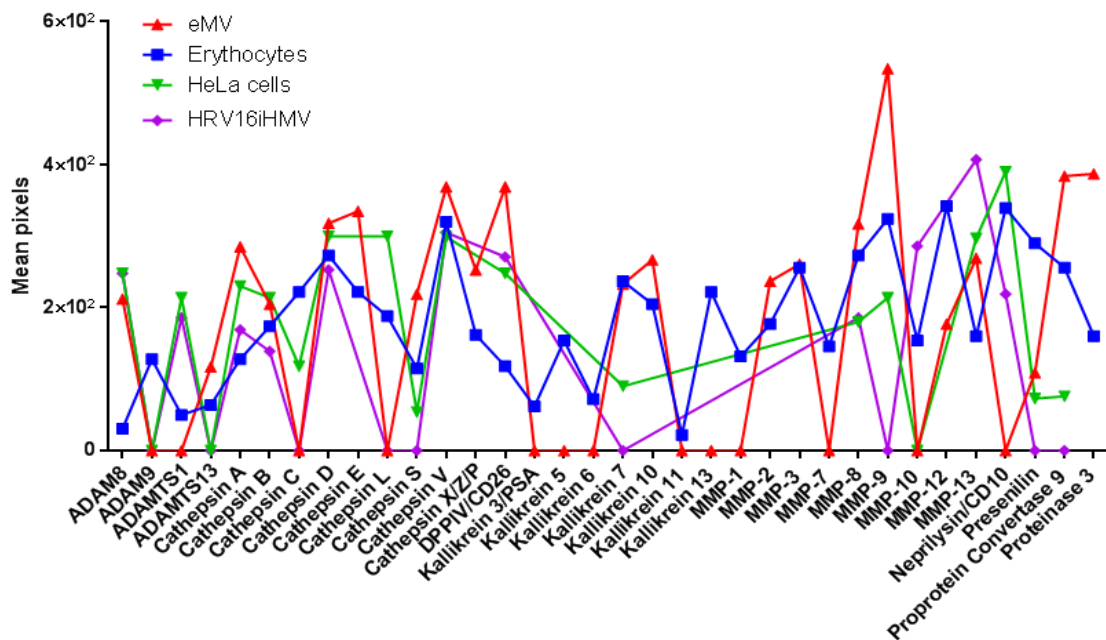


Fig. 3.2.3.4. The comparison of proteases present in all samples. The graph identifies positive and negative expression/signals highlighting the differences between the samples, where MV shows less proteases binding than their parent cells. It also shows the proteases that were not present in all samples (at the bottom of the Y-axis and at numeric value of 0 mean pixels in the X-axis).

3.2.3.3 Discussion

CTS's and MMP's demonstrate substantive expression in this study. This is important because they are responsible for a variety of cellular photolytic (chemical compound is broken down by photons) mechanisms. Involved in the maturation of protein in the immune system, hormone generation and signalling transition on mammalian, which play a general role as intracellular acidic proteases in endolysosomal compartments (Stoka, *et al.*, 2016). Therefore, they are able to control pH level and therefore catalyse key proteins.

CTS's of the A, B, D, V, and XZP classes were found to be markedly abundant in all samples, showing more than 3.0×10^2 / mean pixels. Interestingly, CTS's are lysosomal proteases, which can exert their proteolytic activity in the extracellular space in ECM remodelling (Fonović & Turk, 2014), leading to the assumption that MV analysed here may play a role in membrane remodelling, and therefore can act as an effective mechanism whereby diverse cellular behaviours can be regulated. This concept is particularly important when considering processes and cell behaviours that need to be deployed promptly, transiently, and wherein cell–cell and cell–matrix interactions are constantly changing (Daley, *et al.*, 2008).

An example found to be present in all the samples is CTSX. This protease is capable of cleaving regulatory motifs at C-terminus, which affects the function of targeted molecules. Through the activation of β_2 integrin receptor Mac-1, active CTSX increases adhesion of monocytes/macrophages to fibrinogen and regulates the phagocytosis (Kos, *et al.*, 2009). By activation of Mac-1 receptor (CD11c/CD18), CTSX also dominates adhesion of monocytes, macrophages and dendritic cells (Sándor, *et al.*, 2016), that is necessary in the commencement of adaptive immunity and also through the other β_2 integrin receptor, Lymphocyte Function-associated Antigen 1 (LFA-1) which is involved in the proliferation of T lymphocytes. By modulating the activity of LFA-1, CTSX generates cytoskeletal rearrangements and morphological arrangements of T lymphocytes. This promotes ameboid-like migration in 2-D and 3-D barriers and enhancing homotypic aggregation. C-terminal amino acids of α and γ enolase cleavage by CTSX terminates their neurotrophic activity distressing neuronal cell survival and neuritogenesis (Kos, *et al.*, 2009), which clearly contributes to the survival and function of MV expressing this protease.

The presence of MMP8 and MMP13 in all samples is a further highlighting expression that was observed in this study. These are collagenases (able to cleave the collagen triple helix into characteristic 3/4 and 1/4 fragments). In addition, collagenases can perform proteolytical processes in other ECM proteins, as well as a number of bioactive molecules such as IL-8, protease-activated receptor-1, MMP-8 targets type I collagen and MMP-13 preferentially cleaves type II collagen (Fanjul-Fernández, *et al.*, 2010). Therefore implying that MV may reflect local changes in the extracellular microenvironment.

KLK's family did not in general demonstrate presence in the samples used here. However, KLK7 was present in HeLa, erythrocyte, and eMV samples. KLK10 demonstrated enrichment in erythrocyte and eMV samples only. It is widely accepted that KLK's possess potential membrane-active properties as a fundamental component in their mode of action (Epanand & Vogel, 1999). It is interesting that the effects of KLK on various biological membrane model systems has been demonstrated and KLKs have shown involvement in a broad range of normal physiologic processes, from the regulation of cell growth to tissue remodelling (Emamia & Diamandis, 2007).

Aichinger *et al.*, (2008) demonstrated that KLK avidly interacts with membrane vesicles without perforating the membranes. Their hypothesis is that lipid rafts of DC cells, are preferential targets of KLK and via its binding and integration KLK might facilitate the uptake and intracellular distribution of ODN1a (a synthetic oligodeoxynucleotide, that is a Toll-like receptor 9 agonist lacking containing cytosine phosphate guanine motifs) and antigens, thus stimulating downstream immunostimulatory functions of the antigen-presenting cell. Suggesting that the samples analysed here could trigger the immune response and decays ECM, showing an ability to avoid recognition as non-self-substances and it contributes towards MV entrance to neighbouring cells.

Neprilysin, a cell surface metallopeptidase, cleaves and inactivates pro-inflammatory and vasoactive peptides, and predisposes the lung vasculature to exaggerated remodelling in response to hypoxia. It showed strong expression in HeLa and HRV16iHMV (more than 4.0×10^2 mean pixels), but not in erythrocyte and eMV samples. In addition to its peptidase activity, basic amino acid residues in the tail of Neprilysin contribute to protein-protein interactions, resulting in modulation of signalling factors. This has been demonstrated in prostate cancer cell lines (Sumitomo, *et al.*, 2005) and it could contribute towards the mechanism of HRV16iHMV interaction with neighbouring cells.

DPPIV, which is a prolyl peptidase that attaches proteins and peptides after a proline amino acid residue, was highly expressed in erythrocytes and eMV, but not in HRV16iHMV. DPP IV is also the CD26 T-cell activating antigen found in almost all human organs and tissues (Misumi & Ikehara, 2013). It is attached to the plasma membrane of endothelia and is also found solubilised in body fluids such as blood plasma. The broad distribution of DPP IV allows access to endocrine peptides, neuropeptides and a broad range of paracrine and autocrine peptides and polypeptides (Green, *et al.*, 2006). High levels of plasma DPPIV are positively correlated with type II diabetes (Müller, 2012), suggesting that its presence in eMV may be an indication of donor characteristics, but this needs to be further assessed to confirm the condition. DPP-IV degrades the active form of the incretin, glucagon-like peptide-1, which is liberated from intestinal L-cells after meal intake and enhances insulin secretion in a glucose-dependent manner, suggesting that MV could have a role in metabolic processes.

The expression of the proteases observed in this chapter, suggests that the MV cargo and function depends on the characteristics present in parent cells (similarly to chapters 3.2.2 and 3.2.3), because MV expressed the similar characteristics (not all) to their sources. The protein interaction network (see Fig.3.2.3.1) show the possible interaction network of the proteases present in eMV. This is because they can potentially change the kinetic properties of enzymes, can pose as a common mechanism to permit for substrate channelling, can create an alternative binding site for small effector molecules, can immobilise or repress a specific protein, can modify the specificity of a protein for its substrate during interaction with alternative binding sites, and act in a regulatory role in either the upstream or downstream level (Phizicky & Fields, 1995). Once more, demonstrating the qualitative and broad potential of MV.

3.2.4 *In silico* analyses of biomolecules identified in eMV samples

The current pace of genome-wide sequence analyses programs, coupled with functional genomic screenings has produced a perplexing array of sequence and biological data to be developed (Michalovich, *et al.*, 2002). The identification of proteins and/or genes of interest in present biological studies requires the application of bioinformatics tools to process a vast number of datasets and access their significance. The enrichment analyses have played an important role in this regard, contributing to the detection of relevant genes amongst a significant amount of listed candidate genes in various high-throughput biological studies (Huang, *et al.*, 2009).

Evaluating the functional properties of protein/gene sets is a routine step in understanding high-throughput biological data and is commonly used to verify their implication in biological pathways, assess whether they are functionally relevant, and to discover unexpected shared functions between the entities of interest. Gene Ontology (GO) analysis is therefore, widely used to generate functional enrichments between candidates genes, due to the use of comprehensive reference information and unified annotations of underlying functions to describe common features including biological processes, molecular functions and cellular components of the biology of the gene products to classify them (Glass & Girvan, 2014; Consortium, 2015).

From a protein function standpoint, the change of annotation from known proteins to a novel target is a useful and practical manner to turn vast quantities of “data” into meaningful information. The importance of these analyses in the medical field/research is increasing due to the possibility of narrowing the search by modelling and discovering new biological properties in a systematic fashion that elucidate key functions of complex networks of bio-interactions (Bayat, 2002).

In this PhD research, the primary focus on GO enrichments was associated with human proteins/genes only. After assessing the patterns of protein present in eMV samples, a list containing proteins conversion to gene names was generated using the String and UniProt database (Appendix III- Table 1).

To systematically detect the functional enrichments among the multiple proteins detected in eMV samples, a comprehensive reference information list including gene and phenotype ontologies, description, alternative names, chromosomal and map location (full list is provided in Appendix III- Table 2) was produced. This list was the raw data

used to explore the connections between the query protein/genes and to detect statistically significant common features among them. With this strategy it was possible to uncover enrichment of cellular component (Fig. 3.2.4.1), molecular function (Fig. 3.2.4.2), biological processes (Fig. 3.2.4.3), and specific biological pathways involved (Fig. 3.2.4.4). This list was created using the FunRich functional enrichment analysis tool (Pathan, *et al.*, 2015), which performs functional enrichment analysis on background databases that are integrated from heterogeneous genomic and proteomic resources. Appendix III, table 3 provides the list of the genes mapped for the data input in detail. HRV16iHMV GO annotations and analyses is presented in Appendix IV.

The statistical significance of enriched and depleted terms was checked using hypergeometric distribution testing. Additionally, the Bonferroni and Benjamini-Hochberg (BH) (also known as False Discovery Rate-FDR) method was applied to correct for multiple testing, each associated with a P-value ($P < 0.05$). This is where GO analyses were aligned to the P value (red bar), P value lower than 0.05 (yellow bar) was also considered significant, and the blue bar indicated the percentage of genes classified in clusters (not mutually exclusive) in a whole analysis. The reason for this is that the product of a single gene could have one or more molecular functions, be associated with different cellular components, and be involved in several biological processes.

In Fig. 3.2.4.1, the first cluster of the cellular components enrichments includes the genes that presented frequencies between 50-75%. This means that ~15 genes of the list (out of 27) were involved in 2 different processes related to plasma membrane and extracellular activities. The following group with a frequency of 25-50% was made by ~10 genes of the list. They were related to regulatory processes of extracellular space, integral to plasma membrane, exosome and lysosome. The cluster of 0-25% frequency was formed by 15 miscellaneous processes with an average of ~2 genes in each of the following categories: membrane fraction, cell surface, Golgi apparatus and endoplasmic reticulum.

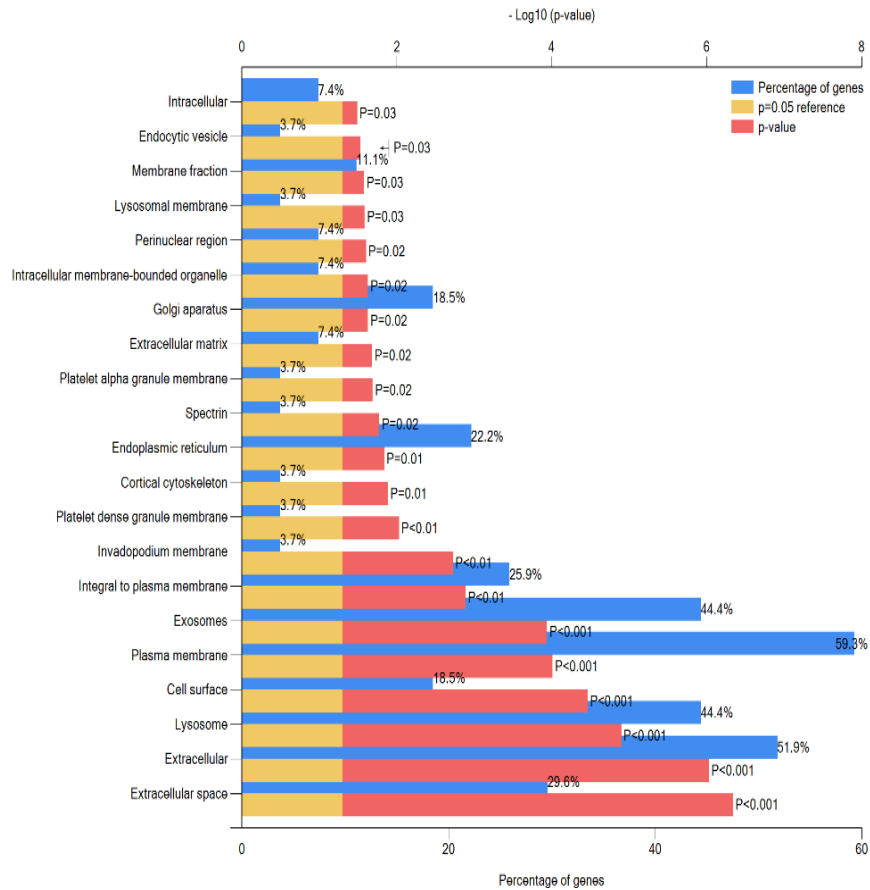


Fig. 3.2.4.1. Cellular component enrichment of biomolecules observed in eMV. Frequency of proteins/genes that shared the same characteristics in relation to its location, at the levels of subcellular structures and macromolecular complexes.

In Fig. 3.2.4.2 the enrichment showed a prevalence of genes (~8) regulating processes that modulate metallopeptidase activity (frequency, rate, extent), which refers to the catalysis of the hydrolysis of peptide bonds using water as a nucleophile (Nagase, 2001). The remaining genes were distributed in 10 miscellaneous processes with an average of ~1 gene per function including receptor activity, transport protein activity, cytoskeletal protein binding, and serine/cysteine peptidase activity.

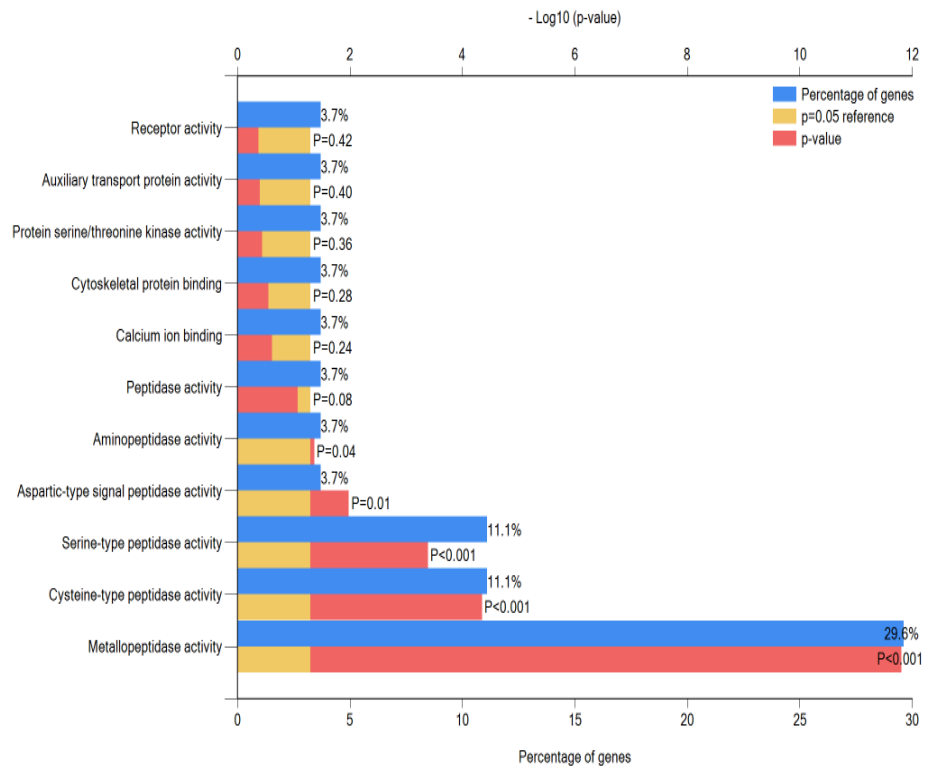


Fig. 3.2.4.2. Molecular function enrichment of biomolecules observed in eMV. The graph shows the frequency of proteins/genes according to their molecular role.

In Fig. 3.2.4.3, the enrichment of biological processes showed a considerable amount of genes (~17) regulating protein metabolism. The rest of the genes were distributed in 6 miscellaneous processes with an average of ~1 gene per process, including immune response, cell communication, signal transduction and others.

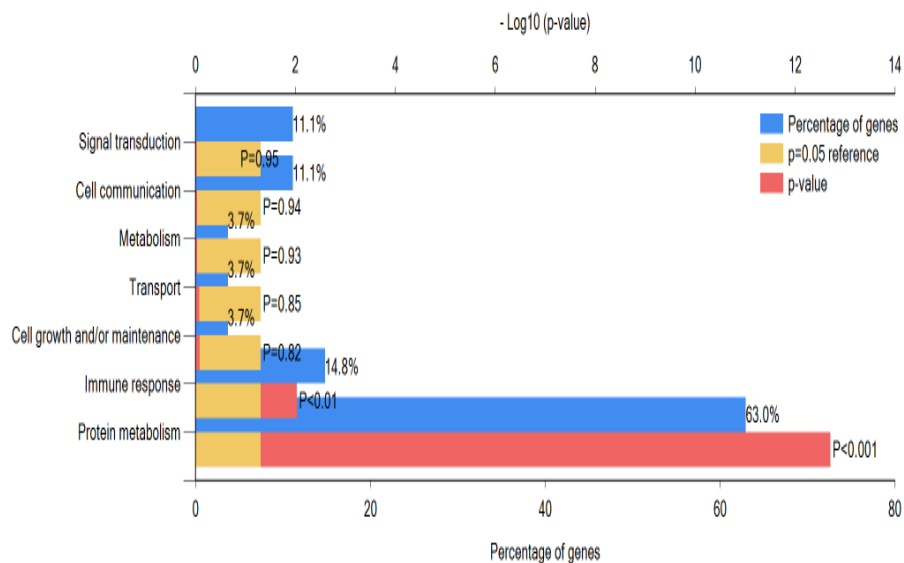


Fig. 3.2.4.3. Biological processes enrichment of biomolecules observed in eMV samples. The figure represents a complex of potential changes on the level of granularity of eMV that is mediated by one or more gene products at the cellular or organisational level. It shows the frequency of proteins/genes grouped according to their involvement in biological processes.

In Fig. 3.2.4.4, the biological pathways showed an enrichment of cell surface interaction by integrin-family with ~15 genes. Within the same cluster of 50-75% frequencies, there was a large number of pathways controlling vital process related to cell growth, apoptosis and metabolism such as the mTOR, IGF, and insulin pathways, showing the same set of ~14 genes involved in that network. The following cluster of 25-50% was made by ~10 genes only related to haemostasis, the physiological process that stops bleeding at the site of an injury while maintaining normal blood flow elsewhere in the circulation (Gale, 2011). The last cluster of 0-25% showed 13 miscellaneous biological pathways with an average of ~4 genes each, including posttranslational regulation, cell signalling events, and cell surface interactions among others.

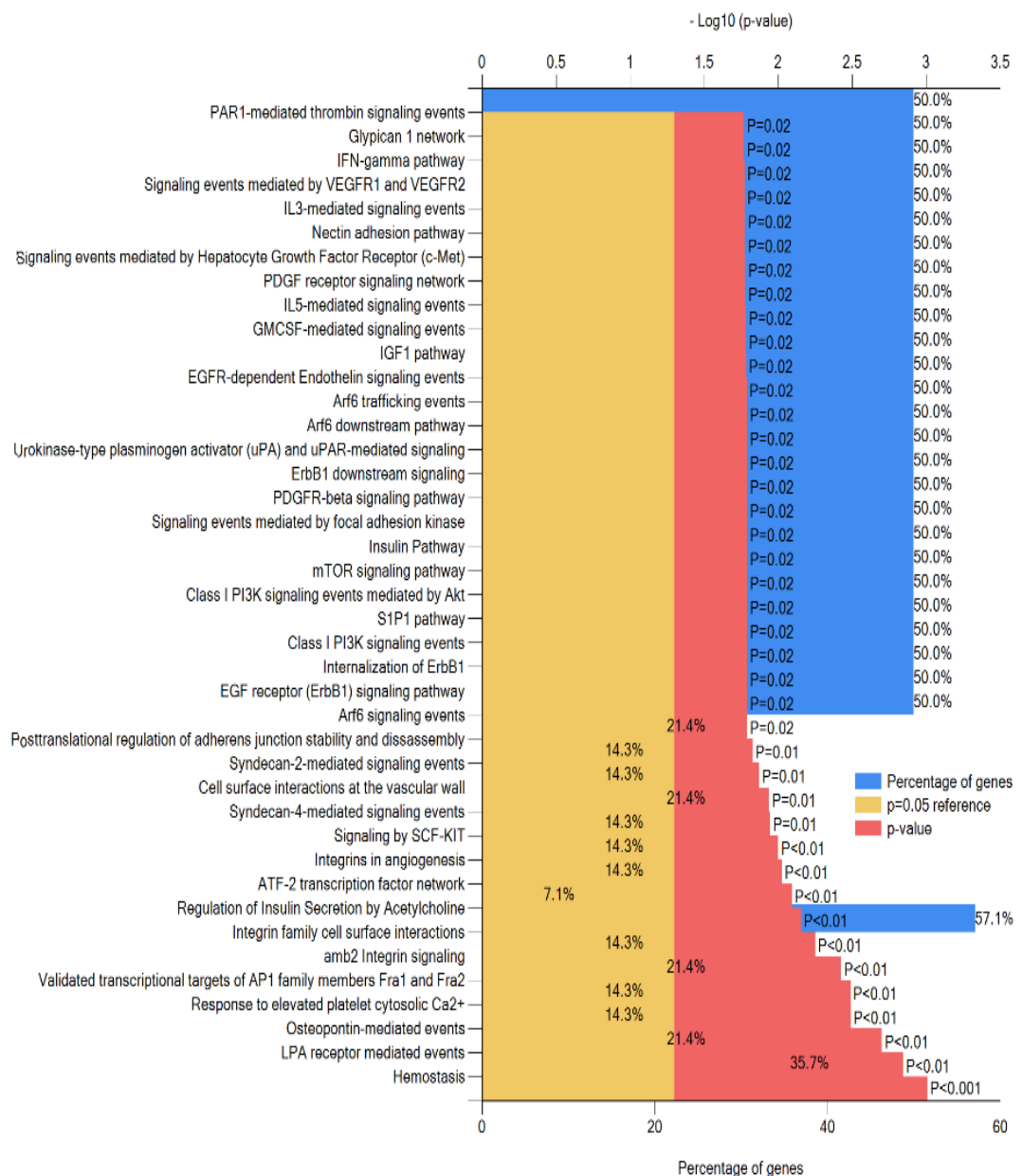


Fig. 3.2.4.4. Biological pathway enrichment of biomolecules observed in eMV. Frequency of proteins/genes grouped according to their biological pathways.

The GO enrichments performed here provided further clarification of the functional roles described for the gene products detected in eMV in this PhD research. Being useful to understand from a system biology perspective the complexity of the network triggered and affected by the bio-information transported in the isolated eMV.

Overall, the highest scores revealed that the cellular locations of the majority of the proteins from the list are in the plasma membrane carrying out extracellular activities. Their molecular function showed a significant representation of processes related to protein metabolism mainly metallopeptidase activity. In terms of biological pathways regulated by this group of proteins, the GO enrichment was consistent with the hypothesis presented in chapter 3.2.1, indicating a prevalence of cell surface interactions in the first place. This is combined with several pathways that control the fate of the cell such as growth, apoptosis and metabolism among others. This brings clarity to the functional role of the eMV characterised in this research, determined by the proteomic information embedded in them.

3.3 Identifying immune related miRNAs: properties that may allow MV to affect the target cell

3.3.1 Introduction

Small RNAs distinguish themselves by their peak length, which varies from 21 to 30 nucleotides and by the mechanisms of biogenesis. The presence of a 5'-uridine, phosphorylation at the 5' end and 2'-O-methylation at the 3' end of the RNA molecule regulate the loading of small RNAs onto effector ribonucleoprotein complexes. MicroRNAs (miRNAs) concern the uttermost rich class of small RNAs in animals (Felekkis, *et al.*, 2010).

miRNAs, are small non-coding RNAs (ncRNAs) of approximately 20 nucleotides in length, that favour Messenger RNA (mRNA) for down-regulation by affiliation with a broad, multi-protein complex known as the RNA Induced Silencing Complex (RISC). RISC assortment depends upon the existence of sequences in each of the target mRNA which are defectively correlated to the miRNA sequence (see Appendix V for miRNA synthesis). The miRNA binding sites usually arise within the 3'-Untranslated Region (UTR) of the mRNA, however, functional miRNA binding sites can also arise within the 5'UTR (Lytle, *et al.*, 2007) or coding region (Forman, *et al.*, 2008). Therefore, it regulates gene expression post transcriptionally by adhering to 3'UTR, coding sequences or 5'UTR of target mRNAs, and resulting in retardation of translation or mRNA degradation.

It is predicted that miRNAs administer approximately 30% of the human protein-coding genome and rule the expression of genes associated with a variety of biological processes, including apoptosis, proliferation, differentiation, and metastasis (Ambros, 2004; Bartel, 2004; Filipowicz, *et al.*, 2008; Almeida, *et al.*, 2011).

miRNAs are assigned sequential numerical identifiers and databases such as miRBase, utilise shorten 3 or 4 letter prefixes to appoint the species, generating unique identifiers, for example *hsa-miR-101* (*hsa* as in *Homo sapiens*). 'miR' is used to label 'mature' sequences, whereas 'mir' denotes the precursor hairpins. The gene identifications are designed to transmit controlled details regarding the functional association among mature miRNAs, such as *hsa-miR-101* in human and *mmu-miR-101* in mouse are orthologous (Griffiths-Jones, *et al.*, 2006).

Lettered suffixes are given to paralogous sequences by which mature miRNAs differ at only one or two positions, for example *mmu-miR-10a* and *mmu-miR-10b* in mouse. Numbered suffixes are applied where well-defined hairpin loci cause indistinguishable mature miRNAs, for example *dme-miR-281-1* and *dme-miR-281-2* in *Drosophila melanogaster* (Griffiths-Jones, *et al.*, 2008; Griffiths-Jones, *et al.*, 2006).

Over time, nomenclature may be subtly and progressively readdressed, as knowledge develops sequences may change for practical redundancy. Current research proposes that only the 5' so-called seed region of the sequence design a compact duplex with the target mRNA and affiliated hairpin precursor sequences may promote mature sequences with only slight resemblance and divergent miRNA numbers. Where two different mature miRNA sequences present to be removed from opposite arms of the same hairpin precursor, for example *miR-17-5p* (5' arm) and *miR-17-3p* (3' arm) (Desvignes, *et al.*, 2015).

It is inadvisable to depend on capitalisation to grant details, such as the *mir/miR* precursor/mature convention. *let-7* and *lin-4* pronounced deviation to the numbering scheme because they are preserved for historical reasons (Ambros, *et al.*, 2003; Griffiths-Jones, *et al.*, 2006).

The discovery of miRNAs adds a new aspect to the interpretation of complex gene regulatory networks (He & Hannon, 2004) and up to now, the possibility of EV as miRNA transporters have been the subject of research in the EV research field (Xu, *et al.*, 2013). This is because miRNAs are understood to regulate the expression of a number of target mRNAs, by modulating a large number of biological processes. They could contribute towards an insight into the molecular changes in the cells that they are extracted/derived from as well as producing diagnostic information and tools (Redis, *et al.*, 2012).

miRNA expression profiles of circulating MV is not a new concept, having been studied in patients with parental hepatocellular carcinoma cells (Xiong, *et al.*, 2013), coronary artery disease (Jansen, *et al.*, 2014), in bone marrow mesenchymal stem (Wang, *et al.*, 2015) and many more. Up to now, they have not been extensively reported in eMV, and none in HeLaMVC or HRV16iHMC. Therefore, this chapter studies a panel of 68 miRNAs for their expression in erythrocytes, eMV, HeLa cells, HRV16iHc, HeLaMVC, and HRV16iHMC.

The immunological panel was selected because it features general markers for multiple immunology-related diseases. Markers specific to certain autoimmune diseases and blood-based cancers which can provide insightful details of parent donor cells and therefore, MV cargo similarities and differences between samples. Also, MV are generally considered heterogeneous naturally and depending on the donor, it can even present more molecules/characteristics in relation of their potential effect on recipient cells.

MV may be able to transfer miRNAs to the neighbouring cells (Zhang, *et al.*, 2015), therefore, it is important to acknowledge its possible targets. For example, during cardiac hypertrophy *miR-23a*, *miR-23b*, *miR-24*, *miR-195*, *miR-199a*, and *miR-214* were upregulated, and this caused an induction of hypertrophic growth in cardiomyocytes *in vitro*. Similarly, *miR-24*, *miR-125b*, *miR-195*, *miR-199a*, and *miR-214* were upregulated in the tissue of patients with end-stage failing human hearts (Zhang, 2008; Ardekani & Naeini, 2010; Thum, *et al.*, 2008).

The Firefly particle (technology used in this research) structure consists of three distinct regions (see Fig. 3.3.1.1), the capture target miRNAs and the encode particles. The particle presence is triggered in the green channel (FC analysis) and the events from all three regions are detected to evidence the bearing of a particle. The fluorescence intensity in the central region determines miRNA quantity and the FC recognises a fluorescent signal in the red channel from the centre of the particle. This arises from the captured and labelled target miRNA and is equivalent to the amount of miRNA recognised in the sample, and the fluorescent code to differentiate distinct miRNAs. By carrying two end regions of assorted fluorescence intensity, a particle code is triggered in the yellow channel, and up to 70 codes are achievable. In all panels each miRNA is independently assigned one of those codes so that data from a blend of particles can be assigned to distinct target miRNAs. Finally, after acquisition, the Firefly Analysis Workbench software processes events from the three regions of the particles and gather them into a single event, providing the affluence data for each target miRNA.

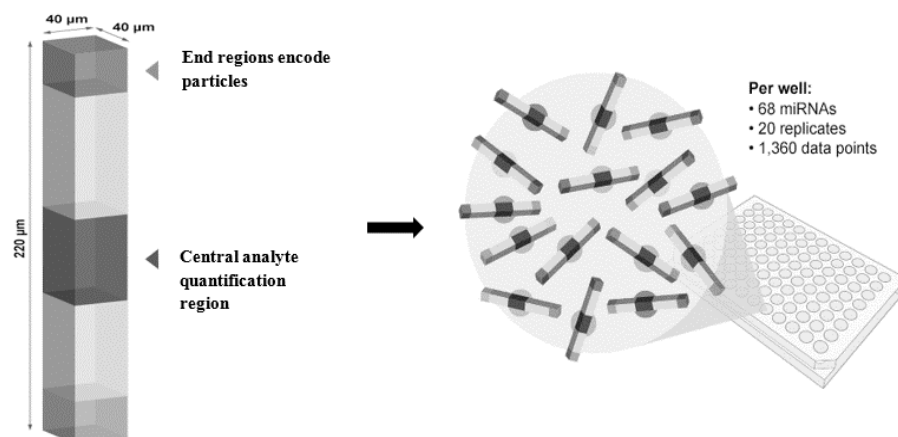


Fig. 3.3.1.1. Firefly particle structure. Adopted from Abcam discover more (2017) and then merged and modified by Roberta Freezor using online Pixlr photo editor. Three distinct regions apprehend target miRNAs and encoded particles are shown. The end regions (top and bottom) encode particles and hold dissimilar fluorescence intensities to promote a fluorescent barcode and in a known panel, all particles that capture a specific miRNA display the same code. Whereas the central analyte quantification region (middle) holds probes to capture an individual target miRNA. When particles are passed through a FC, they act as a series of three cells. By disconnecting the target quantification region from the particle encoding data, the communication between channels and banish the necessity for compensation.

3.3.2 Results

Erythrocytes, eMV control, eMV CaCl₂, eMV CaCl₂ + NHS, HeLa cells, HRV16iHc, HeLaMVC, and HRV16iHVMV samples were prepared as set out in chapters 2.2.1.2, 2.2.2, and 2.2.4. The mirVana™ miRNA Isolation Kit was used for this procedure and the experimental design was followed in accordance with the manufacturer's protocol (chapters 2.2.9.1 and 2.2.9.2). The samples were then submitted to Abcam for profiling (chapter 2.2.9.3), and data analysis was performed using Firefly Analysis Workbench software.

In order to verify the assay performance, Abcam uses two measures in every well: (1) RNA spike-in controls; and (2) particles with no miRNA probe (blank) that defines the background fluorescence. The geNorm-like algorithm was used to regulate the stability reference of housekeeping-genes from a set of examined candidate reference genes in a stated panel. In consequence, a gene expression normalisation factor can be tallied for each sample hinged on the geometric mean of a user-defined number of reference genes, and can be applied to the data in order to select the three most appropriate miRNAs to use for normalisation. To improve the likelihood of identifying three appropriate normalisation candidates, several miRNA targets identified by previous researchers (Qi, *et al.*, 2012; Chen, *et al.*, 2013), and by Abcam in an independent analysis were

automatically included in the fixed panels (in this case the immunology panel) signifying that those miRNA that were recognised as most stable across the samples.

The normalised data used for this study consisted of background-subtraction, using the three most appropriate normalisers *hsa-let-7i-5p*, *hsa-miR-20a-5p* and *hsa-miR-93-5p* (green boxes), and negative miRNA controls *hsa-miR-494-3p* and *hsa-miR-885-5p* (blue boxes), in Fig. 3.3.2.1. These parameters were used to generate all the figures in this chapter, which may include signals at or below the detection threshold. The statistical confidence using multiple measurements of the non-normalised data was used to ascertain the average signal (in arbitrary units) for each miRNA target, as measured in every sample. Averages were calculated across multiple target-specific particles mixed with a sample.

The Multiplex Circulating miRNA assay detects the same miRNA multiple times for every sample, in order to provide the statistical confidence in the results. The Mean fluorescence intensity (MFI) signal is provided with less background, showing a 95% confidence interval between particle methods. The limit of the detection of a probe is calculated from the negative samples, using a combination of two factors: S_{ww} (1) the well-to-well standard deviation of the mean signals; and S_{pp} (2) the mean of the particle-particle standard errors. Then the limit of detection is calculated as $[(3S_{ww})^2 + (4S_{pp})^2]^{1/2}$. To determine whether a particular miRNA signal is detected, the assay background was subtracted from the miRNA signal measured in the samples and the result was compared to a target-specific detection threshold. This is performed when a probe is detected in a particular sample, and if the statistical distribution of the probe's particles in that sample were significantly higher than the distribution of that probe's particles in the negative samples. The limit of detection of a probe is an estimate of the positive fluorescence a probe would have, in order to be determined as significant in a given sample.

Abcam has determined by comparison to dilution series on large numbers of probes, that give a conservative estimate of the limit of detection. If no negative samples are defined, no limit of detection is available. Although most miRNAs exhibit low background signal in negative control wells, there are exceptions where the miRNA probe sequence is complementary to the amplification primers and a higher background signal is measured in negative control wells. The subtraction of the assay background resolves this and there is no effect on the assay, except to slightly decrease the dynamic range of detection of the chosen miRNAs.

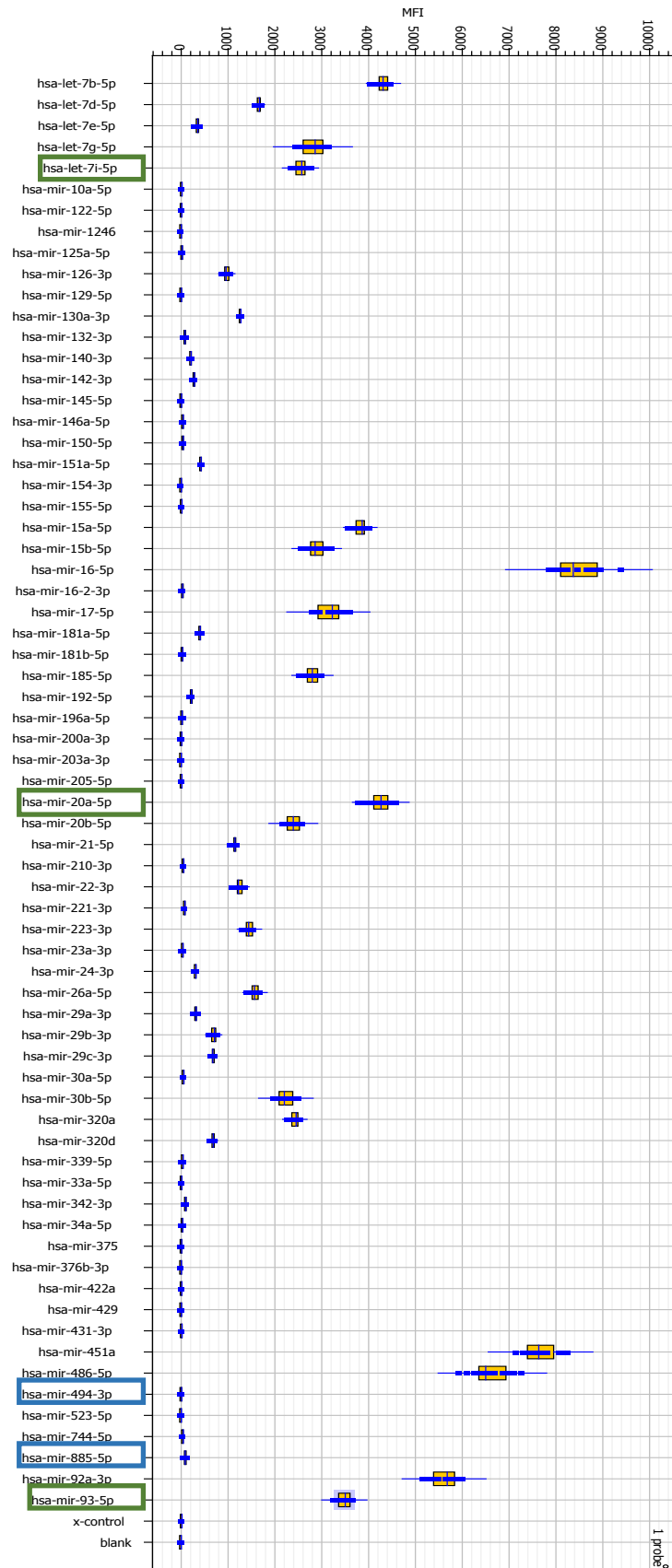


Fig. 3.3.2.1. The average signal in RNA spike-in controls and miRNAs selected for data normalisation. RNA's control and samples were labelled with the immunology panel (68 miRNAs) and analysed with the EMD Millipore Guava 8HT flow cytometry. Due to their stability in signal expression in all samples, *hsa-let-7i-5p*, *hsa-miR-20a-5p* and *hsa-miR-93-5p* were selected to act as normalisers, and *hsa-miR-885-5p* along with *hsa-miR-494-3p* were selected to act as negatives. The graph shows Y axis representing the probes including blank and x-control used here, against the X axis representing the MFI of the signal detected with the FireFly particles.

Additionally, a third quality control measure employed by Abcam is to process a positive control well in parallel with the submitted samples. The positive control well is either pooled human sera or Firefly Control RNA that has been previously characterised by the Multiplex Circulating miRNA Assay. The positive control signals from this study are compared to historical values in Fig. 3.3.2.2.

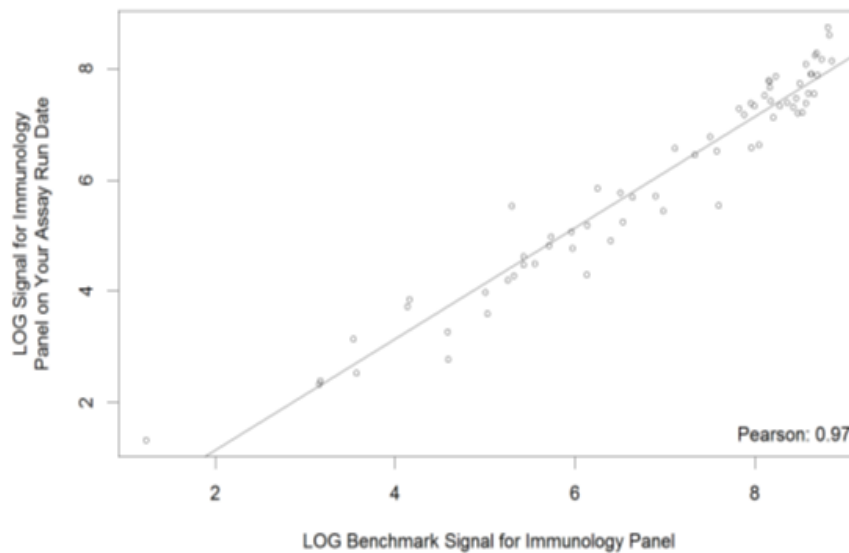


Fig. 3.3.2.2. Comparison of positive RNA spike-in controls to historical values. The graph shows the Y axis representing LOG signal for the immunology panel used for this experiment on the date of the experiment, against the X axis representing the LOG benchmark signal for the immunology panel, providing a presented trend line showing a visual confirmation of the positive correlation.

The heat map (Fig. 3.3.2.3) is a grid of normalised miRNA signal intensities indicated by colour, where orange represents highly expressed miRNA and blue represents lowly expressed miRNA. The miRNA targets with background-subtracted signal show the detection threshold in one or more samples. The white miRNA targets have background-subtracted signals and show the detection threshold across all samples. The signal in low-expressing targets (white) is often masked by sources of noise such as non-specific binding and FC noise. Therefore, it is considered not to meet the chosen threshold of detection and removed from further analyses.

The geNorm-like algorithm, a popular method to assess the substantial reference housekeeping-genes against a set of tested candidate reference genes in a given sample panel, was used for normalisation in circulating miRNA detection. Henceforth, a gene expression normalisation factor can be computed for each sample positioned on the geometric mean of a user-defined number of reference genes. It can be applied to the data

in order to select the three most appropriate miRNAs to be used for normalisation in this data set. To improve the likelihood of identifying three appropriate normalisation candidates (*hsa-let-7i-5p*, *hsa-miR-20a-5p*, and *hsa-miR-93-5p*), several miRNA targets identified by previous researchers (Chen, *et al.*, 2013) were considered and utilised.

According to Pritchard, *et al.*, (2012), *hsa-miR-451*, *486-5p*, *92a* and *16* are significantly increased in haemolysed samples of human plasma and serum, and are highlighted as markers of such which explain why manufacturers include haemolysis markers in fixed panels. Here, only *hsa-miR-451* and *486-5p* were used as haemolysis markers and were excluded from erythrocytes and eMV data only. This is because *hsa-miR-92a* and *hsa-miR-16* were also present in all HeLa cells and their derived MV and expressed at different levels.

hsa-let-7b-5p, *7d-5p*, *7e-5p* and *7g-5p* were present in all samples analysed in this study. And it may be because these miRNAs members, belonging to the same family have identical seed sequence, a highly-conserved region of nucleotides 2 to 8, which is important for target recognition. This also suggests that the *let-7* family members share at least some targets and functions (Su, *et al.*, 2012). *lin-4* and *let-7* were the first two miRNAs identified, and it was discovered in the nematode *Caenorhabditis elegans*. They regulate the schedule of stem-cell division and differentiation. *let-7* and its relatives are vastly preserved over species in sequence and function. Mis-regulation of *let-7* generates a less differentiated cellular state and the development of cell-based diseases such as cancer (Roush & Slack, 2008).

Since not all of the miRNAs were relevant to this study, those miRNAs showing low signal intensity (*hsa-miR-16-2-3p*, *33a-5p*, *125a-5p*, *129-5p*, *140-3p*, *142-3p*, *154-5p*, *155-5p*, *200a-3p*, *205-5p*, *339-5p*, *375*, *376b-3p*, *429*, *431-3p* and *523-5p*), were excluded from analysis, although, *hsa-miR-122-5p* remains in the heat map as a representative example of low signal detection. This was in order to ensure focus on the miRNAs of interest, in order to build a specific miRNA detection profile to gain further insight into the samples submitted for profiling. This can be observed in Fig. 3.3.2.3, where the heatmap is showing merged of each sample (N=3) and excluding triplicates of assay negative, blank and x-control, all normalisers and negatives.

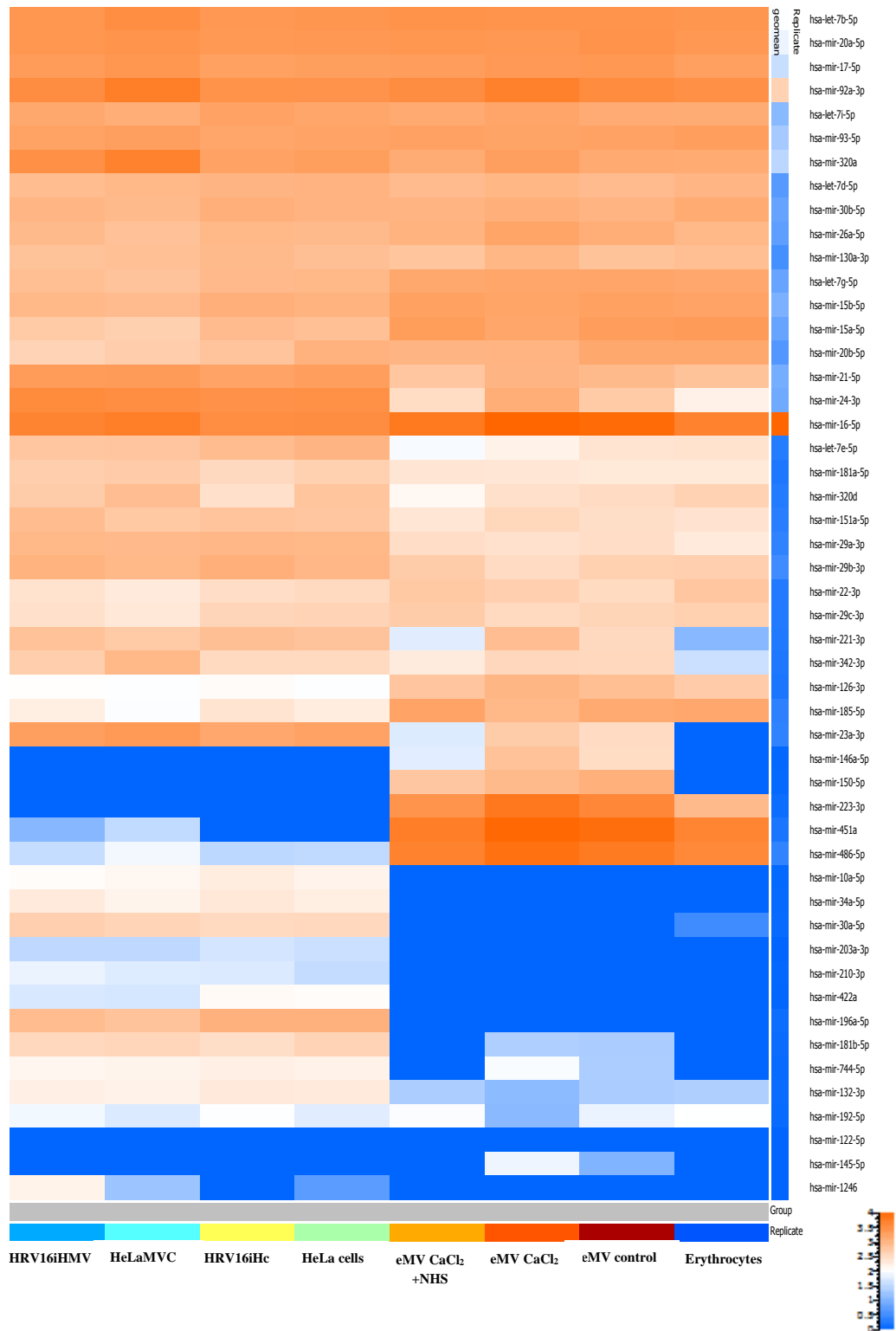


Fig. 3.3.2.3. Expression profile comparison of all samples from merged triplicates. The Heatmap shows the major differences of the submitted samples, highlighting the increased and decreased expression of miRNAs. It also compares MV samples (N=3) derived from different sources showing the major differences of the samples derived from different sources comparing different detected miRNA's. The expression of shared and specific miRNAs for each sample group is shown in different colours, blue for low expression and orange for strong expression.

The potential plasma biomarker that may indicate progression of Gastric Cancer (Zhang, *et al.*, 2015) *hsa-miR-16-5p*, was highly expressed in all samples used for this study. It has been recommended that the candidate reference miRNAs should concern a distinct functional classes, which would fundamentally lessen the likelihood of contradict co-regulation (Mestdagh, *et al.*, 2009). Conversely, the same expression levels of reference miRNAs should be noticeable in all samples, and show low dispersion and no affiliation with a disease (Zampetaki & Mayr, 2012). This was not the case in this study, having been detected at different levels and therefore not used as a normaliser reference. Also, it has been noted that the expression level of *miR-16-5p* could exhibit individual variances (Konishi, *et al.*, 2012) because *miR-16-5p* is a contaminant in haemolysed blood samples, and is not adequate as an optimal internal control. A vast spectrum of miRNAs associated with physiologic and pathologic events can be carefully loaded into the MV, increasing the complexity of the relationship of the miRNA levels between the tissues and circulatory system (Reid, *et al.*, 2011).

hsa-miR-92a-3p was also highly expressed in all samples, and it has also been suggested as a potential reference miRNA (Bignotti, *et al.*, 2016). A search of *hsa-miR-92a-3p* in the miRBase database (Kozomara & Griffiths-Jones, 2014 ; Griffiths-Jones, *et al.*, 2008) has identified gene targets including those involved in cell cycle regulation and cell signalling. It has also proven vital during all stages of mammalian development and necessary for the proliferation of cells, because it is readily available in healthy individuals' serum. However, levels are irregular and seem to alter in response to the onset of certain cancers. As a result of its differing levels of expression observed in all the samples studied here, it could not be used as a normaliser in this study.

Notably, 25 out of 68 miRNA were identified in all samples (apart from normalisers, negatives and haemolysis markers) in Fig. 3.3.2.4. The summary level of expression of the 25 miRNA identified (N=3) can be observed by comparing the Mean Fluorescence intensity (MFI).

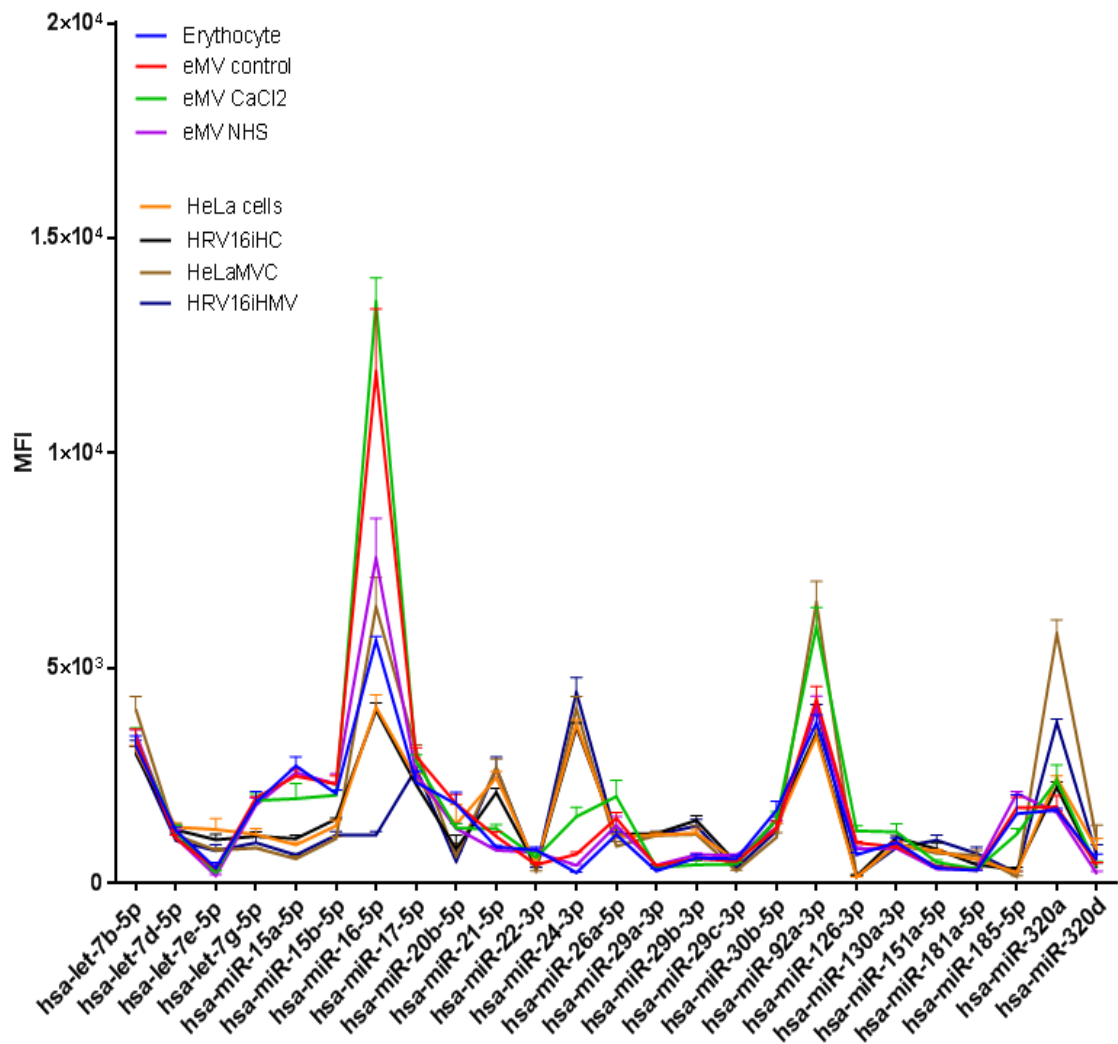


Fig. 3.3.2.4. Summary of miRNAs present in all samples. The graph shows the major differences in expression of the submitted samples, highlighting the increased and decreased expression of miRNAs in each sample (N=3). It also compares MV samples derived from different sources. The analysis was obtained using the GraphPad Prism software version 7.2, where data was arranged in groups and error bars were obtained with the Mean and Error.

In addition to the exclusion of low signal detection of miRNAs in the samples, major differences in miRNA expression between samples were observed. For example, miRNAs *hsa-miR-10a*, *23a-3p*, *24-3p*, *30a-5p*, *34a-5p*, *132-3p*, *196a-5p*, *203a-3p*, *210-3p*, *422a*, *181b-5p* and *744-5p* showed stronger expression in HeLa and their derived MV samples. However, *hsa-miR-23a-3p* was not expressed in erythrocytes, but slightly expressed in eMV samples (Fig. 3.3.2.5).

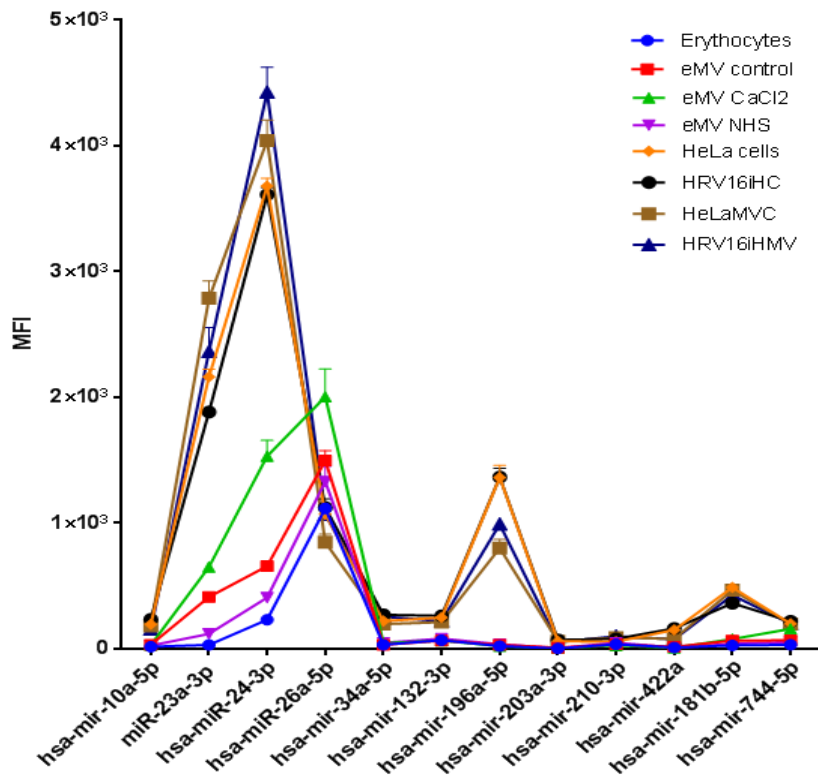


Fig. 3.3.2.5. Summary of miRNAs demonstrating high expression in HeLa cells and their derived MV. The graph compares HeLa cells and their derived MV samples with erythrocytes and eMV samples and demonstrates the major differences of the submitted samples. This is highlighting the increased and decreased expression of a number of miRNAs with higher expression in HeLa and their derived MV. The conclusions were drawn from Fig. 3.3.2.3.

In contrast, *hsa-miR-223-3p* was not detected in HeLa or their derived MV samples, but strongly expressed in erythrocytes and eMV samples. Additionally, *hsa-miR-146a-5p* and *150-5p* were not expressed in erythrocytes, HeLa cells, HRV16iHC and their derived MV, but were expressed in eMV. (Fig. 3.3.2.6).

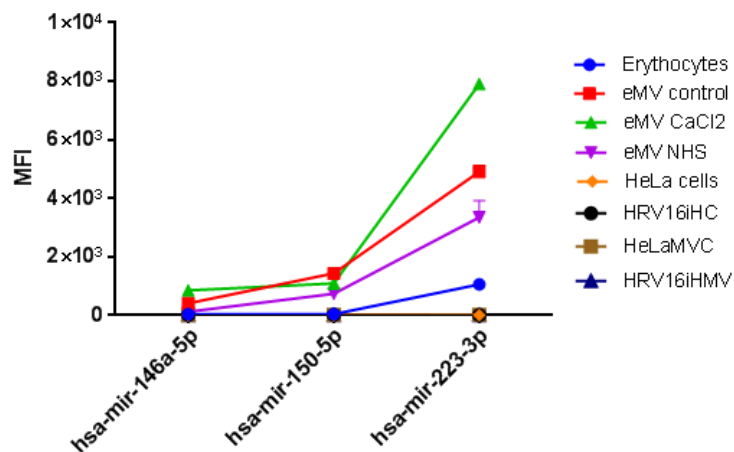


Fig. 3.3.2.6. Summary of miRNAs demonstrating high expression in erythrocytes and their derived eMV. The graph compares the differences between all submitted samples, highlighting the increased and decreased expression of miRNAs in all erythrocytes and eMV, in comparison with HeLa cells and their derived MV.

3.3.3 Discussion

Due to the common assumption that erythrocytes do not express RNA content, one can be confused to find that erythrocytes contain significant amounts of miRNAs (observed in results chapter 3.3.2). This is not only because of their presence, but also, owing to the reasons for miRNA to be present in cells to regulate gene expression by effecting mRNA translation which was believed to be non-existent in erythrocytes (Hamilton, 2010). Nevertheless, the presence of miRNAs in erythrocytes has been reported in Malaria (Rathjen, *et al.*, 2006), and sickle cell disease because of the disease pathogenesis which is dramatically altered in homozygous sickle cell disease erythrocytes and their defect in terminal differentiation (Chen, *et al.*, 2008).

It is understood that erythroid cells misplace their nuclei and active transcription in the course of the reticulocyte stages (see Fig. 1.2.1). miRNAs are credible to participate in a regulatory role in post-transcriptional regulation in erythroid cells, but there is a lack of information explaining the reasons for this, as well as for the presence of miRNAs in erythrocytes. Felli, *et al.*, (2005) reported the role of miRNAs that have been implicated in the process of erythropoiesis, and miRNA expression have been reported in *in vitro* erythroid differentiation also (Choong, *et al.*, 2007), but no reasons were discussed. Therefore, the genomic study of miRNAs in erythrocytes may provide an individual opening to begin to build the understanding of miRNA regulatory roles in erythroid cells (Sangokoya, *et al.*, 2010), and this would further support their feasibility in the eMV studied during this PhD research.

The general analysis of miRNA expression in circulating erythrocytes can contribute towards mechanistic insights into the disease phenotypes of erythrocyte, adding a new feature to erythrocyte characterisation, and can potentially enhance the interpretation of their phenotypic alterations in physiological and pathological adjustment. For example, *hsa-miR-223-3p* was demonstrated as being present in erythrocytes and all eMV samples, but not in HeLa or their derived MV. This is a haematopoietic particular miRNA with essential functions in myeloid lineage development. It performs a crucial part in promoting granulocytic differentiation (O'Connell, *et al.*, 2011), while also being affiliated with the suppression of erythrocytic and megakaryocytic distinction of K562 cells (myelogenous leukaemia cell line) (Yuan, *et al.*, 2009).

It is important to note that, each and every miRNA present in the samples utilised during this PhD research expresses different characteristics, and can also provide insights into

post-transcriptional regulation of gene expression. For example, Pinatel, *et al.*, (2014) predicted that *miR-223* targets revealed enrichment in cell death and survival-related genes and in pathways commonly altered in breast cancer. Their results demonstrated that protein levels for Signal transducer and activator of transcription 5A (STAT5A), Integrin alpha-3 (ITGA3), and NRAS proto-oncogene GTPase were modulated by *miR-223*. They evidenced that STAT5A is a direct *miR-223* target and underlined a feasible correlation between *miR-223* and STAT5A in migration and chemotherapy response, and that *miR-223* has an influential role in breast malignancy that could possibly be investigated therapeutically.

In haematopoiesis, a term used for the formation of blood cellular components, *hsa-miR-150-5p* (present in eMV but not in erythrocytes) regulates genes whose downstream products encourage differentiating stem cells to become megakaryocytes rather than erythrocytes. It also, induces T-cell differentiation (miRBase database). Blood cell-derived EV, containing *miR-150*, have been shown to enter human endothelial cells delivering *miR-150*, which reduced c-Myb (gene- proto-oncogene protein also known as transcriptional activator) expression. This enhanced cell migration of human endothelial cells (Zhang, *et al.*, 2010). This expression is of interest because it suggests a different characteristic and yet another potential use for eMV because once inside neighbouring cells they can potentially share this information with a variety of sources in circulation.

Furthermore, *hsa-miR-146a-5p* (present in eMV control and eMV CaCl₂) has been observed to be involved in the regulation of inflammation, and other biological processes that operate in the innate immune system. This has been reported to be highly upregulated in osteoarthritis cartilage, and could be involved in its pathogenesis (miRBase database). Lopez, *et al.*, (2017) suggested that *miR-146a-5p*, and *miR-24-3p* (present in all samples), are consistent blood markers of antidepressant response and regulators of psychiatrically relevant signalling pathways, and functional annotation clustering analysis disclosed an enrichment of calcium signalling pathways. This is interesting because eMV CaCl₂ demonstrated a particular expression of these these miRNAs. Their results, imply influential implications for the clarification of biological mechanisms involved in clinically relevant antidepressant effects, and propose that these miRNAs could potentially act as correlates or state biomarkers of treatment response. This highlights the potential for the development of diagnostic tools, precautionary approaches, and successful pharmacological interventions for major depressive disorder.

hsa-miR-221-3p is an oncogenic miRNA that targets CD117 (receptor tyrosine kinase protein), which then prevents cell migration and proliferation in endothelial cells. It is also known to be involved in the induction of angiogenesis (miRBase database). This miRNA was present in eMV control, eMV CaCl₂, HeLa, HRV16iHc and their derived MV but not in erythrocytes and eMV CaCl₂ +NHS.

Additionally, several cell-preferentially expressed miRNAs are worth noting. *hsa-miR-342-3p* was present in all samples apart from erythrocytes. This miRNA targets the nuclear factor kappa-light-chain-enhancer of activated B cells known as the NF-κB pathway, and it has a significant role in cell proliferation. Hence it's suitability for the investigation of therapeutic targets (Zhao & Zhang, 2015).

Likewise, HeLa, HRV16iHc and their derived MV also expressed some miRNA specificity, in comparison with erythrocytes and eMV samples. For instance, *hsa-miR-23a* was highly expressed in HeLa and their MV, it was weakly present in eMV control and eMV CaCl₂, but absent in erythrocytes and eMV CaCl₂ + NHS samples. This miRNA is known to regulate the transcriptional repressor Hairy enhancer of split 1 (Kawasaki & Taira, 2003).

In a study by Ru, *et al.*, (2014), *miR-23a* stimulated the replication of human herpes simplex virus type 1 (HSV-1) in HeLa cells. The interferon regulatory factor 1 (IRF1), an innate antiviral molecule is selected by *miR-23a* to advance viral replication. This is because *miR-23a* attaches to the 3'UTR of IRF1 and down-regulates its expression. The suppression of IRF1 expression minimises RSAD2 gene expression, augmenting HSV-1 replication. The ectopic expression of IRF1 abrogated the advancement of HSV-1 replication which is led by *miR-23a*, and the IRF1 advances to innate antiviral immunity by binding to IRF-response elements to control the expression of interferon-stimulated genes (ISGs) and apoptosis, disclosing a complex interaction between *miR-23a* and HSV-1. They hypothesised that *miR-23a* eases HSV-1 replication by regulating IRF1-mediated antiviral signal pathway, and IRF1 mRNA have also demonstrated to be up-regulated after HRV16 infection (Kim, *et al.*, 2015) which may explain why HRV16iHcMV are enriched with this miRNA.

miR-23a has also been observed to be proportionately stable in plasma and serum (Komatsu, *et al.*, 2016) and this is not affected by haemolysis. Therefore it is important to note the possible effects of miRNA profiling when conducting data normalisation and

analysis, so that systematic biases are discarded and detection of disease associated with miRNA biomarkers even from samples affected by haemolysis, are detectable (Blondal, *et al.*, 2013).

In terms of chronic obstructive pulmonary disease (COPD), a pilot study by Fawzy *et al.*, (2016), observed the affiliation of the *miR-196a2* rs11614913 polymorphism with COPD susceptibility and bronchodilator response to short-acting β_2 -agonist. Where, 108 COPD male patients and 116 unrelated controls were used for genotyping rs11614913 polymorphism. When compared with controls COPD patients did not express notable differences in the genotype distribution and allele frequencies of the studied miRNA, but COPD patients with homozygote genotype (CC) results correlated to those with the smallest bronchodilator response post Salbutamol inhalation. The heterozygotes (CT) had an intermediate response, while those with the TT genotype (homozygote dominant) showed the highest response. *miR-196a2* rs11614913 polymorphism is associated with the bronchodilator response of COPD patients, generating a hypothesis of the potential use of *miR-196a2* variant as a pharmacogenetic marker for COPD which also provides an explanation of why *miR-196a* was present in HeLa and their derived MV and absent in erythrocytes and eMV samples.

hsa-miR-181b was present only on HeLa, HRV16iHc and their derived MV. In an investigation by Yang, *et al.*, (2013) into the clinical significance of *miR-181b* expression in non-small cell lung cancer (NSCLC), it was revealed that there was an association of *miR-181b* expression with clinicopathological factors or prognosis of patients analysed. In the beginning of the investigation, *miR-181b* expression was remarkably down-regulated in NSCLC tissues, in comparison with their normal counterparts. Subsequently, the low *miR-181b* expression was observed to be associated with larger tumour size, higher p-TNM stage and positive lymph node metastasis of NSCLC patients. Then, survival analysis revealed that the general survival and disease-free survival of NSCLC patients with low *miR-181b* expression decreased in comparison to those patients with increased *miR-181b* expression. Thus, their study indicates that down-regulation of *miR-181b* may be affiliated with aggressive disease progression and poor prognosis of NSCLC patients. For this PhD research it may indicate that *miR-181b* involvement in lung carcinogenesis could potentially be favourable for MV to be used as a potential prognostic marker for NSCLC.

HRV16 show alteration in the microRNAome of HeLa cells indicating an area for research into infectivity and a potential target for prevention (Gutierrez , *et al.*, 2016). MV can also exert effects on cells by stimulating specific signalling pathways (Mathivanan, *et al.*, 2010). This may suggest that MV may have the ability to alter the transcriptome and signalling activity within recipient cells, allowing them to induce specific phenotypic changes, which support MV as potential therapeutic agents.

miRNAs are highly important because they contribute significantly to the turnover of many proteins, thus inducing effects that may be either stimulatory or inhibitory for target cells which can change gene expression.

The incorporation of miRNAs in eMV may allow them to circulate in the blood while avoiding degradation from blood RNase activity because they are encapsulated (Arroyo, *et al.*, 2011). This is important because miRNAs may contribute significantly to the turnover of many proteins, thus inducing effects that may be either stimulatory or inhibitory for target cells which can change gene expression.

It is interesting that, not all miRNA present in MV samples were present in their parent cells during this PhD research, and so far, there is no clear evidence whether associated miRNA are either inside or just adhere to EV under *in vivo* conditions (Bala, *et al.*, 2015).

After assessing the pattern of miRNAs detected in the eMV samples, further analysis focused on their reported target genes using the miRTarBase database. The analysis generated a list of candidate genes with >14.165 target genes for the miRNA present in eMV samples, with >7.358 being redundant genes (see Appendix VI). The FunRich software classified their functional role in clusters of genes that are not mutually exclusive. The principle here is that previously stated for the GO enrichments produced in chapter 3.2.4, where the product of a single gene could have one or more cellular components (Fig. 3.3.3.1), molecular functions (Fig. 3.3.3.2), be associated with different biological processes (Fig. 3.3.3.3), and be involved in several biological pathways (Fig. 3.3.3.4).

The GO enrichments for the cellular component revealed over 635 locations, with an important representation of genes with functions involved in the nucleus and the cytoplasm. The rest of the categories evaluated here showed lower scores <25% with no specific enrichments.

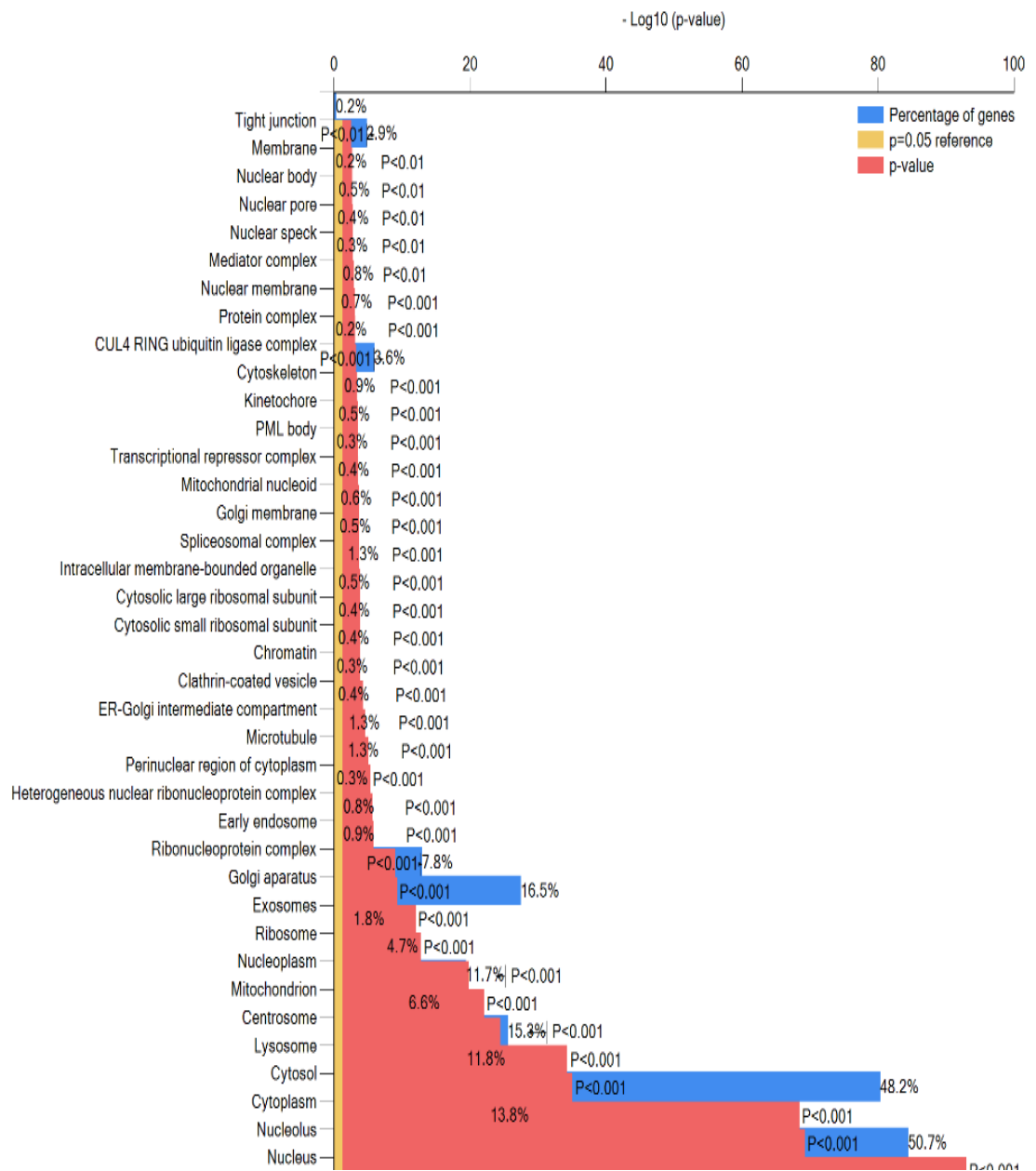


Fig. 3.3.3.1. Cellular component enrichment for target genes of miRNA observed in eMV. Frequency of target genes involved in similar cellular components.

In terms of molecular functions, the wide range of genes showed an overall heterogeneous distribution with low frequencies (0-25%) and no specific enrichments, with DNA binding and transcription showing the highest scores among the miscellaneous single cluster.

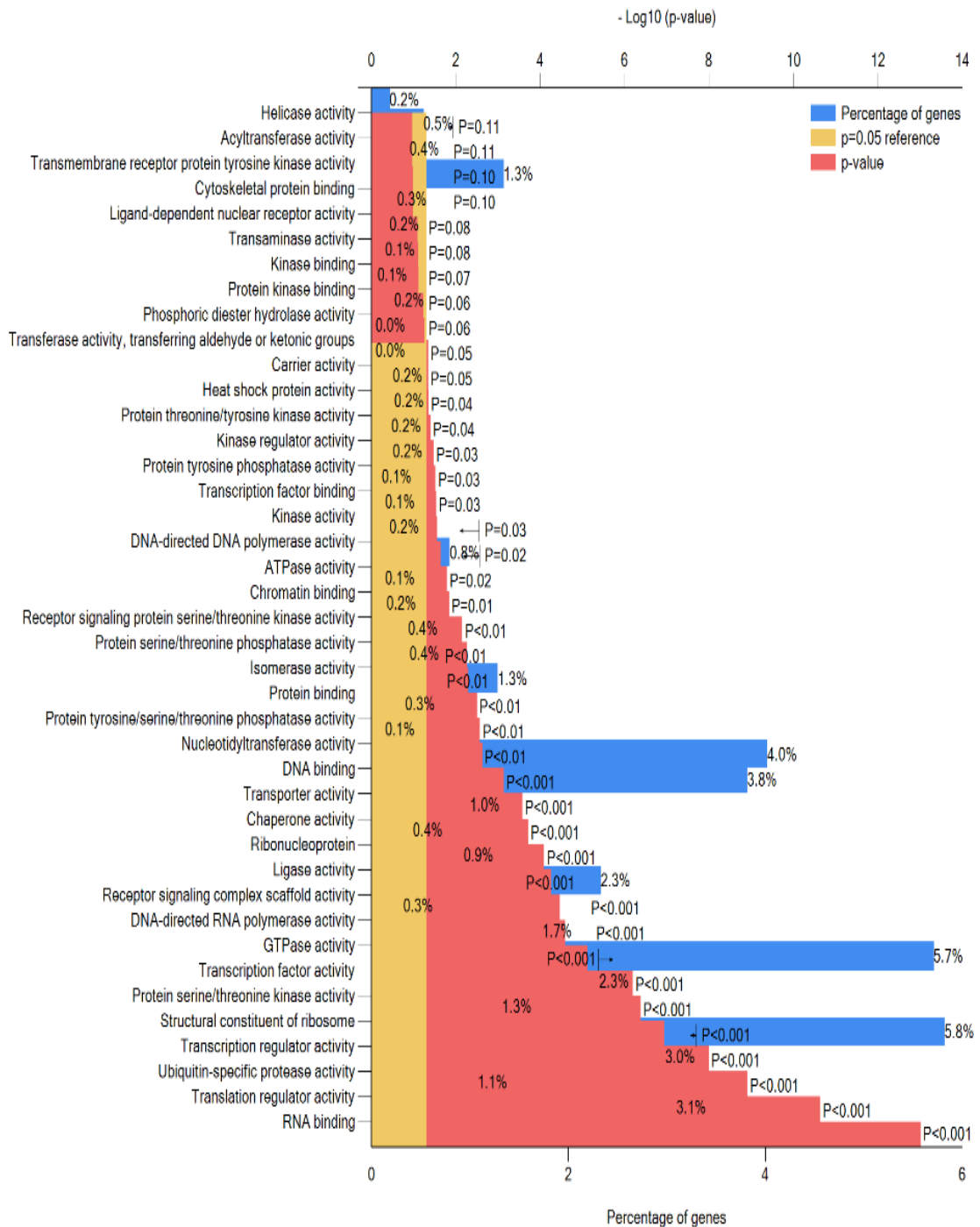


Fig. 3.3.3.2. Molecular function enrichment for target genes of miRNA observed in eMV. Frequency of target genes involved in similar molecular functions.

The biological processes enrichment showed a single cluster (0-25%) of overlapping categories with different levels of representation. Within this group, it is possible to detect the relevance of metabolic processes performed by this set of genes.

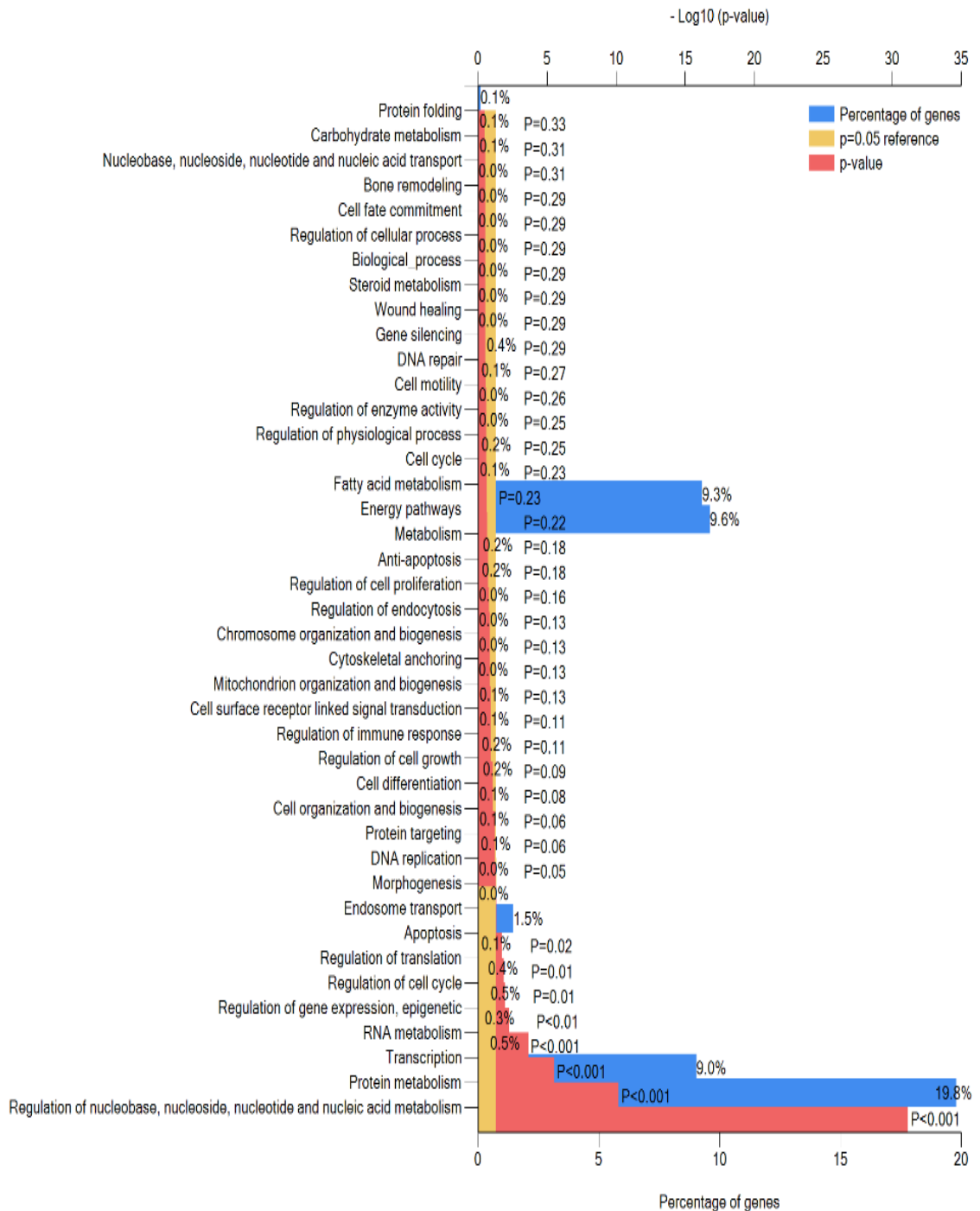


Fig. 3.3.3.3. Biological processes enrichment for target genes for miRNA observed in eMV. Frequency of target genes grouped by biological processes.

In the case of biological pathways, the genes were grouped in two main clusters, one of them involving gene expression only (0-25%) and the other (25-50%) covering a variety of process regulated by the same set of genes, including: signalling events, cell surface interactions, cell adhesion and essential signalling pathways for cell environment recognition such as the mTOR, AKT and IGF1 that control cell fate representing ~28% of the miRNA target genes data input.

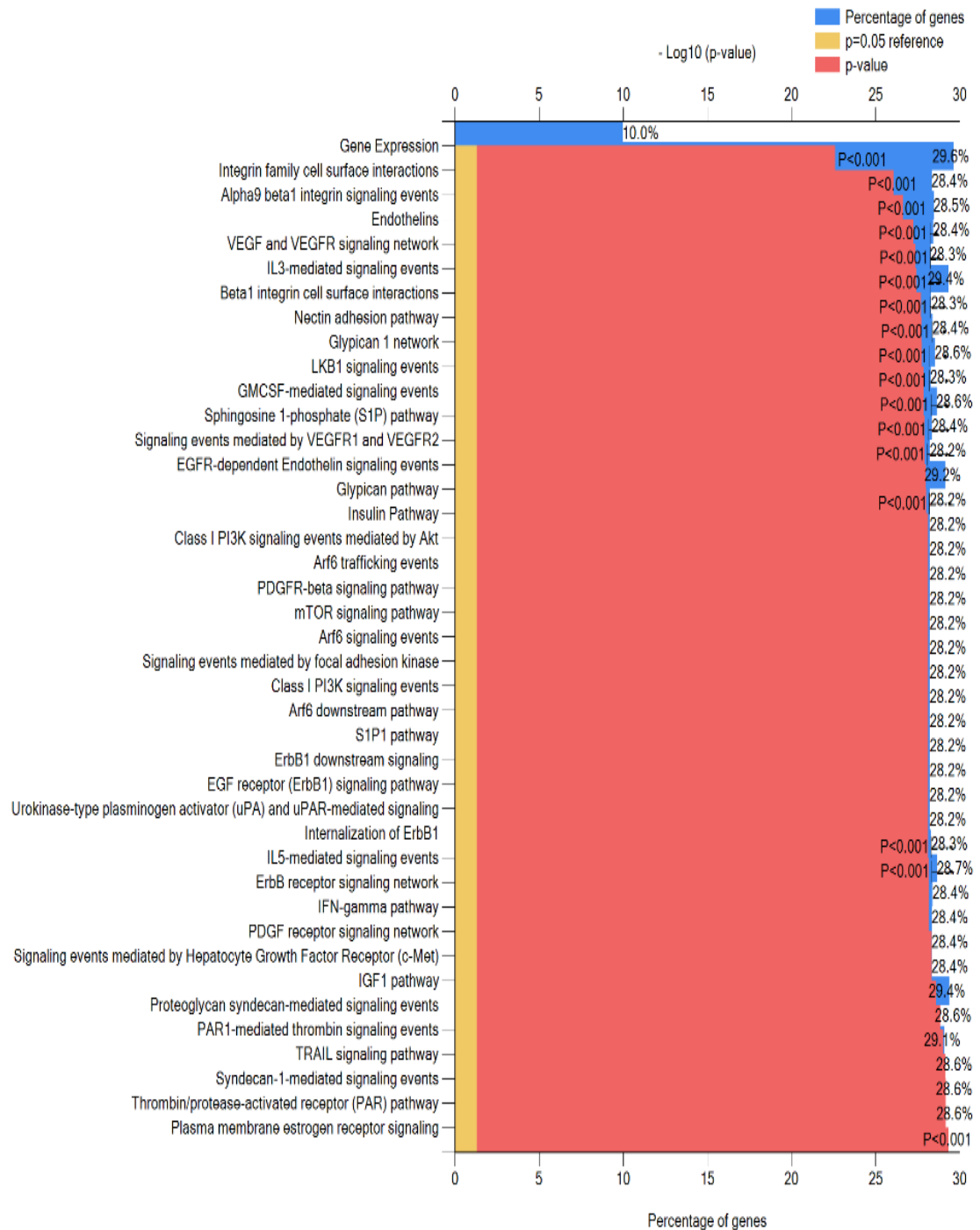


Fig. 3.3.3.4. Biological pathways enrichment for target genes of miRNA observed in eMV. Frequency of target genes grouped by biological pathways. Where, the impact of a series of interactions among genes that leads to a certain product or a change, which can trigger the assembly of neighbouring cells.

Taken together, the GO enrichments generated in this section with the target genes of the miRNAs identified in this study, indicate the prevalence of gene products located in the nucleus and cytoplasm with an involvement in translation according to their frequencies. In this sense, this transcriptional machinery may be responsible for regulating several cellular metabolic processes, which was further supported by the enrichment of a set of biological pathways that operate as rheostats of extracellular stimulus that control cell cycle proliferation and cellular outcome. This is highly relevant to this study since the information transported in the isolated eMV by the set of detected miRNA may be involved in the control of those fundamental cellular processes, also supported by the data collected in chapter 3.2.4.

This association of genes according to categories of processes in which they are involved, facilitates the overview of their potential effects, which allows the tailoring of the subsequent analyses of the query gene list, and provides valuable insights with testable hypotheses for the development of future projects. GO annotations and analysis for HRV16iMV is presented in Appendix VII.

3.4 The interaction of MV on the selected cell lines

3.4.1 Introduction

Cell communication is a major aspect of cell biology because it allows the coordination of biological activities of the organism as a whole by using signalling pathways. The release of MV as free entities containing a variety of biological molecules allowing their engagement with and influencing neighbouring cells became a wide and targeted concept (see chapter 1.7). Cancer cell lines constitute key model systems widely used within biological research. To this end, a variety of cell lines were used to conduct the experiments to observe the effect of MV on their growth rate, including:

1. THP-1, a human leukaemia monocytic cell line that has been extensively used to study monocyte/macrophage functions, mechanisms, signalling pathways, and nutrient and drug transport. It was originally isolated from the peripheral blood of a 1-year-old male patient suffering from acute monocytic leukaemia (Chanput, *et al.*, 2014). This cell line has been widely used to study immune responses, not only in the monocyte state but also in the macrophage-like state. In the monocyte state, it can be differentiated into a macrophage-like phenotype using either phorbol-12-myristate-13-acetate, 1α , 25-dihydroxyvitamin D3 or macrophage colony-stimulating factor (Lund, *et al.*, 2016). Although the latter stimulus is biologically relevant *in vivo*, it is less frequently applied *in vitro*, and it does not apply to this PhD research.
2. Jurkat cells are an immortalised line of T lymphocyte cells that are used to study acute T cell leukaemia, T cell signalling, and the expression of various chemokine receptors susceptible to viral entry, particularly HIV. They originally derived from the peripheral blood of a 14-year-old boy with T cell leukaemia which makes them useful in scientific research because of their ability to produce IL2, a type of cytokine signalling molecule which regulates the activities of white blood cells that are responsible for immunity. Their primary research use is in determining the mechanism of differential susceptibility of cancers to drugs and radiation (Abraham & Weiss, 2004).
3. In 1979 Kaighn, *et al.*, defined the PC-3 a prostate cancer cell line, it was established, characterised and its tumourigenicity from a human prostatic adenocarcinoma metastatic to bone was reported. Culturing the transplanted

tumour cells resulted in a human cell line with features identical to those used initially causing tumour.

PC-3 cells retain characteristics similar to epithelial neoplastic cells, including numerous microvilli, junctional complexes, abnormal nuclei and nucleoli, abnormal mitochondria, annulated lamellae, and lipoidal bodies. However, when compared to normal prostatic epithelial cells, PC-3 cells have a substantially decreased dependence upon serum for growth, do not respond to androgens, glucocorticoids, or epidermal or fibroblast growth factors. As well as divergent morphological development and function, the unique canonical pathways reveal greater diversified features including metabolism, retinoic acid signalling pathway, cell proliferation, and differentiation pathways. The divergence of characteristics in PC-3 cells make them helpful when exploring the biochemical changes in advanced prostatic cancer cells, as well as, when assessing their response to chemotherapeutic agents (Dozmorov, *et al.*, 2009).

4. In 1970 the human breast cancer MCF-7 cell line was first isolated from the breast tissue of a 69-year old Caucasian woman. MCF-7 and other human breast cancer cell lines are useful in many studies including investigating the response of hormone, drug screening, and/or development of multidrug resistance, and the activation, amplification, and overexpression of oncogenes (Vazquez, *et al.*, 2004). MCF-7 cells retained several pathological characteristics associated with the mammary epithelium, including cytokeratin sensitivity, unreceptive to desmin (protein), endothelin (amino acid peptide), and vimentin (protein). Through oestrogen receptors in the cell cytoplasm, PC-3 retain the ability to process oestrogen (as oestradiol), and are therefore useful for *in vitro* breast cancer studies because the cell line can be used as an oestrogen receptor positive control cell line (Pinzone, *et al.*, 2004).
5. For the HRV16 viral infection and their derived MV studies, HeLa cells were used. HeLa cells were the first human cell line established in culture and has since become the most widely used human cell line in biological research. Its application as a model organism has contributed to the characterisation of important biological processes. This cell line originates from a cervical cancer tumour of a patient named Henrietta Lacks, and because it has been continuously sub-cultured (transformed), can now be used as an immortalised bronchial

epithelial cell line. One of the earliest uses of HeLa cells was in the development of the polio vaccine (Landry, *et al.*, 2013).

The study of life cycles of many different viruses, including the HRV (although the natural targets of HRV are original human bronchial epithelial cells) is generally more difficult to obtain and maintain in the relevant primary cell cultures and is normally conducted with HeLa cells. The kinetics of Ribonucleic Acid (RNA) replication, the synthesis and processing of viral proteins, and the general subcellular localisation of key non-structural proteins resembled HeLa cells makes them useful for *in vitro* studies (Amineva, *et al.*, 2011).

All of the cell lines mentioned above present particular and different surface markers, ligands and receptors that can regulate cell adhesion, cell signalling, and adaptive immunity (as previously mentioned in chapter 3.2.1). For instance, THP-1 and Jurkat cells are known to present/express CD9 (Reyes, *et al.*, 2015), a member of the tetraspanin superfamily that interact with other tetraspanins and with different transmembrane and intracellular proteins to facilitate cellular activities in the different subtypes of leukocytes, including intracellular signalling, proliferation, activation, survival, and adhesion (Reyes, *et al.*, 2018). CD9 is understood to interact with CD36 (Huang, *et al.*, 2011; Park, 2014) (also see Fig. 3.2.2.3.1), which showed expression in all MV tested during this PhD research (Fig 3.2.1.3). This demonstrates the potential of MV interacting with cells that for example presents CD9.

The biological significance of EV remains largely of interest, and there is still growing evidence that EV may be important mediators of cell-to cell communication (Karpman, *et al.*, 2017). Their interactions with target cells may be suggested to occur directly by phenotypic, and functional characteristics of cells and may do so by a variety of mechanisms of possible interaction network (see Fig. 3.2.1.3.1, 3.2.2.3.1, and 3.2.3.3.1). This interaction may be accomplished by direct stimulation of target cells with vesicle-based growth factors and/or bioactive lipids, the transfer of a variety of membrane surface receptors, epigenetic reprogramming by transfer of genetic material, and/or protein based transcription factors or the transfer of infectious particles (Ratajczak, 2006; Quesenberry & Aliotta, 2010).

3.4.2 Results

Considering the diversity of the cell lines used during this research (set out in chapter 3.4.1), the aim of this chapter is to observe whether MV interact with neighbouring cells *in vitro*. MV were isolated as set out in chapter 2.2.4 and the experimental design was followed as set out in chapters 2.2.11 and 2.2.12.

To record the interaction between MV and cell lines the Lumascope 500 single colour fluorescence live cell imaging microscope was used. It uses light-emitting diode (LED) light sources, Semrock filters, advanced optical engineering, and complementary metal-oxide-semiconductor sensors to provide near diffraction-limited (theoretical maximum) resolution. The Light Source is detected at 488 nm (bright field and fluorescence) and the excitation filter range between 457-493 nm bright line bandpass, and emission filter at 508-552 nm bright line bandpass (for both fluorescence and bright field). It provides images in formats JPG, BMP, TIF, GIF, and PNG at 1280 x 800 pixels (Labtech, 2014). Due to its compact size, it was placed inside the biological safety cabinet for sample preparation and subsequently inside the tissue culture incubator (37°C in a 5% CO₂) for the duration of the experiment.

Incubation of eMV control (labelled with Annexin V) with THP-1 cells is shown in Fig. 3.4.2.1, where the increase of fluorescence intensity observed in eMV (green fluorescence imaging) was accompanied by unlabelled THP-1 cells (white bright field). After 24 hours of THP-1 cells subculture and incubation, labelled eMV sample was added to the culture flask and observed for 15 minutes, because fluorescence intensity disappeared after 20 minutes of exposure. The aggregation of eMV cluster was observed immediately after the incubation period began. eMV movement towards the THP-1 cell membrane initiated after 4 minutes of incubation (Fig. 3.4.2.1a and b), where the eMV aggregated at first, forming two different clusters, then moved towards the cell membrane. Subsequently, at approximately 7-8 minutes of incubation a single cluster of the eMV was formed, where eMV joined cluster interacts with the cell membrane and finally breaks through the cell membrane (Fig. 3.4.2.1c). The eMV cluster appears to be depositing its contents (engulfment) into the cell (Fig. 3.4.2.1d) at the 11 minute mark after the incubation period. A small cluster joins the previously formed cluster of eMV (bottom right), then the entire cluster moves away from the cell membrane, apparently leaving the deposited residues inside the cell.

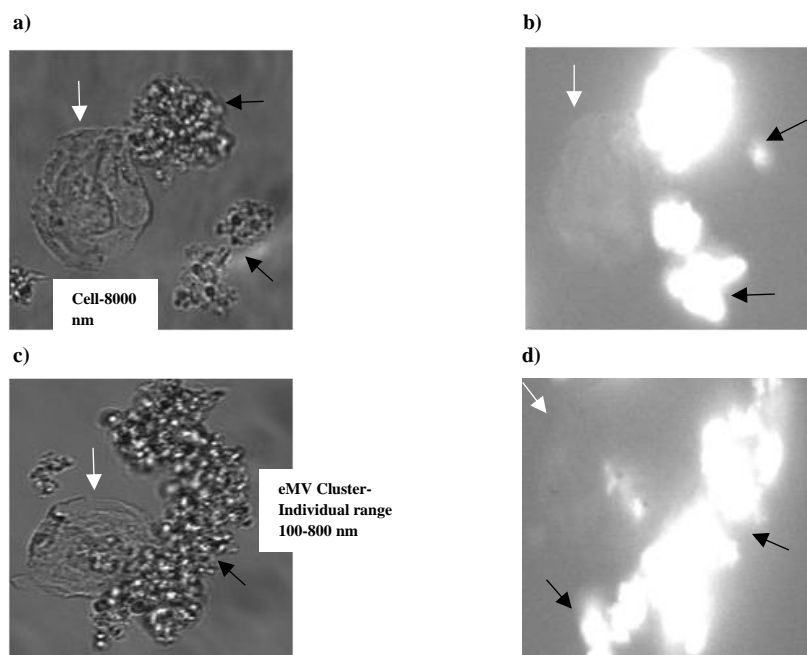


Fig. 3.4.2.1. THP-1 cell and eMV interaction. Photography sequence of eMV interactions with THP-1 cells (100x oil objective lense images) recorded by alternating between bright field and fluorescence. The white arrows indicate the THP-1 cell and the black arrows indicate the eMV Annexin-V labelled. Fig a) and b) show eMV aggregating, and moving towards the cell, approaching the cell membrane (bright field and fluorescent respectively). Whereas Fig c) to d) show the eMV cluster breaching the THP-1 cell membrane and depositing eMV Annexin-V labelled material (bright field and fluorescent respectively) leading to the incorporation of eMV within the cell. After this interaction the eMV cluster moved away from the cell.

Similarly, the phenomenon of eMV control (uninduced) aggregation and their movement towards the Jurkat cell membrane as well as their engulfment was observed. However, in this experiment (Fig. 3.4.2.2) eMV were not labelled with Annexin-V and images were taken under bright field settings only. Also, the eMV cluster does not appear to increase in size (aggregate) over time as observed in Fig. 3.4.2.1, even though the same amount of eMV (ratio 1:1 to cell number) was used. Fig. 3.4.2.2a shows the eMV cluster approaching the cell membrane (at 4 minutes of incubation). Fig. 3.4.2.2b shows what it may be considered an interaction between the eMV cluster and cell membrane (at 7 minutes of incubation), and Fig. 3.4.2.2c suggests the internalisation of the eMV cluster into the cell cytoplasm (at 14 minutes of incubation), but it is not clearly visible.

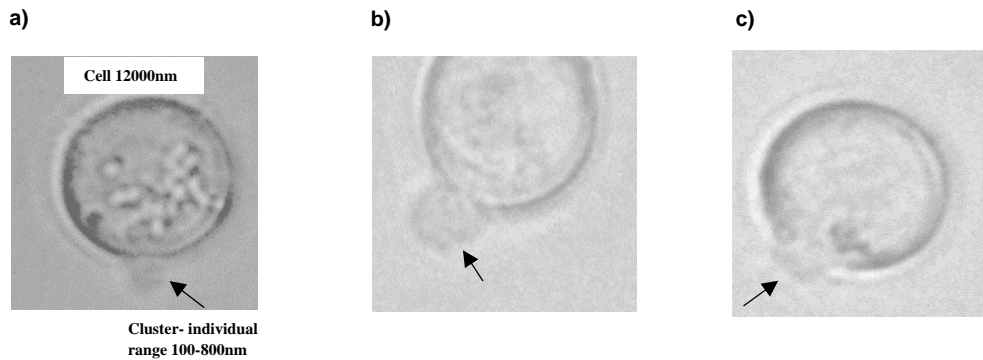


Fig. 3.4.2.2. Jurkat cell and eMV interaction. Time lapse sequence eMV interactions with Jurkat cells (60x objective lens images were taken for 15minutes). Fig. a) shows the eMV cluster approaching the cell membrane, Fig. b) shows the eMV cluster reaching the cell membrane and Fig. c) shows eMV cluster going through the Jurkat cell membrane and depositing the eMV cluster in the cell. The black arrows represent the activity of eMV cluster.

The initial observation (eMV and cell interaction) led to the investigation of how eMV may affect the neighbouring cell, therefore eMV (ratio 1:1 with cell number) was added to the tissue culture flask (different cell lines) and observed to assess whether eMV have an impact on the growth rate of the cell lines FC analysis (see chapter 2.2.5). This is where cells on the exponential phase were seeded into sterile 24 well plates and growth rate (cell number and viability) was assessed by FC every 24 hours for 96 hours (total length of the experiment).

At 0 hours THP-1 (Fig. 3.4.2.3a) and Jurkat cells (Fig. 3.4.2.3b) were $\sim 16 \times 10^5$ / mL (N=3), relatively similar by 24 hours of incubation there was evidence of the growth of both samples (control against eMV treated) but no major differences were observed. There was only a slight decrease in eMV treated cells ($\sim 19 \times 10^5$ / mL) in comparison to the control with $\sim 26 \times 10^5$ / mL. At 48 hours, the difference in cell number/ mL between control and treated eMV appears more obvious ($P > *$ for THP-1 and $P > **$ for Jurkat cells). The trend of the growth rate (number/ mL) decreasing for eMV treated cells continued from 72 hours of observation.

Despite aggregation of eMV being observed in culture, there was no notable migration towards the PC-3 and MCF-7 cell lines, and engulfment was not observed (images not provided here). In contrast to THP-1 and Jurkat cells (decreased effect on the growth rate), no significant effect on the growth rate of PC-3 (Fig. 3.4.2.3c) and MCF-7 (Fig. 3.4.2.3d) cell lines was observed, where the rate of growth was almost at the same rate as control samples.

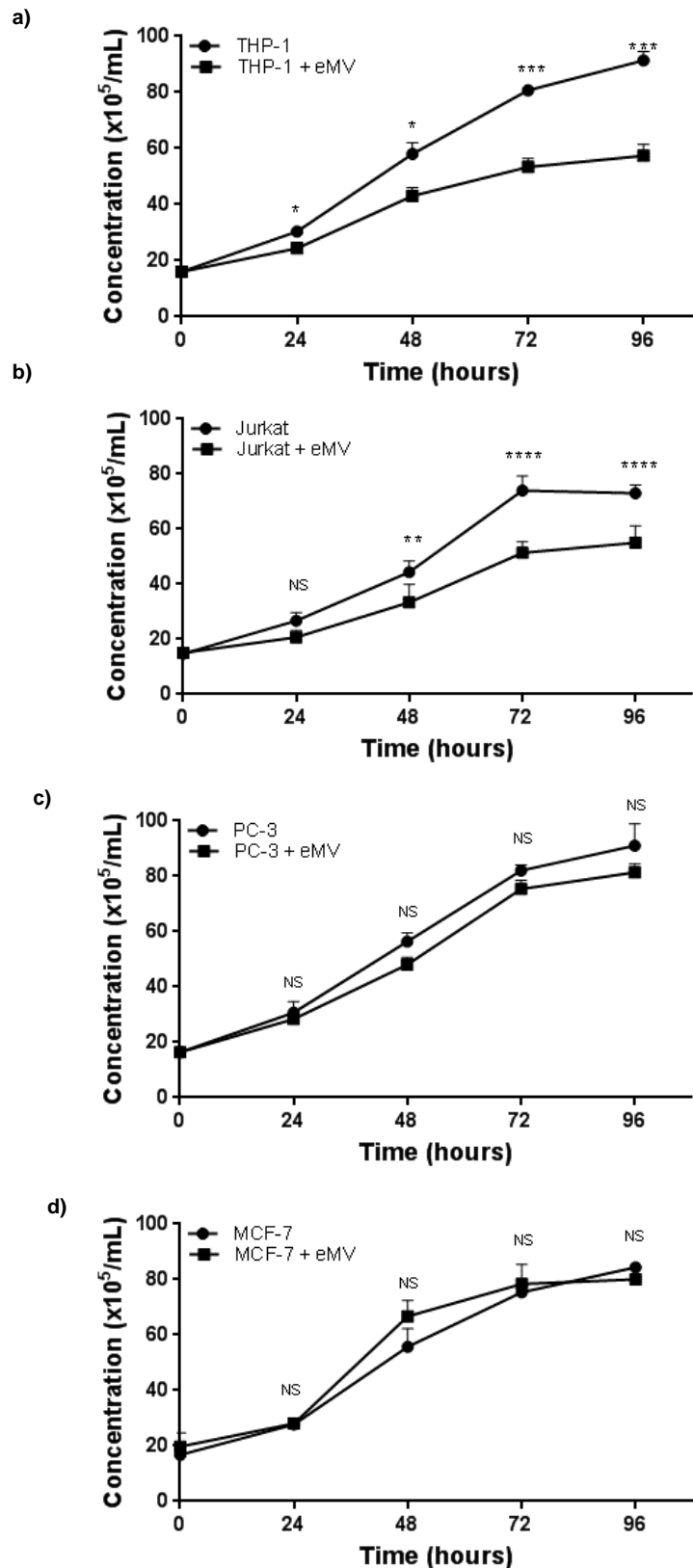
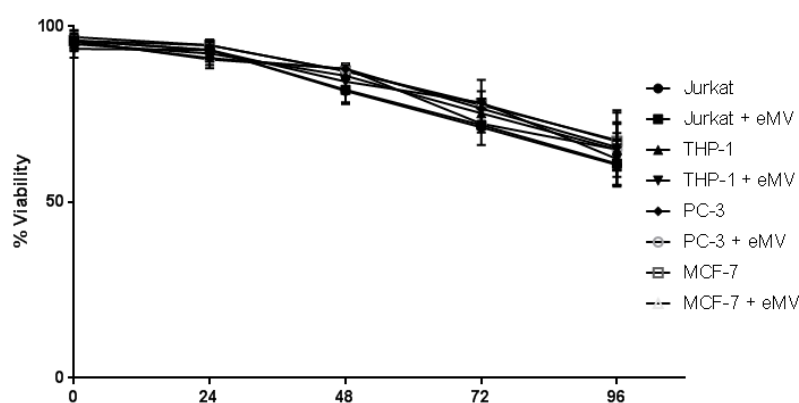


Fig. 3.4.2.3. Growth rate of cell lines - control against eMV treated cells. Where a) represents THP-1, b) Jurkat, c) PC-3 and d) MCF-7 cell lines concentration (x10⁵ / mL) (N=3) over a 96 hour observation period. Statistical analyses were obtained using GraphPad Prism version 7.2, using multiple T test (one unpaired t test per row- per period of time) and statistical significance was determined using the Holm-Sidak method, with alpha = 0.05. The p values (comparison between controls against eMV treated) were considered significant if P<0.05.

In addition to cell number analyses, the percentage viability was also assessed. eMV treated cells had an insignificant effect on the viability of any of the cell lines analysed (Fig. 3.4.2.4). There is no spike in cell death centred on the samples containing the eMV or control samples with general % viability lessening across all the samples from 72 hours into the study, which is expected if cells are left CGM untreated for the period of 96 hours. This demonstrates that eMV clearly have an inhibitory effect, rather than acting as a necrotic protagonist, indicating that they are active players in cell cycle regulation.



P value	Time (hours)			
	THP-1 vs THP +eMV	Jurkat vs Jurkat + eMV	PC-3 vs PC-3 + eMV	MCF-7 vs MCF-7 + eMV
0	0.44182	>0.9999	0.8512	0.6433
24	0.6071	>0.9999	0.8661	>0.9999
48	0.4395	0.9173	>0.9999	>0.9999
72	0.5097	0.5614	0.3933	0.7676
96	0.5927	0.9508	0.9158	0.9632

Fig. 3.4.2.4. % Cell viability of control and eMV treated cell lines. Cell % viability was observed every 24 hours for 96 hours (5 days) in total. The graph highlights the similarities between all samples, where a slight decrease in % viability is observed over time. The P value of all paired data (control vs eMV treated) were all above ($P < 0.05$) which were considered insignificant. Statistical analyses were obtained from GraphPad Prism version 7.2.

Similarly to the eMV and THP-1 cell interaction experiment, Annexin-V-FITC-Conjugated was also used to label the HeLaMVC and HRV16iHMV samples. The labelled MV were added to fully confluent culture dishes (ratio 1:1) after 12 hours of subculture and incubation and MV to cell interaction was observed. This was achieved by utilising an automated system, alternating between bright field and fluorescence which was also visualised using LumaScope™ 500 Series Fluorescence Microscope LED imaging analyses. Observation (by eye) of the outcomes were recorded for 15 minutes.

In Fig. 3.4.2.5, MV involvement/interaction with cell membrane was observed. HeLaMVC (Fig. 3.4.2.5a) and HRV16iHVMV (Fig. 3.4.2.5b) show a certain degree of membrane interaction with HeLa cells, but in contrast to Fig. 3.4.2.1, does not clearly show the cell membrane breakthrough observed with the eMV samples. Also, these MV appear to act as single particles, as aggregation was not observed here at early stages (< 5 minutes) into the experiment. Nevertheless, some aggregation was observed once MV started to approach the cell membrane. The images presented here were taken after 12 minutes of the incubation period and no further MV action could be observed.

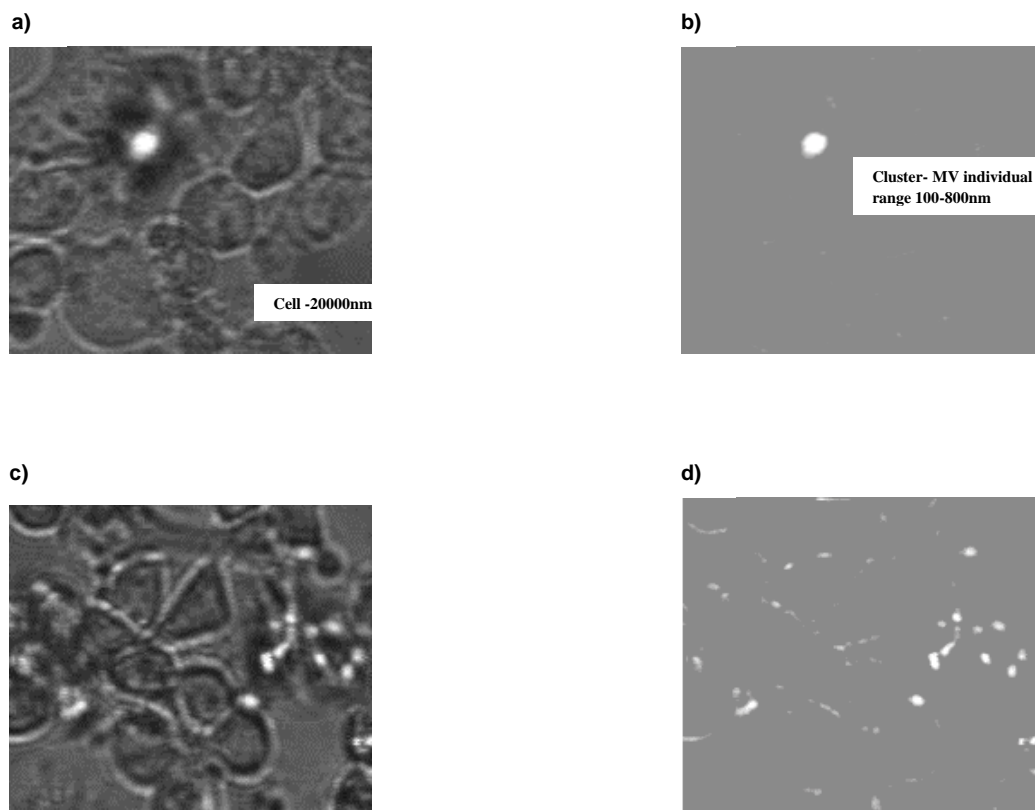


Fig. 3.4.2.5. HeLa cell and their derived MV interaction. Interactions were observed (60x objective lense images) for 15minutes. Fig. a) and b) shows HeLaMVC moving towards the cell and approaching the cell membrane (brightfield and fluorescence) and c) and d) shows HRV16iHVMV surrounding the HeLa cell (bright field and fluorescence respectively) but no major activities were observed.

To test the effects of HRV16 infection rate on the growth rate of HeLa cells, the morphological effect/appearance of MV treated HeLa cells was further investigated after 24 hours of initial infection (Fig. 3.4.2.6), in order to observe whether the HRV16iHVMV (ratio 1:1 to cells) would also infect cells, in comparison to the cells infected with the HRV16 only. Fig. 3.4.2.6a represents healthy cells and did not produce plaques, Fig. 3.4.2.6b HeLa cells were infected with HRV16 (MOI 0.2) and plaques arising due to the infection are shown demonstrating distinguishable characteristics on HeLa monolayers

under these conditions, in comparison to healthy cells. To understand the morphology further, HeLaMVC were introduced to a culture flask and no plaques were visible (no HRV16 particles) in Fig. 3.4.2.6c, in contrast to Fig. 3.4.2.6d where HRV16iHVMV appear to also infect healthy cells, showing a significant amount of plaques.

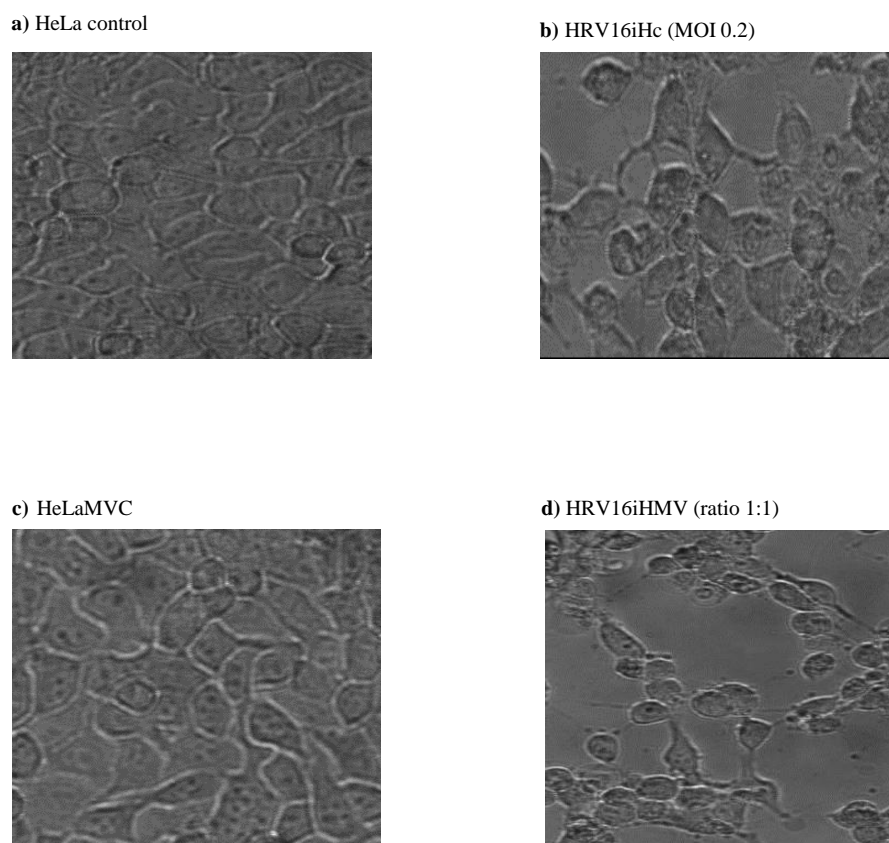


Fig. 3.4.2.6. The impact of HRV16 and MV on the growth of HeLa cells. Where images (bright field) were taken after 24 hours of the initial incubation period showing and comparing the differences and similarities of the samples used. Healthy cells can be observed in Fig. a where no plaques can be observed. Whereas Fig. b shows the HRV16 infection of HeLa cells with the presence of plaques. In addition, HeLa cells were treated with HeLaMVC and no changes in cell morphology can be observed in Fig. c, demonstrating similar morphology/characteristics to Fig.a. In contrast, Fig. d indicates a stronger infection rate of HRV16iHVMV infected HeLa cells than those treated with HRV16 itself, where plaques are strongly presented.

In order to compare the infection rate of HRV16iHVMV with HRV16iHc accordingly it would be required to titrate HRV16iHVMV samples in the same manner as in chapter 2.2.3. However, it was not the aim of this PhD research project. HeLa and their derived MV act as a parallel sample to understand the differences and similarities of MV types and characteristics in comparison to eMV samples.

To further investigate the potential impact of HeLaMVC and HRV16iHVMV on the growth of HeLa cells, cells on the exponential phase were seeded into sterile 24 well plates. Then MV were quantified (FC) and diluted (ratio 1:1) in DMEM and were added to each well

(except controls) containing the HeLa cells. Plates were incubated at 37°C in a 5% CO₂ incubator and left untreated for 24 hours. The cells were counted and viability was determined every 4 hours, after 12 hours of infection (Fig. 3.4.2.7).

In Fig. 3.4.2.7a, no significance in growth rate was observed when comparing HeLa cells with HeLaMVC samples. Whereas Fig. 3.4.2.7b shows statistical significance in the growth rate of HRV16iHVMV treated cells after 16 hours of treatment. In addition, Fig. 3.4.2.7c compares both sets of treated HeLa cells, where HeLa treated with HRV16iHVMV shows a decline of growth after 16 hours into the experiment. Fig. 3.4.2.7d suggests that HRV16iHVMV has an effect on treated cells showing a faster infection rate (P**) after 16 hours of the initial experiment when compared to HeLa infected with HRV16.

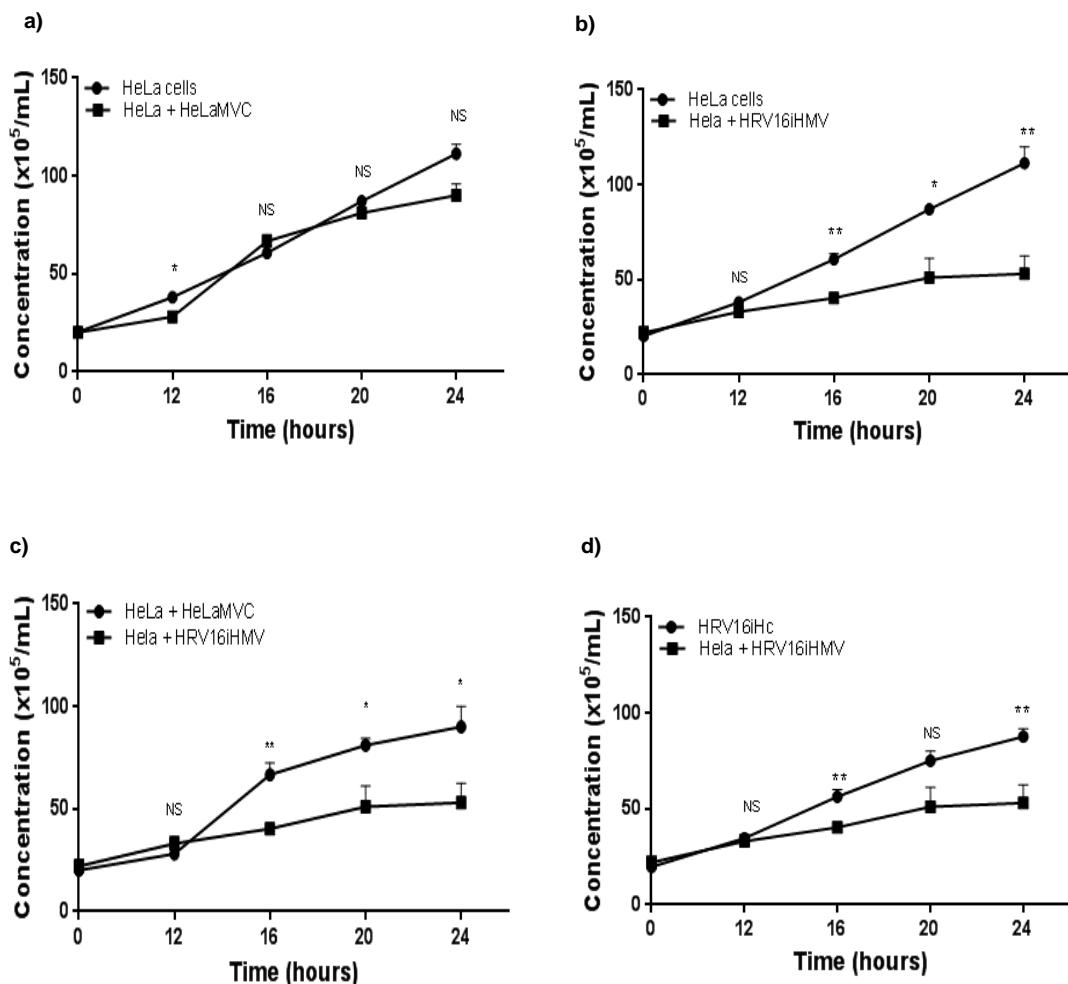
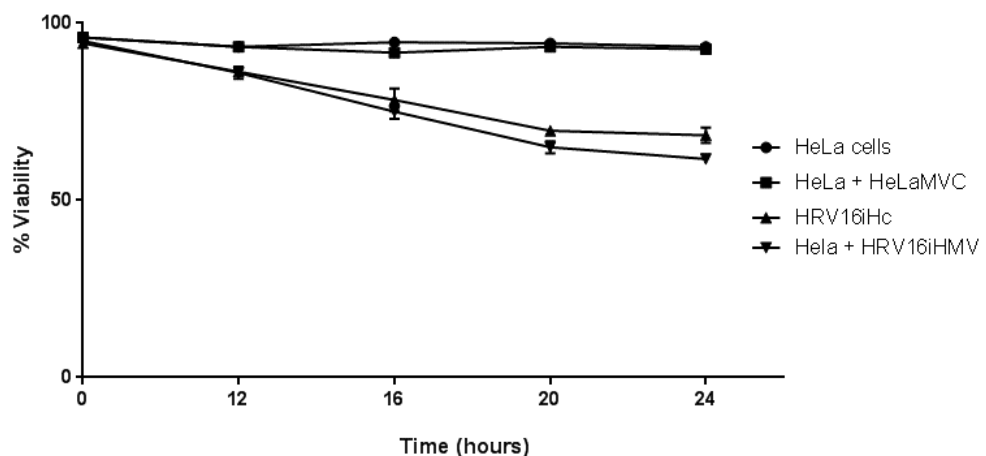


Fig. 3.4.2.7. Growth rate of HeLa cells - control against HeLa cells treated with HeLaMVC and HRV16iHVMV. Where a) represents HeLa cells against HeLa treated with HeLaMVC, b) represents HeLa cells against HeLa cells treated with HRV16iHVMV, and c) comparing HeLa treated with HeLaMVC and HeLa cells treated with HRV16iHVMV. All experiments were performed using triplicates of each sample (N=3). Statistical analyses were obtained using GraphPad Prism version 7.2, using multiple T test and statistical significance was determined using the Holm-Sidak method, with alpha = 0.05. The P values (HeLa cells against HeLa MV treated) were considered significant if P<0.05.

The % viability of HeLa cells against MV treated cells was also observed (Fig. 3.4.2.8), demonstrating a large number of HeLa cells dying with the time of HRV16 infection increasing (after 16 hours of the experiment- 50% infection rate expected after 24hours of initial infection). Healthy HeLa cells treated with HeLaMVC did not demonstrate statistical significance during the experiment. On the other hand, HeLa cells treated with HRV16 and HRV16iHc demonstrated a decline in % viability ($P>^{**}$) after 16 hours of treatment/infection in comparison to HeLa on its own, and those treated with HeLaMVC. However, despite a slight decrease in HRV16iHc treated cells no statistical significance was observed. This was also used as a control factor to investigate the effect of HRV16 on the growth rate of HeLa cells for the extraction of MV (to avoid apoptotic bodies).



P value	HeLa vs HeLa + HeLaMVC	HeLa vs HeLa + HRV16iHc	HeLa + HeLaMVC vs HeLa + HRV16iHc	HRV16iHc vs HeLa + HRV16iHc
0	>0.9999	0.2878	0.2878	0.5614
12	>0.9999	0.0315	0.0315	0.882
16	0.0739	0.0009 ***	0.0018 **	0.4299
20	0.5655	0.0000 ****	0.0002 ***	0.1079
24	0.6213	0.0000****	0.0000 ****	0.0474

Fig. 3.4.2.8. % Cell viability of HeLaMVC and HRV16iHc treated HeLa cells. Where % viability was observed every 4 hours for 24 hours in total after initial incubation period of 12 hours (N=3). The P values of all paired data were considered significant if $P<0.05$. As stated in the table (below graph) only samples compared against HRV16iHc treated cells demonstrated statistical significance, where statistical analyses were obtained using GraphPad Prism version 7.2.

3.4.3 Discussion

During this PhD research eMV did not interact and/or did not have an effect on the growth of PC-3 and MCF-7, which are epithelial cell lines. That may be because these cell lines are widely different cell types (location, form, and function), forming different types of tissues in animals and are derived from different embryonic layers, making them fundamentally unrelated. It is well understood that epithelium refers to a general class of cells that are found throughout the body in various linings of organs including glands, skin, digestive system, breast and prostate. Whereas, endothelial cells are a lining layer of cells or tissue (endothelium- blood vessels and lymphatic's) (Alberts, *et al.*, 2002), particularly present in the interior of the blood vessels at the same location of eMV isolation.

The common structure of the adherens junctions and tight junctions in the endothelium is relatively similar with that of epithelial cells, but there are some cell-specific characteristics. For example, VE-cadherin, claudin-5, and PECAM-1 are endothelial markers, and have not been found in epithelial cells and the morphology of the intercellular cleft in the endothelium vary from that of many epithelia, as tight junction are not only located on the apical side, but may also be united with adherens junctions (Dejana, *et al.*, 2009). Nevertheless, altered tight junction permeability in co-cultures have indicated that these cell types can work conjointly as an operating part of the mucosal barrier (Chowdhury, *et al.*, 2010). However, eMV did not have an impact on the growth rate of PC-3 and/or MCF-7 cell lines during this PhD project and this may be due to the lack of matchable molecules between cell and MV required for the interaction. However, this is an assumption and it requires further investigations to understand the lack of interaction between MV with these cells.

As previously mentioned (chapter 3.4.1) the THP-1 and Jurkat cell lines used here present particular and different surface markers, ligands and receptors that can regulate cell adhesion, cell signalling and adaptive immunity for example, CD9 to CD36 interaction. Other receptors and ligands may have been involved, facilitating the interaction of THP-1 and Jurkat cells with eMV. For instance, the adhesion involving CD2 (a surface antigen found on all peripheral blood T-cells) - CD58 (expressed in all MV tested here Fig. 3.2.1.3e), antigen-specific T-cell receptor interactions with peptides bound MHC molecules (Wang & Reinherz, 2000).

Also, annexin-V was expressed on the surface of all MV tested during this PhD research (see Fig. 3.2.1.2) which may enable MV recognition by PS, a marker for apoptosis receptors on the surface of specific types of target cells. This interaction has been previously described within the context of phagocytosis of apoptotic cells by mononuclear cells using PS receptors including T-cell immunoglobulin and mucin domain (Tim)-1, Tim-4, Stabilin 2, and Brain-specific angiogenesis inhibitor (BAI)-1 (Park, *et al.*, 2007). This could be involved in the uptake of MV. This proposes that Tim1/4 receptors on two adjacent cells could allow the formation of MV/exosome bridges, thereby promoting additional/indirect intercellular interactions (Zhou, 2007). Also, the transfer of PS from vesiculating cells to erythrocytes was implicated in tagging these cells for destruction by phagocytes (Liu, *et al.*, 2009), showing that vesicular transfer of several molecules emerges as a relatively widespread process, that may complement intercellular communication by different mechanisms.

Indeed, PS has been demonstrated to play a critical part in the internalisation of MV derived from cells including monocytes and platelets into endothelial cells (Morelli, *et al.*, 2004; Bruno, *et al.*, 2009). PS has also demonstrated involvement in the uptake of exosomes by dendritic cells (Lima, *et al.*, 2013), but it does not appear to be the case in this PhD study because PS was blocked with Annexin-V label for microscopy analyses. Therefore, the Annexin-V blocking of PS receptors indicates that this may not be the entry site, despite research that has identified a high concentration of PS as one route (Feng, *et al.*, 2010; Mulcahy, *et al.*, 2014). Wei, *et al.*, (2016), demonstrated that blockage of PS sites on hypoxia-induced mesenchymal stem cells (MSC)-MV with Annexin V significantly lowers the incorporation into human umbilical cord endothelial cells (HUVECs). Blocking PS often obliterates MV incorporation at least by endothelial cells, platelets and cancer cells (Del Conde, *et al.*, 2005; Al-Nedawi, *et al.*, 2008). Also, blockage of PS from neuron-derived exosomes using Annexin V not only prevented exosome uptake but also suppressed amyloid β -peptide and A β incorporation into microglia (Yuyama, *et al.*, 2012).

A proposition that follows would be that phagocytes could be particularly susceptible to molecular influences of PS positive MV, beyond their simple destruction. For example, the presence of P-selectin (cell adhesion molecule) ligand on the surface of procoagulant MV, could direct them to P-selectin expressing platelets and endothelial cells (Thomas, *et al.*, 2009). Just as the role of protein milk fat globule-epidermal growth factor 8 (MFG-E8) in promoting the phagocytosis of apoptotic cells, by acting as a bridging molecule

between apoptotic cells and phagocytes has been elucidated (Fricker, *et al.*, 2012). It is believed to facilitate the phagocytic uptake of apoptotic cells by binding PS through 1 domain and with cell surface proteins including CD51 and CD61 through a second domain (Hanayama, *et al.*, 2002) and during macrophage phagocytosis of aged erythrocytes (Föller, *et al.*, 2008).

Nevertheless, the enrichment in signalling molecules alone is not enough to facilitate the signalling functions of EV. In fact, EV also have active lipolytic moieties, including phospholipases, resulting in the the formation of bioactive lipid mediators (fatty acids and prostaglandins). This may interact with peripheral G-protein-coupled receptors and the nuclear receptors in neighbouring cells (Subra, *et al.*, 2010).

The aggregation phenomenon observed in Fig. 3.4.2.1 could be explained by the presence of ADAMTS13 in eMV samples (Fig. 3.2.3.2) simply due to its general function (Zheng, 2013). It processes a large protein called von Willebrand factor, this protein plays a role in clot formation and its unprocessed form of von Willebrand factor interacts easily with cell fragments, that circulate in the bloodstream and are essential for blood clotting. It helps cell fragments attach together and stick to the walls of blood vessels, leading to temporary clots.

Fig. 3.4.2.2 also demonstrated some aggregation (not as much as in Fig. 3.4.2.1). The major differences between the experiments is that the eMV sample in this case was not labelled with Annexin V. Cells and EV membranes present vastly heterogeneous lipid compositions that vary between cell types (van Meer, *et al.*, 2008; Osteikoetxea, *et al.*, 2015), and such variety of lipid composition in membranes is crucial in modulating the interactions of amphipathic proteins with membranes (not studied during this PhD research). Particularly, negatively charged phospholipid including PS (not blocked in this case) and phosphatidylglycerol are well known to impact the kinetics of aggregation and fibril formation of a variety of amyloidogenic proteins on the membrane surface (Galvagnion, *et al.*, 2015; Zhu, *et al.*, 2003; Mizuguchi, *et al.*, 2018).

In addition, while cell lines were undergoing apoptosis/proliferation, they could also have released their own MV or similar properties affecting the neighbouring cells. In a study of MV isolated from THP-1 and Jurkat cells, it was shown that they carry high levels of transforming growth factor- β 1. This suggest that they could have the ability to promote/inhibit the control of cell cycle, cell proliferation, cell differentiation and

apoptosis which caused significantly greater reductions in the growth rate of THP-1 cells (Ansa-Addo, *et al.*, 2010).

In relation to HRV16 and HRV16iHMV treated HeLa cells, it did not increase/decrease in concentration/number, and this may be due to the HRV16 infection dose decreasing their chance of survival, and cell growth rate/effect could therefore not be observed. As for HeLaMVC, no major differences in growth rate were observed within the 24 hours of the experiment. However, HRV16iHMV treated cells showed an advanced infection rate of treated HeLa cells, suggesting that HRV16 particles may be carried in the sample, because according to Lisco, *et al.*, (2009), EV can in general (*in vivo*), interact with viruses and with each other. Either directly or via modulation of host responses by participating in a “War and Peace” interaction between viruses and host.

Some viruses, including HIV, induce the infected cells to release modified EV that facilitate further infection by increasing the pool of susceptible target cells. This is promoted by increasing the number of activated cells, or their susceptibility to viral infection, or by serving as decoys that absorb antiviral antibodies. The capacity of EV to regulate the lifespan of permissive cells and to modify antiviral immune responses may give additional flexibility to the host in responding to viral infection, suggesting that EV formed during viral infection may play either pro- or counter-viral roles (Hoen, *et al.*, 2016).

In this study only much higher infection rate is presented visually in Fig. 3.4.2.6 and 3.4.2.7, and further work is required before any assumptions are made. For example, several HIV proteins and RNAs having already been detected in EV released from HIV-infected cells. One of the viral components released via EV is the HIV transactivation response (TAR) element RNA. The TAR is an RNA stem-loop structure located at the 5' ends of HIV-1 transcripts, which in infected cells is found in TAT (gene that provides instructions for making the liver enzyme, tyrosine aminotransferase), thereby facilitating recruitment of elongation factors and increased production of viral RNA (He, *et al.*, 2010). When transferred via EV, TAR RNA can increase the population of susceptible target cells. Inside EV-targeted cells, the full-length TAR RNA is processed into miRNAs, which silence messenger RNA (mRNA) coding for B-cell lymphoma 2- interacting Protein. The consequential increase in resistance to apoptosis, allows the cell to produce the virus for a longer period, thereby facilitating HIV infection (Narayanan, *et al.*, 2013; Hoen, *et al.*, 2016).

4. A model proposition: eMV may act as delivery vectors in circulation

Human erythrocytes have a flexible biconcave shape and are approximately 7000 nm in size. Their main functions are the transport of oxygen and carbon dioxide. They are also involved in the release of ATP, which may participate in vessel dilation by triggering nitric oxide production (Olearczyk, *et al.*, 2004; Bakhtiari, *et al.*, 2012). Erythrocytes are known to secrete MV and their presence has been observed in a number of diseases by different researchers (see chapter 1.2.1)

eMV range between 100-800 nm in size (Fig. 3.1.2.3) and their biogenesis has been described as a part of erythrocyte senescence and have also been proposed as part of an apoptosis-like process (eryptosis) (Rubin, *et al.*, 2012). An increase of intracellular calcium levels leads to disruption of the erythrocyte membrane asymmetry with concomitant biogenesis. Erythrocytes exposure to inducing agents including CaCl_2 and $\text{CaCl}_2 + \text{NHS}$ leads to a loss of plasma membrane deformability (see chapter 1.2.2), and an increase of their release (amount) was observed during this PhD research (see chapter 3.1.2).

According to the literature used during this PhD research, MV are suggested as being involved in cellular communication (see chapter 1.7). An umbrella term that allows the understanding of how different types of cells can cooperatively perform important bodily processes that are necessary for cell proliferation and their survival. It may also help to understand the binding of eMV to the external surface of their target cells, in which a specific pathway remains unclear. Nevertheless, a number of possible interactions have been suggested by protein interaction networks (Fig. 3.2.1.3.1, 3.2.2.3.1, and 3.2.3.3.1).

EV-cell communication has been proposed as occurring during a variety of processes, which may take place inside the cell, protein-to-protein interaction, endocytosis and other events (chapters 1.4 and 1.7). Intracellular binding and fusion require the involvement of various proteins, including cytoskeletal proteins (actin). Among the latter processes, the ones intensely investigated are EV-virus fusions, which occur with the participation of specific proteins (chapter 1.3.1).

The initial interactions of EV with cells are expected to require specific, high affinity binding of at least two surface proteins (principles of cell communication). One protruding from the EV, and the other from the plasma membrane of the target cells. The investigation into key biomolecules conducted during this PhD research (chapter 3.2), provided the identification of molecules which may play an important role on how eMV may interact with the recipient cell or at least a starting point for further experiments.

To better understand the mechanism by which MV may enter the cells, further analysis is required including the characterisation of potential target cells. For now, the process remains a major challenge and is necessary for elucidating the underlying mechanisms as well as for identifying cell targets.

As the cell travels and circulates in the bloodstream, its trajectory is influenced by viscoelastic and frictional properties, the latter of which is governed by cell surface interactions as well as normal forces exerted by the cell on the channel wall (Byun, *et al.*, 2013). This may also be occurring with MV due to its cargo (surface markers).

After receptor-ligand interaction takes place, which may occur through CD36-CD9, CD58-CD2 and CD63-TIMP1 interactions (see Fig. 3.2.1.3.1), some of these receptors/ligands were present in eMV and ligands/receptors known to be present in THP-1 and Jurkat cells (Wang & Reinherz, 2000; Reyes, *et al.*, 2015; Trim, *et al.*, 2000). Then the ligand-receptor pair relocates as a single component on the plasma membrane. The assembly binds together and diffuses with the receptor, which leads to a chemical environment for the ligand and receptor to adapt. They are then accepted or rejected by each other as allies. The alliance may transduce extracellular signals across the plasma membrane and, through the activation of intracellular signalling pathways, bring about the appropriate functional response (Uings & Farrow, 2000).

For example, integrin-dependent cell adhesion, through integration of cell signalling pathways and cytoskeletal reorganisation are understood to influence cell growth, death, and differentiation (Clark & Brugge, 1995). But, integrin signalling may not simply require cytoplasmic domain associations, it may also use lateral interactions through integrin transmembrane and ectodomains (Wary, *et al.*, 1996), because they tend to assemble into protein complexes (Hotchin & Hall, 1995). This is where they might recruit other molecules including growth factor ligands and phosphatidylinositol 4-kinase, into proximity with integrins (Nakamura, *et al.*, 1995; Berditchevski, *et al.*, 1997).

Furthermore, as previously suggested in chapter 3.2.2.3, integrin proteins may also link specific integrins to Protein Kinase C (PKC) (Zhang, *et al.*, 2001). This is important because understanding of the mechanisms underlying PKC-mediated control of the cell cycle can provide valuable insight into its role in inhibiting cell growth and transformation (Black, 2000). This is of interest because an inhibition of THP-1 and Jurkat cell lines treated with eMV was observed during this research, which may suggest that the activation of PKC on the recipient cell could be the catalyst for this observed inhibition. This is relevant because members of the PKC family have been widely implicated in the regulation of cell growth/cell cycle progression and differentiation (Frey, *et al.*, 2000). Also, PKC was present in eMV samples, see Fig. 3.2.2.2.

The GO enrichment indicated that PKC is heavily involved in these biological functions and pathways (Appendix III; Tables 5 and 6). Using G1 and G2 as checkpoints *in vitro* and *in vivo* systems point to PKC as a key regulator of critical cell cycle transitions, including cell cycle entry and exit. Most of the mechanistic information available relates to the involvement of the PKC enzyme family in negative regulation of these transitions. Cip/Kip cyclin-dependent kinase (known as CDK) inhibitor p21waf1/cip1 (cyclin-dependent kinase inhibitor 1 or CDK-interacting protein 1) are the major target for PKC-mediated inhibition of cell cycle progression (see Appendix VIII). CDK2 activity in the G1 phase is blocked by increased expression of p21waf1/cip1, this leads to hypophosphorylation of the retinoblastoma protein and inhibition of cell cycle progression into the S phase. Whereas in G2, p21waf1/cip1 expression blocks cdc2/cyclin B activity, likely through an indirect mechanism involving inhibition of the CDK2/cyclinA complex, and in turn prevents progression into the M phase. PKC signalling can also activate a coordinated program of pocket protein regulation activities leading to cells leave G1 and enter an alternative G0 state (Chambard, *et al.*, 2007).

Regig & Plataniias (2008), summarised the work in this field based on the relevance of distinct members of the PKC family in the pathophysiology of myeloid and lymphoid Leukaemias. Although most members of PKC promote leukaemic cell survival and growth, others exhibit opposing effects and participate in the generation of anti-leukaemic responses. They concluded that the clinical-therapeutic potential of ongoing work in the future development of novel approaches for the treatment of different types of leukaemias is developing.

The results that are presented in the results chapters of this PhD thesis have provided helpful information into eMV cargo, which opened a range of possibilities for eMV to be involved in different biological processes, due to the large number of molecules identified (chapters 3.2 and 3.3). This may lead to responses to a number of different biological pathways that have been linked to the group of molecules/genes analysed here (proteins/genes and miRNA target genes GO enrichment). The analysed target genes can be regulated in many different ways since a single gene demonstrated involvement in many processes which may be under the regulation of other entities including mutation, repair, and the recombination of the genome (Brown, 2002). During the analysis of these genes, it was possible to distinguish the group of those that were able to regulate the expression of all of the target genes from the miRNAs identified in chapter 3.3.

The universal mechanism of the post-transcriptional regulation of a gene activity through miRNAs indicates they may adapt to a variety of routes (Engels & Hutvagner, 2006). The data obtained during this PhD project, suggests that eMV contain miRNAs which can possibly be involved in up- or down-regulation of the different components. This is because biosynthesis pathways are necessary in some aspects of growth regulation or adaptation to environmental stimuli to cells (Lloyd, 2013).

A deregulation of miRNA expression can result from increased or decreased transcription from their respective miRNA genes by aberrant transcription factor activity. For example, *miR-21* (present in all samples tested here) has been reported at high levels in glioblastomas, pancreas, and breast cancer (Garzon, *et al.*, 2010). When *miR-21* was blocked, an increased activation of caspases and apoptosis was observed in glioblastoma cell lines (Chan, *et al.*, 2005).

Taken together, the study based on eMV characterisation, biomolecules identified and the GO enrichment analyses obtained during this PhD project, a relevant biological model is proposed in Fig. 4.2.1. The proposed model overviews eMV being released from the parent cell, biological molecules which may help eMV to communicate with target cells and, their potential to change gene expression. This is where potential suggestions/conclusions related to the impact of eMV in neighbouring cells may be understood which may be due to a variety of molecular and cellular molecules identified. The model presents information that is currently absent from the EV/MV field.

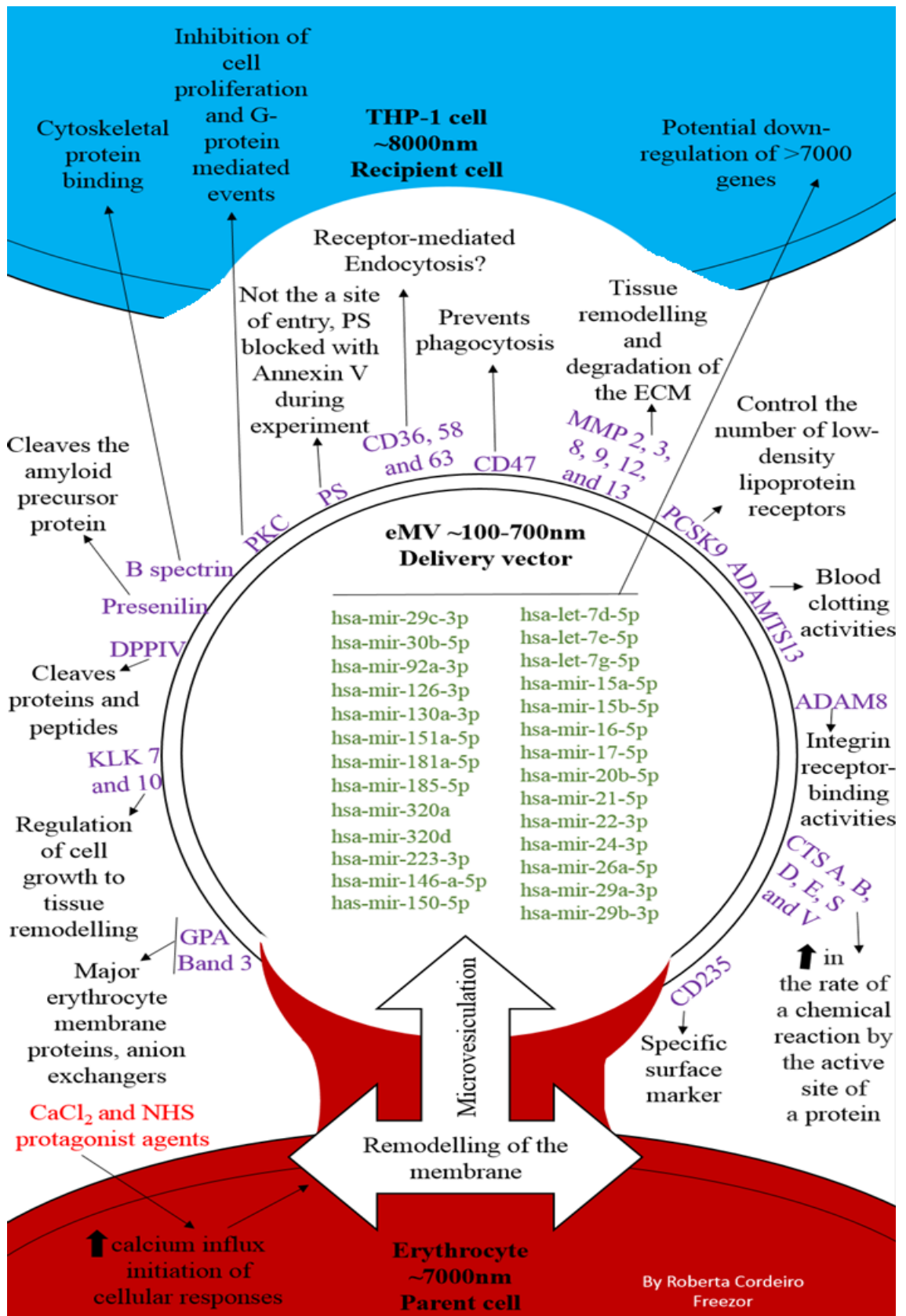


Fig. 4.2.1. Schematic summary of eMV biogenesis, contents, mechanism of communication and potential impact on a THP-1 cell. A representation of the key features identified in eMV during this PhD research. It demonstrates eMV budding directly from the plasma membrane during an increase of intracellular calcium due to the introduction of inducing agents. eMV contains proteins of interest, including tetraspanins CD36, CD58 and CD63 (allows receptor-mediated endocytosis fusion with neighbouring cells) and CD47 (protection against phagocytosis). After MV are secreted, they may be taken up by neighbouring/ target cells via fusion with the plasma membrane, a receptor-ligand interaction. Once inside the cell, eMV can then release their contents including miRNAs, therefore transporting key molecules in which may have an effect on the recipient cell proliferation and overall fate.

5. Conclusions and further work

This PhD research was designed to characterise MV released from uninduced erythrocytes, erythrocytes induced with CaCl₂, and erythrocytes induced with CaCl₂+NHS. The characterisation was based on their amount of release (concentration), their size, and the identification of potential molecules which could allow these MV (eMV) to communicate with cells *in vitro*. And lastly to investigate whether eMV could act as a potential delivery vector. In parallel, HeLa cells, HeLa derived MV, and HeLa infected with HRV16 derived MV were used as a comparative source for all experiments

The first step included the comparison of the amount of MV released from uninduced and induced erythrocytes. This was to investigate whether the induced agents would provide a higher amount of release. The investigation was assessed by FC analyses using samples obtained from the ultracentrifugation procedure compared with SEC. It was observed that erythrocytes released a greater amount of MV when induced with CaCl₂ and CaCl₂+NHS. Classic ultracentrifugation proved to be a faster and more accurate method of isolation when compared to SEC. These findings are helpful and further parameters should be included with these comparisons to gain a better understanding of eMV biogenesis.

For example, to further the work of this PhD research, the inclusion and comparison of erythrocytes induced with NHS only, and other inducing agents including 4-bromo-A23187, lysophosphatidic acid, or phorbol-12 myristate-13 acetate suggested by Nguyen, *et al.*, (2016).

It would also be of interest to take an opposite approach by using Calcium Channel Blockers that are examples of agents that attenuate eMV biogenesis (Harisa, *et al.*, 2017).

A potential clinical application for eMV can be the design of MV modulating therapy based on inhibiting MV biogenesis, by inhibiting their cellular uptake, and/or inhibiting their active components. Mulcahy, *et al.*, (2014), listed several agents that inhibit EV cellular entry including heparin, chlorpromazine, amiloride, Annexin-V and proton pump inhibitor which could be considered for further experiments.

The characterisation of eMV sizes was addressed in this study using different techniques that included FC analyses and qNano. The eMV samples obtained during this PhD research were concluded to be of a size range of between 100-800 nm. The qNano

provided a more accurate measurement of size distribution, but the FC analyses proved to be a faster approach, particularly because the comparison of the size of eMV was not further assessed during subsequent experiments. Alternative techniques are proposed in chapter 3.1.3 (page 66 and 67).

In addition, to compare the MV isolation methods, the classic ultracentrifugation procedure was compared to the Size Exclusion Chromatography column method. This decreased the recovery rate of MV and it added an extra step to the lengthy ultracentrifugation procedure, without demonstrating any advantages in this PhD research. As discussed in chapter 3.1.3 (page 69) alternative approaches are available. Further assessment including proteomic analysis could potentially advance this approach.

Furthermore, random sampling (variability) was not used in this study despite being convenient when the population members are similar to one another on variables, and it ensures a high degree of representativeness for the data obtained because it can critically construct the “representativeness of study samples and generalisability of study results”. These key concepts often can be misconstrued and blended, concealing the general drawbacks of internal and external validity (Kukull & Ganguli, 2012). For this study, eMV samples were derived from the same blood donor and are not to be presented as representative data of the general type of EV population (MV). The results should not be generalised as such, they are derived from uninduced and induced erythrocytes designed samples. Sample size, concentration and isolation methodology were key variables considered in chapter 3.1 when studying the heterogeneity of eMV. This should minimize the possibility that selection factors will have unintended adverse consequences in results, since any effect measured depends on the stimuli used rather than on the comparison of different blood groups as eMV types (control and induced). Factors including sex, age (sample and donor), and total time of isolation may provide different EV yield (total population) because it is noticeable that eMV are composed of diverse subpopulations in relation to size and concentration. It may expand the known EV subpopulation classification, but instead the focus was on eMV derived from uninduced and induced samples.

Nevertheless, random sampling (variability) is an approach recommended for further experiments, especially eMV derived from donors presenting medical conditions that are known to affect erythrocytes. Examples of these conditions include hemolytic anaemia, hemochromatosis, hereditary spherocytosis, iron deficiency anaemia and polycythemia.

This is because elevated levels of eMV release have also been associated with numerous diseases (see chapter 1.2.1, page 13).

The characterisation and optimisation of MV size and concentration mentioned above was a requirement to be able to proceed with the characterisation of the samples in relation to the present of biological molecules, therefore it acted as a starting point.

Subsequently, this study focused on the identification of key biomolecules. This was performed by using immunoblotting techniques including immunophenotyping (surface markers), Western blotting analyses (total proteins) and Proteome Profiler Array (proteases). This is provided in chapter 3.2.

The identification of surface markers, general proteins and proteases within eMV provided an insightful recognition of their biological potential. For example, the potential interaction of CD2 with CD58 among other ligands/receptors identified in chapter 3.2 may facilitate communication/exchange of information by using ligand-receptor molecules to initiate the process. Whereas, by using CD47 (the “do not eat me” signal) eMV may be able to protect themselves in the extracellular environment.

The *in silico* analyses performed in chapter 3.2 (protein interaction network and GO enrichment), provided a detailed set of information that can help unravel the biological functions of eMV. This is because each of the interaction network, biological process and/or pathways identified may form the basis of subsequential research projects, which can support and further this PhD research. The options for further experiments are endless, but the data collected can act as a starting point to understand the complex processes of and biological features of the eMV interacting with neighbouring/target cells.

For example, CD36 was detected in the surface of all eMV samples tested here and it is well understood that CD36 interacts with CD9, a highly conserved cell surface protein CD9 (Wang, *et al.*, 2011). CD9 is known to be expressed on the surface of white blood cells in general, including THP-1 cells (Reyes, *et al.*, 2015). CD9 is relevant for signal transduction, proliferation/apoptosis, cell adhesion and migration among other processes (Sumiyoshi, *et al.*, 2016).

Experiments with THP-1 cells for example, could include the functional assessment and localisation of CD9 on the cell. Functional analyses involving the downregulation of CD9 through genetic manipulation using either Clustered Regularly Interspaced Short Palindromic Repeats (CRISPR)/Cas9-based approaches (Gilbert, *et al.*, 2013) or

transient knock-down by means of mRNA degradation (Fire, *et al.*, 1998), could shed light on the role of CD9 as a rheostat of cell/eMV adhesion and homotypic aggregation. This was previously described as integrin-dependent, which is a critical regulator of vital processes such as fertilisation, where the absence of the protein in oocytes produces a deficient fusion among sperm and egg (Wang, *et al.*, 2011). The knockdown of CD9 from THP-1 cells would prove whether eMV interaction with the cell is dependent on the CD9-CD36 ligand/receptor interaction. This is just one example of an interaction network, but these type of functional analyses are relevant for this study to further elucidate the postulated pathway of cell to eMV interaction.

Then, the identification of immune related miRNA's was conducted using the Firefly particle technology. This was investigated because the presence of miRNAs that function to regulate cellular processes, including cell proliferation, could be a major characteristic that may support MV activities. The data obtained in chapter 3.3.2 provided a detailed set of information that can help to reveal additional biological functions that eMV may be involved with. The options for further investigations here are inestimable, each of the identified miRNA and each of their target genes can provide enough interest for extensive research projects. This is because it has been reported that the presence of miRNAs patterns characterised by their over-/under expression in specific pathologies (Ha, 2011). For example, *let-7* is a tumour suppressor miRNA and its overexpression results in oncogenic loss of differentiation/cell identity (Johnson, *et al.*, 2005), it also prevents early cancer progression by suppressing expression of the embryonic gene HMGA2 (Park, *et al.*, 2007). Therefore, restoring *let-7* levels in cancer is an appealing therapeutic option (Jansson & Lund, 2012).

The use of CRISPR (Chang, *et al.*, 2016) in the case of eMV miRNAs is not feasible because the miRNA found in these samples are as a result of the MV biogenesis, and the erythrocytes lack nuclei and are unable to transcribe mRNA (Warren, 2017). Whether these identified miRNAs were inherited from the erythrocytes membrane or collected in circulation is unknown. Therefore, miRNA biogenesis cannot be edited because MV do not have the cell machinery (including the genome) to carry out this function. Instead, another functional approach can be achieved by the incorporation of locked nucleic acids (LNAs) into a biological model (Pritchard, *et al.*, 2012). After miRNAs purification, miRNAs can be tagged with fluorophore-labelled nucleotides (Nilsen, 2007), leading to the design of oligonucleotides that result in either degradation or steric hindrance of the target mRNA in the recipient cell (Braasch, *et al.*, 2002). This method for specific

inhibition of miRNA function through the interaction with LNA-modified antisense oligonucleotides (Ørom, *et al.*, 2006), has been proved to specifically inhibit both endogenous and exogenously introduced miRNA in *Drosophila melanogaster* cells using a heterologous reporter assay. The method showed stoichiometric and reliable inhibition of the targeted miRNA being applicable to functional studies of miRNA and validation of putative target genes.

Another example is the approach used by Elmén, *et al.*, (2008) that systemically administered LNA-antimiR oligonucleotide complementary to the 5' end of *miR-122*, it is relevant to this study because it suggested that miRNA antagonists comprised of LNA are valuable tools for identifying miRNA targets *in vivo*. Such miRNA antagonists can be used to elucidate the biological role of miRNAs and miRNA-associated gene-regulatory networks in physiological conditions. Their results suggested that this incorporation leads to specific, dose-dependent silencing of *miR-122* without hepatotoxicity in mice.

Following active miRNA load release inside the recipient cell, MV may have the ability to alter the transcriptome and signalling activity within the recipient cells, resulting in the induction of specific phenotypic changes (Camussi, *et al.*, 2010; Bronisz, *et al.*, 2016; van Dongen, *et al.*, 2016), after endocytic activity that can separate properties to be recycled from those that will be degraded in lysosomes (Piper & Katzmann, 2007).

In chapter 1.3, HRV16 was suggested as having a strategy that has evolved to evade cells. For MV to have similar functionality, it may involve alterations in the content of the HRV16iHMV so that it includes components of innate defence against selected viral gene products to be able to replicate, but this was not studied during this PhD research. See GO enrichment, set out in Appendix IV for information regarding molecules identified in chapters 3.1, 3.2, 3.2 and their target genes. It can be hypothesised that the reorganisation of the HRV16 is part of the mission of the HRV16iHMV, and this is to alter the environment in the recipient cells so that it is able to control its dissemination in the host as suggested in Herpes Simplex Virus type 1 infection (Kalamvoki & Deschamps, 2016). This is by restricting its dissemination within the human body, it can propose long-term interactions with the host and increases its chance of transmission, showing potential mechanisms to hijack MV and this could be suggested to be possibly occurring with the HRV16iHMV. However further experiments are required to ascertain this possibility,

which is not a mechanism in which eMV may use, because they are not infectious particles that require a host for survival.

Therefore, it is logical that the next step for this PhD research is to further study the potential to harness the capability of MV to transfer their contents into target cells. This is to confirm whether eMV might be convertible into vehicles for the delivery of therapeutic agents. In addition, because it is well established that cells can be manipulated and have drugs introduced into them, MV may also be manipulated in the same way and thus represent a promising candidate for delivery vectors (Perteghella, *et al.*, 2017), without immune rejection following *in vivo* allogenic administration as suggested for exosomes (Yu, *et al.*, 2014). This is because after being delivered to the target cells, the miRNAs may be able to regulate the translation of the target genes and the function of the recipient cells (Valadi, *et al.*, 2007; Tkach & Théry, 2016).

Despite clinical investigations being in their infancy, the relevance of miRNA transfer in several physiological settings has been postulated in this field. There is emerging evidence that miRNAs transported in EV may be responsible for intercellular communication, but it is yet to be established if the amounts of miRNAs necessary to process that effect are appropriate to confer relevant effects, with regard to physiological impacts *in vivo*.

EV in general demonstrate several possible advantages in terms of their use in regenerative medicine (Beer, *et al.*, 2017) and as delivery vehicles/vectors, because they are stable (membrane bound vesicles), potentially capable inducers of strong signalling pathways due to their cargo (surface markers for instance), and can be produced in higher concentrations when induced compared to uninduced samples (see Fig. 3.1.2.2).

One of the most exciting outcomes of this PhD research was the identification of key molecules in eMV that may contribute to their postulated identity of being genuine biological entities, that are, therefore able to transfer information and substances to recipient cells. The observed membrane interaction with the THP-1 cell and their inhibitory impact (chapter 3.4) during this study demonstrates their potential as a delivery agent.

At this stage, the exact biological mechanisms which eMV use to communicate with neighbouring cells is difficult to predict. Nevertheless, MV have been shown to be an integral part of various immunological systems, as a result of their enriched cargo

consisting of proteins and miRNAs. It is possible they might be able to indirectly activate immune stimulation factors and act as carriers, but this hypothesis needs to be tested in further studies.

eMV are promising biological vectors for drug delivery because they could overcome restrictions of synthetic micro carrier and considered self-molecules due to their ability to permeate the plasma membrane of target cells, as a result of their membrane being able to be amenable to improve specific cell targeting that can deliver their contents to neighbouring cells. Therefore, MV may be suitable for the development of drug delivery cargo, and can be produced at a high level using inducing agents such as CaCl_2 and $\text{CaCl}_2 + \text{NHS}$. EV has shown the capability to deliver drugs to specific tissues, thereby reducing therapeutic doses and decreasing side effects (Sun, *et al.*, 2010).

The results obtained in this study are consistent with knowledge in the EV field, hypothesising that MV not only interact but also have an impact on cell lines *in vitro* (García-Manrique, *et al.*, 2018; Koniusz, *et al.*, 2016). Indeed, results from some studies show that fluorescently labelled EV can be taken up by cells (Svensson, *et al.*, 2013), but others suggest that EV uptake is a particularly specific affair that requires the right combination of ligand and receptor (Mulcahy, *et al.*, 2014; Tomasetti, *et al.*, 2017). This is an assertion this PhD research supports (combination of ligand and receptor- Fig. 3.2.1.3.1).

However, strong evidence about the mechanism of MV influencing other cells *in vivo* is still absent. Implying that more investigation is required to validate these suggestions, including the targeted binding of specific receptors, in order for MV to act as a natural delivery vector. Nevertheless, the characterisation of the MV properties was explored in this research and the data obtained can positively contribute towards the EV field, and further work to identify their true potential for use in the medical field.

References

- Aatonen, M. T. *et al.*, 2014. Isolation and characterization of platelet-derived extracellular vesicles. *J Extracell Vesicles*, Volume 3, p. 10.3402/jev.v3.24692.
- Abcam discover more , 2017. *Firefly particle technology*. [Online] Available at: <http://docs.abcam.com/pdf/kits/firefly-microrna-particle-technology-multiplex-mirna.pdf> [Accessed November 2017].
- Abcam discover more, 2015. *How does the Multiplex Circulating miRNA Assay work?*. [Online] Available at: <http://www.abcam.com/kits/how-does-the-multiplex-circulating-mirna-assay-work> [Accessed 2015].
- Abraham, R. T. & Weiss, A., 2004. Jurkat T cells and development of the T-cell receptor signalling paradigm. *Nature Reviews Immunology*, Volume 4, pp. 301-308.
- Admyre, C. *et al.*, 2007. Exosomes with immune modulatory features are present in human breast milk. *J Immunol*, 179(3), pp. 1969-78.
- Agarwal, S. K., 1990. Proteases cathepsins- A view. *Biochemical education*, 18(2), pp. 67-72.
- Aichinger, M. C. *et al.*, 2008. Unique membrane-interacting properties of the immunostimulatory cationic peptide KLKL(5)KLK (KLK). *Cell Biol Int*, 32(11), pp. 1449-58.
- Alaarg, A., Schiffelers, R. M., van Solinge, W. W. & van Wijk, R., 2013. Red blood cell vesiculation in hereditary hemolytic anemia. *Front Physiol.*, 4(365), pp. 1-15.
- Alberts, B., Johnson , A. & Lewis, J., 2002. The Molecular Mechanisms of Membrane Transport and the Maintenance of Compartmental Diversity. In: *Molecular Biology of the Cell*. 4th edition ed. New York: Garland Science.
- Alberts, B. *et al.*, 2002. Molecular Biology of the Cell. In: *General Principles of Cell Communication*. 4th edition ed. New York: Garland Science.
- Alberts, B., Johnson, A. & Lewis, J., 2002. Blood Vessels and Endothelial Cells. In: *Molecular Biology of the Cell*. 4th ed. New York: Garland Science.
- Alberts, B. *et al.*, 2014. *Molecular Biology of the Cell*. 6th edition ed. New York: Garland Science.
- Alkan, S. *et al.*, 2005. Survival role of protein kinase C (PKC) in chronic lymphocytic leukemia and determination of isoform expression pattern and genes altered by PKC inhibition. *Am J Hematol*, 79(2), pp. 97-106.
- Allan, D. & Thomas, P., 1981. Ca²⁺-induced biochemical changes in human erythrocytes and their relation to microvesiculation. *Biochem. J.* , Volume 198, pp. 433-440.

- Allan, D., Watts, R. & Michell, R. H., 1976. Production of 1,2-Diacylglycerol and Phosphatidate in human erythrocytes treated with calcium ions and ionophore A23187. *Biochem. J.*, Volume 198, pp. 225-232.
- Almeida, M. I., Reisb, R. M. & Calina, G. A., 2011. MicroRNA history: Discovery, recent applications, and next frontiers. *Mutation Research*, 717(1-2), pp. 1-8.
- Al-Nedawi, K. *et al.*, 2008. Intercellular transfer of the oncogenic receptor EGFRvIII by microvesicles derived from tumour cells. *Nat Cell Biol*, Volume 10, p. 619–624.
- Alvarez-Erviti, L. *et al.*, 2011. Delivery of siRNA to the mouse brain by systemic injection of targeted exosomes. *Nat Biotechnol*, 29(4), pp. 341-5.
- Ambros, V., 2004. The functions of animal microRNAs. *Nature*, 7006(431), p. 350–355.
- Ambros, V. *et al.*, 2003. A uniform system for microRNA annotation. *RNA*, 9(3), pp. 277-279.
- Amersham Biosciences, 2002. *Ficoll-Paque PLUS-For in vitro isolation of lymphocytes*. [Online] Available: <http://pro.unibz.it/staff2/sbenini/documents/Protein%20purification%20handbooks/Don't%20move/18115269AB.pdf> [Accessed 12 05 2018].
- Amineva, S. P., Aminev, A. G., Gern, J. E. & Palmenberg, A. C., 2011. Comparison of rhinovirus A infection in human primary epithelial and HeLa cells. *J Gen Virol*, 92(Pt 11), p. 2549–2557.
- Andaloussi, S., Mäger, I., Breakefield, X. O. & Wood, M. J., 2013. Extracellular vesicles: biology and emerging therapeutic opportunities. *Nat Rev Drug Discov*, 12(5), pp. 347-57.
- Anderson, H. C., 1969. Vesicles associated with calcification in the matrix of epiphyseal cartilage. *J Cell Biol*, 41(1), pp. 59-72.
- Andre, F. *et al.*, 2002. Malignant effusions and immunogenic tumour-derived exosomes. *Lancet*, 360(9329), pp. 295-305.
- Andreu, Z. & Yáñez-Mó, M., 2014. Tetraspanins in Extracellular Vesicle Formation and Function. *Front Immunol*, 5(442), pp. 1-12.
- Ansa-Addo, E. A. *et al.*, 2010. Human plasma membrane-derived vesicles halt proliferation and induce differentiation of THP-1 acute monocytic leukemia cells. *J Immunol*, 185(9), pp. 5236-46.
- Ardekani, A. M. & Naeini, M. M., 2010. The Role of MicroRNAs in Human Diseases. *Avicenna J Med Biotechnol*, 2(4), p. 161–179.
- Ardoin, S. P. & Pisetsky, D. S., 2008. The role of cell death in the pathogenesis of autoimmune disease: HMGB1 and microparticles as intercellular mediators of inflammation. *Mod Rheumatol*, 18(4), p. 319–326.

- Arroyo, J. D. *et al.*, 2011. Argonaute2 complexes carry a population of circulating microRNAs independent of vesicles in human plasma.. *Proc Natl Acad Sci U S A.*, 108(12), pp. 5003-8.
- Ayre, D. C. *et al.*, 2015. Dynamic regulation of CD24 expression and release of CD24-containing microvesicles in immature B cells in response to CD24 engagement. *Immunology*, 146(2), pp. 217-33.
- Azevedo, L. C., Pedro, M. A. & Laurindo, F. R., 2007. Circulating microparticles as therapeutic targets in cardiovascular diseases. *Recent Pat Cardiovasc Drug Discov*, 2(1), pp. 41-51.
- Bakhtiari, N. *et al.*, 2012. Red blood cell ATP/ADP & nitric oxide: The best vasodilators in diabetic patients. *J Diabetes Metab Disord*, 11(9).
- Bala, S. *et al.*, 2015. Biodistribution and function of extracellular miRNA-155 in mice. *Scientific Reports*, 5(10721).
- Balasubramanian, K. & Schroit, A. J., 2003. Aminophospholipid asymmetry: A matter of life and death. *Annu Rev Physiol*, Volume 65, pp. 701-34.
- Barclay, A. N. & Brown, M. H., 2006. The SIRP family of receptors and immune regulation.. *Nat. Rev. Immunol.*, Volume 6, p. 457–464.
- Barilla-LaBarca, M. L. *et al.*, 2002. Role of membrane cofactor protein (CD46) in regulation of C4b and C3b deposited on cells. *J Immunol*, 168(12), pp. 6298-304.
- Bartel, D. P., 2004. MicroRNAs: genomics, biogenesis, mechanism, and function. *Cell*, 2(116), p. 281–297.
- Bass, J. J. *et al.*, 2017. An overview of technical considerations for Western blotting applications to physiological research. *Scandinavian Journal of Medicine & Science in Sports*, 27(1), p. 4–25.
- Bayat, A., 2002. Bioinformatics.. *BMJ.* , 324(7344), p. 1018–1022.
- Bazzazi, H., Isenberg, J. S. & Popel, A. S., 2017. Inhibition of VEGFR2 Activation and Its Downstream Signaling to ERK1/2 and Calcium by Thrombospondin-1 (TSP1): In silico Investigation. *Front Physiol*, 8(48), p. eCollection 2017.
- Beer, L., Mildner, M. & Ankersmit, H. J., 2017. Cell secretome based drug substances in regenerative medicine: when regulatory affairs meet basic science.. *Ann Transl Med.* , 5(7), p. 170.
- Berditchevski, F. *et al.*, 1997. A Novel Link between Integrins, Transmembrane-4 Superfamily Proteins (CD63 and CD81), and Phosphatidylinositol 4-Kinase. *J Biol Chem*, Volume 272, pp. 2595-2598.
- Berdowska, I., 2004. Cysteine proteases as disease markers. *Clin Chim Acta*, 342(1-2), pp. 41-69.

Berg, J. M., Tymoczko, J. L. & Stryer, L., 2002. DNA, RNA, and the Flow of Genetic Information. In: *Biochemistry*. 5th edition ed. New York: W H Freeman; 2002.: W H Freeman.

Berg, J. M., Tymoczko, J. L. & Stryer, L., 2002. Proteases: Facilitating a Difficult Reaction.. In: *Biochemistry, 5th edition..* New York: W H Freeman, p. Section 9.1.

Berg, J. M., Tymoczko, J. L. & Stryer, L., 2011. *Biochemistry*. 8th ed. New York: W H Freeman.

Berkman, E. M. & Lawler, S. D., 2018. *Blood group*. [Online] Available at: <https://www.britannica.com/science/blood-group/The-importance-of-antigens-and-antibodies> [Accessed 30 January 2018].

Bervers, E. M. *et al.*, 1992. Defective Ca(2+)-induced microvesiculation and deficient expression of procoagulant activity in erythrocytes from a patient with a bleeding disorder: a study of the red blood cells of Scott syndrome. *Blood*, 79(2), pp. 380-8.

Bhoola, K. D., Figueroa, C. D. & Worthy, K., 1992. Bioregulation of kinins: kallikreins, kininogens, and kininases. *Pharmacol Rev*, 44(1), pp. 1-80.

Bianco, F. *et al.*, 2009. Acid sphingomyelinase activity triggers microparticle release from glial cells. *EMBO J*, 28(8), pp. 1043-54.

Bicalho, B., Holovati, J. L. & Acker, J. P., 2013. Phospholipidomics reveals differences in glycerophosphoserine profiles of hypothermically stored red blood cells and microvesicles. *Biochimica et Biophysica Acta.*, 2(2), p. 317–326.

Bierer, B. E., Barbosa, J., Herrmann, S. & Burakoff, S. J., 1998. Interaction of CD2 with its ligand, LFA-3, in human T cell proliferation. *J Immunol*, 140(10), pp. 3358-3363.

Bignotti, E. *et al.*, 2016. Identification of stably expressed reference small non-coding RNAs for microRNA quantification in high-grade serous ovarian carcinoma tissues. *J Cell Mol Med*, pp. 1-8.

BIO-RAD laboratories, I., 2014. *Flow Cytometry Basics Guide- Bio-Rad Antibodies*. [Online] Available at: <https://www.bio-rad-antibodies.com/static/2015/resources-2015/.../flowcytometry.pdf> [Accessed 02 03 2018].

Blaas, D. & Fuchs, R., 2016. Mechanism of human rhinovirus infections. *Mol Cell Pediatr*, 3(21).

Black, A. R. & Black, J. D., 2012. Protein kinase C signaling and cell cycle regulation. *Front Immunol*, 3(423).

Black, J. D., 2000. Protein kinase C-mediated regulation of the cell cycle. *Front Biosci*, Volume 5, pp. D406-23.

Blondal, T. *et al.*, 2013. Assessing sample and miRNA profile quality in serum and plasma or other biofluids. *Methods*, Volume 59, p. S1–S6.

- Bobrie, A. *et al.*, 2012. Diverse subpopulations of vesicles secreted by different intracellular mechanisms are present in exosome preparations obtained by differential ultracentrifugation. *J Extracell Vesicles*, 1(10), p. 18397.
- Bochkov, Y. A. *et al.*, 2015. Cadherin-related family member 3, a childhood asthma susceptibility gene product, mediates rhinovirus C binding and replication. *Proc Natl Acad Sci U S A*, 112(17), p. 5485–5490.
- Bogdanova, A. *et al.*, 2013. Calcium in Red Blood Cells-A Perilous Balance. *Int J Mol Sci*, 14(5), p. 9848–9872.
- Borges, F. T., Reis, L. A. & Schor, N., 2013. Extracellular vesicles: structure, function, and potential clinical uses in renal diseases. *Braz J Med Biol Res*, 46(10), p. 824–830.
- Bosman, G. J., Werre, J. M., Willekens, F. L. & Novotný, V. M., 2008. Erythrocyte ageing in vivo and in vitro: structural aspects and implications for transfusion. *Transfus Med*, 18(6), pp. 335-47.
- Böyum, A., 1968. Isolation of mononuclear cells and granulocytes from human blood. Isolation of monuclear cells by one centrifugation, and of granulocytes by combining centrifugation and sedimentation at 1 g. *Scand J Clin Lab Invest*, 21(97), pp. 77-89.
- Braasch, D. A., Liu, Y. & Corey, D. R., 2002. Antisense inhibition of gene expression in cells by oligonucleotides incorporating locked nucleic acids: effect of mRNA target sequence and chimera design. *Nucleic Acids Res*, 30(23), pp. 5160-7.
- Bromme, D., Wilson, S., Parks, W. C. & Mecham, R. P., 2011. Role of Cysteine Cathepsins in Extracellular proteolysis. *Extracellular Matrix Degradation*, pp. 23-51.
- Bronisz, A., Godlewski, J. & Chiocca, E. A., 2016. Extracellular Vesicles and MicroRNAs: Their Role in Tumorigenicity and Therapy for Brain Tumors. *Cell Mol Neurobiol*, 36(3), pp. 361-376.
- Brown, T. A., 2002. *Genomes*. 2nd ed. Oxford: Wiley-Liss.
- Bruno, S. *et al.*, 2009. Mesenchymal stem cell-derived microvesicles protect against acute tubular injury. *J Am Soc Nephrol*, 20(5), pp. 1053-67.
- Burger, P. *et al.*, 2012. CD47 functions as a molecular switch for erythrocyte phagocytosis. *Blood*, 119(23), pp. 5512-5521.
- Bushnell, T., 2017. *The Difference Between Linear And Log Displays In Flow Cytometry*. [Online]. Available at: <https://expertcytometry.com/the-difference-between-linear-and-log-displays-in-flow-cytometry/> [Accessed 12 February 2018].
- Byron, A., Morgan, M. R. & Humphries, M. J., 2010. Adhesion signalling complexes. *Curr Biol*, 20(24), p. R1063–R1067.
- Byun, S. *et al.*, 2013. Characterizing deformability and surface friction of cancer cells. *PNAS*, 110(10), pp. 7580-7585.

- Camussi, G. *et al.*, 2010. Exosomes/microvesicles as a mechanism of cell-to-cell communication. *Kidney International*, 78(9), pp. 838-48.
- Canellini, G. *et al.*, 2012. Red blood cell microparticles and blood group antigens: an analysis by flow cytometry. *Blood Transfus*, Volume Suppl 2, p. s39–s45.
- Cantin, R. *et al.*, 2008. Discrimination between exosomes and HIV-1: purification of both vesicles from cell-free supernatants. *J. Immunol. Methods*, 338(1-2), p. 21–30.
- Cardo, L. J., Wilder, D. & Salata, J., 2008. Neutrophil priming, caused by cell membranes and microvesicles in packed red blood cell units, is abrogated by leukocyte depletion at collection. *Transfus Apher Sci*, 38(2), p. 117–125.
- Cassat, J. E. & Skaar, E. P., 2013. Iron in Infection and Immunity. *Cell Host Microbe*, 13(5), p. 509–519.
- Castellana, D., Toti, F. & Freyssinet, J. M., 2010. Membrane micro-vesicles: Macromessengers in cancer disease and progression. *Thromb Res*, 125(Suppl 2), pp. S84–8.
- Castro, C. H. *et al.*, 2011. Looking at the proteases from a simple perspective. *Journal of molecular recognition*, Volume 24, p. 165–181.
- Cerda, S. R. *et al.*, 2006. Protein kinase C delta inhibits Caco-2 cell proliferation by selective changes in cell cycle and cell death regulators.. *Oncogene*, Volume 25, p. 3123–3138.
- Chahar, H. S., Bao, X. & Casola, A., 2015. Exosomes and their role in the life cycle and pathogenesis of RNA viruses. *Viruses*, 7(6), p. 3204–3225.
- Chaineau, M., Danglot, L. & Galli, T., 2009. Multiple roles of the vesicular-SNARE TI-VAMP in postGolgi and endosomal trafficking. *FEBS Letters*, 583(23), pp. 3817-26.
- Chambard, J.-C., Lefloch, R., Pouysségur, J. & Lenormand, P., 2007. ERK implication in cell cycle regulation.. *Biochimica et Biophysica Acta (BBA) - Molecular Cell Research*, 1773(8), pp. 1299-1310.
- Chandler, W. L., 2016. Measurement of Microvesicle Levels in Human Blood Using Flow Cytometry. *Cytometry Part B (Clinical Cytometry)*, Volume 90B, p. 326–336.
- Chang, H. *et al.*, 2016. CRISPR/cas9, a novel genomic tool to knock down microRNA in vitro and in vivo. *Scientific Reports*, 6(22312).
- Chan, J. A., Krichevsky, A. M. & Kosik, K. S., 2005. MicroRNA-21 is an antiapoptotic factor in human glioblastoma cells.. *Cancer Res*, Volume 65, p. 6029–33.
- Chanput, W., Mes, J. J. & Wichers, H. J., 2014. THP-1 cell line: An in vitro cell model for immune modulation approach. *International Immunopharmacology*, 23(1), p. 37–45.
- Chargaff, E. & West, R., 1946. The biological significance of the thromboplastic protein of blood. *J Biol Chem*, 166(1), pp. 189-97.

- Chasis, J. A. & Mohandas, N., 1992. Red blood cell glycoporphins. *Blood*, 80(8), pp. 1869-79.
- Chen, S. Y., Wang, Y., Telen, M. J. & Chi, J. T., 2008. The Genomic Analysis of Erythrocyte microRNA Expression in Sickle Cell Diseases. *PLoS One*, 3(6), p. e2360.
- Chen, X. *et al.*, 2013. A Combination of Let-7d, Let-7g and Let-7i Serves as a Stable Reference for Normalization of Serum microRNAs. *PLoS ONE*, 11(8).
- Choong, M. L., Yang, H. H. & McNiece, I., 2007. MicroRNA expression profiling during human cord blood-derived CD34 cell erythropoiesis. *Exp Hematol*, 35(4), pp. 551-64.
- Chorzalska, A. *et al.*, 2010. The effect of the lipid-binding site of the ankyrin binding domain of erythroid β -spectrin on the properties of natural membranes and skeletal structures.. *Cellular and molecular biology letters.*, Volume 15, pp. 406-423.
- Chothia, C., Gough, J., Vogel, C. & Teichmann, S. A., 2003. Evolution of the protein repertoire. *Science*, 300(5626), pp. 1701-3.
- Chowdhury, F., Howat, W. J., Phillips, G. J. & Lackie, P. M., 2010. Interactions between endothelial cells and epithelial cells in a combined cell model of airway mucosa: effects on tight junction permeability. *Exp Lung Res*, 36(1), pp. 1-11.
- Clark, E. A. & Brugge, J. S., 1995. Integrins and signal transduction pathways: the road taken. *Science*, 268(5208), pp. 233-239.
- Clarkson, Y. L. *et al.*, 2014. β -III spectrin underpins ankyrin R function in Purkinje cell dendritic trees: protein complex critical for sodium channel activity is impaired by SCA5-associated mutations.. *Hum Mol Genet.* , 23(14), p. 3875–3882.
- Clayton, A. *et al.*, 2003. Antigen-presenting cell exosomes are protected from complement-mediated lysis by expression of CD55 and CD59. *Eur J Immunol*, 33(2), p. 522–31.
- Cocucci, E. & Meldolesi, J., 2015. Ectosomes and exosomes: shedding the confusion between extracellular vesicles. *Trends in Cell Biology* , 25(6), pp. 364-372.
- Cocucci, E., Racchetti, G. & Meldolesi, J., 2009. Shedding micro-vesicles: artefacts no more. *Trends Cell Biol*, 19(2), p. 43–51.
- Cohen, F. S. & Melikyan, G. B., 2004. The energetics of membrane fusion from binding, through hemifusion, pore formation, and pore enlargement. *J Membr Biol*, 199(1), pp. 1-14.
- Coleman, M. L. *et al.*, 2001. Membrane blebbing during apoptosis results from caspase-mediated activation of ROCK I. *Nat Cell Biol*, 3(4), pp. 339-45.
- Collino, F. *et al.*, 2010. Microvesicles derived from adult human bone marrow and tissue specific mesenchymal stem cells shuttle selected pattern of miRNAs. *PLoS One*, 5(7), p. e11803.

Conde-Vancells, J. *et al.*, 2010. Candidate biomarkers in exosome-like vesicles purified from rat and mouse urine samples. *Proteomics Clin Appl*, 4(4), pp. 416-25.

Connor, J. & Schroit, J., 1990. Aminophospholipid translocation in erythrocytes: evidence for the involvement of a specific transporter and an endofacial protein. *Biochemistry*, 29(1), p. 37–43.

Consortium, G. O., 2015. Gene Ontology Consortium: going forward. *Nucleic Acids Res.*, 43((Database issue):D1049-56.).

Constantin, B., Meerschaert, K., Vandekerckhove, J. & Gettemans, J., 1998. Disruption of the actin cytoskeleton of mammalian cells by the capping complex actin-fragmin is inhibited by actin phosphorylation and regulated by Ca²⁺ ions. *Journal of Cell Science.*, Volume 111, pp. 1695-1706 .

Cooper, M. G., 2000. *The Cell: A Molecular Approach*. Sunderland(MA): Sinauer Associates.

Craik, C. S., Page, M. J. & Madison, E. L., 2011. Proteases as therapeutics. *Biochem J.*, 435(1), pp. 1-16.

Cruz, C. M. *et al.*, 2007. ATP Activates a Reactive Oxygen Species-dependent Oxidative Stress Response and Secretion of Proinflammatory Cytokines in Macrophages. *J Biol Chem*, 282(5), p. 2871–2879.

Cvjetkovic, A., Lötvall, J. & Lässer, C., 2014. The influence of rotor type and centrifugation time on the yield and purity of extracellular vesicles. *J Extracell Vesicles*, Volume 3, p. eCollection 2014.

Daley, W. P., Peters, S. B. & Larsen, M., 2008. Extracellular matrix dynamics in development and regenerative medicine. *J Cell Sci*, Volume 121, p. 255–264.

De Gassart, A. *et al.*, 2009. Exosomal sorting of the cytoplasmic domain of bovine leukemia virus TM Env protein. *Cell Biology International*, 33(1), p. 36–48.

De Rosa, M. C. *et al.*, 2007. The plasma membrane of erythrocytes plays a fundamental role in the transport of oxygen, carbon dioxide and nitric oxide and in the maintenance of the reduced state of the heme ion. *Gene*, 398(1-2), p. 162–171.

De Villartay, J. P., Rouger, P., Muller, J. Y. & Salmon, C., 1985. HLA antigens on peripheral red blood cells: analysis by flow cytometry using monoclonal antibodies. *Tissue Antigens*, 26(1), pp. 12-9.

Dejana, E. *et al.*, 2009. Organization and signaling of endothelial cell-to-cell junctions in various regions of the blood and lymphatic vascular trees. *Cell Tissue Res*, 335(1), pp. 17- 25.

Del Conde, I., Shrimpton, C. N., Thiagarajan, P. & Lopez, J. A., 2005. Tissue factor-bearing microvesicles arise from lipid rafts and fuse with activated platelets to initiate coagulation. *Blood*, 106(5), p. 1604–1611.

- Dellinger, E. P. & Anaya, D. A., 2004. Infectious and immunologic consequences of blood transfusion. *Crit Care*, 8((Suppl 2)), p. S18–S23.
- Demchenko, A. P., 2013. Beyond annexin V: fluorescence response of cellular membranes to apoptosis. *Cytotechnology*, 65(2), p. 157–172.
- Deregibus, M. *et al.*, 2007. Endothelial progenitor cell derived microvesicles activate an angiogenic program in endothelial cells by a horizontal transfer of mRNA. *Blood*, 110(7), p. 2440–8.
- Diehl, P. *et al.*, 2012. Microparticles: major transport vehicles for distinct miRNAs in circulation. *Cardiovasc Res*, 93(4), p. 633–634.
- Diez-Silva, M. *et al.*, 2010. Shape and Biomechanical Characteristics of Human Red Blood Cells in Health and Disease. *MRS Bull*, 35(5), p. 382–388.
- Desvignes, Dr. T. *et al.*, 2015. microRNA nomenclature: A view incorporating genetic origins, biosynthetic pathways, and sequence variants. *Trends Genet*, 31(11), p. 613–626
- Distler, J. H. *et al.*, 2005. Microparticles as regulators of inflammation: novel players of cellular crosstalk in the rheumatic diseases. *Arthritis Rheum*, 52(11), pp. 3337-48.
- Doherty, G. J. & McMahon, H. T., 2009. Mechanisms of endocytosis. *Annu Rev Biochem*, Volume 78, p. 857–902.
- Dolo, V. *et al.*, 1999. Matrix-degrading proteinases are shed in membrane vesicles by ovarian cancer cells in vivo and in vitro. *Clin Exp Metastasis*, 17(2), pp. 131-40.
- Dozio, V. & Sanchez, J.-C., 2017. Characterisation of extracellular vesicle-subsets derived from brain endothelial cells and analysis of their protein cargo modulation after TNF exposure. *J Extracell Vesicles*, 6(1), p. 1302705.
- Dozmorov, M. G. *et al.*, 2009. Unique Patterns of Molecular Profiling between Human Prostate Cancer LNCaP and PC-3 Cells. *Prostate*, 69(10), p. 1077–1090.
- Dragovic, R. A. *et al.*, 2011. Sizing and phenotyping of cellular vesicles using Nanoparticle Tracking Analysis. *Nanomedicine*, 7(6), pp. 780-8.
- Duffy, M. J. *et al.*, 2011. The ADAMs family of proteases: new biomarkers and therapeutic targets for cancer?. *Clinical Proteomics*, 8(1), p. 9.
- Dunkelberger, J. R. & Song, W.-C., 2010. Complement and its role in innate and adaptive immune responses. *Cell Research*, Volume 20, pp. 34-50.
- Elmén, J. *et al.*, 2008. Antagonism of microRNA-122 in mice by systemically administered LNA-antimiR leads to up-regulation of a large set of predicted target mRNAs in the liver. *Nucleic Acids Res*, 36(4), pp. 1153-62.
- Emamia, N. B. & Diamandis, E. P., 2007. New insights into the functional mechanisms and clinical applications of the kallikrein-related peptidase family. *Molecular oncology*, 1(3), p. 269–287.

- Engels, B. M. & Hutvagner, G., 2006. Principles and effects of microRNA-mediated post-transcriptional gene regulation.. *Oncogene.*, Volume 25, p. 6163–6169.
- Engin, A. B. *et al.*, 2017. Mechanistic understanding of nanoparticles' interactions with extracellular matrix: the cell and immune system. *Particle and Fibre Toxicology*, 14(22).
- Epanand, R. E. & Vogel, H. J., 1999. Diversity of antimicrobial peptides and their mechanisms of action. *Biochim Biophys Acta*, 1462(1-2), pp. 11-28.
- Escrevente, C., Keller, S., Altevogt, P. & Costa, J., 2011. Interaction and uptake of exosomes by ovarian cancer cells. *BMC Cancer*, 11(108).
- Fackler, O. & Grosse, R., 2008. Cell motility through plasma membrane blebbing. *J Cell Biol*, 181(6), pp. 879-884.
- Fadeel, B. & Xue, D., 2009. The ins and outs of phospholipid asymmetry in the plasma membrane: roles in health and disease. *Crit Rev Biochem Mol Biol*, 44(5), p. 264–277.
- Fader, C. M., Sanchez, D. G., Mestre, M. B. & Colombo, M. I., 2009. TI-VAMP/VAMP7 and VAMP3/cellubrevin: two v-SNARE proteins involved in specific steps of the autophagy/multivesicular body pathways. *Biochim Biophys Acta*, 1793(12), pp. 1901-16.
- Fang, Y. *et al.*, 2007. Higher-order oligomerization targets plasma membrane proteins and HIV gag to exosomes. *PLoS Biol*, 5(6), p. e158.
- Fanjul-Fernández, M., Folgueras, A. R., Cabrera, S. & López-Otín, C., 2010. Matrix metalloproteinases: Evolution, gene regulation and functional analysis in mouse models.. *Biochimica et Biophysica Acta* , 1803 (1), p. 3–19.
- Farazi, T. A., Juranek, S. A. & Tuschl, T., 2008. The growing catalog of small RNAs and their association with distinct Argonaute/Piwi family members. *Development* , Volume 135, pp. 1201-1214.
- Fawzy, M. *et al.*, 2016. Association of MicroRNA-196a2 Variant with Response to Short-Acting β 2-Agonist in COPD: An Egyptian Pilot Study. *PLoS ONE*, 11(4), p. e0152834.
- Felekkis, K. & Deltas, C., 2006. RNA Interference: a powerful laboratory tool and its therapeutic implications. *Hippokratia*, Volume 3, pp. 112-5.
- Felekkis, K., Touvana, E., Stefanou, C. H. & Deltas, C., 2010. microRNAs: a newly described class of encoded molecules that play a role in health and disease. *Hippokratia*, Volume 4, p. 236–240.
- Felli, N. *et al.*, 2005. MicroRNAs 221 and 222 inhibit normal erythropoiesis and erythroleukemic cell growth via kit receptor down-modulation. *Proc Natl Acad Sci U S A*, 102(50), pp. 18081-6.
- Feng, D. *et al.*, 2010. Cellular internalization of exosomes occurs through phagocytosis. *Traffic*, 11(5), pp. 675-87.

- Ferguson, R. E. *et al.*, 2005. Housekeeping proteins: a preliminary study illustrating some limitations as useful references in protein expression studies. *Proteomics*, 5(2), pp. 566-71.
- Ferreira, Y. J. *et al.*, 2013. O-253 Human embryos release extracellular vesicles which may act as indicators of embryo quality. Session 66: Embryo quality: does it predict pregnancy?. *ORA*, 28(6), p. 1445–1736.
- Filipe, V., Hawe, A. & Jiskoot, W., 2010. Critical Evaluation of Nanoparticle Tracking Analysis (NTA) by NanoSight for the Measurement of Nanoparticles and Protein Aggregates. *Pharm Res*, 27(5), p. 796–810.
- Filipowicz, W., Bhattacharyya, S. N. & Sonenberg, N., 2008. Mechanisms of post-transcriptional regulation by microRNAs: are the answers in sight?. *Nat. Rev. Genet*, 2(9), p. 102–114.
- Finnegan, E. J. & Matzke, M. A., 2003. The small RNA world. *Journal of Cell Science*, 116(Pt 23), pp. 4689-4693.
- Fire, A. *et al.*, 1998. Potent and specific genetic interference by double-stranded RNA in *Caenorhabditis elegans*. *Nature*, 391(6669), pp. 806-11.
- Fleissner, F., Goerzig, Y., Haverich, A. & Thum, T., 2012. Microvesicles as novel biomarkers and therapeutic targets in transplantation medicine. *Am J Transplant*, 12(2), pp. 289-97.
- Föllner, M., Huber, S. M. & Lang, F., 2008. Erythrocyte programmed cell death. *IUBMB Life*, 60(10), pp. 661-8.
- Fonović, M. & Turk, B., 2014. Cysteine cathepsins and extracellular matrix degradation. *Biochim Biophys Acta*, 1840(8), pp. 2560-70.
- Fonseca, A. M., Pereira, C. F. & Arosa, F. A., 2003. Red blood cells promote survival and cell cycle progression of human peripheral blood T cells independently of CD58/LFA-3 and heme compounds. *Cell Immunol*, Volume 224, p. 17–28.
- Forman, J. J., Legesse-Miller, A. & Collier, H. A., 2008. A search for conserved sequences in coding regions reveals that the let-7 microRNA targets Dicer within its coding sequence. *Proc Natl Acad Sci USA*, 105(39), pp. 14879-14884.
- Frey, M. R. *et al.*, 2000. Protein Kinase C Signaling Mediates a Program of Cell Cycle Withdrawal in the Intestinal Epithelium.. *J Cell Biol.* , 151(4), p. 763–778.
- Fricke, M. *et al.*, 2012. MFG-E8 mediates primary phagocytosis of viable neurons during neuroinflammation. *J Neurosci*, 32(8), pp. 2657-2666.
- Friskin, B. J., 2001. Revisiting the method of cumulants for the analysis of dynamic light-scattering data. *Appl Opt*, 40(24), pp. 4087-91.

- Fuchs, J. E. *et al.*, 2013. Cleavage Entropy as Quantitative Measure of Protease Specificity. *PLoS Comput Biol*, 9(4), p. e1003007.
- Fuchs, R. & Blaas, D., 2010. Uncoating of human rhinoviruses. *Rev. Med. Virol*, Volume 20, p. 281–297.
- Fuchs, R. & Blaas, D., 2012. Productive entry pathways of human rhinoviruses. *Advances in Virology*, Volume 2012.
- Furi, I., Momen-Heravi, F. & Szabo, G., 2017. Extracellular vesicle isolation: present and future. *Ann Transl Med*, 5(12), p. 263.
- Gaggar, A. *et al.*, 2005. Localization of Regions in CD46 That Interact with Adenovirus. *J Virol*, 79(12), p. 7503–7513.
- Gale, A. J., 2011. Current Understanding of Hemostasis. *Toxicol Pathol*. 2011; 39(1): 273–280., 39(1), pp. 273-280.
- Gallagher, P. G. & Forget, B. G., 1996. Hematologically Important Mutations: Spectrin Variants in Hereditary Elliptocytosis and Hereditary Pyropoikilocytosis. *Blood Cells, Molecules, and Diseases*, 22(20), p. 254–258.
- Galtieri, A. *et al.*, 2002. Band -3 protein function in human erythrocytes: effect of oxygenation-deoxygenation. *Biochimica et Biophysica Acta*, 1564(1), pp. 214–218.
- Galvagnion, C. *et al.*, 2015. Lipid vesicles trigger α -synuclein aggregation by stimulating primary nucleation. *Nat Chem Biol*, 11(3), pp. 229–34.
- García-Manrique, P. *et al.*, 2018. Therapeutic biomaterials based on extracellular vesicles: classification of bio-engineering and mimetic preparation routes. *J Extracell Vesicles*, 7(1), p. 1422676.
- Gardiner, C. *et al.*, 2016. Techniques used for the isolation and characterization of extracellular vesicles: results of a worldwide survey. *J Extracell Vesicles*, Volume 5, p. 10.3402/jev.v5.32945.
- Garzon, R., Marcucci, G. & Croce, C. M., 2010. Targeting microRNAs in cancer: Rationale, strategies and challenges.. *Nat Rev Drug Discov.* , 9(10), p. 775–789.
- Gedye, C. A. *et al.*, 2014. Cell Surface Profiling Using High-Throughput Flow Cytometry: A Platform for Biomarker Discovery and Analysis of Cellular Heterogeneity. *PLoS One*, 9(8), p. e105602.
- Giacomini, P. *et al.*, 1997. HLA-C heavy chains free of beta2-microglobulin: distribution in normal tissues and neoplastic lesions of non-lymphoid origin and interferon-gamma responsiveness. *Tissue Antigens*, 50(6), pp. 555–66.
- Giardina, B., Messina, I., Scatena, R. & Castagnola, M., 1995. The Multiple Functions of Hemoglobin. *Critical Reviews in Biochemistry and Molecular Biology*, 30(3), pp. 165–196.

- Gilbert, L. A. *et al.*, 2013. CRISPR-mediated modular RNA-guided regulation of transcription in eukaryotes. *Cell*, 154(2), pp. 442-51.
- Glass, K. & Girvan, M., 2014. Annotation enrichment analysis: an alternative method for evaluating the functional properties of gene sets.. *Sci Rep.*, 4(4191).
- Goel, M. S. & Diamond, S. L., 2002. Adhesion of normal erythrocytes at depressed venous shear rates to activated neutrophils, activated platelets, and fibrin polymerized from plasma.. *Blood.* , 100(10), pp. 3797-803.
- Gould, S. J., Booth, A. M. & Hildreth, J. E., 2003. The Trojan exosome hypothesis. *Proc. Natl. Acad. Sci. U.S.A.*, 100(19), p. 10592–10597.
- Gould, S. J. & Raposo, G., 2013. As we wait: coping with an imperfect nomenclature for extracellular vesicles. *Journal of Extracellular Vesicles*, Volume 2, p. 20389.
- Gov, N. S. & Safran, S. A., 2005. Red Blood Cell Membrane Fluctuations and Shape Controlled by ATP-Induced Cytoskeletal Defects. *Biophys J*, 88(3), pp. 1859-1874.
- Grant, R. *et al.*, 2011. A filtration-based protocol to isolate human plasma membrane-derived vesicles and exosomes from blood plasma. *J Immunol Methods*, 371(1-2), pp. 143-51.
- Green, B. D., Flatt, P. R. & Bailey, C. J., 2006. Dipeptidyl peptidase IV (DPP IV) inhibitors: A newly emerging drug class for the treatment of type 2 diabetes. *Diab Vasc Dis Res*, 3(3), pp. 159-65.
- Greening, D. W. *et al.*, 2015. A protocol for exosome isolation and characterization: evaluation of ultracentrifugation, density-gradient separation, and immunoaffinity capture methods. *Methods Mol Biol*, Volume 1295, pp. 179-209.
- Griffiths, A. J. F. *et al.*, 2000. *An Introduction to Genetic Analysis*. 7th edition ed. New York: W. H. Freeman.
- Griffiths-Jones, S. *et al.*, 2006. miRBase: microRNA sequences, targets and gene nomenclature. *Nucleic Acids Research*, 34(D140-4).
- Griffiths-Jones, S., Saini, H. K., van Dongen, S. & Enright, A. J., 2008. miRBase: tools for microRNA genomics. *Nucleic Acids Res*, Issue 36(Database issue), pp. D154-8.
- Grisendi, G. *et al.*, 2015. Detection of microparticles from human red blood cells by multiparametric flow cytometry.. *Blood Transfus.*, 13(2), p. 274–280.
- Gustafson, C. M., Shepherd, A. J., Miller, V. M. & Jayachandran, M., 2015. Age- and sex-specific differences in blood-borne microvesicles from apparently healthy humans. *Biol Sex Differ*, 6(10), p. eCollection 2015.
- Gutierrez , M. J. *et al.*, 2016. Airway Secretory microRNAome Changes during Rhinovirus Infection in Early Childhood.. *PLoS One.* , 11(9), p. e0162244.

- György, B. *et al.*, 2011. Membrane vesicles, current state-of-the-art: emerging role of extracellular vesicles. *Cell. Mol. Life Sci*, 68(16), pp. 2667-88.
- Haab, B. B., Partyka, K. & Cao, Z., 2013. Using antibody arrays to measure protein abundance and glycosylation: considerations for optimal performance. *Curr Protoc Protein Sci.*, Volume 73, p. 27.6.1–27.6.16.
- Habib, A. *et al.*, 2008. Elevated Levels Of Circulating Procoagulant Microparticles In Patients With B-Thalassemia Intermedia. *Haematologica*, Volume 93, pp. 941-942.
- Hamasaki, N., 1999. The role of band 3 protein in oxygen delivery by red blood cells. *Indian J Clin Biochem*, 14(1), p. 49–58.
- Hamasaki, N. & Okubo, K., 1996. Band 3 protein: Physiology, function and structure. *Cell Mol Bio*, Volume 42, pp. 1025-1040.
- Hamasaki, N. & Yamamoto, M., 2000. Red Blood Cell Function and Blood Storage. *The international journal of transfusion medicine*, 79(4), pp. 191-197.
- Hamilton, A. J., 2010. microRNA in erythrocytes. *Biochem. Soc. Trans*, Volume 38, pp. 229-231.
- Hamilton, K. K., Hattori, R., Esmon, C. T. & Sims, P. J., 1990. Complement proteins C5b-9 induce vesiculation of the endothelial plasma membrane and expose catalytic surface for assembly of the prothrombinase enzyme complex. *J. Biol. Chem*, Volume 265, pp. 3809-3814.
- Hanayama, R. *et al.*, 2002 . Identification of a factor that links apoptotic cells to phagocytes. *Nature*, 417(6885), pp. 182-7.
- Hanson, P. I., Roth, R., Lin, Y. & Heuser, J. E., 2008 . Plasma membrane deformation by circular arrays of ESCRT-III protein filaments. *J Cell Biol*, 180(2), p. 389–402.
- Harisa, G. I., Badranb, M. M. & Alanazi, F. K., 2017. Erythrocyte nanovesicles: Biogenesis, biological roles and therapeutic approach. *Saudi Pharmaceutical Journal*, 25(1), p. 8–17.
- Harry, S., Fairbrother, U. L. C. & Heugh, S. M., 2013. Second International Meeting of ISEV 2013: Boston, USA, April 17th-20th, 2013. *J Extracell Vesicles*, 2(20826).
- Harutyunyan, S. *et al.*, 2013. Viral uncoating is directional: exit of the genomic RNA in a common cold virus starts with the poly-(A) tail at the 3'-end. *PLoS Pathology*, 9(4), p. e1003270.
- Ha, T.-Y., 2011. MicroRNAs in Human Diseases: From Cancer to Cardiovascular Disease. *Immune Netw*, 11(3), pp. 135-154.
- Heemskerk, J. W., Bevers, E. M. & Lindhout, T., 2002. Platelet activation and blood coagulation. *Thromb Haemost*, 88(2), pp. 186-93.

- He, H. *et al.*, 2016. Overexpression of protein kinase C ϵ improves retention and survival of transplanted mesenchymal stem cells in rat acute myocardial infarction. *Cell Death and Disease*, Volume 7, p. e2056.
- Heijnen, H. *et al.*, 1999. Activated platelets release two types of membrane vesicles: microvesicles by surface shedding and exosomes derived from exocytosis of multivesicular bodies and alpha-granules. *Blood.*, 94(11), pp. 3791-9.
- He, J., Lee, J. H., Febbraio, M. & Xie, W., 2011. The emerging roles of fatty acid translocase/CD36 and the aryl hydrocarbon receptor in fatty liver disease. *Exp Biol Med (Maywood)*, 236(10), pp. 1116-21.
- He, L. & Hannon, G. J., 2004. MicroRNAs: small RNAs with a big role in gene regulation. *Nature Reviews Genetics*, Volume 5, pp. 522-531.
- He, N. *et al.*, 2010. HIV-1 Tat and Host AFF4 Recruit Two Transcription Elongation Factors into a Bifunctional Complex for Coordinated Activation of HIV-1 Transcription. *Mol Cell*, 38(3), p. 428–438.
- Hergert, W. & Wriedt, T., 2012. *Mie Theory: A Review*. 1st ed. s.l.:Springer.
- Hess, C. *et al.*, 1999. Ectosomes released by human neutrophils are specialized functional units. *J. Immunol*, 163(8), pp. 4564-73.
- Hind, E. *et al.*, 2010. Red cell PMVs, Plasma-derived vesicles calling out for standards. *Biochemical and biophysical research communication*, 399(4), pp. 465-9.
- Hoeh, E. N., Cremer, T., Gallo, R. C. & Margolis, L. B., 2016. Extracellular vesicles and viruses: Are they close relatives?. *PNAS*, 113(33), p. 9155–9161.
- Holme, P. A. *et al.*, 1994. Demonstration of platelet-derived microvesicles in blood from patients with activated coagulation and fibrinolysis using a filtration technique and western blotting. *Thromb. Haemost.*, 72(5), pp. 666-71.
- Hotchin, N. A. & Hall, A., 1995. The assembly of integrin adhesion complexes requires both extracellular matrix and intracellular rho/rac GTPases. *J Cell Biol.* 1995 Dec;131(6 Pt 2):1857-65., 131(6 Pt 2), pp. 1857-65.
- Hristov M, M., Erl, W., Linder, S. & Weber, P. C., 2004. Apoptotic bodies from endothelial cells enhance the number and initiate the differentiation of human endothelial progenitor cells in vitro. *Blood*, 104(9), pp. 2761-6.
- Huang, D. W., Sherman, B. T. & Lempicki, R. A., 2009. Bioinformatics enrichment tools: paths toward the comprehensive functional analysis of large gene lists.. *Nucleic Acids Res.*, 37(1), p. 1–13.
- Huang, W., Febbraio, M. & Silverstein, R. L., 2011. CD9 Tetraspanin Interacts with CD36 on the Surface of Macrophages: A Possible Regulatory Influence on Uptake of Oxidized Low Density Lipoprotein. *PLoS One*, 6(12), p. e29092.

- Hugel, B. M., Martínez, C., Kunzelmann, C. & Freyssinet, J. M., 2005. Membrane Microparticles: Two Sides of the Coin. *Physiology*, 20(1), pp. 22-27.
- Hulspas, R. *et al.*, 2009. Considerations for the control of background fluorescence in clinical flow cytometry. *Cytometry Part B (Clinical Cytometry)*, Volume 76B, p. 355–364.
- Hunter, M. P. *et al.*, 2008. Detection of microRNA Expression in Human Peripheral Blood Microvesicles. *PLoS ONE*, 3(11), p. e3694.
- Hutchings, C. J., Koglin, M. & Marshall, F. H., 2010. Therapeutic antibodies directed at G protein-coupled receptors. *MAbs*, 2(6), pp. 594-606.
- Igumenova, T. I., 2015. Dynamics and membrane interactions of protein kinase C. *Biochemistry*, 54(32), pp. 4953-4968.
- Inal, J. M. & Jorfi, S., 2013. Coxsackievirus B transmission and possible new roles for extracellular vesicles. *Biochem Soc Trans*, 41(1), pp. 299-302.
- Itzhaky, D., Raz, N. & Hollander, N., 1998. The Glycosylphosphatidylinositol-Anchored Form and the Transmembrane Form of CD58 Associate with Protein Kinases. *J Immunol*, 160(9), pp. 4361-4366.
- Jacobs, S. E., Lamson, D. M., St. George, K. & Walsh, T. J., 2013. Human Rhinoviruses. *Clin Microbiol Rev*, 26(1), p. 135–162.
- Jaken, S. & Parker, P. J., 2000. Protein kinase C binding partners. *BioEssays*, Volume 22, pp. 245-254.
- Janeway, C. A., Travers, P. & Walport, M., 2001. The complement system and innate immunity. In: *Immunobiology: The Immune System in Health and Disease*. 5th edition ed. New York: Garland Science.
- Jansen, F. *et al.*, 2014. MicroRNA expression in circulating microvesicles predicts cardiovascular events in patients with coronary artery disease. *J Am Heart Assoc*, 3(6), p. e001249.
- Jansson, M. D. & Lund, A. H., 2012. MicroRNA and cancer. *Molecular Oncology*, 6(6), pp. 590-610.
- Jayachandran, M., Miller, V. M., Heit, J. A. & Owen, W. G., 2012. Methodology for isolation, identification and characterization of microvesicles in peripheral blood. *J Immunol Methods*, 375(1-2), pp. 207-214.
- Jedezko, C. & Sloane, B. F., 2004. Cysteine cathepsins in human cancer. *Biol. Chem*, 385(11), pp. 1017-1027.
- Jena, B., 2009. Membrane fusion: role of SNAREs and calcium. *Protein Pept Lett.*, 16(7), pp. 712-7.

- Jiang, H. & Sun, S. X., 2013. Cellular Pressure and Volume Regulation and Implications for Cell Mechanics. *Biophys J*, 105(3), p. Biophys J. 2013 Aug 6; 105(3): 609–619.
- Jiang, N., Tan, N. S., Ho, B. & Ding, J. L., 2007. Respiratory protein-generated reactive oxygen species as an antimicrobial strategy. *Nature Immunology*, Volume 8, p. 1114–1122.
- Johnsen, K. B. *et al.*, 2014. A comprehensive overview of exosomes as drug delivery vehicles - endogenous nanocarriers for targeted cancer therapy. *Biochim Biophys Acta*, 1846(1), pp. 75-87.
- Johnson, S. M. *et al.*, 2005. RAS is regulated by the let-7 microRNA family. *Cell*, 120(5), pp. 635-47.
- Johnstone, R. M., Bianchini, A. & Teng, K., 1989. Reticulocyte maturation and exosome release: transferrin receptor containing exosomes shows multiple plasma membrane functions. *Blood*, 74(5), pp. 1844-51.
- Joubert, P.-E., 2014. Cell Surface Pathogen Receptor CD46 Induces Autophagy. In: M. A. Hyatt, ed. *Autophagy: Cancer, Other Pathologies, Inflammation, Immunity, Infection, and Aging*. s.l.:Elsevier, p. 197–209.
- Julian, L. & Olson, M. F., 2014. Rho-associated coiled-coil containing kinases (ROCK)-Structure, regulation, and functions. *Small GTPases*, Volume 5, p. e29846.
- Jy, W. *et al.*, 2011. Microparticles in stored red blood cells as potential mediators of transfusion complications. *Transfusion*, 51(4), pp. 886-93.
- Kadiu, I. *et al.*, 2012. Biochemical and Biologic Characterization of Exosomes and Microvesicles as Facilitators of HIV-1 Infection in Macrophages. *J Immunol*, 189(2), pp. 744-754.
- Kaighn, M. E. *et al.*, 1979. Establishment and characterization of a human prostatic carcinoma cell line (PC-3). *Invest Urol*, 17(1), pp. 16-23.
- Kakhniashvili, D. G., Lee, A., Bulla, J. & Goodman, S. R., 2004. The Human Erythrocyte Proteome Analysis by Ion Trap Mass Spectrometry. *Molecular & Cellular Proteomics*, 3(5), pp. 501-9.
- Kalamvoki, M. & Deschamps, T., 2016. Extracellular vesicles during Herpes Simplex Virus type 1 infection: an inquire. *Virol J*, 13(63).
- Karlsson, M. *et al.*, 2001. “Tolerosomes” are produced by intestinal epithelial cells. *Eur J Immunol*, 31(10), pp. 2892-900.
- Karpman, D., Ståhl, A.-L. & Arvidsson, I., 2017. Extracellular vesicles in renal disease. *Nature Reviews Nephrology*, Volume 13, p. 545–562.
- Kasar, M. *et al.*, 2014. Clinical significance of circulating blood and endothelial cell microparticles in sickle-cell disease. *J Thromb Thrombolysis*, 38(2), pp. 167-75.

- Kato, H. *et al.*, 2008. Length-dependent recognition of double-stranded ribonucleic acids by retinoic acid-inducible gene-I and melanoma differentiation-associated gene 5. *J Exp Med*, 205(7), p. 1601–1610.
- Katzmann, D. J., Odorizzi, G. & Emr, S. D., 2002. Receptor downregulation and multivesicular-body sorting. *Nat. Rev. Mol. Cell. Biol*, 3(12), pp. 893-905.
- Kaur, S. *et al.*, 2014. CD47 Signaling Regulates the Immunosuppressive Activity of VEGF in T Cells. *J Immunol*, Volume 193, pp. 3914-3924.
- Kawasaki, H. & Taira, K., 2003. Hes1 is a target of microRNA-23 during retinoic-acid-induced neuronal differentiation of NT2 cells. *Nature*, 423(6942), pp. 838-42.
- Keerthikumar, S. *et al.*, 2016. ExoCarta: A Web-Based Compendium of Exosomal Cargo. *Journal of Molecular Biology*, 428(4), pp. 688-692.
- Keller, S. *et al.*, 2007. CD24 is a marker of exosomes secreted into urine and amniotic fluid. *Kidney Int*, 72(9), pp. 1095-102.
- Kelwick, R., Desanlis, I., Wheeler, G. N. & Edwards, D. R., 2015. The ADAMTS (A Disintegrin and Metalloproteinase with Thrombospondin motifs) family. *Genome Biology*, 16(1), p. 113.
- Khetsuriani, N. *et al.*, 2008. Novel human rhinoviruses and exacerbation of asthma in children. *Emerg Infect Dis*, 14(11), pp. 1793-6.
- Kim, D. *et al.*, 2012. Anti-CD47 antibodies promote phagocytosis and inhibit the growth of human myeloma cells. *Leukemia*, Volume 26, p. 2538–2545.
- Kim, T. K. *et al.*, 2015. A systems approach to understanding human rhinovirus and influenza virus infection. *Virology*, Volume 486, pp. 146-57.
- Klibi, J. T. *et al.*, 2009. Blood diffusion and Th1-suppressive effects of galectin-9-containing exosomes released by Epstein-Barr virus-infected nasopharyngeal carcinoma cells. *Blood*, 113(9), pp. 1957-66.
- Komatsu, S. *et al.*, 2016. Plasma microRNA profiles: identification of miR-23a as a novel biomarker for chemoresistance in esophageal squamous cell carcinoma. *Oncotarget*, 7(38), pp. 62034-62048.
- Kong, F. *et al.*, 2015. Impact of collection, isolation and storage methodology of circulating microvesicles on flow cytometric analysis. *Experimental and Therapeutic Medicine*, 10(6), pp. 2093-2101.
- Konishi, H. *et al.*, 2012. Detection of gastric cancer-associated microRNAs on microRNA microarray comparing pre- and post-operative plasma. *Brit J Cancer*, 106(4), pp. 740-747.

- Koniusz, S. *et al.*, 2016. Extracellular Vesicles in Physiology, Pathology, and Therapy of the Immune and Central Nervous System, with Focus on Extracellular Vesicles Derived from Mesenchymal Stem Cells as Therapeutic Tools. *Front Cell Neurosci*, 10(109).
- Konokhova, A. I. *et al.*, 2012. Light-scattering flow cytometry for identification and characterization of blood microparticles. *J Biomed Opt*, 17(5), pp. 0570061-8.
- Kooijmans, S. A. *et al.*, 2013. Electroporation-induced siRNA precipitation obscures the efficiency of siRNA loading into extracellular vesicles. *J Control Release*, 172(1), pp. 229-38.
- Kosaka, N. *et al.*, 2010. Secretory mechanisms and intercellular transfer of microRNAs in living cells. *J Biol Chem*, 285(23), pp. 17442-52.
- Kos, J., Jevnikar, Z. & Obermajer, N., 2009. The role of cathepsin X in cell signaling. *Cell Adh Migr*, 3(2), p. 164–166.
- Koumandou, V. L. & Scorilas, A., 2013. Evolution of the plasma and tissue kallikreins, and their alternative splicing isoforms. *PLoS One*, 8(7), p. e68074.
- Kozak, D., Anderson, W. & Trau, M., 2012. Tuning Particle Velocity and Measurement Sensitivity by Changing Pore Sensor Dimensions. *Chemistry Letters*, 41(10), pp. 1134-1136.
- Kozomara, A. & Griffiths-Jones, S., 2014. miRBase: annotating high confidence microRNAs using deep sequencing data. *Nucleic Acids Res*, Issue 42(Database issue), pp. D68-73.
- Kriebardis, A., Antonelou, M., Stamoulis, K. & Papassideri, I., 2012. Cell-derived microparticles in stored blood products: innocent-bystanders or effective mediators of post-transfusion reactions?. *Blood Transfus*, 10(suppl 2), p. s25–s38.
- Kuchel, P. W. & Benga, G., 2005. Why does the mammalian red blood cell have aquaporins?. *Biosystems*, Volume 82, p. 189–196.
- Kukull, W. A. & Ganguli, M., 2012. Generalizability-The trees, the forest, and the low-hanging fruit. *Neurology*, 78(23), pp. 1886-1891.
- Labtech, 2014. *LumaScope 500 - single colour fluorescence live cell imaging microscope*. [Online] Available at: <https://www.labtech.com/lumascope-500-single-colour-fluorescence-live-cell-imaging-microscope> [Accessed 9 11 2017].
- Lagana, A. *et al.*, 2013. Extracellular circulating viral microRNAs: current knowledge and perspectives.. *Front Genet.*, 4(120).
- Lai, C. P. *et al.*, 2014. Dynamic Biodistribution of Extracellular Vesicles In Vivo Using a Multimodal Imaging Reporter. *ACS Nano*, 8(1), p. 483–494.
- Landry, J. J. *et al.*, 2013. The Genomic and Transcriptomic Landscape of a HeLa Cell Line. *G3 (Bethesda)*, 3(8), pp. 1213-24.

- Landsteiner, K. & Donath, J., 1904. Ueber paroxymal haemoglobinurie. *Muench Med Wochenschr*, Volume 51, pp. 1906-8.
- Lässer, C., Jang, S. C. & Lötvall, J., 2018. Subpopulations of extracellular vesicles and their therapeutic potential. *Molecular Aspects of Medicine*, Volume 60, pp. 1-14.
- Lee, T. H. *et al.*, 2011. Microvesicles as mediators of intercellular communication in cancer--the emerging science of cellular 'debris'. *Semin Immunopathol*, 33(5), pp. 455-67.
- Lelièvre, S. A. & Bissell, M. J., 1998. Communication Between the Cell Membrane and the Nucleus: Role of Protein Compartmentalization. *J Cell Biochem Suppl.*, Volume 30-31, p. 250-263.
- Leroyer, A. S. *et al.*, 2008. CD40 ligand+ microparticles from human atherosclerotic plaques stimulate endothelial proliferation and angiogenesis a potential mechanism for intraplaque neovascularization. *J Am Coll Cardiol*, 52(16), pp. 1302-11.
- Leuschner, P. J. F., Ameres, S. L., Kueng, S. & Martinez, J., 2006. Cleavage of the siRNA passenger strand during RISC assembly in human cells. *EMBO Rep*, 7(3), pp. 314-320.
- Levin, S. & Korenstein, R., 1991. Membrane fluctuations in erythrocytes are linked to MgATP-dependent dynamic assembly of the membrane skeleton. *Biophys J*, Volume 60, p. 733-737.
- Liao, J. K., Seto, M. & Noma, K., 2007. Rho Kinase (ROCK) Inhibitors. *J Cardiovasc Pharmacol*, 50(1), p. 17-24.
- Liepins, A., 1983. Possible role of microtubules in tumor cell surface membrane shedding, permeability, and lympholysis. *Cellular Immunology*, 76(1), pp. 120-8.
- Li, L. Y. *et al.*, 2009. Erythrocyte CD58 expression in healthy population undergoing moxibustion: An analysis of 40 cases. *Journal of Clinical Rehabilitative Tissue Engineering Research*, 13(49), pp. 9735-9738.
- Lima, L. G. *et al.*, 2009. Tumor-derived microvesicles modulate the establishment of metastatic melanoma in a phosphatidylserine-dependent manner. *Cancer Lett*, 283(2), pp. 168-75.
- Lima, L. *et al.*, 2013. Intercellular transfer of tissue factor via the uptake of tumor-derived microvesicles. *Thromb Res*, 132(4), pp. 450-456.
- Linares, R. *et al.*, 2015. High-speed centrifugation induces aggregation of extracellular vesicles. *Journal of Extracellular Vesicles*, 4(1).
- Lisco, A., Vanpouille, C. & Margolis, L., 2009. War and peace between microbes: HIV-1 interactions with coinfecting viruses. *Cell Host Microbe*, 6(5), pp. 403-408.
- Liszewski, M. K. & Atkinson, J. P., 2015. Complement regulator CD46: genetic variants and disease associations. *Human Genomics*, 9(7).

- Liu, H. *et al.*, 2008. Photoexcited CRY2 Interacts with CIB1 to Regulate Transcription and Floral Initiation in Arabidopsis. *Science*, 322(5907), pp. 1535-9.
- Liu, M. L., Williams, K. J. & Werth, V. P., 2016. Microvesicles in Autoimmune Diseases. *Adv Clin Chem*, Volume 77, pp. 125-175.
- Liu, P., Sun, M. & Sader, S., 2006. Matrix metalloproteinases in cardiovascular disease. *Can J Cardiol*, 22(Suppl B), p. 25B–30B.
- Liu, R. *et al.*, 2009. Erythrocyte-derived microvesicles may transfer phosphatidylserine to the surface of nucleated cells and falsely 'mark' them as apoptotic. *Eur J Haematol*, 83(3), pp. 220-9.
- Lizarbe, M. A. *et al.*, 2013. Annexin-Phospholipid Interactions. Functional Implications. *Int J Mol Sci*, 14(3), p. 2652–2683.
- Lloyd, A. C., 2013. The regulation of cell size.. *Cell.*, 154(6), pp. 1194-1205.
- Lobb, R. J. *et al.*, 2015. Optimized exosome isolation protocol for cell culture supernatant and human plasma. *J Extracell Vesicles*, Volume 4, p. 10.3402/jev.v4.27031 .
- Lodish , H. *et al.*, 2000. *Molecular Cell Biology*. New York: W. H. Freeman.
- Lodish, H., Flygare, J. & Chou, S., 2000. From stem cell to erythroblast: Regulation of red cell production at multiple levels by multiple hormones. *IUBMB Life*, 62(7), p. 492–496.
- Loffek, S., Schilling, O. & Franzke, C. W., 2011. Biological role of matrix metalloproteinases: a critical balance. *Eur Respir J*, 38(1), p. 191–208.
- Lopez, J. P. *et al.*, 2017. MicroRNAs 146a/b-5 and 425-3p and 24-3p are markers of antidepressant response and regulate MAPK/Wnt-system genes. *Nat Commun*, Volume 8, p. 15497.
- Lötvall, J. *et al.*, 2014. Minimal experimental requirements for definition of extracellular vesicles and their functions: a position statement from the International Society for Extracellular Vesicles. *J Extracell Vesicles*, Volume 3, p. 10.3402/jev.v3.26913..
- Lund, M. E., To, J., O'Brien, B. A. & Donnelly, S., 2016. The choice of phorbol 12-myristate 13-acetate differentiation protocol influences the response of THP-1 macrophages to a pro-inflammatory stimulus. *J Immunol Methods*, Volume 430, pp. 64-70.
- Lutz, H. U. & Bogdanova, A., 2013. Mechanisms tagging senescent red blood cells for clearance in healthy humans. *Front Physiol*, 4(387).
- Lytle, J. R., Yario, T. A. & Steitz, J. A., 2007. Target mRNAs are repressed as efficiently by microRNA-binding sites in the 5' UTR as in the 3' UTR. *Proc Natl Acad Sci USA*, Volume 104, pp. 9667-9672.

- Maas, S. L., De Vrij, J. & Broekman, M. L., 2014. Quantification and Size profiling of Extracellular Vesicles Using Tunable Resistive Pulse Sensing. *J. Vis. Exp*, 92(e51623).
- Macrae, I. J. *et al.*, 2006. Structure of Dicer and Mechanistic Implications for RNAi. *Cold Spring Harbor Symposia on Quantitative Biology*, LXXI(978).
- Mageswaran, S. K. *et al.*, 2014. Binding to Any ESCRT Can Mediate Ubiquitin-Independent Cargo Sorting. *Traffic*, 15(2), p. 212–229.
- Mahmood , T. & Yang, P.-C., 2012. Western Blot: Technique, Theory, and Trouble Shooting. *N Am J Med Sci.*, 4(9), p. 429–434.
- Manjunath, N., Haoquan, W., Sandesh, S. & Premlata, S., 2009. Lentiviral delivery of short hairpin RNAs. *Adv Drug Deliv Rev*, 61(9), p. 732–745.
- Mantel, P. Y. *et al.*, 2013. Malaria-infected erythrocyte-derived microvesicles mediate cellular communication within the parasite population and with the host immune system. *Cell Host Microbe*, 13(5), pp. 521-34.
- Marchesi, V. T. & Steers, J. E., 1968. Selective solubilization of a protein component of the red cell membrane.. *Science.*, Volume 159, pp. 203-204.
- Martinez, M. C., Tual-Chalot, S., Leonetti, D. & Andriantsitohaina, R., 2011. Microparticles: targets and tools in cardiovascular disease. *Trends in Pharmacological Sciences*, 32(11), pp. 659-665.
- Mathivanan, S., Ji, H. & Simpson, R. J., 2010. Exosomes: extracellular organelles important in intercellular communication.. *J Proteomics.*, 73(10), pp. 1907-20.
- McCracken, M. A., Miraglia, L. J., McKay, R. A. & Strobl, J. S., 2003. Protein kinase C delta is a prosurvival factor in human breast tumor cell lines. *Mol Cancer Ther*, 2(3), pp. 273-81.
- McIntyre, C. L., Knowles, N. J. & Simmonds, P., 2013. Proposals for the classification of human rhinovirus species A, B and C into genotypically assigned types. *J Gen Virol*, 94(Pt 8), pp. 1791-806.
- Meckes Jr, . D. G., 2015. Exosomal communication goes viral. *J Virol*, Volume 89, p. 5200–5203.
- Meckes, D. G. & Raab-Traub, N., 2011. Microvesicles and Viral Infection. *Journal of Virology*, 85(24), p. 12844–12854.
- Mellisho, E. A. *et al.*, 2017. Identification and characteristics of extracellular vesicles from bovine blastocysts produced in vitro. *PLoS ONE* , 12(5), p. e0178306.
- MerckmilliporeGroup, 2015. *Guava® easyCyte Flow Cytometers*. [Online] Available at: http://www.merckmillipore.com/GB/en/life-science-research/cell-analysis/guava-easycyte-flow-cytometers/zLWb.qB.7eAAAAE_1rFkifKv,nav?cid=BI-XX-BDS-P-GOOG-FLOW-B322-

1017&gclid=EAIAIQobChMI26vz1ZHV1gIVBeEbCh2HeQx_EAAYASAAEgKwqfD_BwE [Accessed 08 12 2017].

Mestdagh, P. *et al.*, 2009. A novel and universal method for microRNA RT-qPCR data normalization. *Genome Biology*, Volume 10:R64.

Meuer, S. C. *et al.*, 1984. An alternative pathway of T-cell activation: a functional role for the 50 kd T11 sheep erythrocyte receptor protein. *Cell*, 36(4), pp. 897-906.

Michalovich, D., Overington, J. & Fagan, R., 2002. Protein sequence analysis in silico: application of structure-based bioinformatics to genomic initiatives.. *Current Opinion in Pharmacology.*, 2(1), p. 574–580.

Miller, E. K. *et al.*, 2007. Rhinovirus associated hospitalizations in young children. *J Infect Dis*, 195(6), pp. 773-81.

Minasyan, H., 2014. Erythrocyte and blood antibacterial defense. *Eur J Microbiol Immunol (Bp)*, 4(2), p. 138–143.

Mirkowska, P. *et al.*, 2013. Leukemia surfaceome analysis reveals new disease-associated features. *Blood*, 121(25), pp. e149-59.

Misumi , Y. & Ikehara, Y., 2013. Dipeptidyl-peptidase IV. *Handbook of Proteolytic Enzymes*, Volume 3, pp. 3374-3379.

Mitra, S., Cheng, K. W. & Mills, G. B., 2011. Rab GTPases implicated in inherited and acquired disorders. *Semin Cell Dev Biol*, 22(1), pp. 57-68.

Mizuguchi, C. *et al.*, 2018. Effect of Phosphatidylserine and Cholesterol on Membrane-mediated Fibril Formation by the N-terminal Amyloidogenic Fragment of Apolipoprotein A-I. *Scientific Reports*, 8(5497).

Modules, S. T., 2008. *Blood cell lineage*. [Online] Available at: <https://training.seer.cancer.gov/leukemia/anatomy/lineage.html> [Accessed 28 November 2017].

Mohamed, M. M. & Sloane, B. F., 2006. Cysteine cathepsins: multifunctional enzymes in cancer. *Nature Reviews Cancer*, 6(10), pp. 764-775.

Mora, M., Álvarez-Cubela , S. & Oltra, E., 2016. Biobanking of Exosomes in the Era of Precision Medicine: Are We There Yet?. *Int J Mol Sci*, 17(1), p. 13.

Morelli, A. E. *et al.*, 2004. Endocytosis, intracellular sorting, and processing of exosomes by dendritic cells. *Blood*, 104(10), pp. 3257-3266.

Mulcahy, L. A., Pink, R. C. & Carter, D. R., 2014. Routes and mechanisms of extracellular vesicle uptake. *J Extracell Vesicles*, Volume 3, p. e24641.

Müller, G., 2012. Microvesicles/exosomes as potential novel biomarkers of metabolic diseases.. *Diabetes Metab Syndr Obes.* , Volume 5, p. 247–282.

- Müller, H., Schmidt, U. & Lutz, H. U., 1981. On the mechanism of vesicle release from ATP-depleted human red blood cells. *Biochim. Biophys. Acta*, Volume 649, p. 462–470.
- Muntasell, A., Berger, A. C. & Roche, P. A., 2007. T cell-induced secretion of MHC class II-peptide complexes on B cell exosomes. *EMBO J*, 26(19), p. 4263–4272.
- Muralidharan-Chari, V. *et al.*, 2009. ARF6-regulated shedding of tumor cell-derived plasma membrane microvesicles. *Curr Biol*, 19(22), p. 1875–85.
- Murphy, G., 2008. The ADAMs: signalling scissors in the tumour microenvironment. *Nature Reviews Cancer*, Volume 8, pp. 932-941.
- Murtha, P., Tindall, D. J. & Young, C. Y., 1993. Androgen induction of a human prostate-specific kallikrein, hKLLK2: characterization of an androgen response element in the 5' promoter region of the gene. *Biochemistry*, 32(25), pp. 6459-64.
- Nagase, H., 2001. Metalloproteases. *Curr Protoc Protein Sci*, 24(1), pp. 21.4.1-21.4.13.
- Nagase, H., Visse, R. & Murphy, G., 2006. Structure and function of matrix metalloproteinases and TIMPs. *Cardiovascular Research*, 69(3), pp. 562-73.
- Nagy, S. *et al.*, 1998. ATP and integrity of human red blood cells. *Physiol Chem Phys Med NMR*, 30(2), pp. 141-8.
- Nakamura, K., Iwamoto, R. & Mekada, E., 1995. Membrane-anchored heparin-binding EGF-like growth factor (HB-EGF) and diphtheria toxin receptor-associated protein (DRAP27)/CD9 form a complex with integrin alpha 3 beta 1 at cell-cell contact sites. *JCB Home*, 129(6), p. 1691.
- Narayanan, A. *et al.*, 2013. Exosomes derived from HIV-1-infected cells contain trans-activation response element RNA. *J Biol Chem*, 288(27), pp. 20014-33.
- Nelson, P. S., Gan, L. & Ferguson, C., 1999. Molecular cloning and characterization of prostase, an androgen-regulated serine protease with prostate-restricted expression. *Proc Natl Acad Sci USA*, 96(6), pp. 3114-9.
- Nemova, N. N. & Lysenko, L. A., 2013. Biological Significance of Protease diversity. *Paleontological Journal*, 47(9), p. 1085–1088.
- Neumann, F. J., Schmid-Schönbein, H. & Ohlenbusch, H., 1987. Temperature-dependence of red cell aggregation. *Pflugers Arch*, 408(5), pp. 524-30.
- Newton, A. C., 1995. Protein Kinase C: Structure, Function, and Regulation. *The Journal of Biological Chemistry*, Volume 270, pp. 28495-28498.
- Nguyen, D. B. *et al.*, 2016. Characterization of Microvesicles Released from Human Red Blood Cells. *Cell Physiol Biochem*, 38(3), pp. 1085-99.
- Nicholson, A. W., 2014. Ribonuclease III mechanisms of double-stranded RNA cleavage. *Wiley Interdiscip Rev RNA*, 5(1), pp. 31-48.

- Nilsen, T. W., 2007. Mechanisms of microRNA-mediated gene regulation in animal cells. *Trends in Genetics*, 23(5), pp. 243-249.
- Nolte-'t Hoen, E. N. *et al.*, 2012. Deep sequencing of RNA from immune cell-derived vesicles uncovers the selective incorporation of small non-coding RNA biotypes with potential regulatory functions. *Nucleic Acids Res*, 40(18), pp. 9272-85.
- Noris, M. & Remuzzi, G., 2013. Overview of Complement Activation and Regulation. *Semin Nephrol*, 33(6), pp. 479-492.
- O'Connell, R. M., Zhao, J. L. & Rao, D. S., 2011. MicroRNA function in myeloid biology. *Blood*, 118(11), pp. 2960-2969.
- Oldenburg, P.-A., 2013. CD47: A Cell Surface Glycoprotein Which Regulates Multiple Functions of Hematopoietic Cells in Health and Disease.. *ISRN Hematol.* , Volume 2013, p. e614619.
- Olearczyk, J. J. *et al.*, 2004. Nitric oxide inhibits ATP release from erythrocytes. *J Pharmacol Exp Ther*, 309(3), pp. 1079-84.
- Oliveira, M. A. *et al.*, 1993. The structure of human rhinovirus 16. *Structure*, 1(1), p. 51–68.
- Ørom, U. A., Kauppinen, S. & Lund, A. H., 2006. LNA-modified oligonucleotides mediate specific inhibition of microRNA function. *Gene*, Volume 372, pp. 137-41.
- Orozco, A. F. *et al.*, 2009. Placental release of distinct DNA-associated micro-particles into maternal circulation: reflective of gestation time and preeclampsia. *Placenta*, 30(10), pp. 891-7.
- Osteikoetxea, X. *et al.*, 2015. Improved Characterization of EV Preparations Based on Protein to Lipid Ratio and Lipid Properties. *PLoS ONE*, 10(3), p. e0121184.
- Ouagari, K. E., Teissie, J. & Benoist, H., 1995. Glycophorin A Protects K562 cells from natural killer cell attack. *The journal of biological chemistry*, 270(45), p. 26970–26975.
- Palmenberg, A. C. *et al.*, 2009. Sequencing and analyses of all known human rhinovirus genomes reveal structure and evolution. *Science*, 324(5923), pp. 55-9.
- Panagiotou, N., Davies, R. W., Selman, C. & Shiels, P. G., 2016. Microvesicles as vehicles for tissue regeneration: Changing of the guards.. *Curr Pathobiol Rep.* , 4(4), p. 181–187.
- Pantaleo, G. *et al.*, 1987. Transmembrane signaling via the T11-dependent pathway of human T cell activation: Evidence for the involvement of 1,2-diacylglycerol and inositol phosphates. *Eur. J. Immunol.* , 17(55).
- Park, D. *et al.*, 2007. BAI1 is an engulfment receptor for apoptotic cells upstream of the ELMO/Dock180/Rac module. *Nature*, Volume 450, p. 430–434.

- Park, S. M. *et al.*, 2007. Let-7 prevents early cancer progression by suppressing expression of the embryonic gene HMGA2. *Cell Cycle*, Volume 6, pp. 2585-2590.
- Park, Y. M., 2014. CD36, a scavenger receptor implicated in atherosclerosis. *Experimental & Molecular Medicine*, Volume 46, p. e99 .
- Parolini, I. *et al.*, 2009. Microenvironmental pH is a key factor for exosome traffic in tumor cells. *J Biol Chem*, 284(49), pp. 34211-22.
- Passow, H., 1986. Molecular aspects of band 3 protein-mediated anion transport across the red blood cell membrane. *Rev. Physiol. Biochem. Pharmacol*, Volume 103, pp. 61-223.
- Patel, S., Mehta-Damani, A., Shu, H. & Le Pecq, J., 2005. An analysis of variability in the manufacturing of dexosomes: implications for development of an autologous therapy. *Biotechnol Bioeng*, 92(2), pp. 238-49.
- Pathan, M. *et al.*, 2015. FunRich: a standalone tool for functional enrichment analysis. *Proteomics*, 15(15), pp. 2597-2601.
- Pawson, T., Rainaa, M. & Nash, P., 2002. Interaction domains: from simple binding events to complex cellular behavior. *FEBS Letters*, 513(1), pp. 2-10.
- Pegtel, D. M. *et al.*, 2010. Functional delivery of viral miRNAs via exosomes. *Proc Natl Acad Sci U S A*, 107(14), pp. 6328-33.
- Peltola, V. *et al.*, 2008. Rhinovirus transmission within families with children: Incidence of symptomatic and asymptomatic infections. *J Infect Dis*, 197(3), pp. 382-389.
- Pepino, M. Y., Kuda, O., Samovski, D. & Abumrad, N. A., 2014. Structure-Function of CD36 and Importance of Fatty Acid Signal Transduction in Fat Metabolism. *Annu Rev Nutr*, Volume 34, pp. 281-303.
- Persson, B. D. *et al.*, 2010. Structure of the extracellular portion of CD46 provides insights into its interactions with complement proteins and pathogens. *PLoS Pathog*, 6(9), p. e1001122.
- Perteghella, S. *et al.*, 2017. Stem cell-extracellular vesicles as drug delivery systems: New frontiers for silk/curcumin nanoparticles.. *International Journal of Pharmaceutics.*, 520(1–2), p. 86–97.
- Pfeifer, P., Werner, N. & Jansen, F., 2015. Role and Function of MicroRNAs in Extracellular Vesicles in Cardiovascular Biology. *Hindawi Publishing Corporation, BioMed Research International*, 2015(ID 161393), pp. 1-11.
- Phizicky, E. M. & Fields, S., 1995. Protein-protein interactions: methods for detection and analysis. *Microbiological Reviews*, 59(1), p. 94–123.
- Piccin, A., Murphy, W. G. & Smith, O. P., 2007. Circulating microparticles: pathophysiology and clinical implications. *Blood Rev*, 21(3), pp. 157-71.

- Pinatel, E. M. *et al.*, 2014. miR-223 Is a Coordinator of Breast Cancer Progression as Revealed by Bioinformatics Predictions. *PLoS ONE* , 9(1), p. e84859.
- Pinzone, J. J., Stevenson, H., Strobl, J. S. & Berg, P. E., 2004. Molecular and Cellular Determinants of Estrogen Receptor α Expression. *Mol Cell Biol*, 24(11), p. 4605–4612.
- Piper, R. C., Dikic, I. & Lukacs, G. L., 2014. Ubiquitin-Dependent Sorting in Endocytosis. *Cold Spring Harb Perspect Biol.* , 6(1), p. a016808.
- Piper, R. C. & Katzmann, D. J., 2007. Biogenesis and Function of Multivesicular Bodies. *Annu Rev Cell Dev Biol*, Volume 23, p. 519–547.
- Plant, L. J. & Jonsson, A.-B., 2006. Type IV Pili of *Neisseria gonorrhoeae* Influence the Activation of Human CD4+ T Cells. *Infect Immun*, 74(1), p. 442–448.
- Pockley, A. G. *et al.*, 2015. Immune Cell Phenotyping Using Flow Cytometry. *Curr Protoc Toxicol*, 66(18.8), pp. 1-34.
- Pols, M. S. & Klumperman, J., 2009. Trafficking and function of the tetraspanin CD63. *Exp Cell Res*, 315(9), p. 1584–92.
- Poole, J., 2000. Red cell antigens on band 3 and glycophorin A. *Blood Reviews* , Volume 14, pp. 31-43.
- Pospichalova, V. *et al.*, 2015. Simplified protocol for flow cytometry analysis of fluorescently labeled exosomes and microvesicles using dedicated flow cytometer. *J Extracell Vesicles*, 4(25530), p. eCollection 2015.
- Powers, A., Mohammed, M., Uhl, L. & Haspel, R. L., 2007. Apparent nonhemolytic alloantibody-induced red-cell antigen loss from transfused erythrocytes. *Blood*, 109(10), p. 4590.
- Prado, N. *et al.*, 2008. Exosomes from bronchoalveolar fluid of tolerized mice prevent allergic reaction. *J. Immunol*, 181(2), pp. 1519-1525.
- Pritchard, C. C., Cheng, H. H. & Tewari, M., 2012. MicroRNA profiling: approaches and considerations. *Nat Rev Genet*, 13(5), pp. 358-369.
- Pritchard, C. *et al.*, 2012. Blood Cell Origin of Circulating MicroRNAs: A Cautionary Note for Cancer Biomarker Studies. *Cancer Prev Res*, Issue 492.
- Pugin, J. *et al.*, 1998. Cell activation mediated by glycosylphosphatidylinositol-anchored or transmembrane forms of CD14. *Infect Immun*, 66(3), pp. 1174-80.
- Qi, R. *et al.*, 2012. Identification of endogenous normalizers for serum MicroRNAs by microarray profiling: U6 small nuclear RNA is not a reliable normalizer. *Hepatology*, Issue 55, p. 1640–1642.
- Quesenberry , P. J. & Aliotta, J. M., 2010. Cellular phenotype switching and microvesicles. *Adv Drug Deliv Rev.* , 62(12), p. 1141–1148.

- Rand, M. L. *et al.*, 2006. Rapid clearance of procoagulant platelet-derived microparticles from the circulation of rabbits. *J Thromb Haemost*, 4(7), p. 1621–3.
- Rank, A. *et al.*, 2011. Clearance of platelet microparticles in vivo. *Platelets*, 22(2), p. 111–16.
- Rao, M. B., Tanksale, A. M., Ghatge, M. S. & Deshpande, V. V., 1998. Microbiol Mol Biol Rev. *Molecular and biotechnological aspects of microbial proteases*, 62(3), p. 597–635.
- Ratajczak, J. *et al.*, 2006. Embryonic stem cell-derived microvesicles reprogram hematopoietic progenitors: evidence for horizontal transfer of mRNA and protein delivery. *Leukemia*, 20(5), p. 847–56.
- Ratajczak, M., 2006. Microvesicles: from “dust to crown”. *Blood*, Volume 108, pp. 2885–2888.
- Ratajczak, M. & Ratajczak, J., 2016. Horizontal transfer of RNA and proteins between cells by extracellular microvesicles: 14 years later. *Clin Transl Med*, 5(7).
- Rathjen, T., Nicol, C., McConkey, G. & Dalmay, T., 2006. Analysis of short RNAs in the malaria parasite and its red blood cell host. *FEBS Lett*, 580(22), pp. 5185–8.
- Record, M., Carayon, K., Poirot, M. & Silvente-Poirot, S., 2014. Exosomes as new vesicular lipid transporters involved in cell–cell communication and various pathophysiological processes. *Biochimica et Biophysica Acta (BBA) - Molecular and Cell Biology of Lipids*, 1841(1), pp. 108–120.
- Redig , A. J. & Plataniias, L. C., 2008. Protein kinase C signalling in leukemia.. *Leuk Lymphoma*. , 49(7), pp. 1255–62.
- Redis, R. S. *et al.*, 2012. Cell-to-cell miRNA transfer: from body homeostasis to therapy. *Pharmacol Ther*, 136(2).
- Reed , L. J. & Muench, H., 1938. A simple method of estimating fifty percent endpoints. *American Journal of Epidemiology*, 27(1), pp. 493–497.
- Reid, G., Kirschner, M. & van Zandwijk, N., 2011. Circulating microRNAs: association with disease and potential use as biomarkers. *Crit Rev Oncol Hemat*, 80(2), pp. 193–208.
- Reyes, R., Cardeñes, B., Machado-Pineda , Y. & Cabañas , C., 2018. Tetraspanin CD9: A Key Regulator of Cell Adhesion in the Immune System. *Front Immunol*, 9(863), p. eCollection 2018.
- Reyes, R. *et al.*, 2015. Different states of integrin LFA-1 aggregation are controlled through its association with tetraspanin CD9. *Biochimica et Biophysica Acta (BBA) - Molecular Cell Research*, 1853(10, Part A), pp. 2464–2480.

- Riegman, P. H. *et al.*, 1991. Identification and androgen-regulated expression of two major human glandular kallikrein-1 (hGK-1) mRNA species. *Mol Cell Endocrinol*, 76(1-3), pp. 181-90.
- Robbins, P. D. & Morelli, A. E., 2014. Regulation of immune responses by extracellular vesicles. *Nat Rev Immunol*, 14(3), pp. 195-208.
- Robillard, L., Ethier, N., Lachance, M. & Hébert, T. E., 2000. Gbetagamma subunit combinations differentially modulate receptor and effector coupling in vivo. *Cell Signal*, 12((9-10)), pp. 673-82.
- Rodriguez, K., Gaczynska, M. & Osmulski, P. A., 2010. Molecular mechanisms of proteasome plasticity in aging. *Mech Ageing Dev*, 131(2), p. 144–155.
- Roebuck, K. A. & Finnegan, A., 1999. Regulation of intercellular adhesion molecule-1 (CD54) gene expression. *J Leukoc Biol*, 66(6), pp. 876-88.
- Roush, S. & Slack, F. J., 2008. The let-7 family of microRNAs. *Trends in Cell Biology*, 18(10), p. 505–516.
- Rubin, O. *et al.*, 2012. Red Blood Cell Microparticles: Clinical Relevance. *Transfus Med Hemother.*, 39(5), p. 342–347.
- Rubin, O. *et al.*, 2013. Red blood cell-derived microparticles isolated from blood units initiate and propagate thrombin generation. *Transfusion*, 53(8), pp. 1744-54.
- Ruby, J. G., Jan, C. H. & Bartel, D. P., 2007. Intronic microRNA precursors that bypass Drosha processing. *Nature*, Volume 488, pp. 83-86.
- Ru, J. *et al.*, 2014. MiR-23a facilitates the replication of HSV-1 through the suppression of interferon regulatory factor 1. *PLoS One*, 9(12).
- Sadallah, S., Eken, C. & Schifferli, J. A., 2011. Ectosomes as modulators of inflammation and immunity. *Clin Exp Immuno*, 163(1), p. 26–32.
- Sahu, S., Hemlata & Verma, A., 2014. Adverse events related to blood transfusion. *Indian J Anaesth*, 58(5), pp. 543-551.
- Sándor, N. *et al.*, 2016. CD11c/CD18 Dominates Adhesion of Human Monocytes, Macrophages and Dendritic Cells over CD11b/CD18. *PLoS One*, 22(11), p. e0163120.
- Sangkokya, C., LaMonte, G. & Jen-Tsan, C., 2010. Erythrocytes, Isolation and Characterization of MicroRNAs of Human Mature. *Methods Mol Biol*, Volume 667, pp. 193-203.
- Sato, K., Norris, A., Sato, M. & Grant, B. D., 2005. *The C. elegans Research Community- C. elegans as a model for membrane traffic.* [Online] Available at: <http://www.wormbook.org>. [Accessed 19 11 2017].
- Saunderson, S. C., Dunn, A. C., Crocker, P. R. & McLellan, A. D., 2014. CD169 mediates the capture of exosomes in spleen and lymph node. *Blood*, 123(2), p. 208–16.

- Schmidt, O. & Teis, D., 2012. The ESCRT machinery. *Curr Biol*, 22(4), p. R116–R120.
- Schwab, A. *et al.*, 2015. Extracellular vesicles from infected cells: potential for direct pathogenesis. *Front. Microbiol*, 20(6), p. e1132.
- Schwarz, H. P. & Dorner, F., 2003. Karl Landsteiner and major contributions to haematology. *British Journal of Haematology*, 121(4), p. 556–565.
- Seals, D. F. & Courtneidge, S. A., 2003. The ADAMs family of metalloproteases: multidomain proteins with multiple functions. *Genes Dev*, 17(1), pp. 7-30.
- Sehgal, P. B. & Lee, J. E., 2011. Protein trafficking dysfunctions: Role in the pathogenesis of pulmonary arterial hypertension. *Pulm Circ*, 1(1), p. 17–32.
- Shah, J. M. Y., Omar, E., Pai, D. R. & Sood, S., 2012. Cellular events and biomarkers of wound healing. *Indian J Plast Surg*, 45(2), pp. 220-228.
- Shimoda, M. & Khokha, R., 2013. Proteolytic factors in exosomes. *Proteomics*, Volume 13, p. 1624–1636.
- Shukla, S. D. *et al.*, 2017. The main rhinovirus respiratory tract adhesion site (ICAM-1) is upregulated in smokers and patients with chronic airflow limitation (CAL).. *Respiratory Research.*, 18(6).
- Silverstein, R. L. & Febbraio, M., 2009. CD36, a Scavenger Receptor Involved in Immunity, Metabolism, Angiogenesis, and Behavior. *Sci. Signal*, 2(72), p. 3.
- Simons M, M. & Raposo, G., 2009. Exosomes-vesicular carriers for intercellular communication. *Curr Opin Cell Biol*, 21(4), pp. 575-81.
- Sims, P. J., Faioni, E. M., Wiedmer, T. & Shattil, S. J., 1988. Complement proteins C5b-9 cause release of membrane vesicles from the platelet surface that are enriched in the membrane receptor for coagulation factor Va and express prothrombinase activity. *J Biol Chem*, 263(34), pp. 18205-12.
- Sivina, M. *et al.*, 2014. The BTK Inhibitor Ibrutinib (PCI-32765) Blocks Hairy Cell Leukaemia Survival, Proliferation and BCR Signalling: A New Therapeutic Approach. *Br J Haematol*, 166(2), p. 177–188.
- Sloand, E. M. *et al.*, 2004. Transfer of glycosylphosphatidylinositol-anchored proteins to deficient cells after erythrocyte transfusion in paroxysmal nocturnal hemoglobinuria. *Blood*, 104(12), pp. 3782-8.
- Solberg, C., 1988. Storage of Human Red Blood Cells and Platelets. *Upsala Journal of Medical Sciences*, 93(3), pp. 201-214.
- Spalter, S. H. *et al.*, 1999. Normal Human Serum Contains Natural Antibodies Reactive With Autologous ABO Blood Group Antigens. *Blood*, Volume 93, pp. 4418-4424.

- Sparrow, R. L., Healey, G., Patton, K. A. & Veale, M. F., 2006. Red blood cell age determines the impact of storage and leukocyte burden on cell adhesion molecules, glycophorin A and the release of annexin V. *Transfus Apher Sci*, 34(1), pp. 15-23.
- Sprague, D. L. *et al.*, 2008. Platelet-mediated modulation of adaptive immunity: unique delivery of CD154 signal by platelet-derived membrane vesicles. *Blood*, 111(10), pp. 5028-36.
- Stafford, J. H. & Thorpe, P. E., 2011. Increased Exposure of Phosphatidylethanolamine on the Surface of Tumor Vascular Endothelium. *Neoplasia*, 13(4), p. 299–308.
- Stegmayr, B. & Ronquist, G., 1982. Promotive effect on human sperm progressive motility by prostasomes. *Urol Res*, Volume 10, pp. 253-7.
- Stoka, V., Turk, V. & Turk, B., 2016. Lysosomal cathepsins and their regulation in aging and neurodegeneration. *Ageing Res. Rev*, pii: S1568-1637(16), pp. 30067-8.
- Stokes, C. A. *et al.*, 2011. Role of interleukin-1 and MyD88-dependent signaling in rhinovirus infection. *J Virol*, 85(15), pp. 7912-21.
- Subra, C. *et al.*, 2010. Exosomes account for vesicle-mediated transcellular transport of activatable phospholipases and prostaglandins. *J Lipid Res*, 51(8), p. 2105–20.
- Subra, C., Laulagnier, K., Perret, B. & Record, M., 2007. Exosome lipidomics unravels lipid sorting at the level of multivesicular bodies. *Biochimie*, Volume 89, p. 205–212.
- Su, J.-L., Chen, P.-S., Johansson, G. & Kuo, M. L., 2012. Function and Regulation of Let-7 Family microRNAs. *MicroRNA*, 1(1), pp. 34-39.
- Sumitomo, M., Shen, R. & Nanus, D. M., 2005. Involvement of neutral endopeptidase in neoplastic progression. *Biochim Biophys Acta*, 1751(1), p. 52–59.
- Sumiyoshi, N. *et al.*, 2016. The role of tetraspanin CD9 in osteoarthritis using three different mouse models. *Biomedical Research*, 37(5), pp. 283-291.
- Sun, D. *et al.*, 2010. A novel nanoparticle drug delivery system: The anti-inflammatory activity of curcumin is enhanced when encapsulated in exosomes. *Mol. Ther*, 18(9), p. 1606–1614.
- Svensson, K. *et al.*, 2013. Exosome uptake depends on ERK1/2-heat shock protein 27 signalling and lipid raft-mediated endocytosis negatively regulated by caveolin-1. *J Biol Chem*, 288(24), pp. 17713-24.
- Swanson, J. A., 2008. Shaping cups into phagosomes and macropinosomes. *Nat Rev Mol Cell Biol*, 9(8), pp. 639-49.
- Swartz, M. A. & Lund, A. W., 2012. Lymphatic and interstitial flow in the tumour microenvironment: linking mechanobiology with immunity. *Nat Rev Cancer*, 12(3), pp. 210-9.

- Szklarczyk, D. *et al.*, 2015. STRING v10: protein-protein interaction networks, integrated over the tree of life. *Nucleic Acids Research*, Volume 43, pp. D447-52.
- Takahashi, Y. *et al.*, 2013. Visualization and in vivo tracking of the exosomes of murine melanoma B16-BL6 cells in mice after intravenous injection. *J Biotechnol*, 165(2), p. 77–84.
- Tam, J. C. H., Bidgood, S. R., McEwan, W. A. & James, L. C., 2014. Intracellular sensing of complement C3 activates cell autonomous immunity. *Science*, 345(6201), p. 1256070.
- Tanner, M. J., 1993. The major integral proteins of the human red cell. *Baillière's Clinical Haematology*, 6(2), pp. 333-356.
- Tantawy, A. A. *et al.*, 2013. Circulating platelet and erythrocyte microparticles in young children and adolescents with sickle cell disease: Relation to cardiovascular complications. *Platelets*, 24(8), pp. 605-14.
- Taraboletti, G. *et al.*, 2006. Bioavailability of VEGF in tumor-shed vesicles depends on vesicle burst induced by acidic pH. *Neoplasia*, 8(2), pp. 96-103.
- Temme, S., Eis-Hubinger, A. M., McLellan, A. D. & Koch, M., 2010. The herpes simplex virus-1 encoded glycoprotein B diverts HLA-DR into the exosome pathway. *The Journal of Immunology*, 184(1), p. 236–243.
- Thebaud, B. & Stewart, D. J., 2012. Exosomes: cell garbage can, therapeutic carrier, or trojan horse?. *Circulation*, 126(22), pp. 2553-2555.
- Théry, C., 2011. Exosomes: secreted vesicles and intercellular communications. *F1000 Biol Rep*, Volume 3, p. 15.
- Théry, C. *et al.*, 2001. Proteomic analysis of dendritic cell-derived exosomes: A secreted subcellular compartment distinct from apoptotic vesicles. *J. Immunol*, 166(12), pp. 7309-18.
- Théry, C., Ostrowski, M. & Segura, E., 2009. Membrane vesicles as conveyors of immune responses. *Nat Rev Immunol*, 9(8), p. 581–593.
- Théry, C., Zitvogel, L. & Amigorena, S., 2002. Exosomes: composition, biogenesis and function. *Nature Reviews Immunology*, 2(8), p. 569–579.
- Thomas, G. M. *et al.*, 2009. Cancer cell-derived microparticles bearing P-selectin glycoprotein ligand 1 accelerate thrombus formation in vivo. *J Exp Med*, 206(9), p. 1913–1927.
- Thum, T., Catalucci, D. & Bauersachs, J., 2008. MicroRNAs: novel regulators in cardiac development and disease. *Cardiovasc Res*, 79(4), pp. 562-70.
- Tian, T. *et al.*, 2013. Dynamics of exosome internalization and trafficking. *J Cell Physiol*, 228(7), pp. 1487-95.

- Tibaldi, E. V., Salgia, R. & Reinherz, E. L., 2002. CD2 molecules redistribute to the uropod during T cell scanning: Implications for cellular activation and immune surveillance. *Proc Natl Acad Sci U S A*, 99(11), pp. 7582-7587.
- Timperio, A. M., Mirasole, C., D'Alessandro, A. & Zolla, L., 2013. Red Blood Cell Lipidomics analysis through HPLC-ESI-qTOF: application to red blood cell storage. *Journal of Integrated OMICS*, 3(1), pp. 11-24.
- Tissot, J. D. *et al.*, 2013. Blood microvesicles: From proteomics to physiology. *Translational proteomics*, Volume 1, pp. 38-52.
- Tissot, J.-D., Rubin, O. & Canellini, G., 2010. Analysis and clinical relevance of microparticles from red blood cells. *Curr Opin Hematol*, 17(6), pp. 571-7.
- Tkach, M., Kowal, J. & Théry, C., 2017. Why the need and how to approach the functional diversity of extracellular vesicles. *Phil. Trans. R. Soc. B*, Volume 373, p. 20160479.
- Tkach, M. & Théry, C., 2016. Communication by extracellular vesicles: where we are and where we need to go. *Cell*, Volume 164, pp. 1226-1232.
- Tomasetti, M., Lee, W., Santarelli, L. & Neuzil, J., 2017. Exosome-derived microRNAs in cancer metabolism: possible implications in cancer diagnostics and therapy. *Exp Mol Med*, 49(1), p. e285.
- Towner, L. D., Wheat, R. A., Hughes, T. R. & Morgan, B. P., 2016. Complement Membrane Attack and Tumorigenesis: A SYSTEMS BIOLOGY APPROACH. *J Biol Chem.*, 291(29), pp. 14927-38.
- Trajkovic, K. *et al.*, 2008. Ceramide triggers budding of exosome vesicles into multivesicular endosomes. *Science*, 319(5867), pp. 1244-7.
- Tregoning, J. S. & Schwarze, J., 2010. Respiratory viral infections in infants: Causes, clinical symptoms, virology, and immunology. *Clin Microbiol Rev*, 23(1), p. 74-98.
- Trim, J. E. *et al.*, 2000. Upstream Tissue Inhibitor of Metalloproteinases-1 (TIMP-1) Element-1, a Novel and Essential Regulatory DNA Motif in the Human TIMP-1 Gene Promoter, Directly Interacts with a 30-kDa Nuclear Protein. *The Journal of Biological Chemistry*, 275(9), pp. 6657-6663.
- Turk, V., Turk, B. & Turk, D., 2001. New member's review. Lysosomal cysteine proteases: facts and opportunities. *EMBO J*, 20(17), p. 4629-4633.
- Tuthill, T. J., Groppe, E., Hogle, J. M. & Rowlands, D. J., 2010. Picornaviruses. *Curr Top Microbiol Immunol*, Volume 343, p. 43-89.
- Tzur, A. *et al.*, 2011. Optimizing Optical Flow Cytometry for Cell Volume-Based Sorting and Analysis. *PLoS One*, 6(1), p. e16053.

- Uings, I. J. & Farrow, S. N., 2000. Cell receptors and cell signalling. *Mol Pathol*, 53(6), pp. 295-299.
- Urbanelli, L. *et al.*, 2013. Signaling Pathways in Exosomes Biogenesis, Secretion and Fate. *Genes*, Volume 2, pp. 152-170.
- Valadi, H. *et al.*, 2007. Exosome-mediated transfer of mRNAs and microRNAs is a novel mechanism of genetic exchange between cells. *Nat Cell Biol.*, 9(6), p. 654–9.
- Valapala, M. & Vishwanatha, J. K., 2011. Lipid raft endocytosis and exosomal transport facilitate extracellular trafficking of annexin A2. *J Biol Chem*, 286(35), p. 30911–25.
- van Aelst, L. & D'Souza-Schorey, C., 1997. Rho GTPases and signaling networks. *Genes and Dev*, Volume 11, pp. 2295-2322.
- van der Pol, E., Böing, A. N., Gool, E. L. & Nieuwland, R., 2016. Recent developments in the nomenclature, presence, isolation, detection and clinical impact of extracellular vesicles. *J Thromb Haemost*, 14(1), pp. 48-56.
- van der Pol, E. *et al.*, 2012. Classification, Functions, and Clinical Relevance of Extracellular Vesicles. *Pharmacological Reviews*, 64(3), pp. 676-705.
- van der Pol, E. *et al.*, 2014. Particle size distribution of exosomes and microvesicles determined by transmission electron microscopy, flow cytometry, nanoparticle tracking analysis, and resistive pulse sensing. *Journal of thrombosis and haemostasis*, 12(7), p. 1182–1192.
- van Dongen, H. M., Masoumia, N., Witwerb, K. W. & Pegtela, D. M., 2016. Extracellular Vesicles Exploit Viral Entry Routes for Cargo Delivery. *Microbiol. Mol. Biol. Rev*, 80(2), pp. 369-386.
- van Manen, H. J. *et al.*, 2008. Refractive index sensing of green fluorescent proteins in living cells using fluorescence lifetime imaging microscopy. *Biophys J*, 94(8), pp. L67-9.
- van Meer, G., Voelker, D. R. & Feigenson, G. W., 2008. Membrane lipids: where they are and how they behave. *Nat. Rev. Mol. Cell Biol.*, Volume 9, p. 112–124.
- van Niel, G. *et al.*, 2003. Intestinal epithelial exosomes carry MHC class II/peptides able to inform the immune system in mice. *Gut*, Volume 52, pp. 1690-1697.
- van Rooij, E., 2011. The Art of MicroRNA Research. *Circ Res*, 108(2), pp. 219-34.
- van Schravendijk, M. R., Handunnetti, S. M., Barnwell, J. W. & Howard, R. J., 1992. Normal human erythrocytes express CD36, an adhesion molecule of monocytes, platelets, and endothelial cells. *Blood*, 80(8), pp. 2105-14.
- Vance, J. E. & Tasseva, G., 2013. Formation and function of phosphatidylserine and phosphatidylethanolamine in mammalian cells. *Biochimica et Biophysica Acta (BBA) - Molecular and Cell Biology of Lipids*, 1831(3), pp. 543-554.

- VanWijk, M. J., VanBavel, E., Sturk, A. & Nieuwland, R., 2003. Microparticles in cardiovascular diseases. *Cardiovascular Research*, 59(2), p. 277–287.
- Vazquez, S. M. *et al.*, 2004. Three Novel Hormone-Responsive Cell Lines Derived From Primary Human Breast Carcinomas: Functional Characterization. *Journal of cellular physiology*, Volume 199, p. 460–469.
- Verma, R. P. & Hansch, C., 2007. Matrix metalloproteinases (MMPs): Chemical–biological functions and (Q) SARs. *Bioorganic & Medicinal Chemistry*, 15(6), p. 2223–2268.
- Vidal, M., Mangeat, P. & Hoekstra, D., 1997. Aggregation reroutes molecules from a recycling to a vesicle-mediated secretion pathway during reticulocyte maturation. *J. Cell. Sci*, Volume 110, pp. 1867-1877.
- Vogel, R. *et al.*, 2012. Variable pressure method for characterizing nanoparticle surface charge using pore sensors. *Anal Chem*, 84(7), pp. 3125-31.
- Wahid, F., Shehzad, A., Khan, T. & Kim, Y. Y., 2010. MicroRNAs: Synthesis, mechanism, function, and recent clinical trials. *Biochimica et Biophysica Acta (BBA) - Molecular Cell Research*, 1803(11), pp. 1231-1243.
- Walker, E. *et al.*, 2016. Rhinovirus 16 2A Protease Affects Nuclear Localization of 3CD during Infection. *J Virol*, 90(24), pp. 11032-11042.
- Wang, H. X. *et al.*, 2011. The C-terminal tail of tetraspanin protein CD9 contributes to its function and molecular organization. *Journal of Cell Science*, 124(Pt 16), pp. 2702-10.
- Wang, J. J. *et al.*, 1999. Formation and release of virus-like particles by HIV-1 matrix protein. *AIDS*, 13(2), p. 281–283.
- Wang, J.-H. & Reinherz, E. L., 2000. Structural basis of cell–cell interactions in the immune system. *Current Opinion in Structural Biology*, 10(6), pp. 656-661.
- Wang, Q. *et al.*, 2009. Role of double-stranded RNA pattern recognition receptors in rhinovirus-induced airway epithelial cell responses. *J Immunol*, 183(11), p. 6989–6997.
- Wang, Y., Chen, L.-M. & Liu, M.-L., 2014. Microvesicles and diabetic complications–novel mediators, potential biomarkers and therapeutic targets. *Acta Pharmacol Sin*, 35(4), p. 433–443.
- Wang, Y. *et al.*, 2015. Differentially expressed microRNAs in bone marrow mesenchymal stem cell-derived microvesicles in young and older rats and their effect on tumor growth factor- β 1-mediated epithelial-mesenchymal transition in HK2 cells. *Stem Cell Research & Therapy*, 6(185).
- Warren, A. J., 2017. Decoding erythropoiesis. *Blood*, 129(5), pp. 544-545.
- Wary, K. K. *et al.*, 1996. The Adaptor Protein Shc Couples a Class of Integrins to the Control of Cell Cycle Progression. *Cell*, 87(4), pp. 733-743.

- Watanabe, J. *et al.*, 2003. Endotoxins stimulate neutrophil adhesion followed by synthesis and release of platelet-activating factor in microparticles. *Journal of biological chemistry*, Volume 278, pp. 33161-33168.
- Webb, B. L. J., Hirst, S. J. & Giembycz, M. A., 2000. Protein kinase C isoenzymes: a review of their structure, regulation and role in regulating airways smooth muscle tone and mitogenesis. *Br J Pharmacol*, 130(7), p. 1433–1452.
- Wei, X. *et al.*, 2016. Surface Phosphatidylserine Is Responsible for the Internalization on Microvesicles Derived from Hypoxia-Induced Human Bone Marrow Mesenchymal Stem Cells into Human Endothelial Cells. *PLoS One*, 11(1), p. e0147360.
- Wiklander, O. P. B. *et al.*, 2015. Extracellular vesicle in vivo biodistribution is determined by cell source, route of administration and targeting. *J Extracell Vesicles*, 4(26316), p. eCollection 2015.
- Willekens, F. L. *et al.*, 2008. Erythrocyte vesiculation: a self-protective mechanism?. *Br. J. Haematol*, 141(4), pp. 549-56.
- Willekens, F. L. *et al.*, 2005. Liver Kupffer cells rapidly remove red blood cell-derived vesicles from the circulation by scavenger receptors. *Blood*, 105(5), p. 2141–5.
- Willmott, G. R. *et al.*, 2010. Use of tunable nanopore blockade rates to investigate colloidal dispersions. *Journal of physics*, 22(45), p. 454116.
- Witwer, K. W. *et al.*, 2013. Standardization of sample collection, isolation and analysis methods in extracellular vesicle research. *J. Extracell Vesicles*, 27(2), p. 20360.
- Wolf, P., 1967. The Nature and Significance of Platelet Products in Human Plasma. *British Journal of Haematology*, 13(3), p. 269–288.
- Wurdinger, T. *et al.*, 2012. Extracellular Vesicles and Their Convergence with Viral Pathways. *Advances in Virology*, Volume 2012.
- Xiong, J., Miller, V. M., Li, Y. & Jayachandran, M., 2012. Microvesicles at the crossroads between infection and cardiovascular diseases. *J Cardiovasc Pharmacol*, 59(2), p. 124–132.
- Xiong, W. *et al.*, 2013. Comparison of microRNA expression profiles in HCC-derived microvesicles and the parental cells and evaluation of their roles in HCC. *J Huazhong Univ Sci Technolog Med Sci*, 33(3), pp. 346-52.
- Xu, L., Yang, B.-F. & Ai, J., 2013. MicroRNA Transport: A New Way in Cell Communication. *J. Cell. Physiol*, Volume 228, p. 1713–1719.
- Yadav, R. K., Gupta, S. P., Sharma, P. K. & Patil, V. M., 2011. Recent advances in studies on hydroxamates as matrix metalloproteinase inhibitors: a review. *Curr Med Chem*, 18(11), pp. 1704-22.

- Yáñez-Mó, M. *et al.*, 2015. Biological properties of extracellular vesicles and their physiological functions. *J Extracell Vesicles*, 14(4), p. 27066.
- Yang, J., Liu, H., Wang, H. & Sun, Y., 2013. Down-regulation of microRNA-181b is a potential prognostic marker of non-small cell lung cancer. *Pathol Res Pract*, 209(8), pp. 490-4.
- Yang, J., Wei, F., Schafer, C. & Wong, D. T. W., 2014. Detection of Tumor Cell-Specific mRNA and Protein in Exosome-Like Microvesicles from Blood and Saliva. *PLoS One*, 9(11), p. e110641.
- Yim, N. & Choi, C., 2016. Extracellular vesicles as novel carriers for therapeutic molecules. *BMB Rep*, 49(11), pp. 585-586.
- Yoshida, K. *et al.*, 2015. CD47 is an adverse prognostic factor and a therapeutic target in gastric cancer. *Cancer Med*, 4(9), p. 1322–1333.
- Yousef, G. M. & Diamandis, E. P., 2001. The new human tissue kallikrein gene family: structure, function, and association to disease. *Endocr. Rev*, 22(2), p. 184–204.
- Yousef, G. M. *et al.*, 1999. Molecular characterization of Zyme/Protease M/Neurosin (PRSS9), a hormonally regulated kallikrein-like serine protease. *Genomics*, Volume 62, pp. 251-9.
- Yousef, G. M. *et al.*, 2000. The KLK7 (PRSS6) gene, encoding for the stratum corneum chymotryptic enzyme is a new member of the human kallikrein gene family - genomic characterization, mapping, tissue expression and hormonal regulation. *Gene*, 254(1-2), pp. 119-28.
- Yuana, Y. *et al.*, 2013. Cryo-electron microscopy of extracellular vesicles in fresh plasma. *J Extracell Vesicles*, Volume 2.
- Yuan, J.-Y. *et al.*, 2009. MicroRNA-223 reversibly regulates erythroid and megakaryocytic differentiation of K562 cells. *J. Cell. Mol. Med*, 13(11-12), pp. 4551-4559.
- Yu, B., Zhang, X. & Li, X., 2014. Exosomes Derived from Mesenchymal Stem Cells. *Int J Mol Sci*, 15(3), pp. 4142-4157.
- Yu, H., Bowden, D. W., Spray, B. J. & Roch, S. S., 1998. Identification of human plasma kallikrein gene polymorphisms and evaluation of their role in end-stage renal disease. *Hypertension*, 22(2), p. 906–911.
- Yuyama, K., Sun, H., Mitsutake, S. & Igarashi, Y., 2012. Sphingolipid-modulated exosome secretion promotes clearance of amyloid- β by microglia. *J Biol Chem*, 287(14), pp. 10977-89.
- Zampetaki, A. & Mayr, M., 2012. Analytical challenges and technical limitations in assessing circulating miRNAs. *Thromb Haemostasis*, Volume 108, pp. 592-598.

- Zecher, D., Cumpelik, A. & Schifferli, J. A., 2014. Erythrocyte-Derived Microvesicles Amplify Systemic Inflammation by Thrombin-Dependent Activation of Complement. *Arterioscler Thromb Vasc Biol*, 34(2), pp. 313-20.
- Zerial, M. & McBride, H., 2001. Rab proteins as membrane organizers. *Nat Rev Mol Cell Biol*, 2(2), pp. 107-17.
- Zhang, C., 2008. MicroRNAs: role in cardiovascular biology and disease. *Clin Sci (Lond)*, 114(12), pp. 699-706.
- Zhang, J., 2003. Evolution by gene duplication: an update. *TRENDS in ecology and evolution*, 18(6), pp. 292-8.
- Zhang, J. *et al.*, 2015. Circulating MiR-16-5p and MiR-19b-3p as Two Novel Potential Biomarkers to Indicate Progression of Gastric Cancer. *Theranostics*, 5(7), pp. 733-745.
- Zhang, L. *et al.*, 2015. Transfer of microRNAs by extracellular membrane microvesicles: a nascent crosstalk model in tumor pathogenesis, especially tumor cell-microenvironment interactions. *J Hematol Oncol*, 8(14).
- Zhang, X. A., Bontrager, A. L. & Hemler, M. E., 2001. Transmembrane-4 Superfamily Proteins Associate with Activated Protein Kinase C (PKC) and Link PKC to Specific β 1 Integrins. *The Journal of Biological Chemistry*, Volume 276, pp. 25005-25013.
- Zhang, Y. *et al.*, 2010. Secreted monocytic miR-150 enhances targeted endothelial cell migration. *Mol Cell*, 39(1), pp. 133-44.
- Zhao, L. & Zhang, Y., 2015. miR-342-3p affects hepatocellular carcinoma cell proliferation via regulating NF- κ B pathway. *Biochem Biophys Res Commun*, 457(3), pp. 370-7.
- Zheng, X. L., 2013. Structure-function and regulation of ADAMTS13 protease.. *J Thromb Haemost.* , 11(1), p. 11–23.
- Zhenzhen, L. & Roche, P. A., 2015. Macropinocytosis in phagocytes: regulation of MHC class-II-restricted antigen presentation in dendritic cells. *Front. Physiol*, 6(1), p. eCollection 2015.
- Zhou, Z., 2007. New phosphatidylserine receptors: clearance of apoptotic cells and more. *Dev Cell*, 13(6), p. 759–760.
- Zhu, M., Li, J. & Fink, A. L., 2003. The association of alpha-synuclein with membranes affects bilayer structure, stability, and fibril formation. *J Biol Chem*, 278(41), pp. 40186-97.
- Ziegler-Heitbrock, H. W. L. & Ulevitch, R. J., 1993. CD14: Cell surface receptor and differentiation marker. *Trends in Immunology*, 14(3), pp. 121-125.
- Zimring, J. C. *et al.*, 2005. Nonhemolytic antibody-induced loss of erythrocyte surface antigen. *Blood*, 106(3), pp. 1105-12.

Zwaal, R. F. & Schroit , A. J., 1997. Pathophysiologic implications of membrane phospholipid asymmetry in blood cells. *Blood*, Volume 89, p. 1121–32.

Appendices

Appendix I

Abcam miRNA profiling protocol

Sample's volume were adjusted in water such that 5 ng/ μL was in a 25 μL volume. Then, for each sample, 35 μL of the Firefly particles were added to a well of a 96-well filter plate and filtered. Three additional wells for no-sample controls were also prepared.

Subsequently, 25 μL of hybridization buffer was added to each well followed by 25 μL of sample (or water in the case of no-sample controls). The plate was incubated at 37°C for 60 minutes while shaking at 750 rpm. Then, the wells were rinsed twice with 175 μL of 1X Buffer A, and 75 μL of 1X labelling buffer was added to each well. The plate was incubated at RT for 60 minutes while shaking at 750rpm. The wells were rinsed twice with Buffer B followed by one rinse with 1X Buffer A. A catch plate was added to the vacuum manifold (ab204067) and the filter plate was placed under constant vacuum. A 65 μL of 95°C RNase-free water was added twice to each well and the eluant was retained in the catch plate. The particles were stored in the filter plate at 4°C with 75 μL Rinse A for a short period of time until needed.

A 30 μL of the eluant was added to a clean polymerase chain reaction (PCR) plate and mixed with 20 μL PCR master mix. The mixture underwent 27 cycles of PCR amplification followed by 6 cycles of asymmetric amplification.

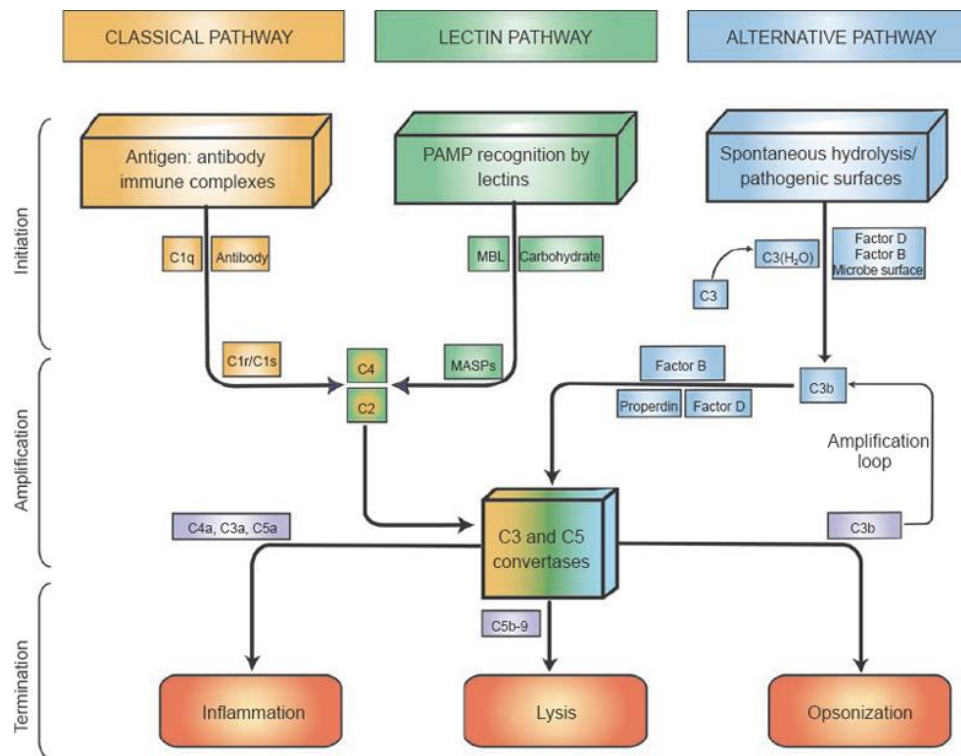
Then, suction was used to remove the rinse A from the particles that was stored in the filter plate at 4°C with 75 μL rinse A. Next, 60 μL of hybridization Buffer was added to each well followed by 20 μL of the PCR product. The plate was incubated at 37°C for 30 minutes while shaking at 750rpm.

The plate was then rinsed twice with 175 μL of 1X buffer A and 75 μL of 1X reporting buffer was added to each well and the plate was incubated at RT for 15 mins while shaking at 750 rpm followed by two rinses with 175 μL of 1X buffer A and then 175 μL of run buffer was added to each well. Samples were then scanned using an EMD Millipore Guava 6HT or 8HT flow cytometer.

Buffers were not specified by manufacturer.

Appendix II

The complement pathway



“Complement can be activated through three pathways: classical, lectin, and alternative. The classical pathway is activated when C1q binds to antibody attached to antigen, activating C1r and C1s, which cleave C4 and C2. The lectin pathway is activated when mannose-binding lectin (MBL) encounters conserved pathogenic carbohydrate motifs, activating the MBL-associated serine proteases (MASPs) and again cleaving C4 and C2. C4 and C2 cleavage products form the classical and lectin pathway C3 convertase, C4bC2a, which cleaves C3 into C3b and C3a. A second molecule of C3b can associate with C4bC2a to form the C5 convertase of the classical and lectin pathways, C4bC2aC3b. The alternative pathway (AP) is activated when C3 undergoes spontaneous hydrolysis and forms the initial AP C3 convertase, C3 (H₂O) Bb, in the presence of Factors B and D, leading to additional C3 cleavage and eventual formation of the AP C3 convertase (C3bBb) and AP C5 convertase (C3bBbC3b). Properdin facilitates AP activation by stabilizing AP convertases.” retrieved from Dunkelberger & Song (2010).

Moreover, opsonins (C3b, iC3b, and C3d - induces phagocytosis of opsonized targets and also serves to amplify complement activation through the alternative pathway) is essential for the induction of the terminal pathway of complement effector generation. The increasing density of C3b during complement activation and amplification leads to a

substrate specificity shift in the generated convertases from C3 to its paralog C5 (terminal pathway at the stage of cleavage) (Janeway, *et al.*, 2001). C3a and C5a, which are potent anaphylatoxins (proinflammatory molecules derived from the cleavage-C4a/C3a/C5a) and has chemotactic activities leaves the large fragment C5b to form the rest of a MAC (terminal assembly of complement components C5b through C9, which can directly lyse targeted surfaces) (Janeway, *et al.*, 2001; Noris & Remuzzi, 2013; Towner, *et al.*, 2016).

Appendix III

Table 1. Protein name to gene name conversion

Surface markers	Gene name
Cluster differentiation 36	CD36
Cluster differentiation 58	CD58
Cluster differentiation 63	CD63
Glycophorin A & B	GYP A and GYP B
Total proteins	Gene name
Glycophorin A	GYP A
Band 3 anion transport protein	SLC4A1
Spectrin beta chain	SPTBN2
Protein Kinase C	PRKC
Cluster differentiation 47	CD47
Proteases	Gene name
Disintegrin Metallopeptidase Domain 8	ADAM8
Disintegrin-like Metallopeptidase with thrombospondin motif 1, 13	ADAMTS13
Cathepsin A	CTSA
Cathepsin B	CTSB
Cathepsin D	CTSD
Cathepsin E	CTSE
Cathepsin V	CTSV
Cathepsin Z	CTSZ
Dipeptidyl peptidase 4	DPP4
Matrix Metalloproteinase 2	MMP2
Matrix Metalloproteinase 3	MMP3
Matrix Metalloproteinase 8	MMP8
Matrix Metalloproteinase 9	MMP9
Matrix Metalloproteinase 12	MMP12
Matrix Metalloproteinase 13	MMP13
Kallikrein 10	KLK10
Proprotein convertase 9	PCSK9
Proteinase 3	PRTN3

Protein names were converted into gene names in order to allow GO enrichment analysis, where column 1 indicates the protein name and column 2 indicates the name of the gene of interest.

The functional enrichments among the multiple proteins/genes present in eMV samples

Table 2. Description of mapped items for protein/gene expression data

Search Term	Gene Symbol	Description	Alternate names	Chromosome	Map location
ADAMTS13	ADAMTS13	ADAM metalloproteinase with thrombospondin type 1 motif, 13	ADAM-TS13 ADAMTS-13 C9orf8 VWF-CP vWF-CP	9	9q34
ADAM8	ADAM8	ADAM metalloproteinase domain 8	CD156 CD156a MS2	10	10q26.3
DPP4	DPP4	dipeptidyl-peptidase 4	ADABP ADCP2 CD26 DPP4 TP103	2	2q24.3
KLK10	KLK10	kallikrein-related peptidase 10	NES1 PRSSL1	19	19q13
MMP2	MMP2	matrix metalloproteinase 2 (gelatinase A, 72kDa gelatinase, 72kDa type IV collagenase)	CLG4 CLG4A MMP-ii MONA TBE-1	16	16q13-q21
MMP3	MMP3	matrix metalloproteinase 3 (stromelysin 1, progelatinase)	CHDS6 MMP-3 SL-1 STMY STMY1 STR1	11	11q22.3
MMP9	MMP9	matrix metalloproteinase 9 (gelatinase B, 92kDa gelatinase, 92kDa type IV collagenase)	CLG4B GELB MANDP2 MMP-9	20	20q11.2-q13.1
MMP12	MMP12	matrix metalloproteinase 12 (macrophage elastase)	HME ME MME MMP-12	11	11q22.3
PCSK9	PCSK9	proprotein convertase subtilisin/kexin type 9	FH3 HCHOLA3 LDLCC1 NARC-1 NARC1 PC9	1	1p32.3
PRTN3	PRTN3	proteinase 3	ACPA AGP7 C-ANCA CANCA MBN MBT NP-4 NP4 P29 PR-3 PR3	19	19p13.3
GYP A	GYP A	glycophorin A (MNS blood group)	CD235a GPA GPERik GPSAT HGpMIV HGpMIXI HGpSta(C) MN MNS PAS-2	4	4q31.21
GYP B	GYP B	glycophorin B (MNS blood group)	CD235b GPB GPB.NV GYPHe.NV GpMIII HGpMIII HGpMIV HGpMIX MNS PAS-3 SS	4	4q31.21
SLC4A1	SLC4A1	solute carrier family 4 (anion exchanger), member 1 (Diego blood group)	AE1 BND3 CD233 DI EMPB3 EPB3 FR RTA1A SW WD WD1 WR	17	17q21.31
CTSA	CTSA	cathepsin A	GLB2 GSL NGBE PPCA PPGB	20	20q13.1
CTSB	CTSB	cathepsin B	APPS CPSB	8	8p22
CTSD	CTSD	cathepsin D	CLN10 CPSD HEL-S-130P	11	11p15.5
CTSV	CTSV	cathepsin V	CATL2 CTS2 CTSU	9	9q22.2
CTSZ	CTSZ	cathepsin Z	CTSK	20	20q13.32
MMP8	MMP8	matrix metalloproteinase 8 (neutrophil collagenase)	CLG1 HNC MMP-8 PMNL-CL	11	11q22.3
MMP13	MMP13	matrix metalloproteinase 13 (collagenase 3)	CLG3 MANDP1 MMP-13	11	11q22.3
ANXA5	ANXA5	annexin A5	ANX5 ENX2 HEL-S-7 PP4 RPRGL3	4	4q27
CD58	CD58	CD58 molecule	LFA-3 LFA3 ag3	1	1p13
CD36	CD36	CD36 molecule (thrombospondin receptor)	BDPLT10 CHDS7 FAT GP38 GP4 GP4V PASIV SCARB3	7	7q11.2
CD63	CD63	CD63 molecule	LAMP-3 ME491 MLA1 OMA81H TSPAN30	12	12q12-q13
SPTBN2	SPTBN2	spectrin, beta, non-erythrocytic 2	GTRAP41 SCA5 SCAR14	11	11q13
CD47	CD47	CD47 molecule	IAP MERG OA3	3	3q13.1-q13.2
PRKC	PRKC	protein kinase C	AAG6 PKC	17	17q22-q23.2

Table 3. Description of cellular components for protein/gene present in eMV samples

Cellular component	No. of genes in the data set	Percentage of genes	Genes mapped from input data set
Extracellular space	8	29.62962963	MMP2,MMP3,MMP9,PCSK9,CTSD,CTSZ,MMP8,MMP13
Extracellular	14	51.85185185	ADAMTS13,DPP4,KLK10,MMP2,MMP3,MMP9,MMP12,PCSK9,CTSA,CTSB,CTSD,MMP8,MMP13,ANXA5
Lysosome	12	44.44444444	DPP4,PCSK9,PRTN3,CTSA,CTSB,CTSD,CTSV,CTSZ,ANXA5,CD36,CD63,CD47
Cell surface	5	18.51851852	ADAMTS13,DPP4,CD36,CD63,CD47
Plasma membrane	16	59.25925926	ADAM8,DPP4,MMP2,MMP9,PRTN3,GYPA,GYPB,SLC4A1,CTSB,ANXA5,CD58,CD36,CD63,SPTBN2,CD47,PRKC
Exosomes	12	44.44444444	DPP4,PCSK9,PRTN3,SLC4A1,CTSA,CTSB,CTSD,ANXA5,CD58,CD36,CD63,PRKC
Integral to plasma membrane	7	25.92592593	ADAM8,GYPB,SLC4A1,CD58,CD36,CD63,CD47
Invadopodium membrane	1	3.703703704	DPP4
Platelet dense granule membrane	1	3.703703704	CD63
Cortical cytoskeleton	1	3.703703704	SLC4A1
Endoplasmic reticulum	6	22.22222222	CTSA,CTSB,CTSD,CTSZ,ANXA5,PRKC
Spectrin	1	3.703703704	SPTBN2
Platelet alpha granule membrane	1	3.703703704	CD36
Extracellular matrix	2	7.407407407	PRTN3,CTSD
Golgi apparatus	5	18.51851852	SLC4A1,CTSA,CTSD,CD36,SPTBN2
Intracellular membrane-bounded organelle	2	7.407407407	MMP2,MMP3
Perinuclear region	2	7.407407407	CTSB,PRKC
Lysosomal membrane	1	3.703703704	CD63
Membrane fraction	3	11.11111111	GYPA,CD36,PRKC
Endocytic vesicle	1	3.703703704	DPP4
Intracellular	2	7.407407407	CTSB,ANXA5
Lamellipodium	1	3.703703704	DPP4
Endosome membrane	1	3.703703704	CD63
Synapse	1	3.703703704	PRKC
Zymogen granule	1	3.703703704	CTSB
Basolateral plasma membrane	1	3.703703704	SLC4A1
Late endosome	1	3.703703704	PCSK9
Apical plasma membrane	1	3.703703704	DPP4
Proteinaceous extracellular matrix	1	3.703703704	ADAMTS13
Nuclear membrane	1	3.703703704	CTSB
Membrane	2	7.407407407	DPP4,CD63
Extracellular region	2	7.407407407	KLK10,CTSD
Perinuclear region of cytoplasm	1	3.703703704	PCSK9
Cytoplasmic vesicle	1	3.703703704	SPTBN2
Cytoplasm	12	44.44444444	ADAMTS13,KLK10,PCSK9,PRTN3,CTSB,CTSD,ANXA5,CD58,CD36,CD63,SPTBN2,PRKC
Mitochondrion	3	11.11111111	SLC4A1,CTSB,CTSD
Endosome	1	3.703703704	CD63
Cytoskeleton	1	3.703703704	CD36
Cytosol	2	7.407407407	SPTBN2,PRKC
Integral to membrane	2	7.407407407	GYPB,SLC4A1
Nucleus	7	25.92592593	ADAMTS13,PCSK9,SLC4A1,CTSB,ANXA5,CD36,PRKC

Table 4. Description of molecular functions for protein/gene present in eMV samples

Molecular function	No. of genes in the data set	Percentage of genes	Genes mapped from input data set
Metallopeptidase activity	8	29.62962963	ADAMTS13,ADAM8,MMP2,MMP3,MMP9,MMP12,MMP8,MMP13
Cysteine-type peptidase activity	3	11.11111111	CTSB,CTSV,CTSZ
Serine-type peptidase activity	3	11.11111111	KLK10,PRTN3,CTSA
Aspartic-type signal peptidase activity	1	3.703703704	CTSD
Aminopeptidase activity	1	3.703703704	PCSK9
Peptidase activity	1	3.703703704	DPP4
Calcium ion binding	1	3.703703704	ANXA5
Cytoskeletal protein binding	1	3.703703704	SPTBN2
Protein serine/threonine kinase activity	1	3.703703704	PRKCA
Auxiliary transport protein activity	1	3.703703704	SLC4A1
Receptor activity	1	3.703703704	CD36
Molecular function unknown	5	18.51851852	GYPB,GYPB,CD58,CD63,CD47

Table 5. Description of biological processes involved in protein/gene present in eMV samples

Biological process	No. of genes in the data set	Percentage of genes	Genes mapped from input data set
Protein metabolism	17	62.96296296	ADAMTS13,ADAM8,DPP4,KLK10,MMP2,MMP3,MMP9,MMP12,PCSK9,PRTN3,CTSA,CTSB,CTSD,CTSV,CTSZ,MMMP8,MMMP13
Immune response	4	14.81481481	GYPB,GYPB,CD58,CD47
Cell growth and/or maintenance	1	3.703703704	SPTBN2
Transport	1	3.703703704	SLC4A1
Metabolism	1	3.703703704	CD36
Cell communication	3	11.11111111	ANXA5,CD63,PRKC
Signal transduction	3	11.11111111	ANXA5,CD63,PRKC

Table 6. Description of biological pathways involved in protein/gene present in eMV samples

Biological pathway	No. of genes in the data set	Percentage of genes	Genes mapped from input data set
Hemostasis	5	35.71428571	CD58, CD36, CD63, CD47, PRKC
LPA receptor mediated events	3	21.42857143	MMP2, MMP9, PRKC
Osteopontin-mediated events	2	14.28571429	MMP2, MMP9
Response to elevated platelet cytosolic Ca2+	2	14.28571429	CD63, PRKC
Validated transcriptional targets of AP1 family members Fra1 and Fra2	3	21.42857143	MMP2, MMP9, PRKC
amb2 Integrin signaling	2	14.28571429	MMP2, MMP9
Integrin family cell surface interactions	8	57.14285714	MMP2, MMP3, MMP9, MMP12, CTSD, MMP13, CD47, PRKC
Regulation of Insulin Secretion by Acetylcholine	1	7.142857143	PRKC
ATF-2 transcription factor network	2	14.28571429	MMP2, PRKC
Integrins in angiogenesis	2	14.28571429	MMP2, MMP9
Signaling by SCF-KIT	2	14.28571429	MMP9, PRKC
Syndecan-4-mediated signaling events	3	21.42857143	MMP2, MMP9, PRKC
Cell surface interactions at the vascular wall	2	14.28571429	CD58, CD47
Syndecan-2-mediated signaling events	2	14.28571429	MMP2, MMP9
Posttranslational regulation of adherens junction stability and disassembly	3	21.42857143	MMP2, MMP3, MMP9
Class I PI3K signaling events	7	50	MMP2, MMP3, MMP9, MMP12, CTSD, MMP13, PRKC
EGF receptor (ErbB1) signaling pathway	7	50	MMP2, MMP3, MMP9, MMP12, CTSD, MMP13, PRKC
PDGFR-beta signaling pathway	7	50	MMP2, MMP3, MMP9, MMP12, CTSD, MMP13, PRKC
Urokinase-type plasminogen activator (uPA) and uPAR-mediated signaling	7	50	MMP2, MMP3, MMP9, MMP12, CTSD, MMP13, PRKC
Internalization of ErbB1	7	50	MMP2, MMP3, MMP9, MMP12, CTSD, MMP13, PRKC
Signaling events mediated by focal adhesion kinase	7	50	MMP2, MMP3, MMP9, MMP12, CTSD, MMP13, PRKC
Arf6 downstream pathway	7	50	MMP2, MMP3, MMP9, MMP12, CTSD, MMP13, PRKC
Arf6 trafficking events	7	50	MMP2, MMP3, MMP9, MMP12, CTSD, MMP13, PRKC
S1P1 pathway	7	50	MMP2, MMP3, MMP9, MMP12, CTSD, MMP13, PRKC
Insulin Pathway	7	50	MMP2, MMP3, MMP9, MMP12, CTSD, MMP13, PRKC
ErbB1 downstream signaling	7	50	MMP2, MMP3, MMP9, MMP12, CTSD, MMP13, PRKC
Class I PI3K signaling events mediated by Akt	7	50	MMP2, MMP3, MMP9, MMP12, CTSD, MMP13, PRKC
mTOR signaling pathway	7	50	MMP2, MMP3, MMP9, MMP12, CTSD, MMP13, PRKC
Arf6 signaling events	7	50	MMP2, MMP3, MMP9, MMP12, CTSD, MMP13, PRKC
EGFR-dependent Endothelin signaling events	7	50	MMP2, MMP3, MMP9, MMP12, CTSD, MMP13, PRKC
IGF1 pathway	7	50	MMP2, MMP3, MMP9, MMP12, CTSD, MMP13, PRKC
IL5-mediated signaling events	7	50	MMP2, MMP3, MMP9, MMP12, CTSD, MMP13, PRKC
GMCSF-mediated signaling events	7	50	MMP2, MMP3, MMP9, MMP12, CTSD, MMP13, PRKC
PDGFR receptor signaling network	7	50	MMP2, MMP3, MMP9, MMP12, CTSD, MMP13, PRKC
Signaling events mediated by Hepatocyte Growth Factor Receptor (c-Met)	7	50	MMP2, MMP3, MMP9, MMP12, CTSD, MMP13, PRKC
IL3-mediated signaling events	7	50	MMP2, MMP3, MMP9, MMP12, CTSD, MMP13, PRKC
Nectin adhesion pathway	7	50	MMP2, MMP3, MMP9, MMP12, CTSD, MMP13, PRKC
IFN-gamma pathway	7	50	MMP2, MMP3, MMP9, MMP12, CTSD, MMP13, PRKC
Signaling events mediated by VEGFR1 and VEGFR2	7	50	MMP2, MMP3, MMP9, MMP12, CTSD, MMP13, PRKC
PAR1-mediated thrombin signaling events	7	50	MMP2, MMP3, MMP9, MMP12, CTSD, MMP13, PRKC
Glypican 1 network	7	50	MMP2, MMP3, MMP9, MMP12, CTSD, MMP13, PRKC
Thrombin/protease-activated receptor (PAR) pathway	7	50	MMP2, MMP3, MMP9, MMP12, CTSD, MMP13, PRKC
Syndecan-1-mediated signaling events	7	50	MMP2, MMP3, MMP9, MMP12, CTSD, MMP13, PRKC
Plasma membrane estrogen receptor signaling	7	50	MMP2, MMP3, MMP9, MMP12, CTSD, MMP13, PRKC
VEGF and VEGFR signaling network	7	50	MMP2, MMP3, MMP9, MMP12, CTSD, MMP13, PRKC
Alpha9 beta1 integrin signaling events	7	50	MMP2, MMP3, MMP9, MMP12, CTSD, MMP13, PRKC
LKB1 signaling events	7	50	MMP2, MMP3, MMP9, MMP12, CTSD, MMP13, PRKC
Endothelins	7	50	MMP2, MMP3, MMP9, MMP12, CTSD, MMP13, PRKC
ErbB receptor signaling network	7	50	MMP2, MMP3, MMP9, MMP12, CTSD, MMP13, PRKC
Sphingosine 1-phosphate (S1P) pathway	7	50	MMP2, MMP3, MMP9, MMP12, CTSD, MMP13, PRKC
N-cadherin signaling events	3	21.42857143	MMP2, MMP3, MMP9
Stabilization of mRNA by HuR	1	7.142857143	PRKC
TRAIL signaling pathway	7	50	MMP2, MMP3, MMP9, MMP12, CTSD, MMP13, PRKC
Glypican pathway	7	50	MMP2, MMP3, MMP9, MMP12, CTSD, MMP13, PRKC
Proteoglycan syndecan-mediated signaling events	7	50	MMP2, MMP3, MMP9, MMP12, CTSD, MMP13, PRKC
Bicarbonate transporters	1	7.142857143	SLC4A1
Regulation of KIT signaling	1	7.142857143	PRKC
Beta1 integrin cell surface interactions	7	50	MMP2, MMP3, MMP9, MMP12, CTSD, MMP13, PRKC
Stabilization and expansion of the E-cadherin adherens junction	3	21.42857143	MMP2, MMP3, MMP9
E-cadherin signaling in the nascent adherens junction	3	21.42857143	MMP2, MMP3, MMP9
E-cadherin signaling events	3	21.42857143	MMP2, MMP3, MMP9
Signal regulatory protein (SIRP) family interactions	1	7.142857143	CD47
Interaction between L1 and Ankyrins	1	7.142857143	SPTBN2
Cell-Cell communication	2	14.28571429	SPTBN2, CD47
Platelet Adhesion to exposed collagen	1	7.142857143	CD36
Regulation of Insulin-like Growth Factor (IGF) Activity by Insulin-like Growth Factor Binding Proteins (IGFBPs)	1	7.142857143	MMP2
FAS (CD95) signaling pathway	2	14.28571429	CTSD, PRKC
Regulation of nuclear beta catenin signaling and target gene transcription	2	14.28571429	MMP2, MMP9
Platelet activation, signaling and aggregation	2	14.28571429	CD63, PRKC
Direct p53 effectors	2	14.28571429	MMP2, CTSD
CD28 dependent Vav1 pathway	1	7.142857143	SPTBN2
Canonical Wnt signaling pathway	2	14.28571429	MMP2, MMP9
CaM pathway	1	7.142857143	PRKC
Calmodulin induced events	1	7.142857143	PRKC
Phospholipase C-mediated cascade	1	7.142857143	PRKC
Ca-dependent events	1	7.142857143	PRKC
DAG and IP3 signaling	1	7.142857143	PRKC
Platelet degranulation	1	7.142857143	CD63
p75(NTR)-mediated signaling	2	14.28571429	MMP3, PRKC
IL8- and CXCR1-mediated signaling events	1	7.142857143	PRKC
EGFR interacts with phospholipase C-gamma	1	7.142857143	PRKC
VEGFR1 specific signals	1	7.142857143	PRKC
Noncanonical Wnt signaling pathway	2	14.28571429	MMP2, MMP9
PLC-gamma1 signalling	1	7.142857143	PRKC

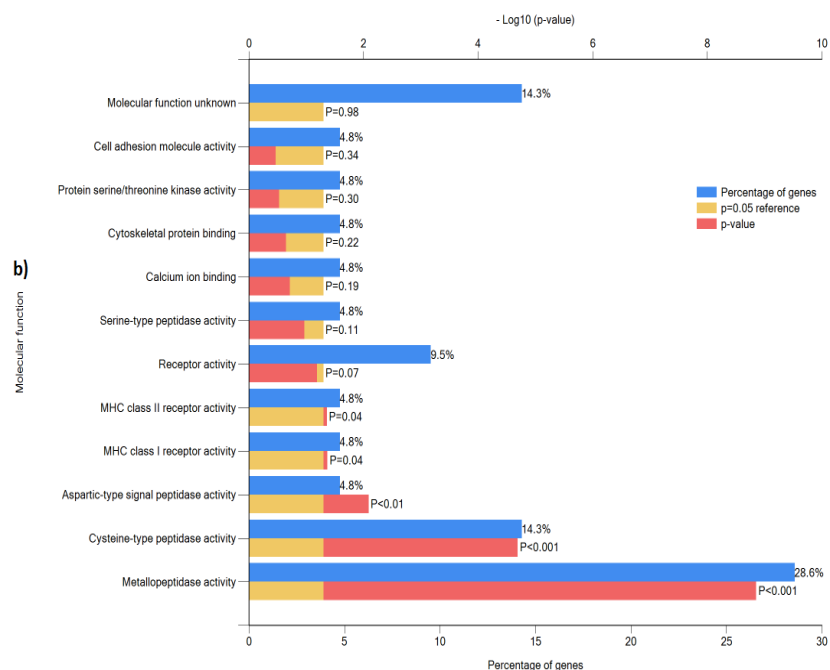
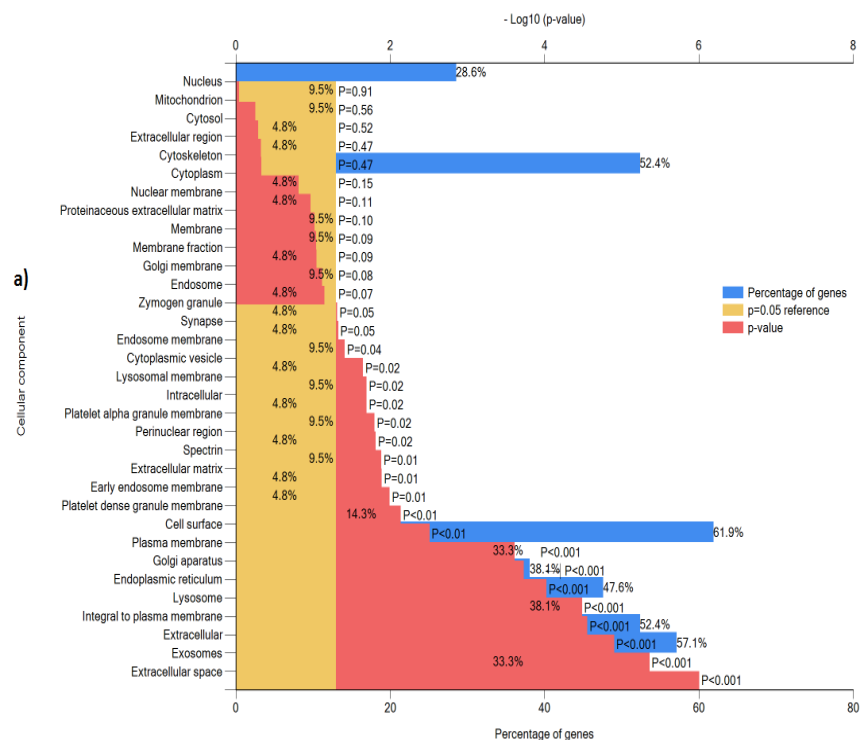
Table 6. Description of biological pathways involved in protein/gene present in eMV samples continued...

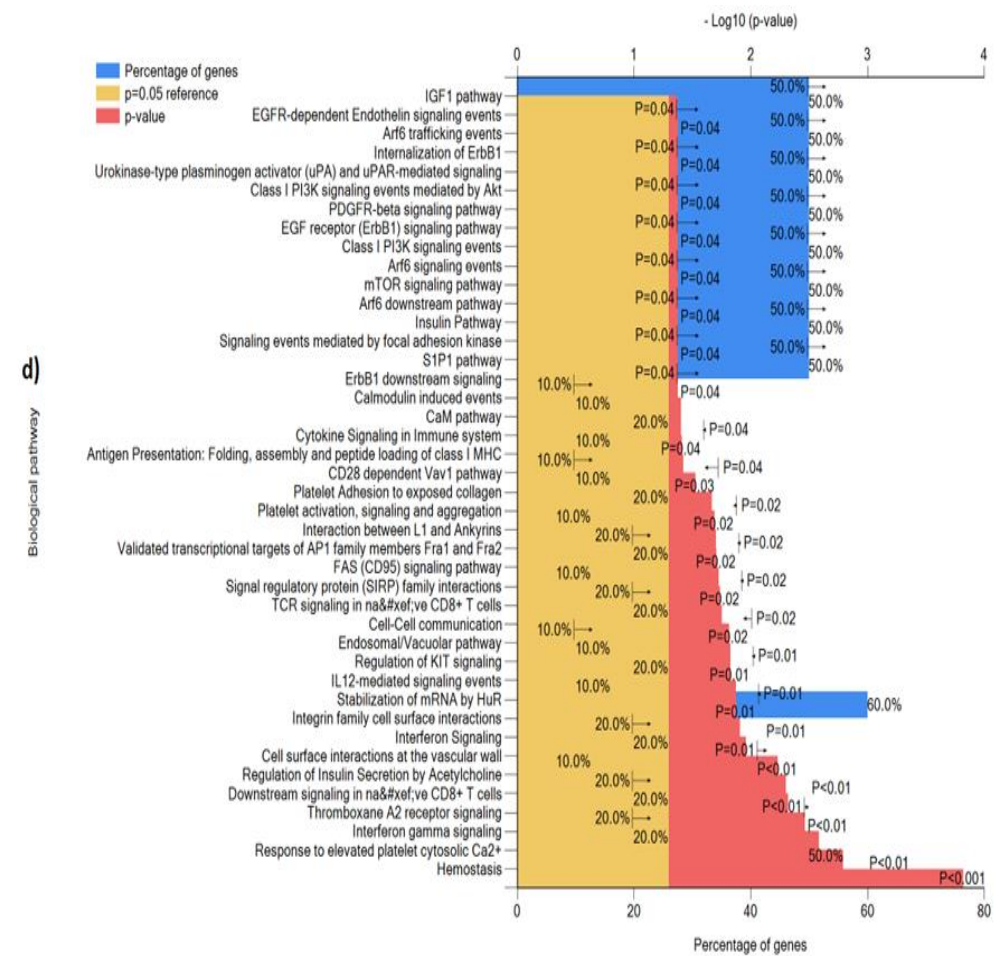
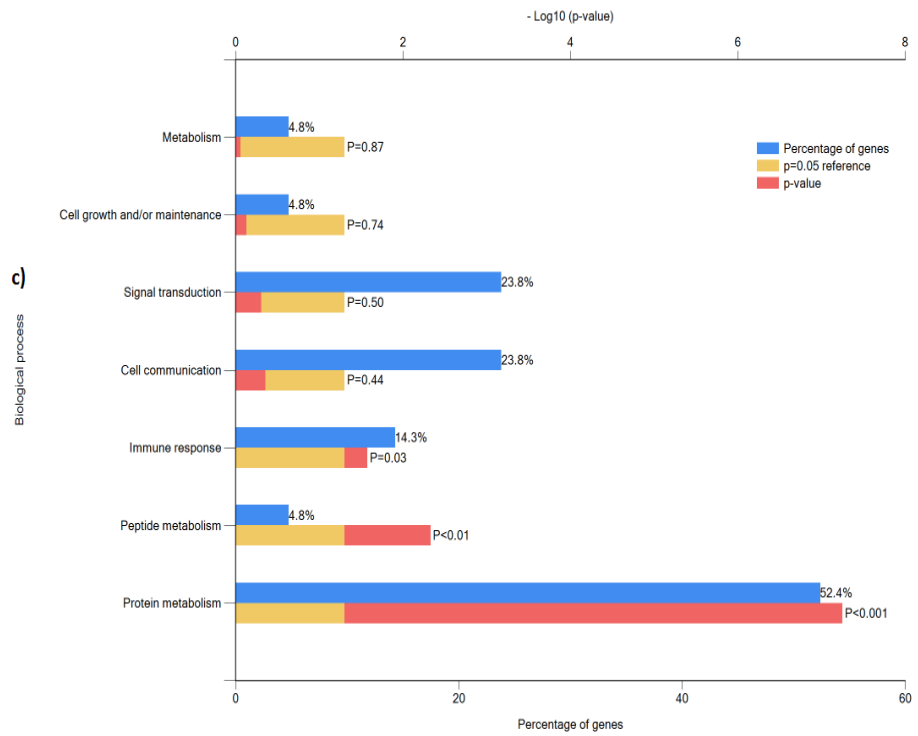
Nephrin interactions	1	7.142857143	SPTBN2
p53 pathway	2	14.28571429	MMP2,CTSD
CXCR4-mediated signaling events	2	14.28571429	MMP9,PRKC
IL8- and CXCR2-mediated signaling events	1	7.142857143	PRKC
Wnt signaling network	2	14.28571429	MMP2,MMP9
Canonical NF-kappaB pathway	1	7.142857143	PRKC
alpha5 and alpha6 Integrin signaling	1	7.142857143	PRKC
RhoA signaling pathway	2	14.28571429	MMP2,PRKC
Regulation of RAC1 activity	2	14.28571429	MMP2,PRKC
Regulation of RhoA activity	2	14.28571429	MMP2,PRKC
RAC1 signaling pathway	2	14.28571429	MMP2,PRKC
Glypican 3 network	2	14.28571429	MMP2,MMP9
CD28 co-stimulation	1	7.142857143	SPTBN2
IL8-mediated signaling events	1	7.142857143	PRKC
PLC beta mediated events	1	7.142857143	PRKC
G-protein mediated events	1	7.142857143	PRKC
FOXO1 transcription factor network	1	7.142857143	MMP2
Ras signaling in the CD4+ TCR pathway	1	7.142857143	PRKC
Beta3 integrin cell surface interactions	1	7.142857143	CD47
Retinoic acid receptors-mediated signaling	1	7.142857143	PRKC
FGF signaling pathway	1	7.142857143	MMP9
Alpha6beta4Integrin	1	7.142857143	PRKC
Regulation of insulin Secretion	1	7.142857143	PRKC
Ceramide signaling pathway	1	7.142857143	CTSD
Angiotensin receptor Tie2-mediated signaling	1	7.142857143	MMP2
ATR signaling pathway	2	14.28571429	MMP2,CTSD
Opioid Signalling	1	7.142857143	PRKC
Costimulation by the CD28 family	1	7.142857143	SPTBN2
Thromboxane A2 receptor signaling	1	7.142857143	PRKC
KitReceptor	1	7.142857143	PRKC
Endogenous TLR signaling	1	7.142857143	PRKC
NCAM signaling for neurite out-growth	1	7.142857143	SPTBN2
CD40/CD40L signaling	1	7.142857143	PRKC
Aurora A signaling	1	7.142857143	PRKC
Downstream signaling in naive CD8+ T cells	1	7.142857143	PRKC
Validated nuclear estrogen receptor alpha network	1	7.142857143	CTSD
Downstream signaling of activated FGFR	1	7.142857143	PRKC
IL23-mediated signaling events	1	7.142857143	PRKC
IL2 signaling events mediated by PI3K	1	7.142857143	PRKC
Signaling events regulated by Ret tyrosine kinase	1	7.142857143	PRKC
Transcriptional Regulation of White Adipocyte Differentiation	1	7.142857143	CD36
TNF receptor signaling pathway	2	14.28571429	CTSD,PRKC
ATM pathway	2	14.28571429	MMP2,CTSD
Downstream signal transduction	1	7.142857143	PRKC
Signaling by PDGF	1	7.142857143	PRKC
AP-1 transcription factor network	3	21.42857143	MMP2,MMP9,PRKC
Validated targets of C-MYC transcriptional activation	1	7.142857143	MMP9
L1CAM interactions	1	7.142857143	SPTBN2
Wnt	1	7.142857143	PRKC
Integration of energy metabolism	1	7.142857143	PRKC
C-MYC transcription factor network	1	7.142857143	PRTN3
Integrin-linked kinase signaling	3	21.42857143	MMP2,MMP9,PRKC
Role of Calcineurin-dependent NFAT signaling in lymphocytes	1	7.142857143	PRKC
Transport of inorganic cations/anions and amino acids/oligopeptides	1	7.142857143	SLC4A1
Signaling by FGFR	1	7.142857143	PRKC
Signaling by EGFR	1	7.142857143	PRKC
Signaling by Aurora kinases	1	7.142857143	PRKC
Regulation of mRNA Stability by Proteins that Bind AU-rich Elements	1	7.142857143	PRKC
PLK1 signaling events	1	7.142857143	PRKC
NGF signalling via TRKA from the plasma membrane	1	7.142857143	PRKC
IL12-mediated signaling events	1	7.142857143	PRKC
Polo-like kinase signaling events in the cell cycle	1	7.142857143	PRKC
IL2-mediated signaling events	1	7.142857143	PRKC
CDC42 signaling events	3	21.42857143	MMP2,MMP9,PRKC
TCR signaling in naive CD8+ T cells	1	7.142857143	PRKC
Regulation of CDC42 activity	3	21.42857143	MMP2,MMP9,PRKC
Developmental Biology	2	14.28571429	CD36,SPTBN2
TCR signaling in naive CD4+ T cells	1	7.142857143	PRKC
EGFR1	1	7.142857143	PRKC
Signalling by NGF	1	7.142857143	PRKC
C-MYC pathway	1	7.142857143	MMP9
Regulation of p38-alpha and p38-beta	1	7.142857143	PRKC
p38 MAPK signaling pathway	1	7.142857143	PRKC
Diabetes pathways	1	7.142857143	MMP2
Axon guidance	1	7.142857143	SPTBN2
BMP receptor signaling	1	7.142857143	PRKC
IL1-mediated signaling events	1	7.142857143	PRKC
Metabolism of mRNA	1	7.142857143	PRKC
Adaptive Immune System	1	7.142857143	SPTBN2
SLC-mediated transmembrane transport	1	7.142857143	SLC4A1
Metabolism of RNA	1	7.142857143	PRKC
Regulation of cytoplasmic and nuclear SMAD2/3 signaling	1	7.142857143	PRKC
TGF-beta receptor signaling	1	7.142857143	PRKC
Regulation of nuclear SMAD2/3 signaling	1	7.142857143	PRKC
ALK1 signaling events	1	7.142857143	PRKC
ALK1 pathway	1	7.142857143	PRKC
Transmembrane transport of small molecules	1	7.142857143	SLC4A1
Immune System	1	7.142857143	SPTBN2
Signal Transduction	2	14.28571429	MMP9,PRKC
Signaling by GPCR	1	7.142857143	PRKC
Metabolism	1	7.142857143	PRKC

Appendix IV

GO assessment of proteins/genes present in HRV16iHVM

The primary focus on GO annotations was associated with human proteins/genes only. After assessing the pattern of protein expression on HRV16iHVM samples, further analyses was focused on the protein to gene name conversion (actual protein coding sequence is often only a small part), using String and UniProt databases and then the cellular component (Fig. a), molecular function (Fig. b), biological processes (Fig. c), and specific biological pathways involved (Fig. d), using the same methodology used in chapter 3.2.4.





The functional enrichments among the multiple proteins present in HRV16iHMV samples

Table 1. Description of mapped items for protein/gene expression data

Search Term	Gene Symbol	Description	Alternate names	Chromosome	Map location
CTSA	CTSA	cathepsin A	GLB2 GSL NGBE PPCA PPGB	20	20q13.1
CTSB	CTSB	cathepsin B	APPS CPSB	8	8p22
CTSD	CTSD	cathepsin D	CLN10 CPSD HEL-S-130P	11	11p15.5
CTSV	CTSV	cathepsin V	CATL2 CTS2 CTSU	9	9q22.2
CTSZ	CTSZ	cathepsin Z	CTSX	20	20q13.32
MMP8	MMP8	matrix metalloproteinase 8 (neutrophil collagenase)	CLG1 HNC MMP-8 PMNL-CL	11	11q22.3
MMP13	MMP13	matrix metalloproteinase 13 (collagenase 3)	CLG3 MANDP1 MMP-13	11	11q22.3
ANXA5	ANXA5	annexin A5	ANX5 ENX2 HEL-S-7 PP4 RPRGL3	4	4q27
CD58	CD58	CD58 molecule	LFA-3 LFA3 ag3	1	1p13
CD36	CD36	CD36 molecule (thrombospondin receptor)	BDPLT10 CHDS7 FAT GP3B GP4 GPIV PASIV SCARB3	7	7q11.2
CD63	CD63	CD63 molecule	LAMP-3 ME491 MLA1 OMA81H TSPAN30	12	12q12-q13
SPTBN2	SPTBN2	spectrin, beta, non-erythrocytic 2	GTRAP41 SCA5 SCAR14	11	11q13
CD47	CD47	CD47 molecule	IAP MER6 OA3	3	3q13.1-q13.2
PRKCA	PRKCA	protein kinase C, alpha	AAG6 PKC-alpha PKCA PRKACA	17	17q22-q23.2
ADAM9	ADAM9	ADAM metalloproteinase domain 9	CORD9 MCMP MDC9 Mltng	8	8p11.22
ADAMTS1	ADAMTS1	ADAM metalloproteinase with thrombospondin type 1 motif, 1	C3-C5 METH1	21	21q22.2
MMP10	MMP10	matrix metalloproteinase 10 (stromelysin 2)	SL-2 STMV2	11	11q22.3
MME	MME	membrane metallo-endopeptidase	CALLA CD10 NEP SFE	3	3q25.2
ICAM1	ICAM1	intercellular adhesion molecule 1	BB2 CD54 P3.58	19	19p13.3-p13.2
CD46	CD46	CD46 molecule, complement regulatory protein	AHUS2 MCP MIC10 TLX TRA2.10	1	1q32
HLA-A	HLA-A	major histocompatibility complex, class I, A	H2A	6	6p21.3

Table 2. Description of cellular components for protein/gene present in HRV16iHMV samples

Cellular component	genes in the dataset	Percentage of genes	Genes mapped from input data set
Extracellular space	7	33.33333333	CTSD, CTSZ, MMP8, MMP13, ADAM9, MMP10, ICAM1
Exosomes	12	57.14285714	CTSA, CTSB, CTSD, ANXA5, CD58, CD36, CD63, PRKCA, MME, ICAM1, CD46, HLA-A
Extracellular	11	52.38095238	CTSA, CTSB, CTSD, MMP8, MMP13, ANXA5, ADAMTS1, MMP10, ICAM1, CD46, HLA-A
Integral to plasma membrane	8	38.0952381	CD58, CD36, CD63, CD47, MME, ICAM1, CD46, HLA-A
Lysosome	10	47.61904762	CTSA, CTSB, CTSD, CTSV, CTSZ, ANXA5, CD36, CD63, CD47, MME
Endoplasmic reticulum	8	38.0952381	CTSA, CTSB, CTSD, CTSZ, ANXA5, PRKCA, MME, HLA-A
Golgi apparatus	7	33.33333333	CTSA, CTSD, CD36, SPTBN2, ADAMTS1, MME, HLA-A
Plasma membrane	13	61.9047619	CTSB, ANXA5, CD58, CD36, CD63, SPTBN2, CD47, PRKCA, ADAM9, MME, ICAM1, CD46, HLA-A
Cell surface	3	14.28571429	CD36, CD63, CD47
Platelet dense granule membrane	1	4.761904762	CD63
Early endosome membrane	1	4.761904762	HLA-A
Extracellular matrix	2	9.523809524	CTSD, MME
Spectrin	1	4.761904762	SPTBN2
Perinuclear region	2	9.523809524	CTSB, PRKCA
Platelet alpha granule membrane	1	4.761904762	CD36
Intracellular	2	9.523809524	CTSB, ANXA5
Lysosomal membrane	1	4.761904762	CD63
Cytoplasmic vesicle	2	9.523809524	SPTBN2, ADAMTS1
Endosome membrane	1	4.761904762	CD63
Synapse	1	4.761904762	PRKCA
Zymogen granule	1	4.761904762	CTSB
Endosome	2	9.523809524	CD63, MME
Golgi membrane	1	4.761904762	HLA-A
Membrane fraction	2	9.523809524	CD36, PRKCA
Membrane	2	9.523809524	CD63, MME
Proteinaceous extracellular matrix	1	4.761904762	MMP10
Nuclear membrane	1	4.761904762	CTSB
Cytoplasm	11	52.38095238	CTSB, CTSD, ANXA5, CD58, CD36, CD63, SPTBN2, PRKCA, ADAM9, MME, ICAM1
Cytoskeleton	1	4.761904762	CD36
Extracellular region	1	4.761904762	CTSD
Cytosol	2	9.523809524	SPTBN2, PRKCA
Mitochondrion	2	9.523809524	CTSB, CTSD
Nucleus	6	28.57142857	CTSB, ANXA5, CD36, PRKCA, ADAM9, HLA-A

Table 3. Description of molecular functions for protein/gene present in HRV16iHVMV samples

Molecular function	No. of genes in the data set	Percentage of genes	Genes mapped from input data set
Metallopeptidase activity	6	28.57142857	MMP8,MMP13,ADAM9,ADAMTS1,MMP10,MME
Cysteine-type peptidase activity	3	14.28571429	CTSB,CTSV,CTSZ
Aspartic-type signal peptidase activity	1	4.761904762	CTSD
MHC class I receptor activity	1	4.761904762	HLA-A
MHC class II receptor activity	1	4.761904762	HLA-A
Receptor activity	2	9.523809524	CD36,CD46
Serine-type peptidase activity	1	4.761904762	CTSA
Calcium ion binding	1	4.761904762	ANXA5
Cytoskeletal protein binding	1	4.761904762	SPTBN2
Protein serine/threonine kinase activity	1	4.761904762	PRKCA
Cell adhesion molecule activity	1	4.761904762	ICAM1
Molecular function unknown	3	14.28571429	CD58,CD63,CD47

Table 4. Description of biological processes involved in protein/gene present in HRV16iHVMV samples

Biological process	No. of genes in the data set	Percentage of genes	Genes mapped from input data set
Protein metabolism	11	52.38095238	CTSA,CTSB,CTSD,CTSV,CTSZ,MMP8,MMP13,ADAM9,ADAMTS1,MMP10,MME
Peptide metabolism	1	4.761904762	MME
Immune response	3	14.28571429	CD58,CD47,HLA-A
Cell communication	5	23.80952381	ANXA5,CD63,PRKCA,ICAM1,CD46
Signal transduction	5	23.80952381	ANXA5,CD63,PRKCA,ICAM1,CD46
Cell growth and/or maintenance	1	4.761904762	SPTBN2
Metabolism	1	4.761904762	CD36

Table 5. Description of biological pathways involved in protein/gene present in HRV16iHMV samples

Biological pathway	genes in the data set	Percentage of genes	Genes mapped from input data set
Hemostasis	5	50	CD58,CD36,CD63,CD47,PRKCA
Response to elevated platelet cytosolic Ca2+	2	20	CD63,PRKCA
Interferon gamma signaling	2	20	ICAM1,HLA-A
Thromboxane A2 receptor signaling	2	20	PRKCA,ICAM1
Downstream signaling in naive CD8+ T cells	2	20	PRKCA,HLA-A
Regulation of Insulin Secretion by Acetylcholine	1	10	PRKCA
Cell surface interactions at the vascular wall	2	20	CD58,CD47
Interferon Signaling	2	20	ICAM1,HLA-A
Integrin family cell surface interactions	6	60	CTSD,MMP13,CD47,PRKCA,ICAM1,HLA-A
Stabilization of mRNA by HuR	1	10	PRKCA
IL12-mediated signaling events	2	20	PRKCA,HLA-A
Endosomal/Vacuolar pathway	1	10	HLA-A
Regulation of KIT signaling	1	10	PRKCA
Cell-Cell communication	2	20	SPTBN2,CD47
TCR signaling in naive CD8+ T cells	2	20	PRKCA,HLA-A
Signal regulatory protein (SIRP) family interactions	1	10	CD47
FAS (CD95) signaling pathway	2	20	CTSD,PRKCA
Validated transcriptional targets of AP1 family members Fra1 and Fra2	2	20	PRKCA,HLA-A
Interaction between L1 and Ankyrins	1	10	SPTBN2
Platelet activation, signaling and aggregation	2	20	CD63,PRKCA
Platelet Adhesion to exposed collagen	1	10	CD36
CD28 dependent Vav1 pathway	1	10	SPTBN2
Antigen Presentation: Folding, assembly and peptide loading of class I MHC	1	10	HLA-A
Cytokine Signaling in Immune system	2	20	ICAM1,HLA-A
Calmodulin induced events	1	10	PRKCA
CaM pathway	1	10	PRKCA
PDGFR-beta signaling pathway	5	50	CTSD,MMP13,PRKCA,ICAM1,HLA-A
mTOR signaling pathway	5	50	CTSD,MMP13,PRKCA,ICAM1,HLA-A
ErbB1 downstream signaling	5	50	CTSD,MMP13,PRKCA,ICAM1,HLA-A
Arf6 signaling events	5	50	CTSD,MMP13,PRKCA,ICAM1,HLA-A
Class I PI3K signaling events	5	50	CTSD,MMP13,PRKCA,ICAM1,HLA-A
EGF receptor (ErbB1) signaling pathway	5	50	CTSD,MMP13,PRKCA,ICAM1,HLA-A
Arf6 downstream pathway	5	50	CTSD,MMP13,PRKCA,ICAM1,HLA-A
Arf6 trafficking events	5	50	CTSD,MMP13,PRKCA,ICAM1,HLA-A
Insulin Pathway	5	50	CTSD,MMP13,PRKCA,ICAM1,HLA-A
Signaling events mediated by focal adhesion kinase	5	50	CTSD,MMP13,PRKCA,ICAM1,HLA-A
Urokinase-type plasminogen activator (uPA) and uPAR-mediated signaling	5	50	CTSD,MMP13,PRKCA,ICAM1,HLA-A
Internalization of ErbB1	5	50	CTSD,MMP13,PRKCA,ICAM1,HLA-A
S1P1 pathway	5	50	CTSD,MMP13,PRKCA,ICAM1,HLA-A
Class I PI3K signaling events mediated by Akt	5	50	CTSD,MMP13,PRKCA,ICAM1,HLA-A
EGFR-dependent Endothelin signaling events	5	50	CTSD,MMP13,PRKCA,ICAM1,HLA-A
IGF1 pathway	5	50	CTSD,MMP13,PRKCA,ICAM1,HLA-A
GMCSF-mediated signaling events	5	50	CTSD,MMP13,PRKCA,ICAM1,HLA-A
IL5-mediated signaling events	5	50	CTSD,MMP13,PRKCA,ICAM1,HLA-A
Signaling events mediated by Hepatocyte Growth Factor Receptor (c-Met)	5	50	CTSD,MMP13,PRKCA,ICAM1,HLA-A
PDGF receptor signaling network	5	50	CTSD,MMP13,PRKCA,ICAM1,HLA-A
Phospholipase C-mediated cascade	1	10	PRKCA
Ca-dependent events	1	10	PRKCA
DAG and IP3 signaling	1	10	PRKCA
Nectin adhesion pathway	5	50	CTSD,MMP13,PRKCA,ICAM1,HLA-A
IL3-mediated signaling events	5	50	CTSD,MMP13,PRKCA,ICAM1,HLA-A
IFN-gamma pathway	5	50	CTSD,MMP13,PRKCA,ICAM1,HLA-A
Signaling events mediated by VEGFR1 and VEGFR2	5	50	CTSD,MMP13,PRKCA,ICAM1,HLA-A
Glypican 1 network	5	50	CTSD,MMP13,PRKCA,ICAM1,HLA-A
PAR1-mediated thrombin signaling events	5	50	CTSD,MMP13,PRKCA,ICAM1,HLA-A
Thrombin/protease-activated receptor (PAR) pathway	5	50	CTSD,MMP13,PRKCA,ICAM1,HLA-A
Syndecan-1-mediated signaling events	5	50	CTSD,MMP13,PRKCA,ICAM1,HLA-A
Plasma membrane estrogen receptor signaling	5	50	CTSD,MMP13,PRKCA,ICAM1,HLA-A
VEGF and VEGFR signaling network	5	50	CTSD,MMP13,PRKCA,ICAM1,HLA-A
Alpha9 beta1 integrin signaling events	5	50	CTSD,MMP13,PRKCA,ICAM1,HLA-A
Platelet degranulation	1	10	CD63
Endothelins	5	50	CTSD,MMP13,PRKCA,ICAM1,HLA-A
LKB1 signaling events	5	50	CTSD,MMP13,PRKCA,ICAM1,HLA-A
ErbB receptor signaling network	5	50	CTSD,MMP13,PRKCA,ICAM1,HLA-A
Sphingosine 1-phosphate (S1P) pathway	5	50	CTSD,MMP13,PRKCA,ICAM1,HLA-A
Beta2 integrin cell surface interactions	1	10	ICAM1
IL8- and CXCR1-mediated signaling events	1	10	PRKCA
VEGFR1 specific signals	1	10	PRKCA
EGFR interacts with phospholipase C-gamma	1	10	PRKCA
TRAIL signaling pathway	5	50	CTSD,MMP13,PRKCA,ICAM1,HLA-A
PLC-gamma1 signalling	1	10	PRKCA
Nephrin interactions	1	10	SPTBN2
Immune System	3	30	SPTBN2,ICAM1,HLA-A
Glypican pathway	5	50	CTSD,MMP13,PRKCA,ICAM1,HLA-A
Proteoglycan syndecan-mediated signaling events	5	50	CTSD,MMP13,PRKCA,ICAM1,HLA-A
Beta1 integrin cell surface interactions	5	50	CTSD,MMP13,PRKCA,ICAM1,HLA-A
IL8- and CXCR2-mediated signaling events	1	10	PRKCA
Adaptive Immune System	2	20	SPTBN2,HLA-A

Table 5. Description of biological pathways involved in protein/gene present in HRV16iHMV samples continued...

Canonical NF-kappaB pathway	1	10	PRKCA
a6b1 and a6b4 Integrin signaling	1	10	PRKCA
CD28 co-stimulation	1	10	SPTBN2
IL8-mediated signaling events	1	10	PRKCA
PLC beta mediated events	1	10	PRKCA
G-protein mediated events	1	10	PRKCA
amb2 Integrin signaling	1	10	ICAM1
Ras signaling in the CD4+ TCR pathway	1	10	PRKCA
Beta3 integrin cell surface interactions	1	10	CD47
AP-1 transcription factor network	3	30	PRKCA,ICAM1,HLA-A
Retinoic acid receptors-mediated signaling	1	10	PRKCA
Regulation of Insulin Secretion	1	10	PRKCA
Alpha6Beta4Integrin	1	10	PRKCA
Ceramide signaling pathway	1	10	CTSD
Immunoregulatory interactions between a Lymphoid and a non-Lymphoid cell	1	10	HLA-A
Costimulation by the CD28 family	1	10	SPTBN2
Opioid Signalling	1	10	PRKCA
TNF receptor signaling pathway	2	20	CTSD,PRKCA
Integrin-linked kinase signaling	3	30	PRKCA,ICAM1,HLA-A
KitReceptor	1	10	PRKCA
Endogenous TLR signaling	1	10	PRKCA
NCAM signaling for neurite out-growth	1	10	SPTBN2
CD40/CD40L signaling	1	10	PRKCA
ATF-2 transcription factor network	1	10	PRKCA
Validated nuclear estrogen receptor alpha network	1	10	CTSD
Aurora A signaling	1	10	PRKCA
Downstream signaling of activated FGFR	1	10	PRKCA
Signaling by SCF-KIT	1	10	PRKCA
IL23-mediated signaling events	1	10	PRKCA
IL2 signaling events mediated by PI3K	1	10	PRKCA
Signaling events regulated by Ret tyrosine kinase	1	10	PRKCA
Transcriptional Regulation of White Adipocyte Differentiation	1	10	CD36
Downstream signal transduction	1	10	PRKCA
CDC42 signaling events	3	30	PRKCA,ICAM1,HLA-A
Interferon alpha/beta signaling	1	10	HLA-A
Signaling by PDGF	1	10	PRKCA
L1CAM interactions	1	10	SPTBN2
Regulation of CDC42 activity	3	30	PRKCA,ICAM1,HLA-A
ER-Phagosome pathway	1	10	HLA-A
Glucocorticoid receptor regulatory network	1	10	ICAM1
Wnt	1	10	PRKCA
Integration of energy metabolism	1	10	PRKCA
Glucocorticoid receptor signaling	1	10	ICAM1
Antigen processing-Cross presentation	1	10	HLA-A
Signaling by FGFR	1	10	PRKCA
Role of Calcineurin-dependent NFAT signaling in lymphocytes	1	10	PRKCA
Signaling by EGFR	1	10	PRKCA
Signaling by Aurora kinases	1	10	PRKCA
LPA receptor mediated events	1	10	PRKCA
Class I MHC mediated antigen processing & presentation	1	10	HLA-A
Developmental Biology	2	20	CD36,SPTBN2
Regulation of mRNA Stability by Proteins that Bind AU-rich Elements	1	10	PRKCA
PLK1 signaling events	1	10	PRKCA
NGF signalling via TRKA from the plasma membrane	1	10	PRKCA
Polo-like kinase signaling events in the cell cycle	1	10	PRKCA
IL2-mediated signaling events	1	10	PRKCA
TCR signaling in naïve CD4+ T cells	1	10	PRKCA
Direct p53 effectors	1	10	CTSD
EGFR1	1	10	PRKCA
Signalling by NGF	1	10	PRKCA
Regulation of p38-alpha and p38-beta	1	10	PRKCA
p75(NTR)-mediated signaling	1	10	PRKCA
p53 pathway	1	10	CTSD
p38 MAPK signaling pathway	1	10	PRKCA
CXCR4-mediated signaling events	1	10	PRKCA
Regulation of RhoA activity	1	10	PRKCA
RAC1 signaling pathway	1	10	PRKCA
RhoA signaling pathway	1	10	PRKCA
Regulation of RAC1 activity	1	10	PRKCA
Syndecan-4-mediated signaling events	1	10	PRKCA
Axon guidance	1	10	SPTBN2
BMP receptor signaling	1	10	PRKCA
IL1-mediated signaling events	1	10	PRKCA
Metabolism of mRNA	1	10	PRKCA
ATR signaling pathway	1	10	CTSD
Metabolism of RNA	1	10	PRKCA
Regulation of nuclear SMAD2/3 signaling	1	10	PRKCA
Regulation of cytoplasmic and nuclear SMAD2/3 signaling	1	10	PRKCA
TGF-beta receptor signaling	1	10	PRKCA
ATM pathway	1	10	CTSD
ALK1 signaling events	1	10	PRKCA
ALK1 pathway	1	10	PRKCA
Signaling by GPCR	1	10	PRKCA
Metabolism	1	10	PRKCA
Signal Transduction	1	10	PRKCA

Appendix V

Ribonucleic acid (RNA) is a linear molecule composed of four types of smaller molecules called ribonucleotide bases: adenine (A); cytosine (C); guanine (G); and uracil (U). Each ribonucleotide base consists of a ribose sugar, a phosphate group, and a nitrogenous base. Unlike Deoxyribonucleic Acid (DNA), RNA is single-stranded. Additionally, RNA in comparison to DNA contains ribose sugars rather than deoxyribose sugars, resulting in RNA being unstable and more prone to degradation (Alberts, *et al.*, 2014). The primary role of RNAs is to convert the genetic information stored in DNA into proteins (Berg, *et al.*, 2002).

RNA is synthesized from DNA by an enzyme known as RNA polymerase, during a process called transcription (DNA is copied to messenger RNA). The new RNA sequences are complementary to their DNA template, rather than being identical copies of the template. RNA is then translated into proteins by structures called ribosomes. While some RNA molecules are passive copies of DNA, many play crucial, active roles in the cell. For example, some RNA molecules are involved in switching genes on and off, and other RNA molecules make up the critical protein synthesis machinery in ribosomes (Alberts, *et al.*, 2014).

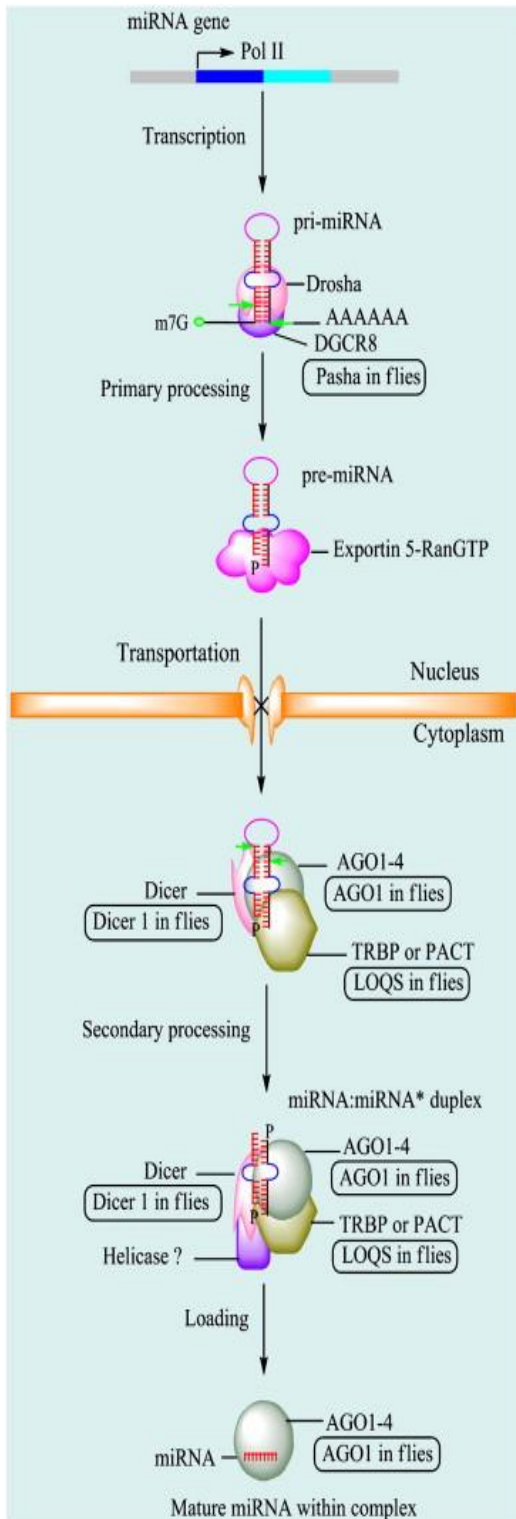
There are three major types of RNA involved in the translation process (protein synthesis) where Messenger RNA (mRNA) carries the genetic information copied from DNA in the form of a series of three bases, each of which specifies a particular amino acid; Transfer RNA (tRNA) is the key to deciphering the code words in mRNA, where each type of amino acid has its own type of tRNA, which binds it and carries it to the growing end of a polypeptide chain if the next code word on mRNA calls for it. Then correct tRNA with its attached amino acid is selected at each step, because each specific tRNA molecule contains a three-base sequence that can base-pair with its complementary code word in the mRNA; and Ribosomal RNA (rRNA) associates with a set of proteins to form ribosomes. These complex structures physically move along an mRNA molecule, catalyse the assembly of amino acids into protein chains. They also bind tRNAs and various accessory molecules that are necessary for protein synthesis (Griffiths, *et al.*, 2000; Lodish, *et al.*, 2000).

Small ncRNAs function by guiding sequence-specific gene silencing at the transcriptional and/or post-transcriptional level, through a mechanism known as RNA interference (RNAi) (Felekis & Deltas, 2006).

Briefly, the RNAi pathway involves two phases:

1. During the initiation phase, the double stranded RNA (dsRNA) molecules are either in the form of a hairpin or a longer dsRNA is processed into a short, interfering RNA (siRNA) by the RNase II enzymes Dicer, a helicase with RNase motif- functions as a molecular ruler to produce dsRNA fragments 25 nucleotides in length (Macrae, *et al.*, 2006) and Drosha, a ribonuclease (RNase) III double-stranded RNA-specific ribonuclease and subunit of the microprocessor protein complex that generate staggered cuts on each side of the RNA helix (Nicholson, 2014) and,
2. During the execution phase, siRNAs are loaded into the effector complex RNA-induced silencing complex (RISC), disentangled during and the single-stranded RNA hybridizes with mRNA target (Leuschner, *et al.*, 2006). The gene specific inactivation occurs by hybridization to and degradation of the target mRNA or by translation inhibition (Felekis, *et al.*, 2010).

The animal miRNA synthesis pathway



“The miRNA genes are transcribed by RNA polymerase II (Pol II), which results in the production of a pri-miRNA. Drosha, along with DiGeorge syndrome critical region gene-8 (DGCR-8; Pasha in flies), mediates the initial processing step (primary processing) that produces a ~ 65 nucleotide (nt) pre-miRNA. The pre-miRNA has a short stem of 2–3 nt 3' overhangs, which is recognised by exportin 5 (EXP5) that mediates transport to cytoplasm. In the cytoplasm, RNase III Dicer is thought to catalyse the second processing step (secondary processing), which generates the miRNA/miRNA* duplex. Dicer, TRBP or PACT (LOQS in flies), and Argonaute1–4 (Ago 1–4) (Argonaute 1 in flies) are responsible for pre-miRNA processing and RISC (RNA-induced silencing complex) assembly. An unknown helicase is thought to mediate unwinding of the duplex. One strand of the duplex remains the mature miRNA (miRNA) on Ago, whereas the miRNA* or passenger strand is degraded. The figure shows the mammalian miRNA synthesis pathway and fly factors are in the squares.” Retrieved from Wahid, *et al.*, (2010).

Appendix VI

Gene ontology methodology for miRNA data

Due to a large number of target genes generated by each miRNA, only instructions on how to produce the data and graphs can be provided, which is readily available as follows:

1. In order to obtain the target genes for each miRNA of interest, please go to miRTarBase website (<http://mirtarbase.mbc.nctu.edu.tw/php/search.php>). On the home page select Search by miRNA, then select Human for species available from the drop down menu.

Search...

Search Example

miRTarBase Home Search Browse Statistics Help Download Contact Us

By miRNA By Target Gene By Pathway By Validated Method By Disease By Literature Advanced Search

Search miRTarBase

Species: Human

Select one search option

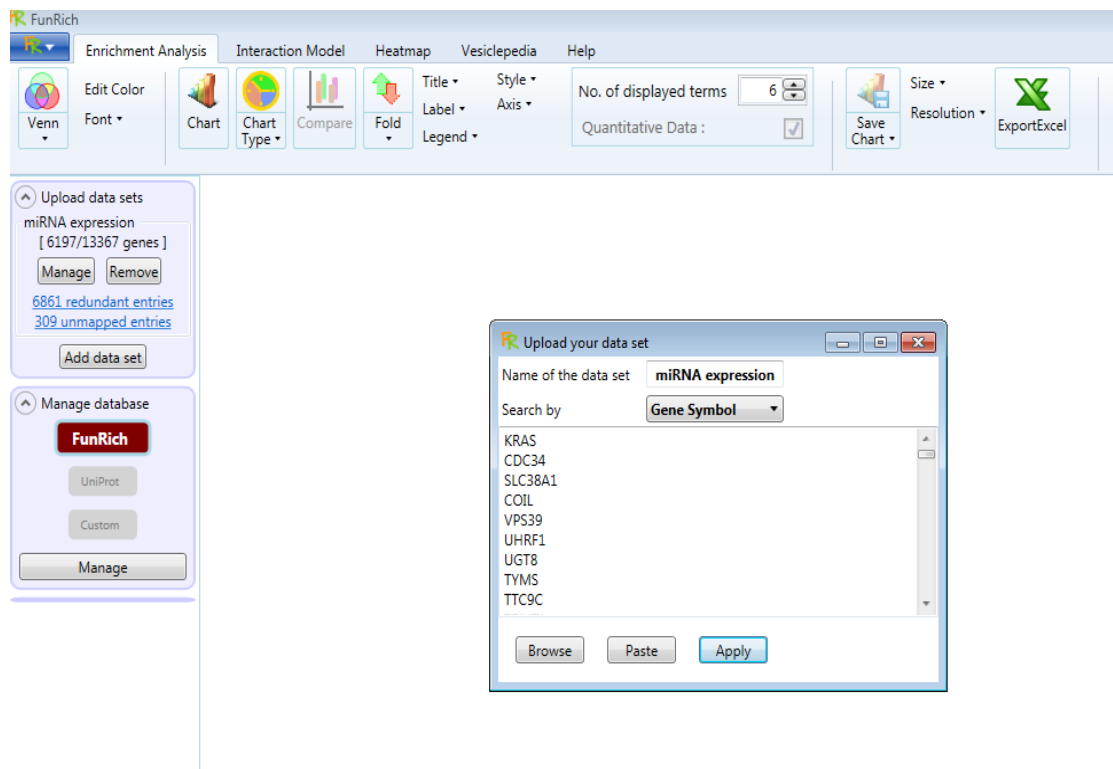
(a) miRNA ID: 23a-3p

(b) miRNA Family:

Submit Cancel

This step will generate a large list for the miRNA of interest (each miRNA generally targets > 500 genes).

2. Download FunRich software for free at <http://www.funrich.org/download>.
3. Upload the data or copy and paste the target gene name/code retrieved from miRTarBase website to create a data set using FunRich software.



This step will allow the generation of enrichment analysis of the target genes for each, or for multiple miRNAs of interest.

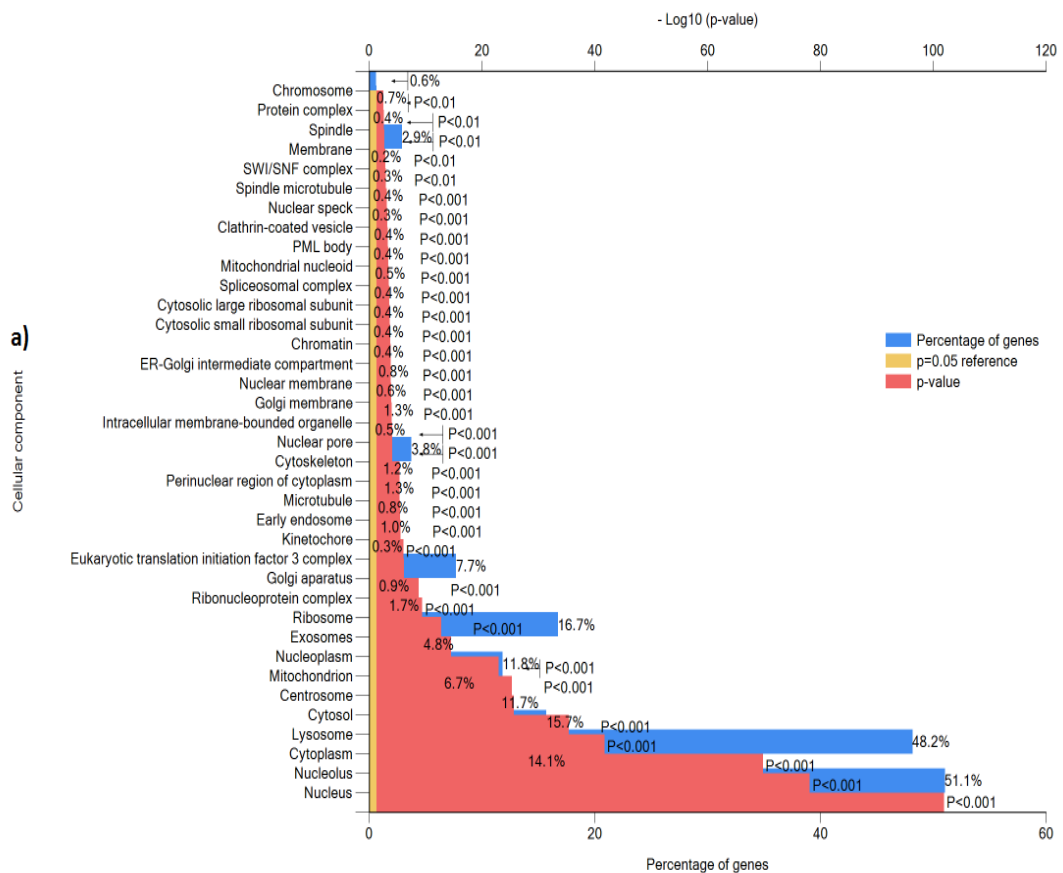
4. In order to obtain the full report of the enrichment analysis, simply save the generated report on the ExportExcel option available from the menu.

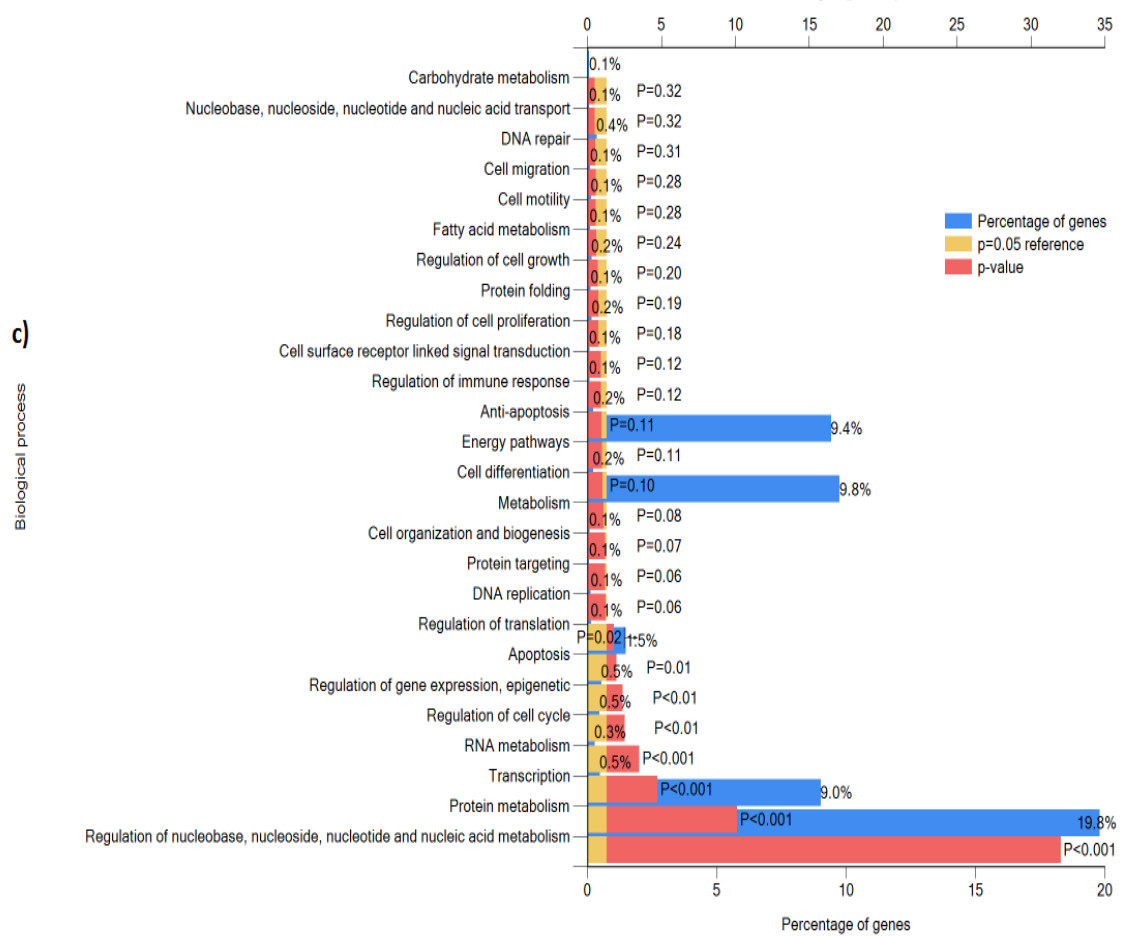
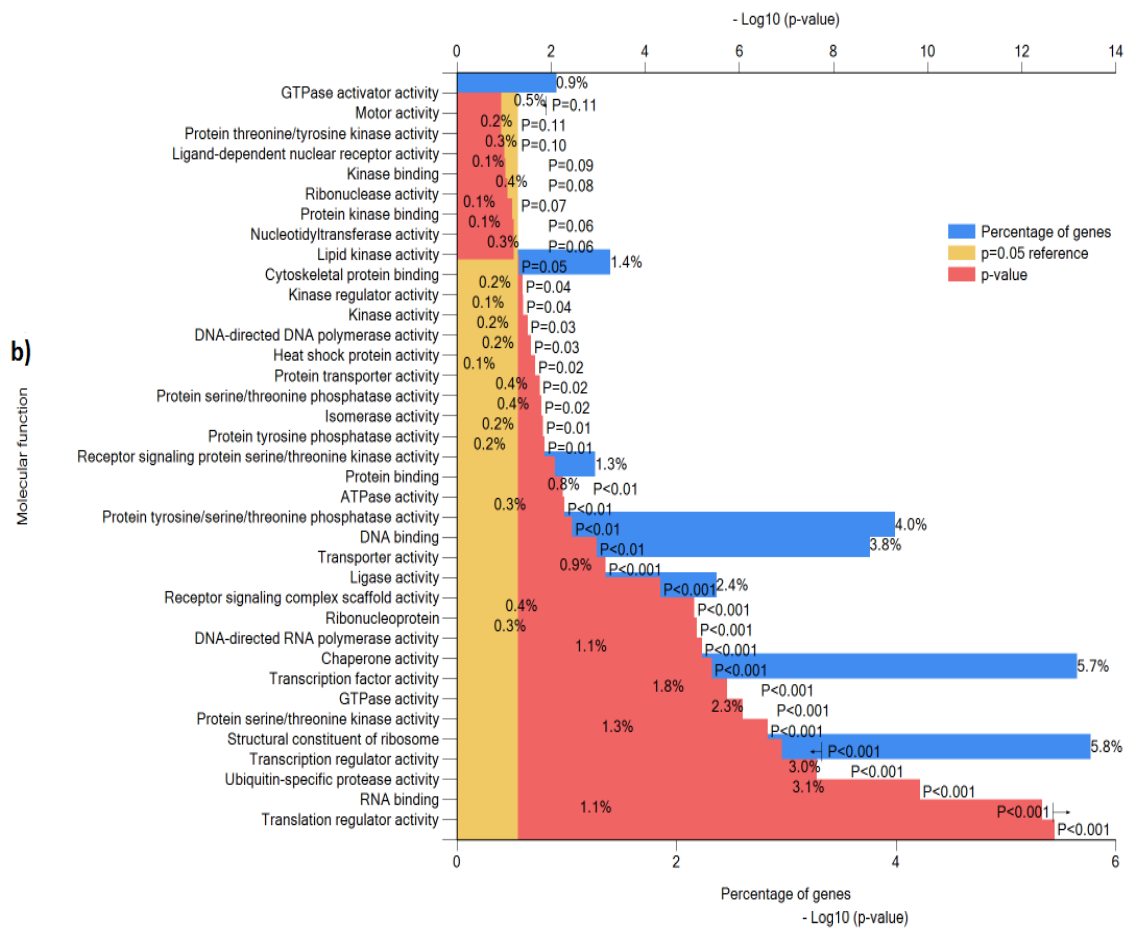
Appendix VII

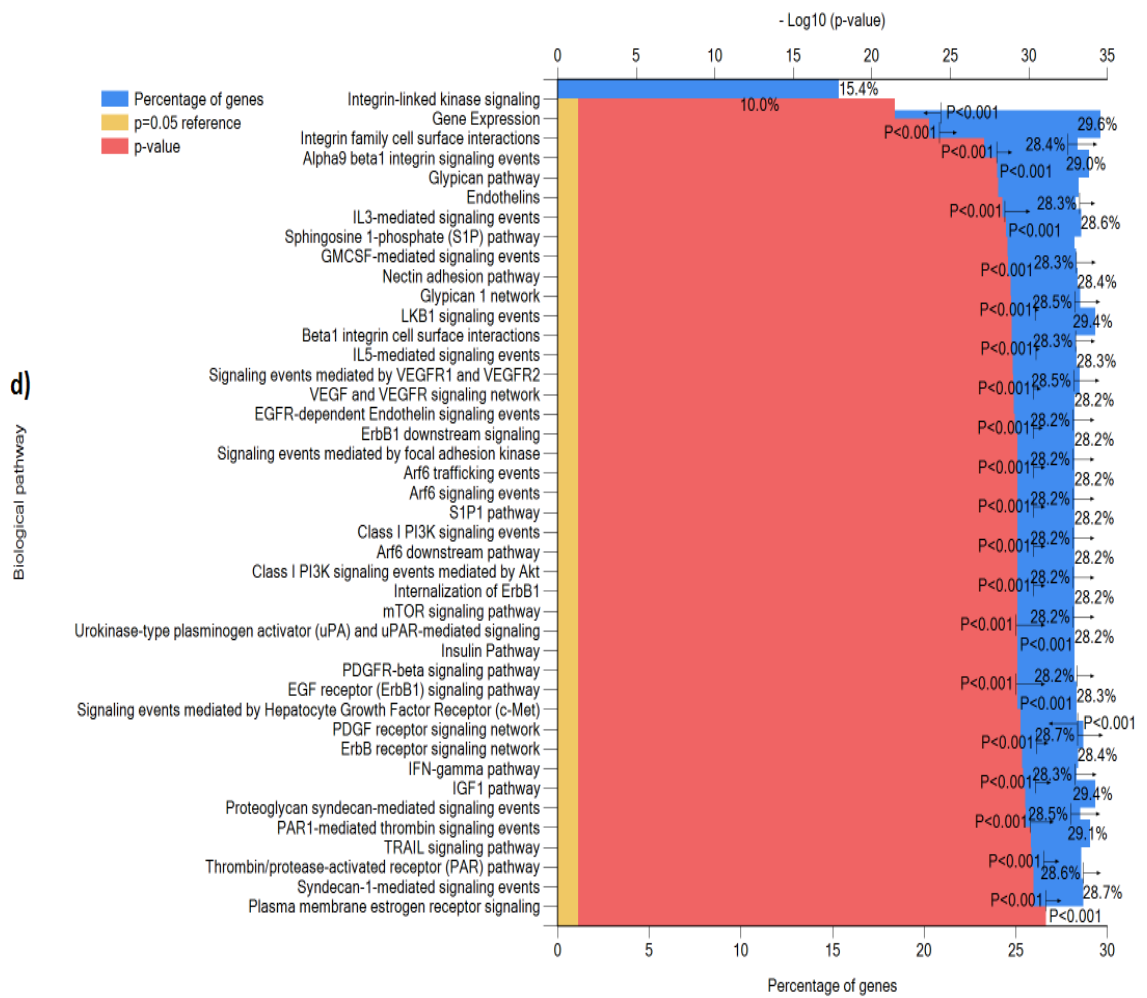
GO assessment of target genes for miRNA present in HRV16iHMV

After assessing the pattern of expression of miRNAs in HRV16iHMV samples, further analyses was focused on the reported target genes using miRTarBase database. The analyses generated a list of candidate genes with >15.866 target genes for the 29 miRNA present in the MV samples, with >8.880 being redundant genes. The FunRich software classified their targets in clusters of genes that are not mutually exclusive, the reason for this is that the product of a single gene could have one or more cellular components (Fig. a), molecular functions (Fig. b), be associated with different biological processes (Fig. c) and be involved in several biological pathways (Fig. d).

The graphs were created with the use of the FunRich functional enrichment analysis tool software, which performs functional enrichment analyses on background databases that are integrated from heterogeneous genomic and proteomic resources. The Hypergeometric distribution test was performed to check the statistical significance of enriched and depleted terms. In addition, the Bonferroni and Benjamini-Hochberg (BH) (also known as the False Discovery Rate (FDR)) method was also implemented to correct for multiple testing, each associated with a p-value ($p < 0.05$).

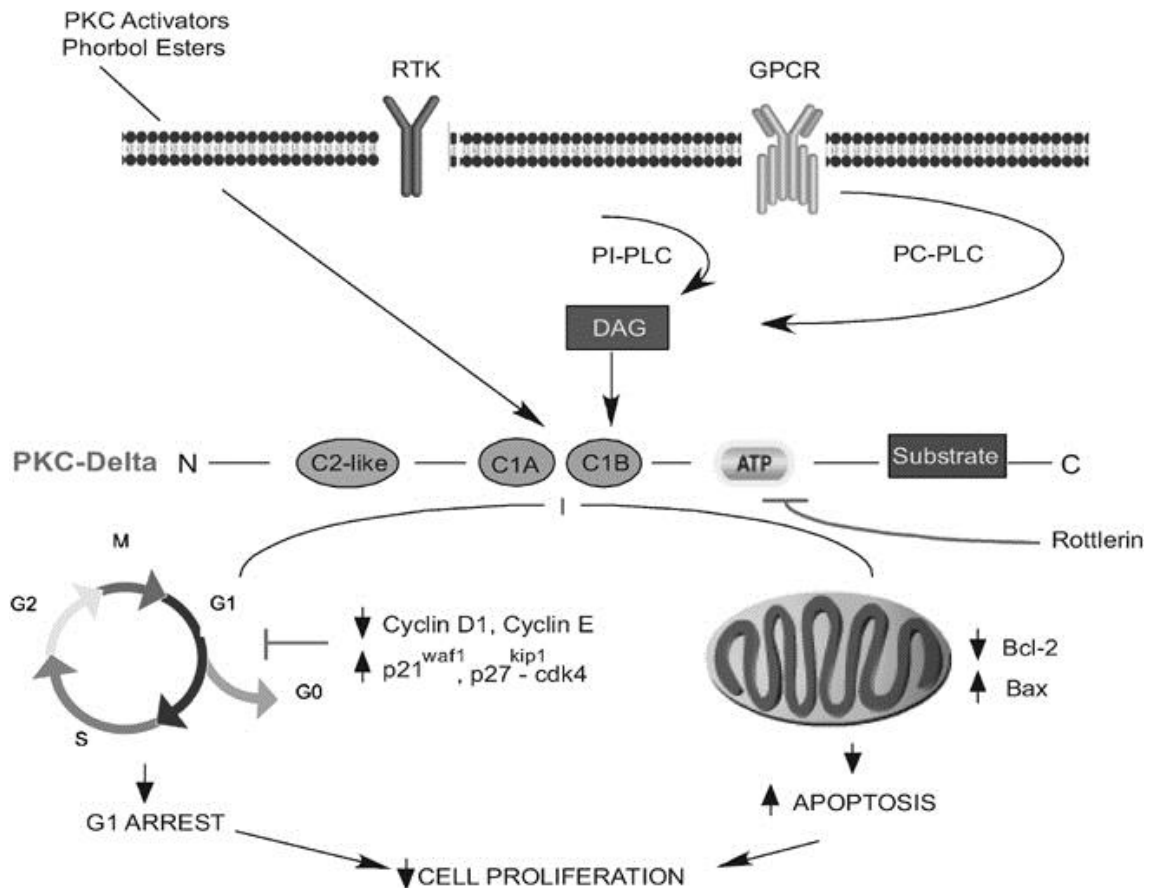






Appendix VIII

Protein kinase C δ inhibits Caco-2 cell proliferation by selective changes in cell cycle and cell death regulators



“A Proposed model for PKC- δ antiproliferative functions in Caco-2 cells. PKC- δ signalling suppresses G1-S progression by inhibiting the expression levels of G1 cell cycle activators, cyclin D1 and cyclin E, and upregulating G1 cell cycle inhibitor p21Waf1 as well as p27Kip1-cdk4 complex. PKC- δ signals also inhibit cell survival by downregulating antiapoptotic Bcl-2 and increasing proapoptotic Bax. These tumour suppressor pathways inhibit mitogenic signalling and enhance cell death that result in decreased cellular proliferation of colon cancer cells. Suppresses G1-S progression by inhibiting the expression levels of G1 cell cycle activators, cyclin D1 and cyclin E, and upregulating G1 cell cycle inhibitor p21Waf1 as well as p27Kip1-cdk4 complex. PKC- δ signals also inhibit cell survival by downregulation.” Retrieved from Cerda, *et al.*, (2006).